University of Southampton

Internalisation and Trafficking Characteristics of CD7 and CD38 on a Human T-ALL Cell Line in Relation to Immunotoxin Potency

By

Sarah Alice Field

Doctor of Philosophy

Faculty of Medicine, Health and Biological Sciences

Simon Flavell Leukaemia Research Unit

Division of Cancer Sciences

February 2002

UNIVERSITY OF SOUTHAMPTON

ABSTRACT

FACULTY OF MEDICINE, HEALTH AND BIOLOGICAL SCIENCES
DIVISION OF CANCER SCIENCES

Doctor of Philosophy

Internalisation and Trafficking Characteristics of CD7 and CD38 on a Human T-ALL Cell Line in Relation to Immunotoxin Potency

by
Sarah Alice Field

The therapeutic potency of an immunotoxin (IT) is determined on the antibody moiety binding to a specific cell surface target antigen, its subsequent internalisation and ultimately translocation of the toxin component from an intracellular vesicular compartment to the cytosol. Once in the cytosol, the toxin kills the cell apoptotically by catalytically inactivating ribosomes. It is of paramount importance that appropriate target molecules are selected that will ensure optimally efficient delivery of toxin to the appropriate intracellular compartment. It has been previously reported that immunotoxin therapy directed against more than one target molecule is more effective in vivo than when only one single antigen is targeted against (Flavell et al.,1998, 2001).

In this study, the enhanced cytotoxic effect of the anti-CD7 IT HB2-Saporin and the anti-CD38 IT OKT10-Saporin used in combination when compared to their use singly was demonstrated on the human T-ALL cell line HSB-2 both in vivo and in vitro. In an in vitro cell proliferation assay and the in vivo SCID mouse model, OKT10-Saporin was shown to be more effective than HB2-Saporin, but neither individual IT was as potent as their combined use. In contrast, HB2-Saporin performed best in the short term protein synthesis inhibition assay (PSI) and the combination of two ITs demonstrated an intermediate potency between that of the two individual ITs. Three explanations were proposed for the improved efficacy of using two ITs simultaneously: 1) co-ligation of CD7 and CD38 might alter the individual internalisation characteristics; 2) targeting against two molecules overcomes the heterogeneity of antigen expression on tumour cells or 3) using two immunotoxins increases the amount of toxin delivered to the target cell. It is possible that all three explanations are valid.

Flow cytometry and confocal microscopy were used to determine the internalisation and intracellular routing characteristics of CD7 and CD38 on the T-ALL cell line HSB-2, when ligated by antibody individually or in combination. These studies indicate that CD7 and CD38 have very different internalisation kinetics. CD7 clears very rapidly from the cell surface following ligation by antibody, whereas only 50% of CD38 molecules internalise over a 24 hr duration. When CD7 and CD38 were ligated by antibody simultaneously, no change to the internalisation characteristics or intracellular routing of either antibody was apparent. In these studies it has become clear that there is no direct correlation between internalisation, intracellular routing and cytotoxic potency.

Brefeldin A was used as a tool to investigate what intracellular routes these ITs may follow within the cell. These were preliminary studies and further work is required.

These studies revealed that no single factor determines IT potency. Internalisation rate is only important if degradation is avoided and trafficking occurs to an appropriate intracellular compartment from which the toxin component can translocate.

Contents

I declare that the data presented in this thesis is my own original work.

List of Figures

List of Tables

Acknowledgements

I would like to thank my supervisors Drs. David and Bee Flavell for their ongoing help, advice and support over the past 4 years. I would also like to thank Dr. Peter Lackie for becoming my supervisor at such a late stage in my PhD and for all his help with the EM studies. He has been very encouraging throughout the whole write-up process.

Thanks to all my work colleagues Armorel, Tony, Sarah and Christine for all their practical advice and for keeping me sane throughout my PhD. Thanks to all those in the Biomedical Imaging Unit, especially Roger and Anton, who have spent endless hours with me obtaining and processing all my confocal and EM images.

My special thanks to all my friends who have kept me going with this PhD and have put themselves out for me on so many occasions, especially Duncan, Becky, Richard, Fay and Katie.

I owe my parents the biggest thanks for always supporting me in everything I do.

All the work detailed in this thesis has been undertaken with the financial support of the charity Leukaemia Busters.

Abbreviations

Ab	-	Antibody
ADCC	-	Antibody Dependent Cell-mediated Cytotoxicity
ADP	-	Adenosine diphosphate
ATP	-	Adenosine triphosphate
AF568	-	Alexa Fluor 568
ALL	-	Acute Lymphoblastic Leukaemia
ANLL	-	Acute Nonlymphoblastic Leukaemia
ARF	-	ADP-ribosylation factor
Asn	-	Asparagine
Asp	-	Aspartate
BFA	-	Brefeldin A
BSA	-	Bovine Serum Albumin
CALLA	-	Common acute lymphoblastic leukaemia antigen
CGy	-	Centi-Gray
CNS	-	Central Nervous System
CD	-	Cluster of differentiation
Cys	-	Cysteine
DABCO	-	1,4-Diazabicylco-[2,2,2]-octane
DT	-	Diphtheria toxin
EM	-	Electron microscopy
E.coli	-	Escherischia coli
EDTA	-	Ethylenediaminetetraacetic acid
EF-2	-	Elongation factor
EGF	-	Epidermal Growth Factor
ER	-	Endoplasmic reticulum
Fab	-	Fragment antigen binding
Fc	-	Fragment crystalisable
FITC	-	Fluorescein isothiocyanate
GI	-	Gastrointestinal
GDP	-	Guanosine diphosphate
Gln	-	Glutamine
Glu	-	Glutamate
Gly	-	Glycine
GTP	-	Guanosine triphosphate
His	-	Histidine
HRP	-	Horseradish peroxidase
HAMA	-	Human anti-mouse antibody
HATA	-	Human anti-toxin antibody
HLA	-	Human leucocyte antigen
Ig	-	Immunoglobulin
IT	-	Immunotoxin
IC_{50}	-	Concentration that produces a 50% inhibition compared to untreated controls
I^{125}	-	Iodine-125

kD	-	Kilo-Daltons
LDL	-	Low density lipoprotein
MAb	-	Monoclonal antibody
MFI	-	Mean Fluorescence Intensity
MDR	-	Multiple drug resistance
MVB	-	Multivesicular body
NAD	-	Nicotinamide adenine dinucleotide
NaN_3	-	Sodium azide
NHL	-	Non-Hodgkins lymphoma
NK	-	Natural Killer
P-gp	-	P-glycoprotein
PBS	-	Phosphate buffered saline
PAP	-	Pokeweed antiviral protein
PE	-	Pseudomonas exotoxin
pI	-	Isoelectric point
PSI	-	Protein Synthesis Inhibition
RIPs	-	Ribosome inactivating proteins
RNA	-	Ribonucleic acid
RTA	-	Ricin A chain
RTB	-	Ricin B chain
Ser	-	Serine
SCID	-	Severe Combined Immunodeficient
SDS-PAGE	-	Sodium dodecyl sulphate polyacrylamide gel electrophoresis
SD	-	Standard deviation
sIg	-	Surface immunoglobulin
TGN	-	Trans-Golgi network
TMs	-	Transmembrane domains
TCA	-	Trichloroacetic acid
Trp	-	Tryptophan
Tyr	-	Tyrosine
VLS	-	Vascular Leak Syndrome
VTC	-	Vesicular tubular clusters

Chapter 1
Introduction

1.1 Acute Lymphoblastic Leukaemia in Childhood

Acute leukaemia is the most common type of childhood malignancy (Poplack and Reaman 1988). Of the approximately 2000 cases diagnosed in The United States and 600 in the UK each year, three quarters are acute lymphoblastic leukaemia (ALL) and the remaining quarter are acute nonlymphoblastic leukaemia (ANLL). The peak incidence of childhood ALL occurs at approximately 4 years of age. This malignancy is twice as common in caucasians than non-caucasians and is more common in boys than in girls (Hanson and Mulvihill 1980). The exact cause of this disease is unknown but is believed to be due to a multitude of predisposing or contributing factors such as environmental and genetic factors, viruses, and immunodeficiency states.

About fifty years ago, before the introduction of chemotherapy to leukaemia therapy, all children afflicted with ALL surrendered to the disease within two months of diagnosis. Due to the gradual improvement in therapy of ALL over the years, 60 to 70% of children currently diagnosed with the disease can expect prolonged (>5 year) disease-free survival and most of these patients are likely to be cured (Poplack 1988, Chessels 2000). These developments in anti-leukaemia treatments include the identification of effective single agent chemotherapy, followed by the development of combination chemotherapy, the introduction of maintenance treatment, the use of central nervous system (CNS) prophylactic therapy, and the use of intensified therapy.

1.1.1 Clinical Presentation

ALL is characterised by the uncontrolled growth and proliferation of immature lymphoid cells. It is thought to be a clonal disease since it is presumed to result from the malignant transformation of a single aberrant progenitor cell that has the ability to self-renew indefinitely (Poplack and Reaman 1988). Children with ALL commonly present symptoms such as pallor, fatigue, petechiae, bleeding and fever. These symptoms are due to the underlying anaemia, thrombocytopenia and neutropenia that result from the failure of normal haematopoiesis. Symptoms like lymphadenopathy, hepatomegaly and splenomegaly reflect the extramedullary leukaemic involvement. These symptoms tend to

vary in duration from days to weeks, or even months. Although anorexia is common, the occurrence of significant weight loss is rare. Bone pain may manifest itself which is a sign of leukaemic lymphoblasts infiltrating the periosteum and the bone.

The onset of ALL is often accompanied by many non-specific symptoms like malaise, anorexia, irritability, and low-grade fever which can make it hard to diagnose since these are common to a number of non-malignant conditions. These include juvenile rheumatoid arthritis, infectious mononucleosis, aplastic anaemia and acute infectious lymphocytosis. Diagnosis is by means of a bone marrow aspirate. Although the presence of greater than 5% lymphoblasts indicates the manifestation of leukaemia, most laboratories require a minimum of 25% leukaemic blast cells in the aspirate before confirming the diagnosis. Less than 5% of children with ALL present with CNS leukaemia at the time of diagnosis (Bleyer and Poplack 1985).

There are various immunological subtypes of ALL and these differ in their clinical presentation. For example, patients with T-cell disease tend to be older boys who present with high initial leukocyte counts and frequently have a mediastinal mass. These patients often have a poor prognosis. Patients suffering from B-cell precursor ALL, which only accounts for a small percentage of the overall childhood ALL population, have a much poorer prognosis, whereas those patients whose leukaemia cells are CALLA positive have a more favourable prognosis (Crist *et al.,* 1984, Crist *et al.,* 1985). Infants of less than a year of age with B-cell ALL have an immune and molecular phenotype that is characteristic of the earliest stages of B-cell differentiation. Studies have shown that these patients develop ALL with a uniquely poor prognosis (Crist *et al.,* 1986, Dinndorf and Reaman 1986).

1.1.2 Prognostic Factors

It is important to be able to identify how favourable or unfavourable a prognosis is, as it allows treatment to be tailored to the different risk groups that a patient may be placed in. Patients showing indications of poor prognosis will be given more intensive therapy, whereas those who show signs of a better prognosis will receive a less intensive therapy regime with the intention of being equally effective but hopefully reducing the occurrence of treatment-associated side effects.

The initial leukocyte count and age at the time of diagnosis have been shown to be the two most reliable indicators of prognosis for remission duration as well as patient survival. The relationship between leukocyte count and prognosis follows a linear trend: - the higher the white blood cell count, the worse the prognosis (Hammond *et al.*, 1986). Very young (<2 years) and older (>10 years) sufferers of ALL have a poorer prognosis compared with patients of an intermediate age (Sather 1986). Infants of under one year of age have the worst prognosis (Reaman *et al.*, 1985, Crist *et al.*, 1986).

Many other factors have been correlated with prognosis and include cytogenetic profile, gender, race, degree of organomegaly, lymphadenopathy, presence or absence of a mediastinal mass, initial haemoglobin, initial platelet count, French-American-British (FAB) classification, immunological subtype, immunoglobulin levels at diagnosis, day 14 marrow response, and HLA type (Hammond *et al.*, 1986, Kalwinsky *et al.*, 1985, Leikin *et al.*, 1981, Miller *et al.*, 1980, Miller *et al.*, 1981, Reaman *et al.*, 1985, Rogentine *et al.* 1973, Sather 1986). Several of these characteristics have been shown to depend on other factors and so therefore do not stand alone as a prognostic factor.

Leukaemia is a clonal disease resulting from genetic mutations and the transformation of a single early progenitor lymphoid cell. There has been much research into the aetiology of acute leukaemia but this still remains largely unknown (Sandler and Ross 1997). Several cytogenetic abnormalities have been described in ALL. Over 50% of all ALL cases carry chromosomal translocations (O'Connor and Weiss 1999).

Cytogenetic abnormalities in ALL were initially identified by routine banding techniques, but due to advances in technology the use of polymerase chain reaction (PCR) and fluorescent in situ hybridisation (FISH) has enabled more sensitive and specific analysis of these changes (Martinez-Climent 1997). These genetic alterations may be numerical or structural and contribute considerably to the understanding of the pathogenesis of acute leukaemias.

Table 1.1 contains a summary of the chromosomal abnormalities, describing their frequency and their clinical features. The chromosomal abnormalities discussed here are just a few examples of those found in patients with ALL of which there are too many to mention, for more details see reviews Pui 1998, Thandla and Aplan 1997.

Table 1.1. Cytogenetic findings in acute lymphoblastic leukaemia

Abnormality	**Frequency (%ALL)**	**Clinical features**
Hyperdiploidy		
47 to 50 chromosomes	15-20%	Intermediate prognosis
>50 chromosomes	25-35%	Common ALL, good prognosis
Diploidy	8-10%	Intermediate prognosis
Hypodiploidy	5-8%	Intermediate/poor prognosis
t(9;22)-Ph' chromosome	1-2%	Poor prognosis
t(12;21)	16-22%	Common ALL, probably good prognosis
t(1;19)	5%	Average prognosis
t(4;11) other 11q23	5-8%	Infant ALL, poor prognosis
t(8;14)	1-2%	B-ALL
14q11, 7q35, 7p15	1-2%	All associated with T-ALL
p53 mutation	3-30%	Relapse in T-ALL

Several prognostically relevant biological markers have been identified for patients with leukaemias of a B-cell lineage immunophenotype, but unfortunately there has not been as much success with identifying such markers of leukaemias of the T-cell lineage. Recently, the absence of CD2 antigen from leukaemia cells of the T-cell lineage has been strongly correlated with failure of treatment in both standard and poor prognosis groups. One important observation from this study is that absence of CD2 on leukaemia cells in standard prognosis T-lineage ALL predicted a significantly worse outcome than CD2-positive patients including those classified as high-risk (Uckun *et al.*, 1996).

1.1.3 Treatment

The treatment of childhood leukaemia has improved enormously over the past years with >75% with ALL cured of the disease. Therapy currently fits into three main treatment phases; 1) remission induction, 2) consolidation therapy including the delivery of CNS preventive therapy and 3) maintenance therapy. The initial treatment is used to induce remission of the ALL and consists of a basic two-drug combination of vincristine and prednisone. These two drugs induce remission in 85% of children suffering from ALL, but this rate can be increased to approximately 95% by the addition of a third drug, often L-asparaginase or an anthracycline. The addition of a third drug to the combination is also found to increase the duration of the remission induced (Frei and Sallan 1978).

The idea of consolidation therapy is to administer a period of intensified chemotherapy immediately remission has been induced. Different drugs from the initial therapy are used with the aim to prolong the duration of remission in high-risk patients, and to reduce the emergence of resistant clones. It is during this stage of treatment that therapy is usually directed at the CNS.

The CNS is a major site of relapse and CNS leukaemia is almost invariably followed by bone marrow relapse. In some studies, the incidence of this form of relapse was as high as 75%. For this reason, CNS preventive therapy was undertaken. This may consist of an 1800 cGy (centi-Gray) dose of cranial irradiation followed by five doses of intrathecal methotrexate. Alternative approaches have included triple intrathecal chemotherapy with methotrexate, cytosine arabinoside and hydrocortisone alone; intermediate-dose methotrexate, alone or with concomitant intrathecal methotrexate; intrathecal methotrexate alone; or a high-dose systemic methotrexate (Bleyer and Poplack 1985, Freeman *et al.*, 1983, Haghbin *et al.*, 1975, Nesbit *et al.*, 1981, Sullivan *et al.*, 1982). Regimes of chemotherapy alone, such as these, have been shown to be as effective for CNS protection as cranial irradiation and intrathecal methotrexate for patients with good prognosis or at an intermediate risk of CNS relapse (Freeman *et al.*, 1983, Sullivan *et al.*, 1982).

Maintenance therapy has been shown to prevent most patients from relapsing within 2 months of termination of the initial treatment. The most common form of maintenance therapy is administration of methotrexate on a weekly or twice weekly basis and 6-mercaptopurine on a daily basis. The addition of intermittent pulses of vincristine and

prednisone is sometimes used to prolong remission duration, although is not needed for all patients (Leikin *et al.*, 1981, Rivera *et al.*, 1987). Maintenance therapy is generally continued for a period of 2 ½ to 3 years. Patients who successfully complete the maintenance therapy without relapse generally have a good prognosis, but some patients relapse while receiving this treatment which can often be an indication that they have developed multiple drug resistance (MDR) and other forms of treatment are required.

Despite the increasing success of intensive chemotherapy and bone marrow transplantation, there are still a substantial number of patients with T-cell ALL or T-cell non-Hodgkin's lymphoma (NHL) who will eventually relapse. Adult patients suffering from ALL who achieve long-term tumour-free survival following standard or high-dose therapy and stem cell rescue are in the minority. It is therefore very clear that the development of novel agents to effectively treat relapsed T-lineage ALL is required. One form of treatment that has shown some clinical promise against haematological malignancies is immunotoxin therapy (Bachier and LeMaistre 1995, Caron and Scheinberg 1994, Frankel *et al.*, 1996).

1.1.3.1 The Mechanisms and Side-Effects of Chemotherapeutic Agents

1.1.3.1.1 Vincristine Sulphate

This drug, also known as Oncovin, and Vinasar, blocks mitosis by binding specifically to tubulin, hence preventing the ability of the protein to polymerise into microtubules. Disruption of the microtubules of the mitotic apparatus arrests cell division in metaphase. The inability to segregate chromosomes correctly during mitosis presumably leads to cell death. Vincristine is relatively non-toxic and has only mild myelosuppressive activity. Unwanted effects of this drug include severe neurological manifestations. Alopecia occurs in up to 20% of patients treated with this drug. Occasionally leukopenia, thrombocytopenia, anaemia, polyuria, dysuria, fever and gastrointestinal (GI) symptoms occur.

1.1.3.1.2 L-Asparaginase

Most cells can synthesise enough L-asparagine (L-Asn) for protein synthesis but certain tumour cells including ALL cells cannot produce as much as they require and hence need an exogenous source of this amino acid. L-asparaginase is an enzyme that destroys the exogenous supply of L-Asn so that tumour cells become depleted and die apoptotically but

normal cells survive by making their own supply of L-Asn intracellularly. Asparaginase is essentially a foreign protein and may cause an anaphylactic reaction. It may also interfere with blood clotting, raise blood sugar levels and liver enzymes and cause liver disease in some patients. The most common side effect is vomiting. It is not myelosuppressive. As it produces ammonia as a by-product of its reaction, it may cause toxicity in patients with liver dysfunction. It has also been associated with pancreatitis.

1.1.3.1.3 Anthracyclines

The main toxicity of anthracyclines (e.g. doxorubicin, epirubicin, aclarubicin and idarubicin) is on topoisomerase II (a DNA gyrase). Its activity is markedly increased in proliferating cells. Doxorubicin intercalates in the DNA and stabilises the DNA-topoisomerase II complex after the strands have been nicked during mitotic segregation, thus causing the process to seize at this point (Epstein 1988). Doxorubicin has many side effects including cumulative, dose-related cardiac damage which may lead to dysrhythmias and heart failure. This may be due to the generation of free radicals. Anthracyclines attack fast growing tissue, mucal and light intestine resulting in hair loss and damage to the GI epithelium. Epirubicin is less cardiotoxic than doxorubicin. These drugs are myelosuppressive.

1.1.3.1.4 Methotrexate

This drug is a folate antagonist which kills cells during the S phase of the cell cycle, and therefore is most effective when cells are in the logarithmic stage of growth. Methotrexate prevents the use of folates for the synthesis of purine nucleotides and thymidylate which are in turn essential for DNA synthesis and cell division. Methotrexate is only partially selective for tumour cells and is toxic to all rapidly dividing normal cells, such as those of the bone marrow and the intestinal epithelium. Side effects other than damage to those tissues may also include pneumonitis. High doses may cause nephrotoxicity due to precipitation of the drug or metabolite in the renal tubules.

1.1.3.1.5 Cytosine Arabinoside

This drug, commonly known as ara-C or cytarabine, is an analogue of the naturally occurring nucleoside 2'deoxycytidine and as such, it can become incorporated into DNA. It exhibits cell phase specificity; primarily killing cells undergoing DNA synthesis (S-phase) and can also block the progression of cells from the G_1 phase to the S-phase under

certain conditions. The mechanism of action of cytarabine is not fully understood but it is thought to act through the inhibition of DNA polymerase. Its main unwanted effects are on the bone marrow and the GI tract. It causes both nausea and vomiting.

1.1.3.2 Drug resistance

The resistance that tumour cells may develop to chemotherapy drugs can be either primary (in which case the resistance is present at the time the drugs were first administered) or acquired (in which case it has developed during the treatment with the drug). Acquired resistance may be due to adaptation of the tumour cells or to mutation. However the resistance originated, these resistant cells expand by selection during treatment and eventually overgrow the sensitive cells (Goldie and Coldman 1983). Examples of various mechanisms of resistance are briefly discussed here.

Firstly, there could be a decrease in the amount of drug taken up by the cell which is one of the mechanisms of resistance to methotrexate where there is a decrease in the membrane transport into the cell (Assaraf and Schimke 1987; Trippett *et al.,* 1992). Secondly, alterations to the target enzyme may prevent the chemotherapy agent from working properly. Again, resistance to methotrexate is a fine example of this whereby dihydrofolate reductase is altered in such a way as to decrease the affinity of the drug for this enzyme or that there is an increase in the concentration of the enzyme in these cells making the drug inefficient (Pauletti *et al.,* 1990). Other mechanisms of resistance to methotrexate include the possible decreased polyglutamation of the drug (Li *et al.,* 1992) and decreased thymidylate synthase activity (Curt *et al.,* 1985) preventing the drug from working efficiently in its normal manner.

Other mechanisms include the insufficient activation of a drug such as with cytarabine when it does not undergo phosphorylation, or the increase in inactivation of the drug, also seen when using cytarabine. Resistance to L-asparaginase arises through the induction of the capacity of tumour cells to synthesise asparagine. Anthracyclines fail to kill tumour cells which have developed a modified topoisomerase II.

One of the biggest causes of resistance to these agents is the decrease in accumulation of the drugs inside cells due to an increase in expression of P-glycoprotein (P-gp), an ATP-dependent drug transport protein. This protein is encoded by the *mdr* gene present on

chromosome 7 and is responsible for MDR to several structurally unrelated cytotoxic compounds such as anthracyclines, the vinca alkaloids and many others. It is not the only membrane transporter to confer MDR but is the most common. The physiological role of this protein is thought to be for the protection of cells against environmental toxins.

Recently the concept as to how this protein works has changed and it is now thought that P-gp may function as a 'flippase' within the plasma membrane (Higgins and Grottesman 1992). It may translocate drugs actively (ATP-dependent) from the cytosolic inner lipid leaflet of the plasma membrane to the outer lipid leaflet, enabling the drugs to leave the plasma membrane by diffusion.

Several non-cytotoxic drugs are able to act as substrates for this protein and reverse MDR. Examples of these are calcium-channel blockers (e.g. verapamil), some anti-hypertensives (e.g. reserpine), some antihistamines (e.g. terfenadine) and some immunosupressants (e.g. cyclosporine). However, these approaches are of limited value due to the intrinsic toxicities of these agents and the high doses required *in vivo* to exert a reversed effect. One new approach that may overcome the problem of MDR would be to use antibodies, which have very different cytotoxic mechanisms, which would circumvent the drug resistance mechanisms. One category of antibody-based drugs that may be of value here are immunotoxins (ITs).

1.2 Immunotoxins

ITs are chimeric molecules in which a cell type-specific ligand is coupled to a variety of catalytic ribosome inhibiting protein toxins or toxin fragments. The most common ligand used for the specific delivery of the toxin into the cell is a monoclonal antibody (MAb) directed against an antigen expressed at high levels on a tumour cell surface (an example of which can be seen in figure 1.1). The toxins used to construct these hybrid molecules are either bacterial toxins such as Pseudomonas exotoxin (PE), Diphtheria toxin (DT) or plant toxins including ricin, abrin, pokeweed antiviral protein (PAP), saporin and gelonin. Bacterial toxins are well suited to the construction of fusion toxins, whereas plant toxins tend to be conjugated to the ligand by disulphide bond chemistry. Plant toxins are well suited to this type of therapy since they possess extreme potency.

An IT acts by selectively binding to the surface of the target cell, followed by internalisation into the cell interior, after which the toxin becomes translocated to the cytosol where it catalytically inhibits ribosomes and thus kills the cell. Unlike other forms of immunotherapy (such as radioimmunotherapy which can target the cell that the conjugate is bound to and surrounding cells), an IT has no bystander effect, as it must be taken into the cell i.e. internalised after binding to the target antigen. Only antibody-toxin conjugates that induce internalisation after binding to the cell surface will be toxic to the target cell population.

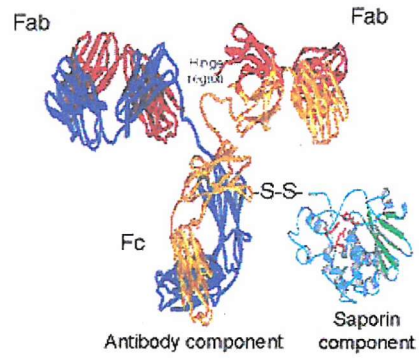

Figure 1.1 A molecular ribbon diagram of a typical immunotoxin.

The main advantage of using ITs over conventional chemotherapy and radiotherapy is that they display a relatively low non-specific toxicity *in vivo* since leukaemia cells are targeted to a greater extent than normal tissue. Another benefit of the use of ITs is that as the mechanism of cytotoxicity is completely different from that used by conventional chemotherapy it is possible that the problems caused by MDR may be overcome.

Several investigators have used different ribosome-inactivating protein (RIP) containing ITs and recombinant ITs for *in vivo* treatment of haematological malignancies including ALL, with mixed results in early clinical trials (Uckun 1993, Vitetta *et al.,* 1993, Uckun and Reaman 1995, Grossbard and Nadler 1994, Sausville *et al.,* 1995, Grossbard *et al.,* 1992). The efficiency may vary greatly from one IT to another. ITs have generally been found to be a lot less active than the original whole toxins they are formed from, towards the target cells, especially if only a fragment of the toxin has been used since there is a reduction in transport of the toxin to the cytosol. There are several factors that limit the efficiency of an IT in the treatment of cancer and these include insufficient tumour and

tissue penetration, non-specific toxicity, and immunogenicity. These will be discussed in greater detail in section 1.4.

1.2.1 Toxins used in the construction of immunotoxins

The toxins most commonly used to construct ITs are of bacterial or plant origin. They are cytotoxic by inhibiting protein synthesis. Such toxins are classified as either type I (hemitoxins) or type II (holotoxins) RIP toxins. Type II toxins contain both a binding domain and an enzymatically toxic domain which are typically linked by a disulphide bond. Such toxins include ricin, abrin, mistletoe lectin and modeccin. In contrast, type I toxins contain an enzymatic domain but no binding domain. These toxins are relatively non-toxic to mammalian cells in their native form because of their lack of binding capacity. Toxins that are classified in this group include saporin, PAP and gelonin.

1.2.1.1 Structures and functions of toxins

1.2.1.1.1 Ricin

Ricin is probably the most commonly used and investigated of all the toxins for the construction of ITs. Ricin is purified from the castor bean plant *Ricinus communis*. It is a 60kD glycoprotein, type II RIP that consists of two functional 30kD subunits. This heterodimer consists of an A and B chain that are connected by a disulphide bond as shown in figure 1.2(a) (Katzin *et al.*, 1991, Rutenber and Robertus 1991).

The B chain possesses the two functional binding domains of the toxin. These domains enable the toxin to bind to galactose-containing glycoproteins on the plasma membrane of eukaryotic cells (Randy *et al.*, 1988, 1991). There is evidence to suggest that the translocation function is closely associated with the binding site (Marsh J.W. & D.M. Neville, Jr. unpublished results). Site 1 (of the two galactose binding sites) is a low affinity site with the key residues Trp^{37}, Asp^{22}, Asn^{46} and Gln^{47}. Site 2 is a higher affinity domain and has the important residues Tyr^{248}, Asp^{234}, Gln^{256} and Asp^{255} within the binding site.

The catalytic, enzymatic region that causes the release of adenine 4324 from 28S rRNA of the large (60S) subunit of eukaryotic ribosomes resulting in protein synthesis inhibition is known to be located on the A chain. Residues Glu^{177} and Arg^{180} are located in the active site and are particularly important to the toxin's activity. This has been demonstrated by

the great reduction in enzymatic activity of the A-chain when either of these residues were mutated (Day *et al.,* 1996). Ricin A chain (RTA) can be isolated from the B chain using chemical and chromatographic techniques or may be generated by genetic recombination (Thorpe *et al.,* 1988, Piatak *et al.,* 1988, Ghetie *et al.,* 1991). These modifications to ricin are illustrated in figure 1.2(b). The RTA has also been shown to display some degree of translocating function (Esworthy & Neville, Jr 1984) although not as great as that possessed by the B chain.

Galactose-containing glycoproteins are extensively distributed in mammalian cells, hence making ricin highly toxic to many human cells, which is why native ricin is not an ideal choice of toxin to use as an IT. RTA chain was used alone in the production of ITs to try to overcome the non-selective toxicity displayed by ITs made using native ricin. Unfortunately ITs made with RTA are more specific, in terms of their toxicities, but are as much as 100-fold less active (Weil-Hillman *et al.,* 1985). Even with the absence of the B chain in the IT, non-specific toxicity on macrophages and hepatic non-parenchymal cells can still be observed (Fulton *et al.,* 1988a, Fulton *et al.,* 1988b). This is thought to be due to the glycosylated side residues binding to mannose receptors in the liver (Bourrie *et al.,* 1986).

Chemically blocking ricin's galactose binding sites with galactose, lactose or a glycopeptide (figure 1.2c) before using it in treatment has been another approach to counteract the non-selective binding of native ricin (Thorpe *et al.,* 1985, Lambert *et al.,* 1991). It has been observed that the presence of the B chain enhances the cytotoxic action of the enzymatic A chain even though the binding sites are blocked. This may be due to the contribution of the translocation function from the B chain.

Another alternative is to deglycosylate RTA chemically (as shown in figure 1.2biii). A longer half-life in mice, resulting in increased therapeutic index (Fulton *et al.,* 1988a, Fulton *et al.,* 1988b) is seen when deglycosylated RTA is incorporated into an IT. The deglycosylated RTA IT has a decreased entrapment by the liver (which is normally mediated by the carbohydrate residues on the A chain) and is cleared from the blood more slowly creating a greater opportunity for the IT to localise within the tumour target (Blakey *et al.,* 1987). The half-life of the IT can be further prolonged when the disulphide bond between the antibody (Ab) and the toxin is formed in a sterically hindered fashion

using derivatising agent 4-succinimidyloxycarbonyl-α-methyl-α(2-pyridyldithio) toluene (SMPT) thus protecting the bond from reduction (Thorpe *et al.*, 1987, Thorpe *et al.*, 1988).

Only RTA is needed to translocate into the cytosol. Using a fusion protein of single chain ricin is not a very viable option, as the ligand cannot separate from the A chain prior to translocation.

Resistance to ricin has been developed through mutation imparted by aberrantly high sialyltransferase activity. The toxin binds to terminal galactosyl residues of complex carbohydrates on the cell surface and elevated transferase activity blocks these binding sites through addition of neuraminic acid.

1.2.1.1.2 Saporin

Saporin is a single-chain non-glycosylated basic protein (figure 1.2d) with a molecular weight of 29.5 kD and an isoelectric point (pI) in the alkali range (≥9.5) (Stirpe *et al.*, 1983). It is a type I RIP or hemitoxin. Since it only consists of an enzymatic domain (Stirpe *et al.*, 1983) and has no binding domain of it's own, it is relatively non-toxic to mammalian cells. There are a number of isoforms of saporin and saporin 6 is the most abundant. Saporin 6 is purified from the seeds of *Saponaria officinalis* (Gasperi-Campani *et al.*, 1985, Stirpe *et al.*, 1983) in which it is contained in surprisingly high amounts (7% of the total seed protein). These seeds appear to be the richest source of a RIP (Stirpe *et al.*, 1983). It is one of the most active RIPs against isolated ribosomes or acellular systems.

Although saporin uses the same mechanism to inhibit protein synthesis as ricin great differences in their cytotoxicity *in vitro* and *in vivo* can be observed. An IT prepared with saporin and anti-Thy1.1 mAb OX7 produced a superior anti-tumour effect to an analogous IT made from RTA when administered to mice bearing allografts of Thy1.1 expressing AKR-A lymphoma cells (Thorpe *et al.*, 1985). This conjugate has been found to be 1000 times more efficacious *in vivo* than was first suggested by an *in vitro* cytotoxicity assay (Thorpe *et al.*, 1985, Blakey *et al.*, 1988). An *in vivo* experiment has suggested that saporin may have a more efficient way of entering the cytosol (Blakey *et al.*, 1988).

Saporin contains no O- or N-linked carbohydrates (Stirpe *et al.*, 1983) and is similar to PAP in this respect (Barbieri *et al.*, 1982). It has no carbohydrate residues and is not glycosylated (Stirpe *et al.*, 1983), and may use this to escape the carbohydrate recognition system of the liver. For this reason and the fact that saporin is resistant to proteolytic inactivation (Siena *et al.*, 1988), it is possible to understand why immunotoxins constructed with it have a relatively longer blood half-life when compared to ITs made with ricin. The greater stability seen with saporin may also contribute to its better anti-tumour efficacy as well as its greater non-specific toxicity seen in mice.

1.2.1.1.3 Pseudomonas exotoxin

PE is a 613 amino acid long single chain protein (figure 1.2e). This 66 kD single chain toxin (Gray *et al.*, 1984) is secreted by the bacterium *Pseudomonas aeruginosa* and has three functional domains necessary for cellular intoxication. The three-dimensional structure was determined by Allured *et al.*, (1986). The functions of each of the domains were determined by expressing the products of different portions of its gene in *E. coli* (Hwang *et al.*, 1987).

Domain Ia consists of amino acids 1 to 252 and is the binding domain of the toxin (demonstrated in *E.coli* by Hwang *et al.*, 1987). Domain II is contained within amino acids 253 to 364 and is responsible for translocating the toxin to the cytosol. It is a small domain containing six alpha helices. Between helix A and B there is a loop containing three arginine (Arg) residues, which lie on the surface of the molecule. Arg residues at positions 276 and 279 are thought to be required for cytotoxicity (Jinno *et al.*, 1989). A proteolytic site for furin cleavage located between amino acids 279 and 280 can be found within this domain (Chiron *et al.*, 1994; Ogata *et al.*, 1992). The function of domain Ib (amino acids 365-399) is unknown but deletion of this region appears not to affect the toxicity of PE (Siegall *et al.*, 1991). Domain III (amino acids 400 through to 613) contains the ADP-ribosylating enzyme, which inactivates elongation factor (EF-2) and also contains the C-terminal fragment, which directs the toxin to the endoplasmic reticulum (ER). Deletion mapping shows that amino acids 400-600 are essential for ADP-ribosylating activity (Siegall *et al.*, 1989).

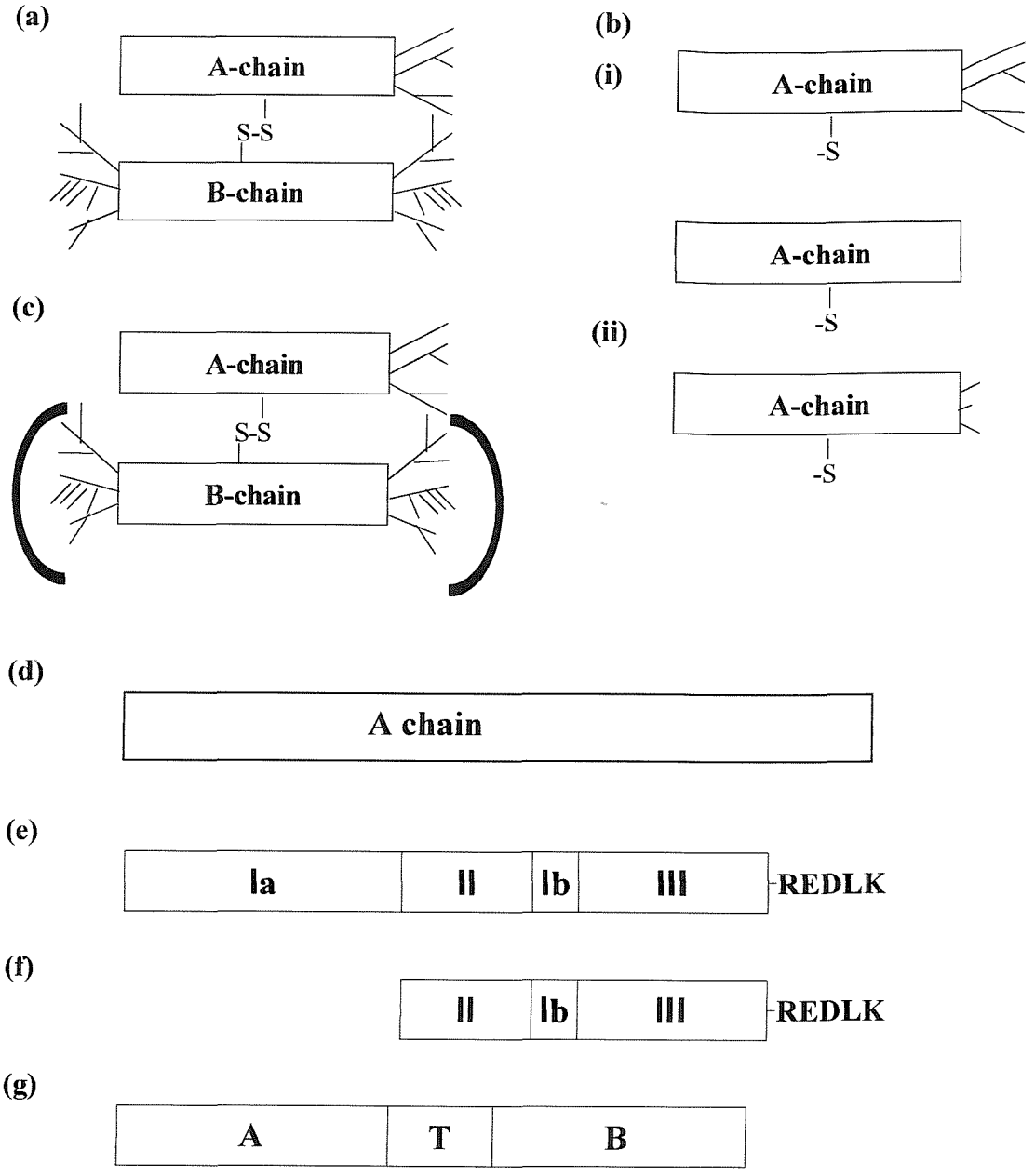

Figure 1.2 The structures of some of the toxins used to construct immunotoxins. **(a)** Whole ricin is composed of a catalytic A-chain disulphide bonded to the binding B-chain. Derivatives of the native toxin have been used to dramatically reduce the uptake by the liver. These include **(b)(i)** RTA (produced by reducing the whole ricin), **(ii)** rRA (made in E. coli and so does not possess glycosylated amino acids), **(iii)** chemically deglycosylated RTA (dgA). **(c)** One approach to prevent non-specific toxicity of whole ricin is to chemically treat or 'block' it (bR). **(d)** Saporin is a hemitoxin which only consists of the catalytic chain and is not glycosylated. **(e)** PE is 613 amino acids long and contains three functional domains as described in detail in section 1.2.2.3. Domain III contains the ADP-ribosylating domain which inactivates EF-2 resulting in cell death. **(f)** PE40 is a truncated form of PE devoid of domain Ia. **(g)** DT is 535 amino acids long and is composed of the enzymatic A domain, the binding B domain and the translocation or transmembrane T domain. (Illustration redrawn from Kreitman 1999.)

ITs (which can also be referred to as chimeric toxins when the ligand is not an Ab) produced by adding a receptor ligand (such as TGF-α, IL-2, and IL-4) at the carboxyl end of the recombinant form of the toxin, PE40 (figure 1.2f), displayed poor cytotoxic ability (Chaudhary *et al.,* 1990). This is possibly because the carboxyl terminus of domain III may have an additional role in the cytotoxic action of PE. Chaudhary *et al.,* (1990) have also demonstrated that mutations at the carboxyl end of PE, especially of the last 5 amino acids, results in molecules with full ADP-ribosylation activity but with greatly reduced cytotoxicity.

1.2.1.1.4 Diphtheria toxin

Diphtheria toxin (DT) is encoded and produced by lysogenic β-phage containing bacterium, *Corynebacterium diphtheria* (Greenfield *et al.,* 1983). It is a 58 kD single polypeptide chain consisting of 535 amino acids (figure 1.2g). Located at the N-terminus is the 21 kD A fragment and at the C-terminal end is the 37 kD B subunit. A tryptic-sensitive bond separates the two domains so that the toxin is functionally a two-chain structure. A single disulphide bond spans the tryptic-sensitive region. DT is a highly toxic molecule. The toxin is lethal for susceptible animals (including man) in doses as small as 100ng/kg or less.

The A fragment is the domain that inhibits protein synthesis by ADP-ribosylating EF-2 in an identical manner to that achieved by PE. The B fragment mediates binding to specific receptors at the cell surface (Pappenheimer 1977). The crystal structure of DT shows evidence for a third domain which is thought to be involved in the translocation/transmembrane (T) domain and is located in the centre of the molecule (Pappenheimer 1977).

DT inactivates elongation factor (EF-2) by ADP ribosylation at a diphthamide residue at His^{715} (explained in more detail later) using NAD^+ as a cofactor (Iglewski and Kabat 1975, Omura *et al.,* 1989). The key residue to NAD^+ binding was identified to be Glu^{148} (Carroll and Collier 1984) and corresponds to glutamic acid at position 553 on PE (Carroll and Collier 1987). This residue is probably only a few angstroms away from the catalytic site.

DT binds to the cell surface via the carboxyl end of the B fragment. This function may be abolished or greatly diminished by deletion of 15 kD or 6 kD fragment from the C terminus (Pappenheimer 1977) by point mutations at positions 390 and 525 (Greenfield *et al.,* 1987), or by chemical cleavage and release of the C-terminal residues (Myers *et al.,* 1988). Amino acids 220 to 373 at the N-terminal end of the B fragment are mainly hydrophobic residues, hence this region is thought to be involved in the translocation of the enzymatic domain of DT, possibly by forming a pore which enables the A fragment to pass through to the cytosol. Trp^{153} is one of only two Trp residues in the A fragment and is considered to be important for ADP-ribosylation because chemical modification of this residue sees a block in enzymic activity (Michel *et al.,* 1977).

Although PE and DT act in a similar fashion they differ greatly in amino acid sequence. The enzymatic domain is near the C-terminus in PE but near the N-terminus in DT. The opposite is true for the binding site.

1.2.2 Protein toxin entry, routing and translocation within the cell

The first necessary step in ricin intoxication is cell surface binding. Ricin binds to a large number of different surface molecules as it binds to both glycoproteins and glycolipids with terminal galactose. It has been seen to bind all over the cell surface by electron microscopy (EM) using either ricin-gold conjugates or ricin bound to the enzyme horse-radish peroxidase (HRP) (van Deurs *et al.,* 1989, Sandvig *et al.,* 1991).

The second step of ricin intoxication involves internalisation from the cell surface to intracellular compartments. Ricin has been demonstrated to be taken up by clathrin-dependent and independent mechanisms (van Deurs *et al.,* 1989, Sandvig *et al.,* 1991, Hansen *et al.,* 1991). Clathrin-dependent uptake was demonstrated by morphological studies in which the ricin-gold conjugate was located in clathrin-coated pits. Clathrin coated pits are interfered with and paralysed when the cytosol is acidified to below pH 6.5 (Sandvig *et al.,* 1991, Sandvig *et al.,* 1987). Under these acidic conditions or in cells overexpressing mutant dynamin (which is unable to cause budding of clathrin coated vesicles), ricin was still internalising between 40-80% of control values and was still able to intoxicate cells (Sandvig *et al.,* 1991, Moya *et al.,* 1985). This indicates that ricin is also internalised via a clathrin-independent mechanism.

There is evidence to suggest that the clathrin-independent mechanism may comprise of more than one process as it gives rise to large vesicles in some systems (Haigler *et al.*, 1979), but in HEp-2 cells the pre-endosomal vesicles formed by this mechanism had a diameter of 95 nm which is smaller than the clathrin coated vesicles in these cells (Hansen *et al.*, 1991). It has now become obvious that clathrin-independent endocytosis can be different from uptake by caveolae and macropinocytosis (Sandvig and van Deurs 1999). Clathrin-independent endocytosis of ricin occurs even when uptake from caveolae and clathrin-dependent are inhibited by extraction of membrane cholesterol or by nystatin treatment (a cholesterol binding drug), which leads to the disappearance of caveolae and inhibits formation of invaginated clathrin-coated pits, indicating that there must be an alternative clathrin-independent mechanism.

After endocytosis, the internalised membrane and its contents are delivered to endosomes in which sorting for further routing in the cell takes place. From here, ricin may be recycled back to the plasma membrane, enter lysosomes where it is degraded or accumulates in the *trans*-Golgi network (TGN) (as is the case for approximately 5% of endocytosed ricin). The presence of ricin in the TGN was determined by tyrosine sulphation of the A chain which could only occur in the Golgi apparatus (Rapak *et al.*, 1997) or by EM to visualise a ricin-HRP conjugate in this intracellular compartment (Sandvig and van Deurs 1996).

The next step in the intracellular routing of ricin involves the post-Golgi sorting of ricin to a translocation-competent compartment. Brefeldin A is capable of blocking ricin toxicity in sensitive cells without interfering with the transport of the toxin to the TGN, suggesting that a distal compartment is critical for intoxication by ricin (Yoshida *et al.*, 1991). Membrane flow from the Golgi back to the ER allows retrieval of resident ER lumenal proteins via a receptor recognising a carboxy terminal tetrapeptide present in ER lumen proteins, KDEL, in mammalian cells. Although ricin does not have this sequence there is a proposed requirement of intracellular ricin B chain (RTB) binding activity. It is proposed that the RTB will bind to a galactose on a recycling glycoprotein, which must have travelled the anterograde secretory route at least as far as the TGN, where galactosyl transferase is located, to transport ricin back in to the ER. Calreticulin, a molecular chaperone, contains a terminally galactosylated oligosaccharide (determined by metabolic labelling with [^{3}H] galactose) which is mainly retained in the ER was shown to interact

with the holotoxin in such a way (Day *et al.*, 2001). Studies have also shown that addition of the KDEL sequence increases the toxicity of ricin (Wales *et al.*, 1992; Wales *et al.*, 1993). The use of transdominant mutants of GTPases involved in vesicular traffic followed by incubation with ricin showed a decrease in ricin toxicity when modified GTPases which regulate ER-Golgi traffic (Rab1, ARF1, and Sar1) were used but no change to intoxiciation when endosome-related GTPases (dynamin element 1, Rab5 and Rab9) were mutated (Simpson *et al.*, 1995). This indicates that retrograde transport of toxins occurs via the active recycling of toxin-specific receptors between the ER and the terminal compartments of the Golgi stack and that ricin must reach the ER to produce cell toxicity.

The penultimate step in intoxication is membrane translocation. It is currently believed that ricin uses the ER associated degradation (ERAD) pathway (used by misfolded proteins) to enter the cytosol via the Sec61p translocon (Simpson *et al.*, 1999; Wesche *et al.*, 1999). This hypothesis is supported by such evidence as using the proteasome inhibitor, lactacystin, which sensitises cells to ricin and increases cytosolic RTA, and the precipitation of sulphated and deglycosylated RTA with anti sec61α (Wesche *et al.*, 1999). First, the cleavage of the interchain disulphide bond linking the A and B chain is essential for cytotoxicity (Sandvig *et al.*, 1976) and is thought to occur in the ER lumen. This process leads to the unfolding of the A chain and the exposure of a hydrophobic stretch (at the C-terminus) which might be required for transport to the cytosol (Lord and Roberts 1998) by triggering interactions with membranes, chaperones or Sec61p translocons directly. A mutation within this sequence has been shown to inhibit translocation without reducing the catalytic activity of the toxin (Lord and Roberts 1998). The RTA may be perceived as an ERAD substrate although it is not known how. Once translocated into the cytosol the A chain must rapidly regain its native conformation to make it resistant to proteolytic degradation. Only a small proportion of the ricin translocated manages to avoid degradation by the proteasome. Once in the cytosol, ricin is able to inactivate ribosomes and inhibit protein synthesis.

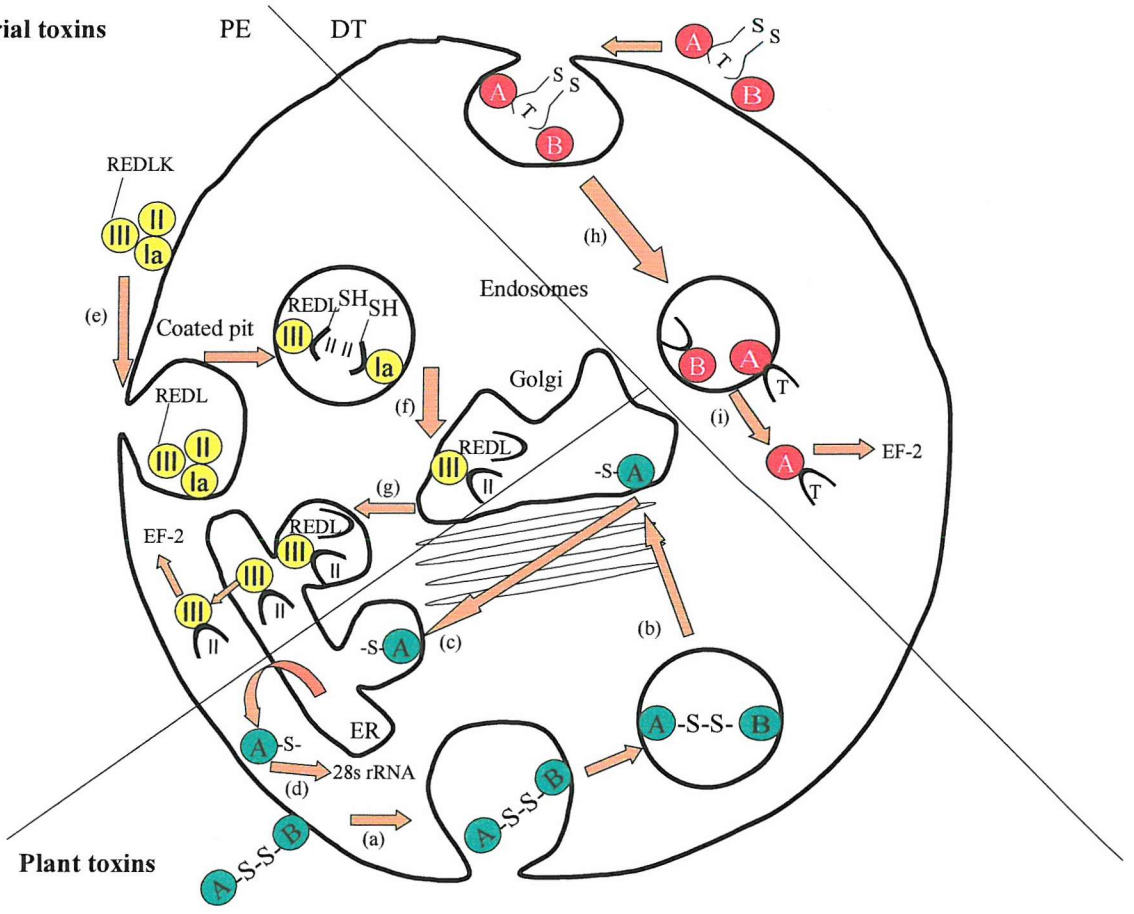

Figure 1.3 Protein toxin entry, routing and translocation within the cell. The modes of toxin entry and routing for plant toxins like ricin (bottom left) and the bacterial toxins PE and DT (top left and right respectively). Most plant toxins are internalised (a) and thought to travel through the Golgi apparatus (b) before translocating to the cytosol via the ER (c). Once in the cytosol they inhibit protein synthesis by preventing the interaction between elongation factor-1 and –2 (EF-1 and EF-2) with the 60S ribosomal subunit (described in section 1.2.4.2). PE is actively taken up by the cell and undergoes both removal of the carboxy-terminal lysine residue (e) and processing between residues 279 and 280 (f), resulting in a 37 kD C-terminal toxin fragment ending in the residues REDL. These residues bind to the KDEL receptor which is believed to transport this active fragment from the Golgi to the ER (g), from where it is thought to translocate to the cytosol. Once internalised, DT undergoes processing between residues 193 and 194 (h). The catalytic A chain then translocates to the cytosol (i) through the endosome with the help of the translocation (T) domain which is thought to form an ion channel. PE and DT inhibit protein synthesis by ADP-ribosylating EF-2. (Illustration redrawn from Kreitman 1999.)

Brefeldin A (BFA) blocks anterograde vesicular flow from the ER to the Golgi but does not affect retrograde membrane traffic from the Golgi to the ER. The Golgi stacks disappear and are absorbed into the ER (Pelham *et al.*, 1991). BFA blocks intoxication of cells by ricin and PE (Yoshida *et al.*, 1991), but offers no protection of Vero cells from DT. This enhances the proposal that DT enters the cytosol from endosomes whereas ricin and PE need to enter or pass through Golgi stacks before translocation can occur.

PE binds to α2-macroglobulin receptors on the surface of cells via its binding site in domain Ia. It internalises in clathrin-coated pits into endocytic vesicles and maybe other endosomal compartments to the transreticular Golgi (Kounnas *et al.*, 1992). A cleavage occurs while the toxin is in the endosome in the arginine rich loop. This results in the breaking of a peptide bond between Arg^{279}-Gly^{280}. Any changes to Arg^{276} and Arg^{279} creates a dramatic reduction in cytotoxicity (M.Ogata V.K.C., I.P., + D.F., unpublished results). Two fragments are generated by the proteolysis and they are only held together at this point by a disulphide bond between Cys^{265} and Cys^{287}. Reduction of this bond generates the 37 kD C-terminal fragment, which comprises the active toxin. The location where the reduction takes place is unknown. Translocation to the cytosol can only take place once this active fragment has been produced (Ogata 1990).

All this evidence shows the importance of the ER retention signal to the intoxication process of PE and indicates the ER as part of this process. However, unlike ricin, internalised PE has not been observed in the Golgi apparatus or the ER and has only been visualised in endosomes (Morris *et al.*, 1983; Jinno *et al.*, 1989). There is now evidence to suggest that PE can translocate from recycling endosomes in an ATP-driven process (Taupiac *et al.*, 1996; Alami *et al.*, 1997), at least in some cell types such as lymphocytes. Exposure to acidic pH is considered to be a prerequisite for translocation (Taupiac *et al.*, 1996; Alami *et al.*, 1997). Wherever PE translocates from, amino acids 280 to 313 are thought to be responsible for mediating the translocation event (Theuer *et al.*, 1994, Theuer *et al.*, 1993) into the cytosol where the ADP-ribosylating enzyme within amino acids 400-602 inactivate EF-2 (Carroll & Collier 1987).

DT like PE seems to use a clathrin dependent endocytic mechanism (Morris *et al.,* 1985, Morris *et al.,* 1983). DT is proteolytically cleaved outside the cell between Arg^{193} and Ser^{194} (Pappenheimer 1977) which are located within a disulphide loop formed by Cys 186 and 201. Once this has occurred DT is able to bind to a complex of heparin-binding epidermal growth factor (EGF)-like growth factor precursor and CD9 on the cell surface (Pappenheimer 1977). DT can be found concentrated in coated pits and is internalised by endocytosis.

The pH of the interior of endocytic vesicles and lysosomes is pH 5.5 which is approximately 2 pH units less than the extracellular fluid (Tycko and Maxfield 1982). In the acidic environment of the endosome (and possibly any other acidic endocytic compartment it may locate in), DT unfolds and the hydrophobic regions of the B fragments become exposed (Sandvig *et al.,* 1981, Kagan *et al.,* 1981, Blewitt *et al.,* 1985, Montecucco *et al.,* 1985). TM8 (amino acids 326-347) and TM9 (amino acids 358-376) domains form a hairpin which inserts into the membrane of the endosome and forms a channel through which the enzymatic A fragment in extended form translocates to the cytosol (vanderSpek *et al.,* 1994). This means the hydrophilic residues of the A fragment are shielded from contact with the hydrocarbon tails of the lipids (Kagan *et al.,* 1981, Hoch *et al.,* 1985). DT appears to translocate from early endosomes (Lemichez *et al.,* 1997). Stenmark *et al.,* (1988) demonstrated that binding of DT to specific receptors is a requirement for translocation into the cytosol.

1.2.3 Toxin mechanisms of action

There are two main mechanisms of cytotoxicity employed by the toxins discussed, both of which involve the inhibition of protein synthesis. The plant toxins share a common mechanism and the bacterial toxins share another. Bacterial toxins act by modifying elongation factor 2 and plant toxins target a site on the 60S ribosomal subunit.

1.2.3.1 ADP-ribosylation of EF-2 by bacterial toxins

During unmodified protein synthesis EF-2 forms binary complexes with GTP and GDP (Mizumoto *et al.,* 1974, Henriksen *et al.,* 1975). The factor will associate with pre-translocation ribosomes if it is in the presence of GTP (Nygärd & Nilsson 1984), which facilitates the translocation of the peptidyl tRNA from the ribosomal A site to the P site (Skogerson & Noldave 1967, Tanaka *et al.,* 1977). This reaction is coupled to a factor-

and ribosome-dependent hydrolysis of GTP, and results in the formation of an EF-2·GDP·ribosome complex with the release of inorganic phosphate (Mizumoto *et al.*, 1974, Montanaro *et al.*, 1971, Baliga & Munro 1972, McKeehan 1972, Chuang & Weissbach 1972).

When the toxin is present within the cytosol it binds nicotinamide adenine dinucleotide (NAD) within its active site cleft. This site is located around the glutamic acid residue at 553 on PE (Carroll and Collier 1987) and the glutamic acid residue at 148 on DT (Carroll and Collier 1984). NAD is an essential cofactor for the toxin catalysed reaction. Once bound to the toxin, NAD is hydrolysed and an ADP-ribosyl moiety from it is transferred to EF-2 in the following reaction:

$$NAD^+ + \text{EF-2} \xrightarrow{\text{PE/DT}} \text{ADP-ribose-EF-2} + \text{nicotinamide} + H^+$$

(Honjo *et al.*, 1968, Honjo *et al.*, 1971)

The ADP-ribosylation site is thought to be at a histidine residue located at position 715 which has been post-translationally modified to a diphthamide residue also known as 2-[3-carboxyamido-3- (trimethylammonio)propyl]histidine (Omura *et al.*, 1989, Ness *et al.*, 1980) (figure 1.4). ADP-ribosylation does not occur unless the biosynthesis of diphthamide has occurred. This is demonstrated by amino acid substitutions at positions 584 (serine to glycine), 714 (isoleucine to asparagine) and 719 (glycine to aspartic acid), which prevent the production of diphthamide and hence the ADP-ribosylation (Foley *et al.*, 1995).

Figure 1.4. Proposed structure of diphthamide (Ness *et al.*, 1980)

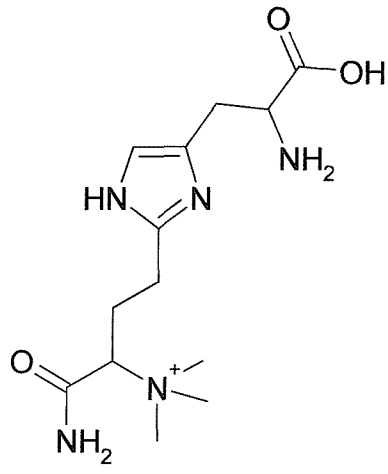

ADP-ribosylation of EF-2 is characterised by a loss of its non-specific affinity for high molecular mass RNA and its dissociation from the complexes with mono- and polyribosomes (Sitikov *et al.*, 1984). The ADP-ribosylated factor is still able to bind with GTP (Montanaro *et al.*, 1971, Chuang and Weissbach 1972) and form an EF-2·GTP·ribosome complex (Chuang and Weissbach 1972, Kloppstech *et al.*, 1969), but it is approximately 40-50% less active in pretranslocation complex formation than the native factor (Nygärd and Nilsson 1985). The ribosylated factor still possesses GTPase activity in such a complex (Kloppstech *et al.*, 1969) and so is capable of participating in one round of the elongation cycle (Carrel *et al.*, 1991). Therefore, in summary, inhibition of the translocation process caused by DT or PE is due to the reduced affinity of ADP-ribosylated EF-2 for pretranslocation ribosomes and the site of ADP-ribosylation on the factor is within the functional domain responsible for the pretranslocation attachment (Nygärd and Nilsson 1985).

The interaction between toxin, NAD and EF-2 is a highly specific one. This is demonstrated by studies showing that nothing other than EF-2 is ADP-ribosylated in the presence of NAD^+ and toxin, not even the prokaryotic equivalent EF-G in bacteria, nor the mitochondrial elongation factor G (Richter & Lipmann 1970). The interaction with NAD is also very specific since it cannot be replaced by any of its analogues such as αNAD^+, $NADP^+$, or NADH (Pappenheimer 1977). Although DT and PE are immunologically distinct and differ in proteolytic susceptibility (Iglewski and Kabat 1975), they are both believed to catalyse this reaction. They are thought to produce modifications at the same site on EF-2, since the modifications created are non-additive.

It has been shown that after 90 minutes of incubation with DT at 37°C there is an exponential reduction in the uptake of amino acids (Pappenheimer 1977). It has been reported that approximately 4000 molecules of DT can bind specifically to the surface of one cell (Boquet and Pappenheimer 1976), although only a small proportion of these may actually reach the cytoplasm. This is not too much of a hindrance to its cytotoxicity as a single molecule of fragment A of DT is sufficient to kill a cell (Yamaizumi *et al.*, 1978).

1.2.3.2 Inactivation of the 60S ribosomal subunit by plant toxins

Endo *et al.*, demonstrated that type I and the active A chains of type II RIPs possess a unique RNA N-glycosidase activity. They selectively cleave the N-glycosidic bond of adenine^{4324} of the 28S eukaryotic mammalian rRNA in a hydrolytic fashion (Endo *et al.*, 1987ab, Stirpe *et al.*, 1988, Zamboni *et al.*, 1989). All the adenine residues that may be cleaved by ricin and saporin are located in a loop and stem sequence of rRNA which has a GAGA sequence in the loop. This may be the recognition structure used by the toxins (Endo *et al.*, 1991).

The adenine cleaved by these toxins is adjacent to the site of cleavage of rRNA by a group of highly specific RNases from fungi: α-sarcin from the mould *Aspergillus giganteus* (Endo *et al.*, 1982), restrictocin and mitogillin from *Aspergillus restrictus* (Lopez-Otin *et al.*, 1984, Fando *et al.*, 1985) that cleave the phosphodiester bond between G^{4325} and A^{4326} on rat liver RNA (Endo *et al.*, 1982). The toxin does not break the RNA chain, but the depurination of the RNA makes it susceptible to hydrolysis at alkaline pH, and at acidic pH in the presence of anilin (Olsnes and Kozlov 2001).

The modification of the 60S subunit affects the site(s) on the ribosome that is involved in the specific interaction with EF1·GTP and EF2·GTP, which are required for aminoacyl tRNA binding and peptidyl-tRNA translocation respectively. Inactivation occurs by inhibition of the EF-1 hydrolysis of GTP and blocking of the EF-2-dependent interaction of GDP, GTP or GTP analogues with the ribosome (Benson *et al.*, 1975, Gasperi-Campani *et al.*, 1978, Gessner *et al.*, 1980). This results in loss of EF-1 dependent binding of aminoacyl-tRNA and EF-2 dependent translocation and an eventual arrest of protein synthesis

No cofactor is required for the catalytic inactivation of sensitive ribosomes and a single molecule of RTA can inactivate 1500 ribosomes per minute (Olsnes *et al.*, 1975). A single A-chain can inactivate ribosomes faster than the cell can make new ones and therefore in theory it can take as little as one molecule of ricin to kill a cell (Eiklid *et al.*, 1980). Type II RIPs have been found to be as much as 10^6-fold more potent than the type I RIPs in their ability to inactivate ribosomes by cells in culture. These differences in potency are thought to be due to lack of a B chain containing the ability to bind to and

mediate the penetration of the catalytic enzymatic subunit I to the cell. Ippoliti *et al.*, (1992) have demonstrated that saporin-6 interacts with at least one ribosomal protein of the 60S ribosomal subunit of yeast ribosomes (28S rRNA).

1.3 Target Antigens on Leukaemia Cells

Leukaemia cells express a wide variety of well-characterised antigens on their cell surface, which can act as potential targets for immunotoxin therapy. Antigen characteristics are arguably the most important determinant for success of this kind of treatment. The ideal target antigen would be one which is expressed solely on tumour cells and not on the normal cellular counterpart, but none are totally leukaemia or tumour specific. The next best situation would be for there to be high expression levels of the target molecule on tumour cells with low expression on the healthy cells. If this was not possible, and the antigen was not expressed by life sustaining tissue (e.g. heart, liver, brain), or on a stem cell population and the cells could be regenerated from another cell unaffected by the immunotoxin therapy, then higher expression levels of the molecule could very well be tolerated on non-target cells. The consequence of this would be a transient complete or partial ablation of the normal cellular counterpart. A disadvantage to this may be that the antigens on the normal cells may compete for Ab binding of the immunotoxin and therefore decrease the amount of drug delivered to the tumour cell population.

There are several requirements to look for when choosing an antigen target. Firstly, the molecule should be homogeneously expressed amongst the tumour cell population in order to eradicate all the cancerous cells and reduce the possibility of tumour regrowth. This may not be totally necessary, as it could be possible to use cocktails of immunotoxins to be sure of targeting the whole tumourous population (Flavell *et al.*, 1992). Secondly the antigen needs to be expressed on the cell surface, as the immunotoxins cannot gain access to and bind to intracellular antigens (Frankel *et al.*, 1986). The modulation characteristics of the cell surface molecule are important because typically it has been found that antigens that readily endocytose make exceedingly effective immunotoxin targets (Trowbridge *et al.*, 1981, van Horssen *et al.*, 1995, Preijers *et al.*, 1988). This is not always the case though as preferential routing to the ribosomes as opposed to the lysosomes is also required (FitzGerald & Pastan 1989, Stevenson 1993, May *et al.*, 1991). An intact Ab to an antigen that does not internalise but has an exposed Fc fragment can trigger complement or antibody-dependent cell-mediated cytotoxicity (ADCC) (Ritz *et al.*,

1987). Another consideration is that a shed antigen interferes with the binding of an Ab to its intended target (Press *et al.*, 1994).

Antigens that have proved to be useful tumour targets include tumour-specific transplantation antigen (TSTA), virus-specified antigens and a number of differentiation antigens (Stevenson 1993). Cluster of differentiation (CD) molecules are defined as any group of antigens restricted to a limited number of cell lineages and to certain stages of cell differentiation. CD codes are only assigned to antigens that have three or more monoclonal antibodies from independent laboratories that recognise them. They are the type of antigen most commonly targeted with immunotoxins. Many CD antigens are particularly good for selectively targeting cells because they are specific to few cells and certain stages of that cells development and so therefore reduces non-specific toxicity.

Receptors for growth factors are another potential target molecule. If these molecules are selected with antibodies, growth inhibition may be produced. For example, epidermal growth factor and IL-2 receptors are both overexpressed in some cancers (FitzGerald and Pastan 1989) which makes them good targets for immunotoxin therapy as their continued functional expression is needed for those cells to keep on proliferating.

1.3.1 CD7

1.3.1.1 Tissue distribution

CD7 is the earliest marker antigen expressed in the T lineage, being found on T cell precursors in the foetal liver and thorax prior to thymic colonisation, and in thymus and bone marrow (Haynes *et al.*, 1989). CD7 is lineage-restricted. It is expressed on haemopoietic stem cells, most human thymocytes and a major subset of peripheral blood T cells (Haynes *et al.*, 1989). CD7 is a T-cell differentiation antigen and is the earliest antigen to appear during T-cell ontogeny (Lobach *et al.*, 1985). CD7 is also found on 80-85% of circulating T cells, thymocytes, and natural killer (NK) cells (Haynes *et al.*, 1979, Haynes *et al.*, 1980). CD7 expression on NK cells has been found to be highest on freshly isolated cells. This level of CD7 expression appears to decrease with IL-2 activation (Rabinowich *et al.*, 1994). The CD7 antigen is a common marker on many immature T-cell malignancies including T-cell ALL (where it is the most prevalently expressed antigen) and T-cell lymphoblastic lymphoma (Haynes *et al.*, 1989). For this reason it makes an excellent marker to target immunotherapies against immature T-cell

malignancies. Anti-CD7 monoclonal antibodies are currently being investigated for novel therapies for T-cell ALL (Pauza *et al.*, 1997). In contrast to the CD7 expression on T-cell ALL, most mature T-cell malignancies are $CD7^-$ (Haynes *et al.*, 1981, Haynes *et al.*, 1983, Broder *et al.*, 1980).

1.3.1.2 CD7 Structure

CD7 is a 40 kD glycoprotein, which has an N-terminus with significant sequence homology with the variable region of immunoglobulin (Ig) κ-chains and T cell receptor TCRγ chains. This single Ig-like domain classifies CD7 as a member of the Ig gene superfamily and is separated from the transmembrane sequence by four tandem repeats of a consensus sequence Xaa-Pro-Pro-Xaa-Ala-Ser-Ala-Leu-Pro forming a stalk or Ig-hinge like region adjacent to the plasma membrane (Aruffo *et al.*, 1987) (figure 1.5). There are also two N-linked glycosylation sites (Asn-X-Ser/Thr) in this region of the extracellular domain. The fact that there is a high degree of sequence conservation in the N-terminus of the CD7 molecule suggests that it folds into a tertiary structure comprised of a β-barrel with anti-parallel strands (Aruffo *et al.*, 1987). At the C-terminal end of the Ig-like barrel there are 48 additional amino acids including Cys-10 and Cys-117 which are predicted to form a disulphide bridge causing amino acids 107-117 to fold back under the Ig-like barrel. This structure is thought to sit back onto the stalk or Ig-hinge-like region of the molecule to form an extended structure like that proposed for the CD8 hinge (Aruffo *et al.*, 1987, Ware *et al.*, 1989). The hydrophobic transmembrane sequence of CD7 only traverses the plasma membrane once and the molecule is terminated with a short cytoplasmic tail. A putative ligand binding site has been found. This site is thought to be at the N-terminal end of the Ig-like barrel where the amino acids located at 32-36, 46-49, and 89-96 correspond to the Ig-κ-CDR or hypervariable regions. Human K12 has been discovered to be a binding partner for CD7 (Lyman *et al.*, 2000). It is thought that it plays a costimulatory role in T cell activation (Leta *et al.*, 1995).

1.3.1.3 CD7 Function

When cross-linked by antibodies CD7 has been shown to participate in many signalling pathways either by itself or in conjunction with complexed proteins. One example of this was discovered by Ledbetter and colleagues (Ledbetter *et al.*, 1987) who found that cross-linking of CD7 in TCRαβ T cells induced rapid mobilisation of cytoplasmic calcium.

This rise in intracellular calcium levels was linked with T-cell activation and induction of cytokine mRNA (Carrel *et al.*, 1991). The rapid rise in intracellular calcium can also lead to induction of integrin-mediated adhesion to fibronectin, ICAM-1, and VCAM-1 (Carrera *et al.*, 1988, Ledbetter *et al.*, 1987, Shimizu *et al.*, 1992).

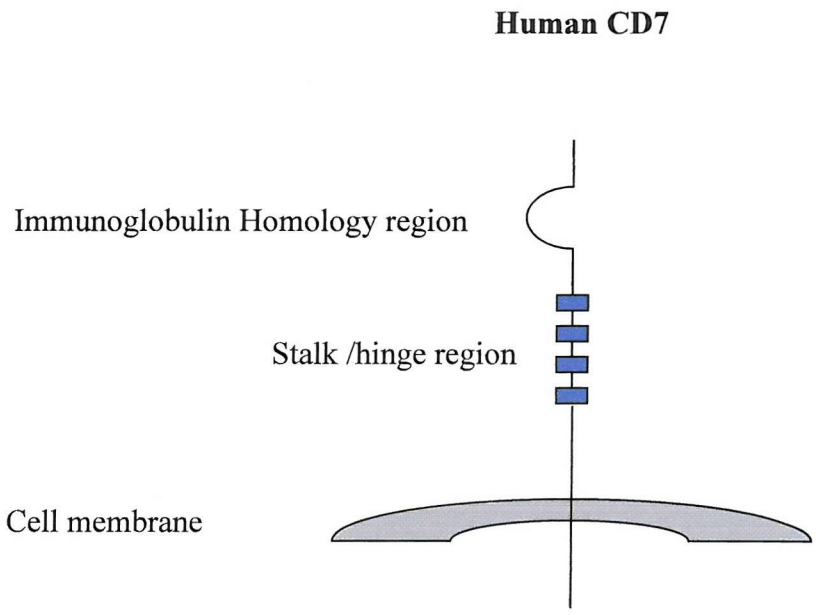

Figure 1.5. Schematic representation of human CD7 molecule (redrawn from Sempowski *et al.*, 1999).

Recent studies suggest that CD7 is involved in T and NK cell activation via both tyrosine kinase dependent and independent pathways. There have also been several studies which have detected the presence of proteins with newly phosphorylated tyrosine residues discovered in both T and NK cells after the interaction of human CD7 (hCD7) with an anti-CD7 mAb (Rabinowich *et al.*, 1994, Lazarovits *et al.*, 1994, Chan *et al.*, 1994). Lavarovits and colleagues (1994) have demonstrated the association between hCD7 and a tyrosine kinase whose major substrate is CD45 (Lazarovits *et al.*, 1994). Immunoprecipitation studies by the same group have provided evidence that CD3 and CD45 are associated with CD7 and that hCD7 may exist as a homodimer. Thus, it was seen to be possible that hCD7 may form an oligomeric complex in the plasma membrane with the protein phosphatase CD45, the TCR/CD3 complex, and a tyrosine kinase (Lazarovits *et al.*, 1994).

Triggering CD7 on T cells may play a role in the signal transduction that induces an upregulation of IL-2 and IL-2Rα, resulting in T cell proliferation (Jung *et al.*, 1992). Jung *et al.*, (1986) has also suggested that CD7 has a possible function in regulating T cell differentiation. It also leads to the induction of TNF-α, TNF-β and granulocyte-macrophage colony-stimulating factor (GM-CSF) production (Carrel *et al.*, 1991).

Cross-linking of CD7 using mAb on NK cells stimulates increases in free cytoplasmic calcium, secretion of IFN-γ, NK cell proliferation, adhesion to fibronectin, and NK cytotoxic activity (Carrel *et al.*, 1991).

1.3.1.4 CD7 as a target antigen

There has been much interest in using CD7 as a target antigen for immunotoxin therapy over the past decade for the reasons discussed above. Such studies have yielded promising results. CD7 was first targeted using Ab 3A1 conjugated to PAP, and was reported to eliminate 99.96% of leukaemic cells from normal bone marrow with only slight toxicity to stem cells (Ramakrishnan *et al.*, 1985). DA7 IT, which consists of the anti-CD7 MAb 3A1E and deglycosylated RTA (dgA), has had its antitumour activity tested against established T-ALL lines and fresh patient cells in sever combined immunodeficient (SCID) mice. This immunotoxin has also undergone a Phase I clinical trial (Frankel *et al.*, 1997, Vallera *et al.*, 1996, Jansen *et al.*, 1992). In the phase I trials there were two partial responses and one minimal response seen. Patients with minimal lymphoma burden or T-cell large granular lymphocyte (LGL) leukaemia were shown to be the most responsive. Although human anti-mouse antibodies (HAMA) were observed in these patients the concentrations detected were minimal (<55ng/ml) and human anti-ricin Ab levels were only elevated (190ng/ml) in one of the patients. Unfortunately vascular leak syndrome (VLS) presented with hypoalbuminaemia, dyspnoea, pulmonary oedema, aphasia, and peripheral oedema but this cleared over a two week period. The anti-CD7 IT HB2-Saporin developed in this laboratory has shown selective cytotoxic activity against HSB-2 (T-ALL) cells in SCID mice (Morland *et al.*, 1994).

1.3.2 CD38

1.3.2.1 Tissue distribution

The tissue distribution of CD38 appears to be dependent on the differentiation and activation state of the cell, for example, resting B and T cells are $CD38^-$ but activated B and T cells are positive for the antigen. CD38 is found on early cells of the T and B cell lineages but not on most mature resting peripheral lymphocytes. It is present on thymocytes, pre-B cells, germinal centre B cells, mitogen-activated T-cells, and Ig-secreting plasma cells (Jackson and Bell 1990). The majority of medullary thymocytes, germinal centre lymphoblasts, and plasma cells also express CD38 along with some follicular cells in the lymph nodes, and activated lymphoid and myeloid cells (Malavasi *et al.*, 1984, Santos-Argumedo *et al.*, 1993). It is expressed on approximately 80% of resting NK cells and monocytes. The distribution of CD38 in tumour leukocyte expansions and continuous lines of both myeloid and lymphoid origin make it a good potential target for immunotoxin therapy. Evidence that suggests leukaemias that immortalise early differentiation stages maintain CD38 expression is also encouraging in this respect, but it appears that more differentiated leukaemias are $CD38^-$ (with exceptions such as myeloma) (Malavasi *et al.*, 1984). Approximately 50% of B-lineage leukaemias express CD38 but a significant proportion of normal bone marrow cells are also $CD38^+$, particularly precursor cells (Malavasi *et al.*, 1984).

1.3.2.2 CD38 Structure

CD38 is a monomorphic single chain glycoprotein of molecular weight 45kD (Malavasi *et al.*, 1992, Cotner *et al.*, 1981, Terhorst *et al.*, 1981). It is a type II integral membrane protein (figure 1.6) with a short N-terminal cytoplasmic tail, long extracellular C-terminal domain and single membrane-spanning region (Jackson and Bell 1990). It has four N-linked oligosaccharide chains and is resistant to trypsin digestion but susceptible to V8 Staphylococcus aureus protease (Barclay 1993).

The gene encoding the human CD38 antigen has been cloned from T-cell lines and normal lymphocytes (Jackson and Bell 1990) and is located on chromosome 4 (Katz *et al.*, 1983).

There is data to indicate that there may be a naturally occurring soluble, high molecular weight form of the antigen (Funaro *et al.*, 1995, Umar *et al.*, 1996). The soluble form can be found in cell culture supernatants of alloactivated T lymphocytes, and $CD38^+$ tumour

lines. It can also be detected in amniotic fluids and in serum and ascites of myeloma patients. The soluble form is approximately 39 kD in size compared to the 45 kD of the transmembrane form of the antigen and is spontaneously released from the cell membrane (Funaro *et al.*, 1996). The difference in molecular weight is due to the lack of 21 cytoplasmic amino acids and the 23 transmembrane residues (Jackson and Bell 1990). The high molecular weight form of CD38 was discovered in HL-60, a myeloid cell line, after induction with *all-trans* retinoic acid (ATRA) (Umar *et al.*, 1996).

Figure 1.6. Schematic representation of CD38 (based on a diagram from the Leucocyte Antigen Facts Book).

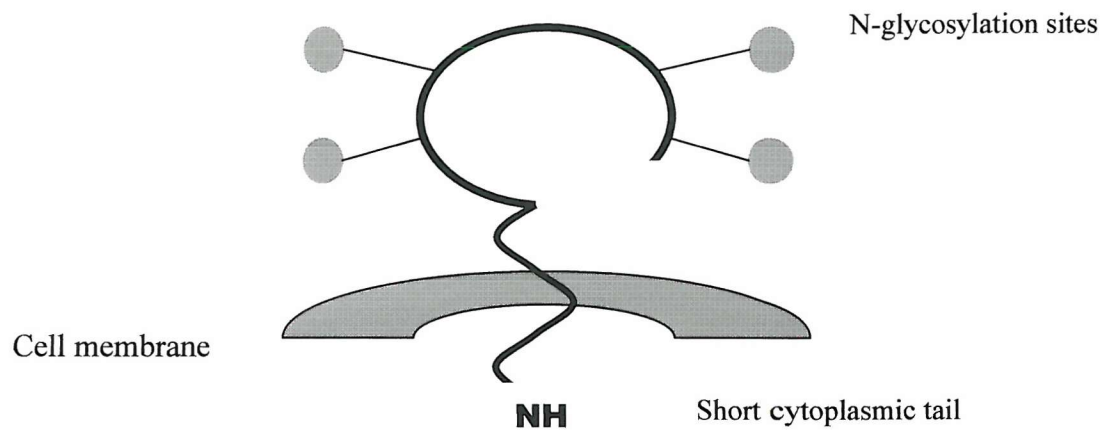

1.3.2.3 CD38 Function

CD38 is a very versatile molecule with many functional roles. Its functions include the supression of lymphopoiesis (Kumagai *et al.*, 1995), the rescue of human germinal centre B cells from apoptosis (Zupo 1994), mediating adhesion of lymphocytes to endothelium and cytokine production (Mehta *et al.*, 1996, Ausiello 1996) after activation of CD38.

CD38 may play an important role in signal transduction and CD38 cross-linking has been found to cause activation and proliferation of T cells, thymocytes and NK cells in the presence of IL-2 and/or accessory cells (Funaro *et al.*, 1990). The proliferation induced by CD38 is much less than that produced when the T cell receptor /CD3 complex is stimulated. CD38 can also function synergistically with CD3 and CD2 to induce activation and proliferation. The activation pathway triggered by CD38 in peripheral blood lymphocytes was found to induce the transduction of IL-2, tumour necrosis factor α

and granulocyte-macrophage colony-stimulating factor at levels similar to those obtained via CD3 stimulation, but transcription levels of IL-2, interferon-γ (IFN-γ) and IL-10 were lower than with CD3 activation. These results suggest that different activation pathways are involved in cell triggering through CD3 and CD38 (Malavasi *et al.*, 1992).

CD38 appears to mediate adhesion to endothelial cells, probably through a direct interaction with a ligand located on the surface of these cells, which is a characteristic CD38 shares with selectins.

CD38 has been found to be a bifunctional ectoenzyme which posseses both ADP-ribosyl cyclase and ADP-ribosyl hydrolase functions. This quality of CD38 was discovered when significant amino acid sequence homology was seen when compared to that of the ADP-ribosyl cyclase protein of the mollusc *Aplysia californica* (States *et al.*, 1992). ADP-ribosyl cyclase is an enzyme involved in the production of cyclic ADP-ribose (cADPR), an endogenous second messenger that regulates the immobilisation of intracellular calcium (Lee *et al.*, 1989). ADP-ribosyl cyclase and cADPR hydrolase activities occur on the outer surface of human erythrocytes (Lee *et al.*, 1993). Zocchi *et al.*, (1993) purified a single protein from human erythrocytes that was immunologically identified as CD38 which contained NADase, cyclase and cADPR hydrolase activities. ADP-ribosyl cyclase acts to convert NAD^+ to cADPR which is then hydrolysed by cADPR hydrolase to ADPR (Lee *et al.*, 1993). It is thought that extracellularly produced cADPR may play a role in the differentiation mechanism of both B and T lymphocytes as it has been observed that CD38 antigen is overexpressed during the activation and proliferation of these lineages as well as during myeloid differentiation.

Incubation of CD38 with specific antibodies causes the molecule to internalise and/or shed from the cell surface and also precedes the simultaneous modulation of other cell surface antigens of the immune system (Funaro *et al.*, 1993). The antigens that co-modulate tend to be lineage-restricted and function as signal transducers. There is evidence to suggest there is some kind of association, of both a physical and functional nature, between CD38 and CD3 on T cells as the reduced signalling by CD38 corresponds to a decrease in expression of CD3 (Funaro *et al.*, 1990). CD38 also appears to have similar associations

with surface Igs (sIg), CD19 and CD21 on B cells, and with the low-affinity Ig receptor CD16 on NK cells (Funaro *et al.,* 1993).

1.3.2.4 CD38 as a target antigen

Attempts to produce an efficient immunotoxin using CD38 as a target antigen have also been made, with some promising results. Flavell *et al.,* have developed the anti-CD38 IT OKT10–Saporin IT which is currently being used in a phase I trial in patients with multiple myeloma and may eventually be used against B-cell lymphoma and B- and T-lineage ALL (Flavell *et al.,* 1996, 1997, Flavell *et al.,* 1995). Although there have been some concerns about the expression of CD38 by normal myeloid progenitor cells (Vooijis *et al.,* 1995), preclinical toxicological studies performed show that while there is toxicity for progenitors, which give rise to CFU-GEMM, CFU-G, CFU-M, BFU-E by OKT10-Saporin there is none exerted against primitive long term culture initiating cell (LTCIC) (Gibson and Flavell, unpublished observations). This cell type is all that is necessary for re-establishing all of the above CFU progenitors in long term culture, but transient reversible myelosupression will still occur. This is now being investigated directly in patients receiving OKT10-Saporin.

1.4 Factors limiting efficacy of antibody-based therapies

Although the concept of a selective cytotoxic agent is an attractive one, there are many factors which prevent Ab-based therapies being as therapeutically effective as they could be. One of these factors is the short half-life of immunotoxins in the blood.

Life threatening vascular leak syndrome (VLS) is the main dose limiting factor affecting immunotoxins (Vitetta 1993). VLS involves extravasation of fluids and proteins from the vasculature into the periphery. This major dose-limiting toxicity might prevent the administration of therapeutic doses of immunotoxin. There are now studies looking into the administration of fibronectin during IT treatment to limit the development of VLS (Baluna *et al.,* 1996) and also the use of pentoxyphyline to treat VLS (Edwards *et al.,* 1992). There are now suggestions that some toxins (including ricin) possess a three amino acid sequence motif, (x)D(y) where x = L, I, G, or V and y = V, L, or S, which enables them to bind to a receptor on endothelial cells and inflict damage that results in VLS (Baluna *et al.,* 1999). Fibronectin is thought to bind to endothelial cells using the same motif and presumably inhibits toxicity of ricin by blocking the site to which it would bind.

There still needs to be more investigations to gain a better understanding of the development of this disease and how it may be possible to counteract it.

An immunotoxin selectively targets a cell population by binding to a specific antigen molecule on the cell surface. As an IT has no bystander effects it is of paramount importance that all of the leukaemia cell population is selected for the tumour to be successfully killed, since it only takes a few cells to be missed by the therapy for a relapse to occur. It is neccessay for the leukaemia stem cell to express the target antigen and not just the daughter leukaemia cells that have a limited proliferative ability. The problem with using a single target antigen for IT therapy is that antigen heterogeneity may occur. In this event, a subpopulation of the leukaemia cells may be negative for the selected antigen target and is not attacked by the therapy, allowing the tumour to continue developing.

This problem may be overcome by the use of cocktails of immunotoxins that target more than one antigen expressed on the leukaemia cell surface. This has been demonstrated to be a highly effective strategy in a SCID mouse model of B-cell lymphoma and T cell leukaemia (Flavell *et al.,* 1997, Flavell *et al.,* 2001). The approach of constructing various ITs with different toxins might also be used to avoid the manifestation of resistance to this kind of treatment. Resistance to IT therapy may also be overcome by using ITs alongside conventional chemotherapies.

Patients being treated with ITs may produce both HAMA and human anti-toxin Ab (HATA) responses causing the immune system to reject these foreign proteins. An immune response against the IT can occur at any time after the treatment but usually within 2-3 weeks of initiation of treatment (Frankel *et al.,* 1986) and may prove problematic when retreating with these agents. However, it is only the anti-IT antibodies that neutralise the enzymatic portion of the molecule or interfere with selective binding that may actually interfere with IT efficacy (Vallera 1994). This accounts for only a small proportion of anti-IT antibodies produced. Rodent variable Ig regions can be "humanised" with human Ig gene sequences that present fewer xenogenic peptide sequences and hence reduce the immunogenicity of the Ab moiety of ITs (Hale *et al.,* 1988). There is no easy solution to reduce HATA reactions but to change toxins once such a response has been seen. Immunosuppression with cyclophosphamide or total nodal irradiation to create a

temporary immune unresponsiveness may also be employed to combat these reactions (Frankel *et al.*, 1986).

To be fully functional, ITs need to gain access to all cells within the tumour. This makes haematological malignancies the ideal tumour to study because ITs can gain easy access to the whole tumour population. A need for physically smaller ITs has been considered to allow easier access to tumour cells. Intact MAb ITs have the advantage of high potency, longevity and stability, whereas Fab' ITs are more effective in localising to tumour tissue (Spitler *et al.*, 1987) and can also show similar levels of cytotoxicity.

Different antigens have different efficiencies of internalisation and of delivering toxin to the appropriate compartments in the target cell. As mentioned previously, readily endocytosed antigens can make exceedingly effective ITs (Trowbridge *et al.*, 1981), so ways of increasing the efficiency of this process may improve the therapeutic index of this type of treatment. A common problem of targeting antigens with immunotoxins is that the ITs are often preferentially directed to lysosomes which then leads to degradation of the drug and resultant reduction in cytotoxic effects. In these cases good internalisation characteristics are not the only properties needed to make an efficient IT (May *et al.*, 1991).

Much work has been done on finding ways to improve the intracellular routing of ITs. One of the approaches tested to improve the efficiency of translocating the toxin from the endosome to the cytosol was to conjugate a peptide sequence from a virus to the IT. In pilot studies Flavell *et al.*, have shown that a 22mer peptide sequence derived from Influenza virus haemagglutinin 2 (HA-2) significantly improved the potency of an anti-CD19 IT (BU12-Saporin IT) against $CD19^+$ cells, both *in vitro* and *in vivo* in SCID mice when conjugated to the IT (unpublished data). The mechanism of this enhancement was thought to be due to the fusogenic properties contained within the peptide sequence which assist the passage of infective virions across the endosomal or other intracellular vesicular membrane into the cytosol.

Another common approach that has been investigated is the use of lysosomotropic amines and carboxylic ionophores to improve IT efficacy. These agents are known to increase intralysosomal pH (Seglen *et al.*, 1979) and inhibit degradation of the IT. Manske and

colleagues (1986) observed that there was almost a total absence of IT in the lysosome, whereas there was accumulation in large non-lysosomal vacuoles close to or belonging to the trans-Golgi apparatus, when monensin was used (Manske *et al.,* 1986). This approach has severe limitations due to the high intrinsic toxicity of these agents.

Studies investigating the effects of these molecules on IT potency have had varied conclusions, some observing great enhancement of cytotoxicity (Ippoliti *et al.,* 1998, Casellas *et al.,* 1984, Krönke *et al.,* 1986) and others seeing none (Raso *et al.,* 1984, Fulton *et al.,* 1986). Much more needs to be done in this area of research.

1.5 Endocytosis and intracellular routing of immunotoxins

The endocytosis and intracellular routing of immunotoxins are arguably the most important factors that affect their potency, and for this reason there has been considerable interest in this topic. If a greater understanding of the pathways by which immunotoxins reach their target can be gained then ways of manipulating these processes can more readily advance.

Internalisation is necessary for intoxication of the cells to occur by ITs. Pirker *et al.,* (1985) has shown that antibodies that internalise more readily generally make better ITs than those that do not. ITs are toxins conjugated to a ligand, Ab or other directing molecule and most ITs will enter the cell via receptor-mediated endocytosis. In these cases the first step made by ITs is to bind to a cell surface receptor and form a ligand-receptor complex (L-R). These complexes diffuse laterally within the cell membrane until they encounter a clathrin-coated pit in which they get taken up into the cell. The clathrin-coated vesicle goes on to form endosomes or receptorsomes, which move away from the cell surface by saltatory motion.

In the case of Ab directed immunotoxins, the majority of the IT is directed to lysosomes where it is degraded. The reason that these ITs are still cytotoxic is that it is possible for a small proportion of the internalised IT molecules to escape from some intracellular location into the cytosol (Pastan *et al.,* 1986). Ways of overcoming this dose-limiting situation have already been investigated. One of them is to expose cells to adenovirus and IT simultaneously as this enables them to enter the same endocytic vesicle. The result of this is that the IT can be released into the cytosol as a result of the virus disrupting the

intracellular vesicular membrane and shows enhanced cytotoxicity (FitzGerald *et al.*, 1983). This would also avoid degradation in lysosomes.

Intracellular routing depends greatly upon the signals contained within the receptor or antigen targeted by the IT (Neville 1987). In contrast to this, the translocation of the active moiety of an IT is partly controlled by the individual toxin itself (Neville 1987). This could explain why the intracellular route taken by one particular toxin can differ partially when it is conjugated to different antibodies.

The intracellular pathways taken by many immunotoxins against various surface antigens still remain largely unclear and need defining. The problem of visualising the pathway of immunotoxins is probably largely a result of the small quantities required to reach the cytosol to cause cytotoxicity. Most of the data obtained on this subject indicates that the majority of immunotoxins probably follow one of the pathways proposed in a model by Oeltmann & Frankel (1991). All immunotoxins must bind to cell surface receptor or antigens which are subsequently endocytosed via coated and/or uncoated pits and vesicles. The endocytosed material is generally found within endosomes. Once in endosomes the IT may be transported back to the plasma membrane, on to the lysosome where it will be degraded or on to the TGN. The exact location from which the toxin moiety of the IT translocates to the cytosol is not always known. DT may enter the cytosol directly from acidified endosomes or lysosomes, whereas ricin may enter the cytosol from the TGN, the Golgi stacks or the ER.

1.6 Endocytosis defined

It is of critical importance to understand endocytic processes with respect to different cell surface antigens that internalise following ligation with IT. This understanding could help to identify a suitable target molecule for IT treatment and make it possible to manipulate these processes. For this reason, the following section will focus on the intracellular organelles that have been found to be part of IT pathways once endocytosed.

'Endocytosis' is a very general term, which was used by De Duve in 1963 to encompass all variant forms of basic cellular transport mechanisms. It refers to the processes by which cells ingest extracellular materials by trapping them within inward invaginations of the plasma membrane that pinch off to form intracellular vesicles (Silverstein *et al.*, 1977).

The intracellular vesicles may be in the form of phagosomes, pinosomes, coated vesicles or primary food vacuoles. The process varies depending on the cell type studied and the mode of endocytosis involved.

Endocytosis serves to maintain cellular homeostasis by recovering protein and lipid components that are inserted into the plasma membrane by ongoing secretory activity (Mellman 1996). It is an essential process for sustaining organismal homeostasis, enabling the control of an extraordinary array of activities required for existence as part of a multicellular community. For example, transmission of neuronal, metabolic and proliferative signals, the uptake of many essential nutrients, the regulated interaction with the extracellular environment, and the ability to mount a defence against any invading micro-organisms.

Endocytosis can be divided into two main types, phagocytosis and pinocytosis. Phagocytosis, is the internalisation of particulate matter that is larger than a few tenths of a micrometer in diameter and hence is visible by light microscopy. Binding of opsonised particles to cell surface receptors, which are capable of transducing a phagocytic stimulus to the cytoplasm, triggers uptake by phagocytosis. This stimulus results in the polymerisation of actin local to the site of particle attachment causing pseudopod extensions that engulf the particle into a cytoplasmic phagosome (Greenberg *et al.,* 1990). Once the phagosome has formed, it rapidly fuses with an endosome and/or lysosome thus exposing its contents to hydrolytic enzymes (Steinman *et al.,* 1983, Rabinowitz *et al.,* 1992). Examples of receptors that mediate phagocytosis on mammalian cells are the IgG Fc receptors, some integrins (eg complement receptor), and lectins (eg mannose receptor) (Kielian & Cohn 1980, Mellman *et al.,* 1983, Wright & Silverstein 1983).

Pinocytosis is the uptake of smaller substrates, which range from insoluble particulates to low molecular weight solutes and even fluid itself. Pinocytosis can be subdivided into fluid phase where substances enter cells in fluid content and absorptive where cell binding is essential for entry into the cell.

There are also two types of adsorptive endocytosis. Firstly, there is the internalisation of markers that bind in a non-specific fashion to the cell surface, for example, cationic ferritin binding to anionic sites on the plasma membrane. Secondly, endocytosis of

ligands can be mediated by binding to specific receptors on the cell surface and this mechanism is known as receptor mediated endocytosis (RME). Many molecules are taken up into cells via this mechanism, including lysosomal enzymes (Besterman and Low 1983), polypeptide hormones such as EGF (Carpenter & Cohen 1976), insulin (Maxfield *et al.,* 1978), and thyroid hormones (Cheng *et al.,* 1980), plasma transport proteins eg LDL (Brown & Goldstein 1979), asialoglyoproteins (Ashwell & Morell 1974) and α_2-macroglobulin (Willingham *et al.,* 1979).

As RME is the form of endocytosis that is most associated with IT transport within the cell, this is the form of endocytosis reviewed in the following text.

1.6.1 Receptor-mediated endocytosis (RME)

The concept of RME was first formulated in 1974 based on biochemical studies to explain how the regulation of cellular cholesterol metabolism depended on sequential cell surface binding, internalisation and intracellular degradation of plasma low density lipoprotein (LDL) (Goldstein & Brown 1974). This was later confirmed by morphological studies where LDL receptors could be seen concentrated in coated pits that pinched off from the cell surface to form coated vesicles carrying the LDL to the cell interior (Anderson *et al.,* 1976, 1977).

RME has received a lot of attention over the last decade or so, which has focussed on the pathways of physiologically and pathologically important molecules and their receptors. Although RME varies considerably between cell type and different receptor-ligand systems a general description of receptor-mediated endocytosis can be summarised as follows (Goldstein *et al.,* 1979, Pastan & Willingham 1981, Bretscher & Pearse 1984):

1) Endocytosis is initiated when macromolecules bind to specific cell surface receptors, which are usually diffusely distributed on the plasma membrane.
2) The receptor-ligand (R-L) complex formed slides laterally into coated pits.
3) Within minutes the coated pits invaginate into the cell and are generally assumed to pinch off to form coated endocytic vesicles.
4) These vesicles soon shed their coats to enable them to fuse together to form endosomes, the contents of which are acidified by ATP-driven pumps (Tycko & Maxfield 1982, Helenius *et al.,* 1983). The acidic environment within the endosome

often causes the R-L complex to dissociate and part company, with the ligand being degraded in lysosomes and the receptor being recycled to the plasma membrane (Bron *et al.*, 1985), although this is not always the case.

Over 25 receptors have been seen to participate in RME. Cellular uptake of lysosomal enzymes is also mediated via this mechanism and occurs when the mannose-6-phophate residues attached to this class of protein are recognised by their respective receptor. Some toxins and viruses use RME to enter cells by binding opportunistically to receptors that normally function in the uptake of other substances.

It appears that there is one common feature to all receptor-mediated endocytosis, which is that all receptors enter cells via coated pits and are then delivered to the same type of acidified endosomes, after which the pathways can be seen to diverge (Pastan & Willingham 1981, Via *et al.*, 1982, Carpentier *et al.*, 1982). There are four main pathways that can be taken by R-L complexes once they are in early endosomes (Courtoy 1993):

1. *Receptors that recycle but their ligand is degraded.* This is the classic pathway for the endocytosis of LDL, asialoglycoproteins (Gal/GalNAc), α_2-macroglobulin and insulin. The acidic environment of the endosome causes the ligand to dissociate from its receptor (Brown *et al.*, 1983, Helenius *et al.*, 1983), after which the ligand is transported to lysosomes and degraded. The receptor is believed to leave the endosome by incorporating itself into the membrane of a vesicle that buds off the endosome surface. This route is well suited to receptors that transport ligands into the cells at a high rate. Receptors may be reused every 10-20 minutes via this mechanism, which enables the uptake of hundreds of ligands in the lifetime of one receptor (10-30hr). The receptors for this pathway must be very stable to withstand denaturing under the acidic conditions of the endosome and must undergo a significant conformational change for the ligand to be released (DiPaola & Maxfield 1984).
2. *Receptors that recycle with their ligands.* An example of a ligand that follows this route is transferrin (Octave *et al.*, 1983). In this case, the R-L complex does not dissociate in the endosome. Transferrin has been shown to remain bound to its receptor at pH 5 *in vitro* whereas EGF and LDL do not display this property (Klausner *et al.*, 1983, Dautry-Varsat *et al.*, 1983). The low pH in the endosome causes iron to dissociate from transferrin leaving apotransferrin-receptor complex to recycle to the

plasma membrane. This happens via a network of membrane tubules and vesicles that eventually lead it back to the cell surface (Geuze *et al.,* 1984). The neutral pH at the cell surface then results in dissociation of apotransferrin enabling the receptor to bind holotransferrin.

3. *Receptor that degrades and ligand that is targeted to lysosomes.* EGF is an example of a ligand that fits into this category. Dissociation of the ligand from the receptor occurs once in the endosome and both are degraded probably as a result of subsequent cotransport to lysosomes (Carpenter & Cohen 1979). The mechanism by which this occurs is unclear. In some cells, EGF can escape degradation and recycle to the plasma membrane as observed in cultured fibroblasts (Carpenter & Cohen 1979).
4. *Receptors that are transported and a ligand that is targeted to lysosomes.* The receptor that carries polymeric IgA across epithelial surfaces such as across liver cells for excretion into the bile is an example of this kind of pathway. The receptor-IgA complex is incorporated into vesicles and carried into the cell (Renston *et al.,* 1980). At some stage the receptor is clipped proteolytically. This enables part of the receptor with Ig still bound to it to be released from the membrane. The released receptor fragment is called the secretory component. The IgA containing vesicle eventually migrates to the bile canalicular face of the hepatocyte, where it discharges IgA/secretory component adduct into bile.

1.6.2 Intracellular compartments important to trafficking of ITs

In order for an IT to be cytotoxic it must be transported to the ribosomes in the cytosol. Reviewed here are some of the compartments and organelles that are thought to be part of this trafficking process.

1.6.2.1 Endosomal functions and characteristics

1.6.2.1.1 Early endosomes

Early endosomes, which are also referred to as endosome-I (Helenius *et al.,* 1983) or peripheral endosomes, are located close to the plasma membrane. They are denoted 'early' because they are the first compartment entered by a pulse of endocytic tracers. They are tubulo-vesicular structures, with the vesicular structures ranging in diameter between 0.4-1 μm with tubular projections of several micrometres. They are often seen to

have an electron-lucent interior with a plaque-like electron-dense region, which covers portions of the cytosolic surface.

For receptors engaged in rapid recycling the early endosome is the site that hosts the initial dissociation of the receptor-ligand complex. This is thought to occur because of the slightly acidic (pH 6.3-6.8) environment within this compartment. Enveloped viruses were used as intracellular pH probes to determine such values (Kornfeld & Mellman 1989). Endosome acidification is generated by means of an ATP-driven proton pump (Galloway *et al.*, 1983) which is electrogenic. It is modulated in early endosomes by the presence of Na^+, K^+-ATPase which reduces the degree of acidification comparative to late endosomes and lysosomes (Fuchs *et al.,* 1989). The degree of acidification found within various endosomal populations has been seen to correlate well with their functions.

Early endosomes next engage in the physical separation or sorting of receptors from dissociated ligands, and other macromolecules internalised in the fluid phase. The mechanism for this is thought to be a geometric one. Receptors accumulate in tubular extensions as a result of their greater surface area, whereas the greater fractional volume within the vesicular regions of the early endosome allows accumulation of the soluble contents. Morphological data of the segregation of the asialoglycoprotein from its receptor using immunolocalisation demonstrates this quite clearly (Geuze *et al.,* 1983). The tubular elements then pinch off or serve as sites for budding of carriers of recycling receptors and the larger vesicular elements proceed to late endosomes and lysosomes for degradation.

The kinetics of receptor recycling suggest that these peripheral elements are the site from which a significant proportion of receptors are recycled back to the plasma membrane. However, there is evidence (especially from studies of transferrin receptor trafficking) that a significant proportion of recycling receptors are also routed through the juxtanuclear compartment of the endosome (Yamashiro *et al.,* 1984, Hopkins 1983).

1.6.2.1.2 Recycling receptors

Recycling endosomes or vesicles are a network of 60-80 nm diameter tubules which contain receptors targeted for recycling to the plasma membrane. They are less acidic than early endosomes and are generally distributed throughout the cytoplasm, often

concentrated in the pericentriolar area (Hopkins & Trowbridge 1983, Yamashiro *et al.*, 1984, Gagescu *et al.*, 2000). They have frequently shown direct continuity with the vacuoles of the early endosome, but the direct relationship between these two compartments is unclear. It is possible that the recycling vesicles arise from the tubular extensions of the early endosomes.

Some recycling vesicles fuse directly with the plasma membrane, whereas some translocate to the perinuclear cytoplasm on microtubule tracks. Here they accumulate as a distinctive population of vesicles and tubules closely opposed to the microtubule organising centre (MTOC) (Hopkins & Trowbridge *et al.*, 1983). These perinuclear recycling vesicles appear to contain an intracellular pool of recycling receptors. Up to 75% of all transferrin receptors are found within these vesicles (van der Sluijs *et al.*, 1992). Recycling direct from the early endosome only takes 2-3 minutes, whereas it takes 5-10 minutes from the perinuclear recycling vesicles.

1.6.2.1.3 *Late endosomes*

Late endosomes are defined by the kinetics of the appearance of endocytic tracers and tend to be located in the perinuclear region of the cell. They differ morphologically from early endosomes in that they exist as large spherical structures, often with deep invaginations of the limiting membrane which gives rise to multivesicular bodies (MVBs). Late endosomes contain hydrolytically active lysosomal hydrolases and are likely to initiate the degradative process. These lysosome–like characteristics can sometimes lead to late endosomes being referred to as pre-lysosomes or the pre-lysosomal compartment.

The function of the late endosome appears to be in the transport of internalised ligands to lysosomes (Schmid *et al.*, 1988). Transport to the lysosomes appears to require microtubules (Gruenberg *et al.*, 1989). Late endosomes can be distinguished from lysosomes by histochemical detection of arylsulphatase or acid phosphatase.

Transfer of material from early endosomes to late endosomes involves the dissociation of vacuolar elements from the early endosome network, and their subsequent migration on microtubules to the perinuclear cytoplasm where they fuse with late endosomes (Mellman *et al.*, 1996). Carrier vesicles may be formed from late endosomes. Formation of carrier vesicles is often accompanied by an increase in the number of internal vesicles they

contain. Carrier vesicles and subsequent structures thus take on the general appearance of classical MVBs (Hopkins *et al.*, 1990). Transfer of material between late endosomes and lysosomes appears to be a direct fusion event, resulting in a transient hybrid organelle (Mullock *et al.*, 1998). Lysosomes are also multivesicular, but completely lack mannose-6-phosphate receptors.

1.6.2.1.4 Transport intermediates

MVBs are endocytic vesicles that occur to a variable extent in most cells. Profiles of structures giving the appearance of an MVB can be seen in both early and late endosomes (Griffiths 1996). These endosomal structures are vacuoles, of 200-800nm in diameter, containing small (40-80nm diameter) vesicles (van Deurs *et al.*, 1993). In exogenous tracer studies, early labelled elements in the peripheral cytoplasm tend to contain fewer vesicles than those of the juxtanuclear area. In the later labelled elements of the juxtanuclear area these vacuoles become typical multivesicular bodies with their lumena often filled with closely packed vesicular profiles.

While some MVBs have been found to contain acid phosphatase activity and mannose-6-phosphate receptors, dual labelling studies have shown that endosomal MVB can exist in the juxtanuclear area for some time (<15 min) before they acquire a range of demonstrable hydrolases (Miller *et al.*, 1986, Harding 1983). Griffiths and Simon (1986) suggested that the fusion of TGN-derived vesicles with a MVB may be an event that converts a late endosomal compartment into a lysosome, but how MVBs acquire acid hydrolase activity and thus transform into lysosomes is not known.

1.6.2.2 Golgi Apparatus and the trans Golgi network (TGN)

The Golgi apparatus is a central way station for protein secretion from cells, or delivery to the cell surface or to lysosomes (Farquhar and Palade 1998, Warren and Malhotra 1998). The simplest model used to describe the Golgi apparatus is one where the Golgi stack is comprised of 3-8 discrete flattened cisternae and associated 60-70 nm diameter vesicles. The Golgi stack has a defined polarity with the cis cisternae being the face that accepts material from the ER, and the trans cisternae being the face where material accumulates prior to secretion.

The Golgi apparatus could be seen as a combined assembly line and logistics centre. It houses the enzymes responsible for the synthesis of complex carbohydrate structures found on many proteins or lipids and these are summarised in figure 1.7. The *cis*- and *trans* faces are important sites for the sorting of proteins and lipids for delivery to specific subcellular destinations.

Griffiths and Simons (1986) propose that the TGN is a specialised organelle on the trans side of the Golgi stack that is responsible for routing proteins to lysosomes, secretory vesicles, and the plasma membrane from the Golgi complex. The distinction between the trans cisterna and the TGN is often determined by the nonoverlapping localisations of thiamine pyrophosphatase reactivity (*trans*) and acid phosphatase (TGN) as demonstrated by cytochemistry (Novikoff and Novikoff 1977). The TGN appears to be the only site within the Golgi complex of clathrin localisation. Budding structures have been seen on the rim of the cisternae in the Golgi stack but as these cannot be labelled by antibodies against clathrin, it is believed that different proteins must form these structures (Griffiths *et al.*, 1985). It has also been suggested that a link between the exocytic and endocytic pathways exists at the TGN (Griffiths and Simons 1986).

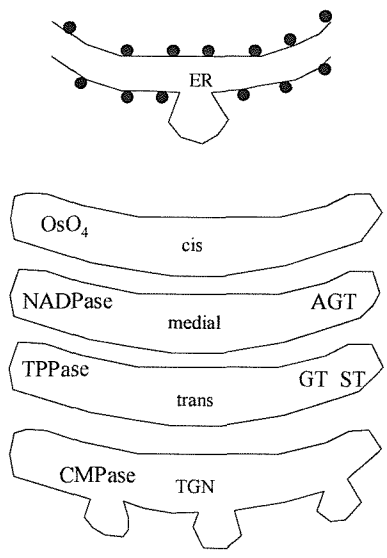

Figure 1.7 Simple model of the Golgi complex.

The major feature is the presence of three main compartments. Proteins move sequentially through these compartments and undergo modifications. The *cis* compartment is the major site for sorting of secretory and ER-derived proteins. Here the removal of mannose takes place by mannosidase II and the presence of strong reducing agents can be detected by osmium tetroxide reduction (Friend 1969). Nicotinamide adenine dinucleotide phosphatase (NADPase) (Smith 1980) and N-acetylglucosamine-transferase I (AGT) (Dunphy *et al.*, 1985) are usually attributed to the *medial* cisternae. Thiamine pyrophosphatase (TPPase), galactosyl transferase (GT) (Roth and Berger 1982) and sialyl transferase are most often detected in the *trans* cisternae. The TGN is distinguished from the *trans* compartment by the presence of acid phosphatase (CMPase).

A dispersed tubulovesicular system has now been described which is suggested to serve as an intermediate compartment linking the ER and Golgi (Schweizer *et al.*, 1990). It is known as the ER-Golgi intermediate compartment (ERGIC) or vesicular tubular clusters (VTC) and is thought to transfer proteins between organelles in the early parts of the

secretory pathway and in the retrieval of resident ER proteins (Pelham 1995). It has recently become evident that the Golgi stacks are dynamic structures which are possibly less compartmentalised than previously assumed. For this reason, there is revived interest in the idea that Golgi cisternae may be transient structures that move in a *cis-trans* direction carrying proteins through the stacks. For a detailed discussion of the 'cisternae maturation' and the 'vesicular' model of the Golgi see review Griffiths 2000.

A candidate population of small shuttle vesicles has been identified by morphological studies on isolated stacks incubated in the presence of ATP and cytoplasmic extract (Orci *et al.,* 1986). The buds and vesicles, which appear in these studies, are approximately 100nm in diameter and appear to bear some form of coating on their cytoplasmic surfaces for which there is no evidence of it being composed of clathrin. Orci *et al.,* (1986) suggest that these vesicles, unlike their clathrin-coated counterparts may be concerned primarily with bulk transport; selective routing along the biosynthetic pathway being required only after the Golgi stack has been traversed.

Initiation of vesicle formation is thought to require the presence of a small GTPase ADP-ribosylation factor (ARF) complexed to GDP, and a BFA-sensitive exchange factor (Donaldson *et al.,* 1992, Franco 1996). Association of ARF to the Golgi membrane follows the exchange of GDP for GTP. Subsequently, ARF-GTP recruits a cytosolic complex, coatomer or AP-1 to the membrane, possibly through the activation phospholipase D (Ktistakis *et al.,* 1996). Assembly of coat proteins results in deformation of the membrane to form a coated bud, which then pinches off to form a coated vesicle containing the proteins to be transported. Hydrolysis of ARF-bound GTP is a requirement for the disassembly of the coat proteins and the subsequent fusion of the vesicle with the target membrane (Tanigawa *et al.,* 1993).

Coatomers consist of either COP-I or COP-II proteins. It is generally believed that COP-II-coated vesicles are obligate intermediates in anterograde transport from the ER to the Golgi complex (Barlowe 1998, Aridor *et al.,* 1998). In mammalian cells, these vesicles have been found to coalesce to form the VTCs mentioned previously, which shuttle anterograde cargo from ER to Golgi complex (Morin-Ganet 2000). COP-I coated vesicles on the other hand may function both in the transport from ERGIC to the Golgi stacks and

in the anterograde retrograde pathways (Scales *et al.*, 1997, Schekman and Mellman 1997).

There is still much debate on the transport systems operating between the compartments of the Golgi stacks especially since cell-free systems fail to demonstrate the vesicular transport described above. *In vitro* studies have shown the possibility of a nonvesicular mechanism for intra-Golgi transport (Happe & Weidman 1998) which is also ARF independent. It is uncertain whether these studies indicate that the in vivo mechanism of intra-Golgi transport is not faithfully reproduced in vitro, or that intra-Golgi transport really does occur by a non-vesicular mechanism.

1.6.2.3 Lysosomes

Steinman *et al.*, (1983) define lysosomes as membrane bounded vacuoles rich in acid hydrolases. Primary lysosomes are described as the package of acid hydrolases formed by the concerted action of rough ER and the Golgi apparatus. A secondary lysosome is an acid hydrolase rich vacuole that has acquired substrates by endocytosis or by autophagy.

There are a number of criteria used to identify "mature" secondary lysosomes. When studied under phase-contrast microscopy the lysosome granules are phase-dense and can usually be easily distinguished from mitochondria and lipid droplets. In thin sections, lysosomes can usually be seen to contain an amorphous electron-dense content and sometimes membranes and particulates. They can also be labelled with endocytic tracers and with acid hydrolase cytochemistry.

Mature lysosomal granules concentrate in the perinuclear region. The size and number of such compartments varies greatly depending on the cell type, environment and endocytic loads. For example, under routine culture conditions, macrophages contain more than 1000 lysosomes which occupy 2-5 % of the cell volume, and have a surface area 10-20 % of the plasma membrane area (Steinman *et al.*, 1976).

Weak bases, such as chloroquine, ammonium chloride and acridine orange, tend to accumulate in lysosomes because of their low internal pH (the pH of lysosomes in macrophages is 4.5-5.0) (Okhuma & Poole 1981; Poole & Okhuma 1981). Once in lysosomes these substances become protonated and most are rendered impermeable. It is

generally accepted that an energy-dependent proton pump acidifies lysosomes (Ohkuma *et al.*, 1982, Poole and Okhuma 1981), although there is evidence that impermeable anions may contribute to the low pH via a Donnan equilibrium (Reijngoud and Tager 1977).

Lysosomes degrade proteins, lipids, nucleic acids and saccharides and are the principle site of intracellular digestion (Bainton 1981). The biological materials destined for degradation are either ingested by endocytosis whereby they are shuttled to lysosomes in early and late endosomes, or large particles are taken up by phagocytosis into specialised cells (e.g. macrophages) which results in the formation of phagolysosomes (Mellman *et al.*, 1986). A third vesicular structure, an autophagosome, which contains obsolete parts of the cell itself, is also able to fuse with lysosomes causing degradation of its contents.

1.6.3 Retrograde transport

Newly synthesised proteins in the ER undergo dynamic folding/unfolding reactions which aid the assembly and maturation of secretory and membrane proteins. ER-specific chaperones and folding enzymes that work to prevent non-productive interactions and irreversible aggregation of proteins (Rothman 1989) mediate these processes. Only once proteins are correctly folded are they allowed to leave the ER and proceed to the Golgi complex and beyond. Incompletely folded, misfolded or unassembled proteins are retained and/or degraded, and thus the ER serves an important quality control function in the secretory pathway (Doms *et al.*, 1993). The ER is the sole compartment that exhibits this quality control mechanism. This can be seen for example with unassembled class I molecules that are exported from the ER which have been found to be cycled back to the ER, whereas the properly assembled class I molecules are efficiently transported to the cell surface (Hsu *et al.*, 1991).

Once released from the ER, secretory proteins can enter the Golgi apparatus in vesicles that fuse with the *cis* side and then go on to exit the Golgi after modification in transport vesicles from the *trans* side (Palade 1975). There are resident Golgi enzymes that can be transported in the *cis*-to-*trans* direction with the secretory flow which must be recycled constantly by retrograde transport in the opposite direction (Pelham 1988). There are also resident proteins present in the ER lumen and membrane that can escape this compartment and reach the Golgi where they can acquire oligosaccharide side chains, before being returned to the ER by retrograde transport. These ER proteins can be recognised by the

presence of a C-terminal tetrapeptide sequence, typically KDEL, HDEL or KKXX (Pelham 1989, Pelham 1988). These proteins are thought to be recognised by virtue of these retrieval signals by a membrane-bound receptor located in the Golgi apparatus, or in an intermediate compartment between the ER and Golgi complex, which can then enter the retrograde pathway and return these proteins to their source. In the case of the KDEL receptor, retrieval can occur from all Golgi cisternae including the TGN.

The KDEL receptor is thought to be a seven transmembrane domain (Townsley *et al.*, 1993) responsible for the retrieval of ER proteins from the Golgi complex. It is only a temporary resident of the Golgi complex because upon binding a KDEL-containing ligand it is transported to the ER where the ligand is released.

Lewis and Pelham (1990) have identified the KDEL receptor in human cells on the *ERD2* gene. From the work of Townsley *et al.*, (1993) it has been discovered that most of the residues affecting KDEL binding can be found in the luminal half of the proposed membrane-spanning segments or to one of the luminal loops. There is a good correlation between the functionally significant residues and those that are evolutionarily conserved, although as with many other proteins, there are also a number of highly conserved residues that may be altered without affecting the function of the receptor. Mutations that abolished KDEL binding were mainly restricted to transmembrane domains (TMs) 1, 2, 5, and 6 and to the luminal loop between TM 2 and 3. It has also been noted that alterations to all but one of the conserved acidic and basic residues in TMs can affect binding and hence it is plausible that these contribute to the hydrophilic pocket that can accept the highly polar KDEL ligand. This data also corresponds to the finding that changes to the luminal end of TM2 can affect the specificity of ligand recognition by the receptor (Lewis and Pelham 1992).

Mutants have been tested that included changes to all the cytoplasmically exposed residues of erd2, except for four alanines (Townsley *et al.*, 1993). There was no good evidence for a retrograde transport signal in this portion of the receptor which was surprising since many of the receptors active in the endosomal system contain cytoplasmic signals, and the KKXX signal thought to specify retrieval of ER membrane proteins is also cytoplasmic (Jackson *et al.*, 1993). It may be that such a signal exists but may be redundant.

Alteration of residue D^{193} had the effect of allowing ligand binding to occur normally, but prevented ligand-induced movement of the receptor to the ER. This residue sits in the hydrophobic sequence which is probably in the membrane spanning region in TM7. It couldn't be replaced by any other charged residue whilst retaining its function. For these reasons, D^{193} is considered to mediate the recycling of ligand-receptor complexes from the Golgi complex to the ER. The mechanism by which it does this is still to be elucidated.

1.6.4 Actions of Brefeldin A

The fungal isoprenoid antibiotic BFA has been used as a valuable tool to analyse membrane transport in the secretory pathway. It has mainly been noted for its inhibitory effects on anterograde protein transport beyond the Golgi (Misumi *et al.*, 1986; Oda *et al.*, 1987), the rapid disassembly of the Golgi complex (Lippincott-Schwartz *et al.*, 1989), and the retrieval of resident and itinerant Golgi proteins to the ER (Doms *et al.*, 1989). BFA causes the *cis, medial* and *trans* cisternae of the Golgi complex to redistribute to the ER. These effects can be seen to occur very rapidly after the addition of BFA, but reverse with equal rapidity once the drug has been washed out of the system. For example, once BFA is removed, the Golgi apparatus reforms within a few minutes indicating that the ER and Golgi have an intrinsic ability to self-sort.

The mechanism of action of BFA remains unclear but it is likely to involve inhibition of the binding of a 110 kD protein to the Golgi membranes in intact cells and in vitro (Donaldson *et al.*, 1990). This protein known as β-COP, shares limited homology with the clathrin-coated vesicle component β-adaptin, and forms a complex with other non-clathrin coat proteins (Serafini *et al.*, 1991). This non-clathrin coat is thought to play a critical role in budding of Golgi derived transport vesicles or in regulating formation of tubules that may be involved in transport in the Golgi (Orci *et al.*, 1991). The earliest observed effect of BFA is the dissociation of β-COP complexes from the Golgi membranes. This precedes any changes in Golgi structure observed by light microscopy. It is not known whether BFA disrupts the Golgi structure and transport directly by interfering with the association of β-COP with Golgi membranes (Lippincott-Schwartz *et al.*, 1991).

In vitro this dissociation is followed by the formation of continuous tubular connections between Golgi cisternae, which is to be expected if one of the roles of the coat is to prevent the formation of such tubules (Orci *et al.,* 1991). *In vivo* the fusion of Golgi cisternae seems to occur rapidly. Long tubules can be seen to emanate from the Golgi region, in a microtubule manner and eventually fuse with the ER (Lippincott-Schwartz *et al.,* 1990). Formation of these structures may be explained by the unmasking of microtubule motor attachment sites that are normally covered by coat proteins. These motors may pull out uncoated tubules, which would then fail to pinch off into vesicles, but would be capable of fusion. A similar mechanism is used normally for tubule formation but they do not fuse with heterologous compartments.

Effects of BFA have also been identified on endosomes, lysosomes, and the TGN (Lippincott-Schwartz *et al.,* 1991). The Golgi and endosomal effects appear to be species-specific. For example, in rat and bovine cells both organelles are affected, but in Madin-Darby canine kidney (MDCK) cells the Golgi complex is resistant while endosomes remain sensitive to the drug (Hunziker *et al.,* 1991; Lippincott-Schwartz *et al.,* 1991).

In MDCK cells, early endosomes form a tubular network in a microtubule-dependent manner, but the uptake of endocytic markers from the basolateral surface, recycling of receptors to the plasma membrane, and degradation of endocytosed material in (pre)lysosomes appear to be unaffected. In these cells, it seems that only transcytosis is altered. It is the formation of transcytotic vesicles, rather than their transport and fusion that is inhibited (Hunziker *et al.,* 1991). This could be explained by BFA-induced dissociation of a coat protein specific to transcytosis, which would result in the prevention of the formation of discrete transcytotic vesicles.

In rat and bovine cells, tubular networks extend from the TGN and fuse with early endosomes (Wood *et al.,* 1991, Lippincott-Schwartz *et al.,* 1991). This results in the formation of a mixed TGN/endosomal compartment that is still capable of receiving endocytosed material, recycling receptors to the cell surface, and delivering macromolecules to a degradative compartment which may not necessarily be mature lysosomes. Since the late endosomes/prelysosomal compartment of this system appears unaffected, it would suggest that these organelles do not arise by maturation of early endosomes, at least not in these cells.

Even lysosomes have been shown to be moderately sensitive to BFA, as they form a modest microtubule-dependent network (Lippincott-Schwartz *et al.,* 1991). This response to the drug suggests the possible association of some coat proteins with the organelle indicating that transport out of this structure may occur.

From this data it is apparent that some transport steps are affected but not others. This leads us to the possibility that BFA targets only specific coat proteins, which would leave other transport processes untouched.

1.7 Aims of the project

ITs are used as a novel approach to treat cancer both *in vivo* by specifically targeting a tumour population and *ex vivo* by purging bone marrow of leukaemic cells prior to transplantation. The treatment of haematological malignancies with ITs has resulted in mixed responses in early clinical trials (Uckun 1993, Vitetta *et al.,* 1993, Uckun and Reaman 1995, Grossbard and Nadler 1994, Sausville *et al.,* 1995, Grossbard *et al.,* 1992). Much of this is due to the heterogeneity within and between MAb-toxin conjugate preparations (Bachier and LeMaistre 1995, Caron and Scheinberg 1994, Frankel *et al.,* 1996). The ITs used in this work directed against CD7 and CD38 are both selectively potent cytotoxic agents, although each IT performs differently in various assays such an *in vitro* protein synthesis inhibition assay, and long term outgrowth assay as well as in therapy studies in mice xenografted with human leukaemia cells. Research carried out in this laboratory has focussed on the increased therapeutic effect that is often observed when a combination of two or more ITs are used simultaneously against a variety of leukaemia cell lines (Flavell *et al.,* 2001, Flavell *et al.,* 1997, Flavell *et al.,* 1992, Flavell *et al.,* 1995). In these studies, the final concentration of the two combined ITs was no greater than when each IT was used alone. This project was intended to investigate the individual mechanisms and factors affecting the cytotoxicity of the individual ITs and determine how these might be affected when both antigens are ligated simultaneously with ITs in a way that may cause an increase in the cytotoxicity produced.

The purpose of the first experimental chapter is to determine whether or not the phenomenon described earlier of increased cytotoxicity when ITs were directed against

two antigens simultaneously would be observed on the T-cell acute lymphoblastic leukaemia cell line HSB-2. A protein synthesis inhibition assay, cell proliferation assay and *in vivo* SCID-HSB-2 leukaemia mice model was used to investigate this.

The second experimental chapter uses flow cytometric analysis to monitor the modulation of the cell surface antigens CD7 and CD38 when ligated individually or simultaneously by monoclonal antibodies or their equivalent ITs. This investigation is intended to determine whether any alterations to internalisation kinetics or characteristics occur when both antigens are ligated simultaneously that may account for the increase in cytotoxicity observed when two ITs are used simultaneously. Scatchard analysis is also conducted on these two antibodies and their respective ITs to determine the effect that antigen density and affinity of the Ab moiety for the antigen has on IT cytotoxicity.

The third experimental chapter uses BFA as a tool for determining part of the routing of the HB2- and OKT10-Saporin ITs. In particular the focus is on whether or not the Golgi apparatus plays an important role in the intracellular pathways of these two ITs, and whether using BFA affects their cytotoxicities.

Finally, the fourth experimental chapter focuses on the use of confocal laser scanning microscopy and electron microscopy to study the binding patterns and intracellular trafficking of the two monoclonal antibodies used to construct the ITs. This is used to determine whether or not the differences in intracellular routing is responsible for the differences in cytotoxicity of each individual IT and to see if co-ligation of the two antigens alters the routing in a way more conducive for cytotoxicity.

It is hoped that this work has helped in clarifying some of the mechanisms and factors that affect the efficacy of these agents. By gaining a better understanding of these trafficking processes, and the mechanism of the enhanced cytotoxicity obtained when using two ITs simultaneously, work can be focussed on finding ways to enhance the performance of these agents in patients.

Chapter 2

Materials and Methods

2.1 Solutions and Buffers

All buffers were purchased from either BDH Merck or Sigma-Aldrich Company Ltd unless otherwise stated.

2.1.1 General Buffers

2.1.1.1 Phosphate-Buffered Saline (PBS) pH 7.4

NaCl	35.06g	7.012g
Na_2HPO_4	17.20g	3.44g
KH_2PO_4	3.95g	0.79g
Dilute with dH_2O to	5L	1L

2.1.1.2 Flow cytometry wash solution

PBS	1000ml
NaN_3	1g

2.1.1.3 Binding buffer

PBS	1000ml
BSA (Fraction V) 1% (w/v)	10g
NaN_3 0.1% (w/v)	1g

2.1.1.4 Blocking solution

PBS	1000ml
BSA (Fraction V) 1% (w/v)	10g

2.1.1.5 Dialysis buffer

PBS	5000ml
EDTA (1mM)	1.86g

2.1.1.6 Dialysis Buffer for Fab preparation

20mM Na_2HPO_4	14.2g
10mM EDTA	18.6
dH_2O	5000ml

Should be pH 7.0.

2.1.1.7 Digestion Buffer for Fab preparation

Cysteine-HCl	4.22mg
Phosphate Buffer pH 10	12ml

2.1.1.8 Dialysis Buffer and Digestion Buffer for F(ab)$_2$ Preparation

20mM $C_2H_3O_2Na \cdot 3H_2O$	2.72g	13.61g
dH_2O	1000ml	5000ml

pH to 4.5 using 100% Glacial Acetic Acid

2.1.1.9 Carbonate Buffer

Na_2CO_3	132.5g
NaCl	29.2 g

Make up to 5000ml with dH_2O and adjust the pH to 9 with 5M HCl.

2.1.1.10 0.1M Sodium Bicarbonate pH 8.4

$NaHCO_3$	8.4g
Distilled Water	1000ml

2.1.2 Solutions and Buffers for SDS-PAGE

2.1.2.1 1M Tris-HCl pH 8.8

Tris (g)	60.57 g

Dissolve in approx. 300 ml dH_2O.

Adjust pH to 8.8 with 5M HCl (approx. 13.4 ml)

Make up to 500 ml with dH_2O.

2.1.2.2 1M Tris-HCl pH 6.8

Tris (g)	60.57 g

Dissolve in approx. 300 ml dH_2O.

Adjust pH to 6.8 with 5M HCl (approx. 91ml)

Make up to 500 ml with dH_2O.

2.1.2.3 Stock 50% Acrylamide

NB Acrylamide is a cumulative neurotoxin but it is safe once it is in solution. Therefore weighing out and dissolving should be performed in a fume cupboard while wearing a mask and gloves. Once in solution it should be stored in the dark by covering the bottle with tin foil and placing in a cupboard.

Acrylamide (g) 48.75% (w/v)	48.75	121.875	243.75	487.5
Bisacrylamide (g) 1.25% (w/v)	1.25	3.125	6.25	12.5
H_2O to (ml)	100	250	500	1000

2.1.2.4 SDS 10% (w/v)

SDS (g)	10	25	50
dH_2O (ml)	100	250	500

2.1.2.5 Ammonium Persulphate 1.5% (w/v) (amperes)

Ammonium Persulphate	150	mg
dH_2O	10	ml

2.1.2.6 Electrode Buffer Stock (x10) pH ~8.3

Glycine (1.92M)	144.13 g
Tris (0.25M)	30.28 g
dH_2O	1000 ml

2.1.2.7 Sample Buffer

10% (w/v) sodium dodecyl sulphate (SDS)	10g
10% (v/v) 2-mercaptoethanol	10ml
50% (W/V) sucrose	50g
0.005% Bromophenol blue	0.005g
0.125 M Tris-HCl pH 6.8 to	100ml
(= 1:8 dilution 1M Tris-HCl pH 6.8)	

2.1.2.8 Overlay Buffer

1M Tris-HCl pH 8.8	19ml
dH_2O	40ml
Ethanol	25ml
Bromophenol Blue	1-2 crystals

2.1.2.9 Destain

Methanol	750	1500	ml
Acetic acid	500	1000	ml
H_2O	2900	5800	ml

2.1.2.10 Coomassie Blue Stain

0.3% (W/V) Coomassie	1.2	1.5g
Destain solution (above)	400	500ml

Stir until dissolved then filter through filter paper before use.

2.1.2.11 Running Buffer for SDS Gels

dH_2O	1780ml
SDS 10% (w/v) solution	20ml
Electrode Buffer	200ml

2.1.3 Composition of SDS-polyacrylamide gels (Laemmli System)

2.1.3.1 Separating gel (50 ml)

	Final Concentration			
	5%	7.5%	10%	12.5%
1M Tris-HCl pH 8.8 (mls)	18.75	18.75	18.75	18.75
dH_2O (mls)	24.625	22.125	19.625	17.125
Acrylamide (50% w/v) (mls)	5.00	7.50	10.00	12.50
Degas then add				
10% W/V SDS (mls)	0.50	0.50	0.50	0.50
TEMED (mls)	0.031	0.031	0.031	0.031
1.5% W/V amperes (mls)	1.125	1.125	1.125	1.125

2.1.3.2 Stacking gel 15 ml (30 ml)

	Final Concentration			
	3%		5%	
1M Tris-HCl pH 6.8 (mls)	1.875	(3.75)	1.875	(3.75)
dH_2O (mls)	11.55	(23.10)	10.95	(21.90)
Acrylamide (50% w/v) (mls)	0.90	(1.80)	1.5	(3.00)
Degas then add				
10% w/v SDS (mls)	0.15	(0.30)	0.15	(0.30)
TEMED (mls)	0.015	(0.03)	0.015	(0.03)
1.5% W/V ampers.(mls)	0.525	(1.05)	0.525	(1.05)

2.1.4 pH elution buffers

2.1.4.1 Citrate-Phosphate Buffer; pH range ~2.5 to 7.0

(a) 0.1M Citric acid; 19.21 g/l (M.W. 192.1)

(b) 0.2M Dibasic sodium phosphate; g/l

Mix citric acid and sodium phosphate solutions in the proportions indicated and adjust the final volume to 100ml with deionised water. Adjust the final pH using a sensitive pH meter.

pH	2.6	3.0	3.4	3.8	4.2	4.6	5.0	5.4	5.8	6.2	6.6	7.0
ml of Citric acid	44.6	39.8	35.9	32.3	29.4	26.7	24.3	22.2	19.7	16.9	13.6	6.5
ml of sodium phosphate	5.4	10.2	14.1	17.7	20.6	23.3	25.7	27.8	30.3	33.1	36.4	43.6

2.1.4.2 Glycine-HCl Buffer; pH range 2.1 to 4.0

(a) 0.1M Glycine: 7.5 g/l (M.W.75.0)

(b) 0.1M Hydrochloric acid

Mix 50 ml of glycine and indicated volume of hydrochloric acid. Mix and adjust the final volume to 100 ml with deionized water. Adjust the final pH using a sensitive pH meter.

pH	2.2	2.4	2.6	2.8	3.0	3.2	3.4	3.6
ml of HCl	44.0	32.4	24.2	16.8	11.4	8.2	6.4	5.0

2.1.5 100 mM Phosphate Buffer pH 6.5 (Iodination buffer)

Prepare buffers A and B in deionised water:

A) 100mM KH_2PO_4	13.609 g/L
B) 100mM Na_2HPO_4	14.196 g/L

Mix seven parts (350mls) of A with three parts (150mls) of B and adjust the pH using either A to make it lower and B to make it higher.

2.1.6 Confocal reagents

2.1.6.1 Confocal fixative

PBS (autoclaved for 20 minutes at 121°C)	100ml
Paraformaldehyde 4% (w/v)	4g

Stirred on a hotplate set at approximately 60°C for 20 minutes, avoiding boiling the solution. Once fully dissolved the solution was passed through a folded filter paper and stored at 4°C. Paraformaldehyde is not very stable and can come out of solution after short periods of standing, and so was made up fresh every time.

2.1.6.2 Mountant containing an antifade agent

x10 antifade solution:

1, 4 Diazobicyclo (2, 2, 2) octane (DABCO)	2g
Tris-HCl, pH5.5	10mls

Mountant containing antifade:

Glycerol	18mls
X10 antifade solution	2mls

2.1.6.3 Toluidine Blue solution

Toluidine powder	1g
Sodium tetraborate (borax)	1g
Distilled water	200ml

2.1.7 Solutions for EM studies

2.1.7.1 Piperazine (PIPES) buffer

Piperazine-NN'-bis-2-ethanesulphonic acid (PIPES) 60.48g

10M Sodium hydroxide (NaOH)

The piperazine was mixed with 900ml of distilled water. The 10M sodium hydroxide solution was added to bring the pH up to 7.2. It was then made up to 1L with distilled water to produce a 0.2M solution of PIPES buffer.

2.1.7.2 Sodium alginate

A gram of sodium alginate powder was sprinkled on to 20ml distilled water on a magnetic stirrer. This was stirred until totally dissolved and gelatinous (approximately 30 minutes) and was stored frozen until needed.

2.1.7.3 Reynolds lead stain

$Pb(NO_3)_2$	1.33g
$Na_3C_6H_5O_7.2H_2O$	1.76g
Distilled water	30ml
1M NaOH	8ml

The lead nitrate and sodium citrate were placed into the distilled water in a very clean container. The solution was shaken for 1 minute and then intermittently for 30 minutes to produce a milky suspension. The sodium hydroxide was added and shaken until clear. Hen the solution was made up to 50ml with fresh distilled water.

2.1.7.4 Sucrose +10k PVP

2.3M sucrose in PBS	40ml
PVP 10K	10g
1.1M Na_2CO_3	2.0ml

Stirred for 3-4 hours and then left for a few hours or overnight to allow the bubbles to leave the solution.

2.1.7.5 Uranyl acetate/methyl cellulose

A normal 3% (saturated) uranyl acetate in water solution was filtered through a Millipore filter (0.2μm) before each use. One part uranyl acetate was mixed with nine parts methyl cellulose, both were at 4°C. Embedding was carried out on ice at 4°C.

2.2 General Protocols

2.2.1 Culturing the Human acute T-cell leukaemia cell line HSB-2

The HSB-2 cell line was derived from a patient with T-cell acute lymphoblastic leukaemia (T-ALL) (Adams *et al* 1970) and obtained from the American Tissue Culture Collection (ATCC, Bethesda, MD). Cells were cultured in antibiotic-free RPMI-1640 medium (Sigma-Aldrich Company Ltd., Dorset, UK) containing 10% FetalClone foetal calf serum (Pierce and Warriner, UK now known as Perbio), and supplemented with 1mM L-glutamine and 1mM sodium pyruvate (Sigma-Aldrich Company Ltd., Dorset, UK). Hereafter it will be referred to as R10 medium. The cells were maintained continuously in the logarithmic phase of growth by passage at regular intervals in a humidified atmosphere of 5% CO_2/95% air in an incubator at 37°C.

2.2.2 Cell quantification and viability

Cell densities were determined using 0.4% (w/v) Trypan Blue in PBS (filter sterilised) and a haemocytometer. 50μl of trypan blue was mixed with 50μl of cell suspension. This was then transferred to both chambers of the haemocytometer via capillary action. The cells were counted in all of the small squares in the grid.

To calculate the number of cells/ml of cell suspension the counts from both chambers were added together, divided by 10 and multiplied by 10^5. I.e.

$23+24 / 10 \times 10^5 = 4.7 \times 10^5$ cells/ml.

Cell viability was assessed using the principle that live cells will exclude 0.4% Trypan blue but dead cells will not. Any cells found to exclude the dye were considered to be viable. Cells were used at 95% or greater viability.

2.3 Conjugations and Purifications

2.3.1 Antibody Production

The anti-CD7 and anti-CD38 antibodies HB2 and OKT10 respectively were produced by growing their respective hybridomas in DMEM (with high glucose content) in static culture. Once confluent the HB2 hybridoma cells were transferred to an Acusyst R hollow fibre bioreactor system (Endotronics Inc., Minneapolis, MN) and OKT10 hybridoma cells were cultured on an Integra Technomouse hollow fibre system (Integra Biosciences, Cramlington, UK) as per manufacturers instructions. Supernatants containing Ab were harvested periodically. The first stage in the purification of both antibodies from these harvests was an ammonium sulphate precipitation to produce a crude extract. Further purification of Ab was conducted by anion exchange chromatography on a DEAE-Sepharose column with a sodium chloride gradient, followed by gel filtration on Sephacryl S200HR (Sigma-Aldrich Company Ltd., Dorset, UK). HB2 and OKT10 antibodies are both of the IgG_1 subclass. Flow cytometry and immunohistochemical staining of sections of frozen tonsil have confirmed the specificity of these antibodies.

2.3.2 Saporin Production

Seeds of the Soapwort plant *Saponaria officinalis* were kindly supplied by Chiltern Seeds, Ulverston, Cumbria, UK. The SO6 isoform of saporin was extracted from the seeds using the method of Stirpe *et al* (1983). The crude extract was then purified to homogeneity by cation exchange chromatography on carboxymethyl-sepharose with a sodium chloride gradient followed by gel filtration on a Sephacryl-S200HR column (Sigma-Aldrich Company Ltd., Dorset, UK). The product gave a single band on SDS-PAGE of 29,500 D molecular weight, and was immunoreactive with both polyclonal and monoclonal anti-saporin antisera on ELISA.

2.3.3 Immunotoxin construction

The immunotoxins HB2-Saporin (anti-CD7) and OKT10-Saporin (anti-CD38) were constructed by conjugating HB2 or OKT10 Ab to saporin using the heterobifunctional cross-linking reagent N-succinimidyl 3-(2-pyridyldithio)-propionate (SPDP) (Pharmacia, Uppsala, Sweden) as described previously (Thorpe *et al.*, 1985). Immunotoxins produced using this method contained a non-hindered disulphide bond between the Ab and saporin moiety. Gel filtration on a Sephacryl S200-HR column was used to remove any free saporin from the conjugate. A column containing Carboxymethyl-Sepharose (Sigma-

Aldrich Company Ltd., Dorset, UK) was used to remove any free Ab from the immunotoxin as described by Lambert *et al.*, (1985). The immunotoxin was dialysed into PBS pH7.2 and sterilised through a 0.2μm filter. Aliquots were stored at -80°C.

2.3.4 Preparation of Fab' Fragments

Fab' fragments of mouse monoclonal IgG_1 were prepared using Pierce ImmunoPure® Fab' Preparation kit (Pierce and Warriner, Rockford, IL). The method was carried out according to the manufacturer's instructions. Briefly, an Ab was dialysed overnight against 20mM disodium hydrogen orthophosphate containing 10mM ethylenediaminetetraacetic acid (EDTA) pH 7.0 (section 2.1.1.6). Antibodies were taken off dialysis and concentrated to 20mg/ml in an amicon chamber under nitrogen pressure. 500μl of digestion buffer was added to 500μl of Ab. The 1ml sample was then added to a tube containing equilibrated immobilised papain (supplied within the kit). This solution was rotated overnight at 37°C. Protein A columns were equilibrated with ImmunoPure® IgG Binding Buffer. The solubilised Fab', Fc fragments and undigested IgG were recovered and applied to the column. The columns were washed with ImmunoPure® Binding Buffer and the eluate containing the Fab' fragments was collected. The fragments were dialysed against PBS and 1mM EDTA pH 7.4 (section 2.1.1.5) overnight in dialysis tubing with a 12-14 kD MW cut-off. After dialysis, the F(ab) fragments were measured on the UV spectrophotometer at 280nm to determine their protein content.

$$\text{Protein concentration (mg/ml)} = \frac{OD_{280}}{1.45}$$

The samples were passed through a 0.2μm filter.

Samples were tested by flow cytometry and SDS-PAGE to confirm the absence of an Fc region.

2.3.5 Preparation of F(ab')$_2$ Fragments

$F(ab')_2$ fragments of mouse monoclonal IgG_1 were prepared using the Pierce ImmunoPure® $F(ab')_2$ Preparation Kit (Pierce and Warriner, UK now known as Perbio). This method was carried out according to the manufacturer's instructions. Briefly, an Ab was dialysed overnight against a 20mM sodium acetate buffer at pH 4.5. Once taken off dialysis the Ab was concentrated to 20mg/ml. 500μl of the 20mM sodium acetate (pH

4.5) digestion buffer (section 2.1.1.8) was added to 500µl of Ab. The 1ml sample was then added to a tube containing equilibrated immobilised pepsin. This solution was rotated overnight at 37°C. Protein A columns were equilibrated with ImmunoPure® Binding Buffer. The solubilised $F(ab')_2$, Fc fragments and undigested IgG were recovered and applied to the column. The columns were washed with ImmunoPure® Binding Buffer and the eluate containing the $F(ab')_2$ fragments contaminated with small Fc fragments no longer capable of binding to protein A, was collected. Samples were then purified on a Superdex column.

Before samples were used for flow cytometry studies they were further dialysed against PBS containing 1mM EDTA pH 7.4 (section 2.1.1.5) and were passed through a 0.2µm filter. Samples were tested by flow cytometry and SDS-PAGE to confirm that there was no Fc fragment still attached to the fragments.

2.3.6 Preparation of fluorescein-conjugated antibodies

Antibodies were directly conjugated to fluorescein isothiocyanate (FITC) for flow cytometry and confocal microscopy studies. Using the following protocol, 20mg of Ab was dialysed overnight against carbonate buffer pH 9.0 (section 2.1.1.9). This was done to remove any trace amounts of primary amine-containing components or sodium azide in the original buffer and to raise the pH.

FITC (Sigma-Aldrich Company Ltd., Dorset, UK) was dissolved in carbonate buffer at a concentration of 10mg/ml. Following dialysis, 0.05mg of FITC per mg of Ab was added to the Ab (10mg/ml) i.e. 100µl FITC and stirred overnight at 4°C. The reaction mixture was then loaded onto a Sephadex G25 (Pharmacia & Upjohn Ltd, Milton Keynes, UK) column equilibrated in PBS containing 1mM EDTA pH 7.4 to remove unconjugated FITC. Two coloured fractions were visible on the column. Fractions from the first peak were pooled, since the Ab is first to pass through the column, and filter sterilised through a 0.2µm filter (Bibby Sterilin Ltd., Staffordshire, UK).

The concentration of protein in the sample was determined by reading the absorbance of the conjugate at 278nm (A_{278}) and 495nm (A_{495}) as according to Wood *et al* (1965):

$$\text{Protein concentration (mg/ml)} = \frac{A_{278} - (0.26 \times A_{495})}{1.35}$$

where 0.26 is the correction factor to compensate for the absorbance of the dye at 278nm and 1.35 is the extinction coefficient of murine IgG.

The molecular fluorescein/protein ratio (F/P) was calculated by reading the absorbance of the conjugate at 280nm (A_{280}) and 495nm (A_{495}):

$$\text{Molar ratio} = \frac{\text{MW IgG}}{\text{MW FITC}} \times \frac{\text{conc. FITC (mg/ml)}}{\text{conc. IgG (mg/ml)}}$$

$$\text{Simplified to} = \frac{2.87 \times A_{495}}{A_{280} - 0.35 \times A_{495}}$$

assuming a molecular weight for IgG of 160,000 and of 390 for FITC. The formula for calculating the concentration of FITC was $A_{278}/200$ using the extinction coefficient for chromatically pure crystalline isomer I FITC.

2.3.7 Preparation of Alexa Fluor™ 568-conjugated antibodies

The Alexa Fluor™ 568 Protein Labeling Kit (Molecular Probes Europe BV, Leiden, The Netherlands) was used to conjugate this dye to the Ab. The method was carried out according to the manufacturer's instructions. Briefly, an Ab was dialysed overnight against 0.1 M sodium bicarbonate, pH 8.4 (section 2.1.1.10), to remove any trace amounts of primary amine-containing components in the original buffer and to adjust the pH. After dialysis the Ab was diluted to 2mg/ml. 500µl of the protein solution was added to a vial containing an aliquot of reactive dye. The vial was inverted a few times and the mixture was allowed to react for 1 hour at room temperature. The reaction was stopped by the addition of a hydroxylamine solution and allowed to stir for an additional 30 minutes at room temperature. The sample was then loaded onto the purification column (supplied within the kit) and the first visible fraction was collected.

The concentration of protein in the sample was found by reading the absorbance of the conjugate at 280nm (A_{280}) and 577nm (A_{577}):

$$\text{Protein concentration (M)} = \frac{[A_{280} - (A_{577} \times 0.46)]}{203{,}000}$$

where 203,000 is the molar extinction coefficient of a typical IgG and 0.46 is a coefficient factor to account for absorption of the dye at 280 nm.

The degree of labelling was determined as follows:

$$\text{Moles dye per mole protein} = \frac{A_{577}}{91{,}300 \times \text{protein concentration (M)}}$$

where 91,300 is the appropriate molar extinction coefficient of the Alexa Fluor 568 dye (referred to hereafter as AF568) at 577nm.

2.4 Sodium Dodecyl Sulphate Polyacrylamide Gel Electrophoresis (SDS-PAGE)

Sodium dodecyl sulphate-polyacrylamide gel electrophoresis was performed according to the method of Laemmli (1970) on slab gels. The slab gels were prepared as described in section 2.1.3. A separating gel of either 5, 7.5 or 10% (w/v) was formed using the Bio-Rad moulding apparatus. Once the separating gel had been poured, a thin layer of overlay buffer was placed on the top of the gel to ensure polymerisation occurred under anaerobic conditions. When the separating gel had set, the overlay buffer was rinsed off with distilled water and a 3% (w/v) stacking gel was layered on top. Before the stacking gel started to set, a well forming comb was inserted into the gel.

Immediately prior to the electrophoretic run, the well forming comb was removed, the upper and lower chambers were filled with running buffer and the cooling chamber was filled with cold running tap water. The samples were then loaded carefully into the wells.

Electrophoresis was carried out through the stacking gel at 100 volts for 30 minutes before the voltage was increased to 300 volts for the duration of the run. When the dye front was near the bottom of the gel, the run was finished. The gel was taken off and placed in 0.3% (w/v) Coomassie blue stain overnight and then destained with several changes of destain solution over a period of approximately 18h.

2.5 Animal studies

2.5.1 SCID Mice

Specific pathogen-free CB-17 *scid/scid* (SCID) mice of both sexes 6-10 weeks of age were obtained from our own breeding colony and used in all the experimental work described here. The animals were maintained under sterile conditions inside a laminar flow isolator housed on sterile bedding and fed on autoclaved food and filter sterilised

water *ad libitum*. Animals for experimental use were taken out from the isolator and transferred to autoclaved filter top microisolator cages. These animals were housed on sterile bedding as five single-sex animals to a cage, and were continued to be fed with sterile food and water *ad libitum*. All manipulations to these mice were carried out in a laminar flow hood by personnel using aseptic techniques.

2.5.2 Establishment of HSB-2 Leukaemia in SCID Mice

Each SCID mouse was injected intravenously into the tail vein with $2x10^6$ HSB-2 cells in a volume of 200µl of R10 medium. In all therapy studies the cells were injected into the SCID mice seven days prior to the commencement of any kind of treatment.

2.5.3 Therapy Protocols

Therapy was commenced seven days after the mice had been injected intravenously with the HSB-2 cells. Each treatment was given as a bolus injection in a 200µl volume of PBS into the tail vein. Different groups were treated with 10µg doses of either IT, Ab or a combination of both. Where a combination of two ITs, two Abs or an IT plus an Ab were given, the 10µg dose was comprised of 5µg of each component part. All animals were monitored daily throughout the study, and any animal that displayed hind leg paralysis or that were obviously unwell were killed humanely.

2.6 Cell Proliferation Assay

HSB-2 cells (2×10^5) were cultured in 10mls R10 medium in T25 culture flasks in the presence of various concentrations of IT, Ab and combinations of both. The medium for this assay was supplemented with penicillin and streptomycin (P/S) at 100U/ml and 100µg/ml respectively. Control cultures were grown in R10 medium with antibiotics only. Viable cell counts were performed on a regular basis using Trypan Blue dye exclusion (described in section 2.2.2). The various culture conditions are summarised in Table 2.1.

Table 2.1 Summarises the conditions cells were cultured in for the long term cell proliferation assay.

Condition Number	Condition
1	R10 medium + P/S
2	0.5μg/ml OKT10-Saporin IT
3	0.5μg/ml HB2-Saporin IT
4	0.25μg/ml OKT10-Saporin IT + 0.25μg/ml HB2-Saporin IT
5	0.25μg/ml OKT10-Saporin IT + 0.25μg/ml HB2 Ab
6	0.25μg/ml HB2-Saporin IT + 0.25μg/ml OKT10 Ab
7	0.5μg/ml HB2 Ab
8	0.5μg/ml OKT10 Ab
9	0.25μg/ml HB2 Ab + 0.25μg/ml OKT10 Ab

2.7 Protein Synthesis Inhibition Assay

This assay was used to determine IC_{50} values for any cytotoxic agents and to test for toxicity of any agents used on the cells by measuring the incorporation of ^{3}H-leucine into cells after incubation with these reagents.

Fresh R10 medium containing 100U/ml penicillin and 100μg/ml streptomycin was used to make all of the serial dilutions of the reagents to be tested. 100μl of each dilution was added in triplicate to the wells of a flat-bottomed 96-well microtitre plate. In the case of control cultures, 100μl of medium alone was plated. 100μl of a cell suspension containing $5x10^5$ cells/ml (resuspended in R10 medium) was added to give a final density of $5x10^4$ cells per well. Cultures were incubated at 37°C for 48 hr in a humidified atmosphere of 5% CO_2/95% air. After this period 1μCi [^{3}H]-leucine (ICN Biomedicals, Ltd., Basingstoke, UK) was added to each culture well and incubated for a further 14-16 hr. The extent of ^{3}H-leucine incorporation was measured by harvesting the cells onto glass fibre filter discs (Camo, Trondheim, Norway) using a Combi cell harvester (Skatron, Lier, Norway). Discs were dried for 1-2 hr before individual discs were placed into scintillation vials containing 1ml Opti-Fluor O scintillant (Canberra Packard, Pangbourne, UK). The vials were counted for radioactivity on a 1600TR Scintillation analyser (Canberra Packard, Pangbourne, UK) using a protocol specific for measuring tritium. Results were expressed

as a percentage of the ^{3}H-leucine incorporated in untreated cells maintained under identical conditions.

2.8 Flow Cytometric Analysis

The Epics XL Flow Cytometer (Beckman Coulter UK, High Wycombe) equipped with Coulter PC-based analytical software was used for the analysis of surface level immunofluorescence.

2.8.1 Indirect method

One million (or 5 x 10^5) HSB-2 cells were incubated with primary Ab or IT at 10µg/ml for 30 minutes at 4°C. Dilutions of reagents to be tested were prepared in chilled PBS pH 7.4 + 0.1% sodium azide (NaN_3). Irrelevant isotypic controls or PBS were used to indicate non-specific fluorescence levels. Samples were washed twice with wash solution (section 2.1.1.2) at 1500 rpm for 5 minutes to remove excess unbound Ab. 50µl of a 1:50 dilution of fluorescein isothiocyanate (FITC) labelled $F(ab)_2$ sheep anti-mouse IgG (whole molecule) immunoglobulin (Sigma-Aldrich Company Ltd., Dorset, UK) was added to the dry cell pellets, which were resuspended by vortexing and incubated at 4°C for a further 30 minutes. Cells were washed twice with wash solution to remove excess Ab. Pellets were resuspended in 500µl PBS and 0.1% NaN_3, vortexed and read on the flow cytometer.

2.8.2 Direct method

HSB-2 cells (1x10^7) were pelleted at 1500 rpm for 5 minutes and the supernatant aspirated. The cells were then resuspended in 1ml PBS and 0.1% NaN_3. Dilutions of reagents were made in chilled PBS pH 7.4 + 0.1% NaN_3. 10µl of each dilution was added to 100µl of the cell suspension (1x10^6 cells), vortexed and incubated for 20 minutes at room temperature. The cells were washed twice at 1500rpm for 5 minutes with wash solution. Pellets were resuspended in 500µl PBS + 0.1% NaN_3, vortexed and read on the flow cytometer.

Specific protocols were used to select for cells excluding dead cells and debris by using forward and side light scatter to gate with. The fluorochrome was excited with an argon laser light of 488nm and the emission intensity was measured at 515-545nm for FITC.

Five thousand cells were analysed and histograms of cell number against fluorescence intensity were produced for each sample. The mean fluorescence intensity (calculated by the flow cytometer software) was used for sample analysis.

2.8.3 Flow cytometric endocytosis assay

2.8.3.1 Monitoring Individual Endocytosis Trends

This method was based on an approach used by May *et al* (1991). Two conditions were set up for this investigation. To determine the rate of internalisation of cells saturated with Ab, $3x10^7$ cells were incubated with Ab at a concentration of 10μg/ml (in 3ml) for 30 minutes at 4°C in PBS containing 0.1% sodium azide (PBS + 0.1% NaN_3). Excess Ab was removed by washing twice with PBS + 0.1% NaN_3 at 1500 rpm for 5 minutes and then the cells were resuspended in 30mls prewarmed culture medium (R10) at 37°C. The flask was incubated at 37°C for the following time points before samples were taken at: 0, 30minutes, 1, 3, 6, 12, and 24hr.

The endocytosis rate was also monitored in cells continuously exposed to Ab. The cells for this part of the study had been unexposed to Ab for the first time point, but were then resuspended in medium containing a saturating concentration of Ab (10μg/ml). This flask was also incubated at 37°C for the same time points as above.
At each of the times mentioned above, samples (each consisting of $1x10^6$ cells) were taken from both flasks and the cells washed twice in wash solution. Half of the samples were then incubated with 50μl of a 1:50 dilution of a FITC-labelled $F(ab')_2$ sheep anti-mouse IgG secondary Ab (Sigma-Aldrich Company Ltd., Dorset, UK) diluted in PBS + 0.1% NaN_3, for 30 minutes at 4°C. These samples were washed twice with wash solution and then analysed by flow cytometry. The second set of samples were reincubated with the primary Ab, for a further 30 minutes, washed twice and then exposed to the secondary Ab as above before being analysed by the flow cytometer.

To determine the proportion of Ab internalised at each of the time points, control cells were saturated with Ab and detected by the secondary Ab as described above. To measure the amount of non-specific interaction with the cells, an isotypic, irrelevant MAb (BU12) was incubated with the cells before incubation with the secondary Ab. The percentage of Ab modulated from the cell surface was calculated as follows:

$$\% \text{ Ab modulated} = \frac{\text{MFI sample} - \text{MFI isotypic control}}{\text{MFI positive control}} \times 100$$

Where MFI is the mean fluorescence intensity.

Data from these studies were plotted in duplicate as a percentage of the mean fluorescence intensity produced by control cells saturated with the primary Ab and maintained at 4°C to prevent endocytosis occurring.

The same series of experiments were also performed with immunotoxins constructed with both native antibodies to determine if the addition of the saporin molecule to the Ab influenced the internalisation characteristics. Fab' fragments of both antibodies were investigated to determine whether or not bivalent binding was a requirement for internalisation of the antibodies used in these studies. These reagents were used at a molar equivalent concentration (6.25×10^{-5}M) to the antibodies used.

2.8.3.2 Monitoring Combination Endocytosis Trends

2.8.3.2.1 Approach 1

To study the effects of simultaneous co-ligation of CD7 and CD38, both antigens were saturated by IT (HB2 and OKT10 IT respectively). Two flasks were set up with both pulsed and continuous exposure to IT. Cells (3×10^7) were either pulsed with 3ml containing 24.6μg/ml (12.3μg/ml of each individual IT) for 30 minutes at 4°C, washed twice at 1500 rpm for 5 minutes, then resuspended in 30mls of R10 medium at 37°C or resuspended in 30mls R10 medium containing 12.3μg/ml of both HB2 and OKT10 IT. Samples were taken from the flasks at the same time points and were treated as in section 2.8.3.1 except that the cells were labelled with 50μl of a 1:25 dilution of the sheep anti-mouse FITC conjugated secondary Ab. To determine the proportion of Ab internalised at each of the time points, control cells (1×10^6) were saturated with 100μl containing both HB2 and OKT10 IT each at 12.3μg/ml and detected by the secondary Ab as above. To measure the amount of non-specific interaction with the cells, an isotypic, irrelevant IT,

BU12 (anti-CD19), was incubated with the cells at 24.6μg/ml for 30 minutes on ice before incubation with the secondary Ab.

2.8.3.2.2 Approach 2

A second approach was used to show the modulation of each individual antigen in a combination study. This was achieved by using one intact Ab in combination with the $F(ab)_2$ fragment of the second Ab. The pulsed flask was set up by incubating $3x10^7$ cells with 3 mls of PBS + 0.1% NaN_3 containing either 10μg/ml HB2 Ab in combination with 6.875μg/ml OKT10 $F(ab)_2$ or 10μg/ml OKT10 Ab in combination with 6.875μg/ml HB2 $F(ab)_2$, for 30 minutes on ice. The cells were then washed twice at 1500rpm for 5 minutes and resuspended in 30mls R10 medium at 37°C. The continuous exposure flask was set up by resuspending $3x10^7$ cells in 30 mls R10 medium containing the same combinations of Ab and $F(ab)_2$ fragments at 37°C.

Samples were taken from both flasks at times 0, 30 minutes, 1, 3, 6, 9 and 24 hours and either labelled with 50μl of a 1:100 dilution of an anti-mouse IgG (Fc-specific)-FITC conjugate (Sigma-Aldrich Company Ltd., Dorset, UK) for 30 minutes on ice or were reincubated with the combination of Ab and $F(ab)_2$ fragment for 30 minutes at 4°C before being labelled with the same secondary reagent. To determine the proportion of Ab internalised at each of the time points, control cells were saturated with 100μl containing the combination of Ab and $F(ab)_2$ fragment and detected by the secondary Ab as above. To measure the amount of non-specific interaction with the cells, an isotypic, irrelevant Ab and its $F(ab)_2$ fragment (BU12) were incubated with the cells at 10μg/ml and 6.875μg/ml respectively for 30 minutes on ice before incubation with the secondary Ab. The percentage of modulation of Ab was calculated as described in section 2.8.3.1.

2.8.4 Monitoring associations between CD7 and CD38

An investigation to answer whether or not any associations exist between the two antigens CD7 and CD38 was also undertaken. In this experiment, one antigen was ligated with Ab at the start of the experiment to stimulate modulation of the molecule and at various time points the second antigen was detected by the use of a directly labelled Ab to the antigen. A pulsed flask was set up where $3x10^7$ cells were incubated with a saturating

concentration (10μg/ml) of either HB2 or OKT10 Ab in 3mls for 30 minutes at 4°C. The cells were then washed twice at 1500rpm for 5 minutes and resuspended in 30mls R10 medium at 37°C. Samples of 10^6 cells were taken from the flask at each of the following time points: 0, 30 minutes, 1hr, 3hr, 6hr, 9hr and 24hr. The samples were either labelled with 50μl of a 1:50 dilution of the sheep anti-mouse IgG FITC conjugate, washed as before and read on the flow cytometer or were incubated for 30 minutes on ice with 100μl of a 10μg/ml solution of a FITC conjugated Ab (the opposite Ab to that, that the cells had already been incubated with), washed and then read on the flow cytometer.

2.9 Radiosiotopic studies

2.9.1 Radioiodination

Antibodies or ITs were radiolabelled using carrier-free ^{125}Iodine (ICN) and IODO-BEADS® (Pierce and Warriner) according to Manufacturer's instructions. Briefly, one IODO-BEAD® was allowed to react with 1mCi of ^{125}Iodine at room temperature for 5 minutes prior to the addition of 500μg of Ab (or IT) diluted in iodination buffer. The reaction, which took place in a sealed eppendorf, was allowed to proceed for 15 minutes before the reaction was stopped by removing the mixture from the IODO-BEAD®. Gel filtration was performed to remove excess $Na^{125}I$ or unincorporated $^{125}I_2$ from the iodinated Ab. PBS was used as the elution buffer. Econo-Pac 10DG columns (Bio-Rad) were used for this purpose.

2.9.2 Measurement of radioactivity incorporated into protein

As not all of the total activity in a radiolabelled sample is covalently bound to the protein (due to the imperfections of labelling and fractionation procedures) a formula was used to determine the amount of radioactivity incorporated into the Ab.

Two discs of glass fibre filter paper were placed on top of test tubes, 5μl of a labelled sample was added to the middle of each disc and allowed to dry. The radioactivity contained on these discs was counted on an LKB Wallac γ-counter (1282 Compugamma Universal Gamma Counter). These discs were added to tubes containing 2ml 10% (w/v) trichloroacetic acid (TCA) solution, left for 10 minutes while vortexing occasionally before the liquid was discarded. A second 2ml of acid solution was added and left for 10 minutes. After the liquid was discarded, 2ml of ethanol was added and left for 10 minutes,

vortexing occasionally. The ethanol was discarded and the discs left to dry before being placed in clean tubes and the radioactivity measured as before. The radioactivity incorporated into the Ab was calculated as follows:

Total protein-bound radioactivity in sample =

$$\text{mean activity after acid precipitation} \times \frac{\text{total volume of sample}}{\text{volume of aliquot}}$$

And the efficiency of the labelling procedure was calculated as below:

Percentage of sample radioactivity bound to protein =

$$\frac{\text{mean activity after acid precipitation}}{\text{mean activity before acid precipitation}} \times 100$$

This value was taken into account when performing Scatchard analysis from the data produced from these radioactive conjugates.

2.9.3 *Scatchard Plot Analysis*

HSB-2 cells ($1x10^6$) were spun down in capped universals at 1500rpm for 5 minutes. Ab dilutions of 20, 10, 2, 1, 0.2 μg/ml were made by serial dilutions into PBS + 1% BSA and 0.1% NaN_3. Once the cells were spun down, the supernatant was decanted to waste and either 200μl of unlabelled Ab (identical to the labelled Ab of interest) at 20mg/ml or PBS was added to the cell pellets and incubated for 5 minutes at 4°C. 200μl of each dilution of labelled Ab was then added to both sets of tubes and incubated at 4°C for 30 minutes. The samples were washed by spinning the cell suspension on top of a 180μl layer of phthalate oil (made from 1 part dinonyl phthalate oil and 4 parts di-butyl phthalate oil) for 90 seconds at 13,600g. The vessels were frozen in liquid nitrogen and the cell pellet sliced off. Both the cell pellet and the supernatant were counted on the γ-counter.

A Scatchard plot (1949) was performed on this data of Bound (counts from the pellet) against Bound/Free (counts from the pellet divided by the counts from the supernatant). The inverse of the gradient was used to determine the affinity of these reagents for their antigens.

Calculation for the number of binding sites per cell:

Bound	=	no. CPM on x-intercept
Mass of protein bound	=	Bound (CPM)/Specific Activity (CPM/μg protein)
No. moles protein bound	=	Mass (g/l) /molecular weight (ie 160,000)
No. binding sites	=	No.moles x Avogadro's number (6.022×10^{23})
No. binding sites per cell	=	No. binding sites/no. cells

Calculation for the K_D of the Ab:

Gradient	=	$\delta y/\delta x$
K_D	=	(1/gradient)
Divide by specific activity	=	μg/400μl (reaction volume)
Multiply by reaction volume	=	μg/L
Divide by 10^6	=	g/L
Multiply by molecular weight	=	Molarity

2.10 Confocal microscopy studies

2.10.1 Competitive Binding Studies

In competitive binding studies, $1x10^6$ HSB-2 cells were incubated for 30 minutes at 4°C with fluorophore-labelled Ab at a concentration of 20μg/ml in the presence or absence of a 10- or 100-fold mass excess of: 1) the same unconjugated Ab, or 2) an Ab irrelevant for the antigen but relevant for the cell line, or 3) an Ab irrelevant for the antigen and the cell line. This was performed for 30 minutes at 4°C (to prevent endocytosis) before the cells were fixed in paraformaldehyde. All antibodies were of the IgG_1 isotype. Cells were washed twice by centrifugation at 1500rpm for 5 minutes in cold PBS, fixed in 4% paraformaldehyde for 20 minutes at 4°C, and washed twice again before they were immobilised by cytospinning for 5 minutes at 800rpm onto glass slides. The slides were analysed with the Leica TCS 4D Confocal Microscope.

2.10.2 Endocytosis of antibody for viewing under the confocal laser scanning microscope

The cells were labelled with antibodies directly conjugated to fluorophores and incubated at 37°C to allow internalisation of the Ab and its location within the cell to be monitored using confocal laser scanning microscopy.

To follow the internalisation of each individual Ab the following method was used. HSB-2 cells ($1x10^7$) were resuspended in 1 ml of cold PBS containing fluorophore-labelled Ab at a concentration of 20μg/ml and incubated at 4°C for 30 minutes. Excess Ab was removed by washing twice with ice-cold PBS. The cell pellet was then resuspended in 10ml of prewarmed R10 medium and incubated at 37°C. Samples containing $1x10^6$ cells were taken from the flask at 0, 30 minute, 1hr, 3hr, 6hr and 24hr. Samples were washed twice with ice-cold PBS and fixed in 4% (w/v) paraformaldehyde in PBS pH 7.4 for 15 minutes at 4°C. Fixed cells were washed twice with PBS and resuspended in PBS. A cytospin was prepared using 300μl of the sample spun at 800 rpm for 5 minutes using a Shandon Southern Cytospin. The slides were allowed to dry before the cells were counterstained with toluidine blue (0.5% v/v in 0.5% borax). Toluidine blue (0.5% v/v in 0.5% borax) was applied to slides for approximately 20 seconds before being washed off with PBS. This was used as a guide to the outline of the cell and the location of the nucleus since toluidine blue weakly stained the cytoplasm of the cell and densely stained the nucleus. Toluidine Blue fluoresces in the red channel. The slides were then coverslipped using a mountant containing 1,4-diazabicylco-[2,2,2]-octane (DABCO) an antifade agent.

The slides were stored in the dark at 4°C for up to three days before being analysed on the Leica TCS 4D Confocal Microscope.

2.10.3 Co-localisation of OKT10 and HB2 antibodies

For studies investigating the extent of co-localisation between OKT10 and HB2 Ab, the same protocol was followed except that no counterstain was used. For this work, HB2 Ab was directly conjugated to Alexa Fluor™ 568 dye (with an absorption and fluorescence emission maxima of approximately 577nm and 603nm respectively) and OKT10 Ab was directly conjugated to FITC. In this experiment both antibodies were added at 20μg/ml.

A co-localisation analysis program (Leica, UK) was used to analyse the exact location of both probes.

Additional studies were undertaken whereby an Ab that was directly conjugated to FITC ligated one antigen and an unlabelled Ab ligated the other antigen. This was done for both possible permutations. The method was followed as described for tracing the pathway of the individual antibodies (section 2.10.2).

The slides were stored in the dark at 4°C before being analysed on the Leica TCS 4D Confocal Microscope.

***2.10.4** Co-localisation of OKT10 Ab- and HB2 Ab-FITC with transferrin-TRITC*

To take these investigations further and elucidate the intracellular routing of these two antibodies, either OKT10 Ab-FITC or HB2 Ab-FITC was incubated simultaneously with transferrin-TRITC (a generous gift from Dr Rodolfo Ippoliti, Rome). Briefly, $1x10^7$ cells were resuspended in 1ml of cold PBS containing 20μg/ml of the Ab-FITC conjugate and incubated at 4°C for 30 minutes. Excess Ab was removed by washing twice with ice cold PBS at 1500 rpm for 5 minutes. The cell pellet was then resuspended in 10ml of prewarmed R10 medium containing 20μg/ml transferrin-TRITC and incubated at 37°C. Samples containing $1x10^6$ cells were taken from the flask at 0, 15, 30, 45, 60, 90 and 120 minutes. Samples were washed twice with ice cold PBS and fixed in 4% (w/v) paraformaldehyde in PBS pH 7.4 for 15 minutes at 4°C. Fixed cells were washed twice with PBS and resuspended in PBS. A cytospin was performed using 300μl of the cell suspension using a Shandon Southern Cytospin at 800rpm for 5 minutes. The slides were allowed to dry before they were coverslipped using a mountant containing 1,4-diazabicyclo–[2,2,2]-octane (DABCO) an antifade agent. Two channel analysis was undertaken to establish the location of both probes throughout the cell. TRITC has an absorption and fluorescence emission maxima of 544nm and 572nm respectively.

The slides were stored in the dark at 4°C for up to three days before being analysed on the Leica TCS 4D Confocal Microscope.

2.10.5. Co-localisation of CD7 and CD38 with human TGN46

HSB-2 cells ($1x10^7$) were resuspended in 1ml of cold PBS containing 20μg/ml of OKT10 Ab-AF568 or HB2 Ab-AF568 and incubated at 4°C for 30 minutes. Excess Ab was removed by washing twice with ice cold PBS. The cell pellet was then resuspended in 10ml of prewarmed R10 medium and incubated at 37°C. Samples containing 10^6 cells were taken from the flask at time 0, 30, 60, 90 120, 240 and 360 minutes. Samples were washed twice with ice cold PBS and fixed in 4% (w/v) paraformaldehyde in PBS pH 7.4 for 15 minutes at 4°C. Fixed cells were washed twice with PBS and resuspended in PBS. A cytospin was performed using 300μl of the sample spun at 800rpm for 5 minutes. The cells were permeabilised on the slides by 50μl of a 0.5% nonidet (NP40) solution (in PBS) for 15 minutes. This was removed by washing the cells three times for 5 minutes with PBS. The human trans-Golgi network marker TGN46 was labelled using 100μl of a 1μg/ml of a sheep anti-TGN46 Ab (Serotec) for 1 hour at room temperature. Excess Ab was removed by three 5 minute washes with PBS. The anti-TGN46 Ab was detected using 50μl of a 1:200 dilution of a donkey anti-sheep Ab-FITC conjugate (Dako) incubated on the cells for 45 minutes at room temperature. Excess Ab was removed by washing three times for 5 minutes with PBS. Excess wash solution was shaken off and the slides coverslipped using a mountant containing DABCO.

2.11 Electron Microscopy Studies

2.11.1 The effects of Brefeldin A on Organelle Morphology

HSB-2 cells ($1x10^8$) were either exposed to 50μg/ml of brefeldin A (BFA) for 30 minutes at 37°C before excess drug was removed by two washes at 1500rpm for 5 minutes in PBS and the cells were then resuspended in R10 medium without BFA for various periods of time, or the cells were resuspended in R10 medium containing 50μg/ml BFA and incubated at 37°C for the same time intervals. At the following times intervals of 0, 2h, 24h and 48h $1x10^7$ cells were taken from the cultures, washed twice and then fixed in 3% glutaraldehyde and 4% formaldehyde in 0.1M PIPES (pH 7.2) for 1 h. Following fixation, samples were embedded into sodium alginate by centrifuging the suspension at 1250g, decanting the supernatant, adding 2 drops of 5% sodium alginate and dropping 10μl

droplets of the alginate mixture into the fixation buffer with an equal volume of 0.1M calcium chloride to set. Cells embedded in alginate were post-fixed with 1% osmium tetroxide (in 0.1 M PIPES buffer) for 1 hour and then dehydrated by graded ethanol. Cell pellets were set in TAAB resin by incubation with histosol and resin (50:50) overnight and then embedded in Epoxy resin. Ultrathin sections were obtained with an ultramicrotome and observed with a Hitachi H7000 transmission electron microscope; after sections were counterstained by uranyl acetate and Reynolds lead stain.

2.11.2 Preparation of cells for electron microscopy studies

2.11.2.1 Post-fixation method

HSB-2 cells were incubated with a saturating concentration of HB2 (anti-CD7) Ab (10μg/ml) for 30 minutes at 4°C. Excess Ab was removed by washing the cells twice in PBS for 5 minutes at 1500rpm each time. Cells were resuspended in R10 culture medium and incubated at 37°C for 0, 30 or 60 minutes. At these times cells were taken from the flask, washed twice in PBS as before, then fixed for 15 minutes in 2mls of a combination of 3% paraformaldehyde and 0.1% glutaraldehyde at room temperature. After fixation the cells were rinsed and pelleted twice for 5 minutes each using PBS at room temperature. Free aldehyde groups were quenched by treating cells with 2mls of 50mM NH_4Cl in PBS, then washed twice in PBS. Cells were set in agarose blocks for cryosectioning by pelleting the cells into a 2% low melting point agarose. Agarose containing cells was cut into appropriately sized blocks for cryosectioning and treated with 2.3M sucrose containing 10K PVP (cryoprotectant solution). Ultrathin sections were cut in a cryo chamber (as described in section 2.11.4) collected onto carbon coated, formvar EM grids and stored on gelatine plates. The grids were immunolabelled with a 1:20 dilution of anti-mouse IgG-gold conjugate (10nm) in PBS/1% BSA/0.05% Triton X-100 and 0.05% Tween 20 as described in section 2.11.5. Following this, the grids were embedded in methyl cellulose and uranyl acetate (described in section 2.11.6). Grids were viewed on a Hitachi H7000 transmission electron microscope.

2.11.2.2 Pre-fixation method

HSB-2 cells incubated with 10μg/ml HB2 Ab for 30 minutes at 4°C. Excess Ab was removed from the cells by washing twice in PBS as before. Following this, the cells were

incubated with a 1:50 dilution of a goat anti-mouse IgG gold conjugate (15nm) for 1 hour at 4°C, washed twice in PBS and resuspended in R10 medium. Cells were incubated for 0, 30 minutes and 1 hour before they were washed, fixed, quenched and embedded in to agarose as described above. Blocks were cryosectioned, and sections collected onto grids were post fixed in 1% glutaraldehyde (in PBS) before they were embedded in methyl cellulose and uranyl acetate. Cells were viewed on a Hitachi H7000 transmission electron microscope.

2.11.3 Cells in agarose blocks

A 2% low melting point agarose solution was heated to ~60°C to liquify the agarose. The fixed cells were stored in PBS in an eppendorf and 200µl of the agarose solution and 5µl of a suspension of sephadex beads dyed with Evans Blue (2% aq) was added. This cell suspension was pelleted by centrifuging at 3000rpm for 2 minutes while the agarose was still liquid. The sephadex beads were visible by the naked eye after centrifugation and were used to provide an indication of the location of the cells within the agarose. Once the agarose had set, the section that contained the cells was cut using a blade into small blocks for cryosectioning. These blocks were stored at 4°C in 2.3M sucrose in PBS containing 10k PVP overnight for cryopreservation.

2.11.4 Cryosectioning

2.11.4.1 Coating grids for cryosectioning

A 0.2% of polyvinyl Formal Formvar solution was made in 1, 2 Dichloro Ethane (or chloroform). A clean glass slide was immersed in the formvar solution to coat it with a thin layer. A second glass slide was run along the edge of the coated slide to cut the edge of the formvar layer and across the top of the slide. The slide was then placed into a bowl of clean water (filtered to remove dust) at a 45° angle to allow the formvar layer to float on the surface. EM grids were carefully placed on the formvar layer dark side down. A rectangle of parafilm was then lowered on to the formvar layer with the grids to enable it to be taken out of the water. This was allowed to dry before it was coated with a thin layer of carbon.

2.11.4.2 Tissue mounting and freezing

The tissue block was mounted on a pin in the best orientation for sectioning. A thin layer of infiltrating medium covered the block and any excess was drained off using filter paper. The pin was gripped firmly in a pair of long forceps and plunged into liquid nitrogen until frozen. The pin was placed in a small, liquid nitrogen filled container to keep it frozen until ready for transfer to the cutting chamber.

2.11.4.3 Trimming and sectioning

The cryo chamber (Reichert MM80-E) was correctly set up and a reservoir of liquid nitrogen obtained. The chamber was allowed to cool for approximately 30 minutes before starting to reach temperatures of -80 to -90°C. At these temperatures the block face was trimmed to produce a clean edged square or rectangular block face. A few semi-thin sections were then cut and stained with toluidine blue to examine the tissue structures in the block. The temperatures of the cryo chamber, knife and block were reduced further to about -110 to -120°C. Once the lower temperatures had been reached sections of 70 to 90nm thick were cut. An eyelash probe was used to move sections away from the cutting edge ready for retrieval.

2.11.4.4 Retrieval of sections

A medium sized drop of a mixture of 2% methyl cellulose (aq) and 2.3M sucrose mixed 1:1 (Liou and Slot., 1996) was collected on a wire loop about the size of a grid. The sections were collected by lightly touching the sections with the drop whilst viewing the sections under the binocular attachment of the microtome. The loop was then immediately removed from the chamber and touched onto a carbon coated, formvar EM grid which was then inverted onto a gelatine plate. The sections on the gelatine plates were stored at 4°C before staining, but for no longer than overnight.

2.11.5 Immunolabelling

The gelatine plates containing the grids were heated to approximately 40°C. The grids were then washed briefly on three drops of PBS before they were blocked in 1% BSA in PBS for 10 minutes. The excess blocking solution was drained and the grids were incubated with the Ab-gold conjugate diluted in PBS + 1% BSA, 0.05% Triton X-100 and 0.05% Tween 20. They were transferred between three drops of the secondary Ab using a wire loop and left incubating for 1 hour and covered to avoid condensation. The grids

were washed on 6 drops of PBS over a period of 15 minutes and then underwent post-fixation in 1% glutaraldehyde in PBS for 10 minutes. They were then washed three times in PBS over 15 minutes followed by a brief wash for 5 minutes in distilled water to remove any traces of phosphate before being embedded in methyl cellulose and uranyl acetate.

2.11.6 Post-embedding

A mixture of 9 volumes methyl cellulose and 1 volume filtered uranyl acetate (referred to as MC/UA) was made. Each section was washed on three drops of distilled water (to remove any traces of buffer) and transferred between drops by a wire loop. The grids were transferred section side down subsequently onto three drops of MC/UA on parafilm over ice. The sections were left on the final drop for at least 10 minutes. The grids were covered to avoid condensation from forming. Each section was picked up on a separate wire loop; the excess MC/UA was carefully removed with small pieces of hardened filter paper. The grids were left for at least 10-15 minutes for the grids to dry in this support and then carefully removed from the loops. These grids were stored in dry petri dishes.

Chapter 3

Treatment of the T-Cell Acute Lymphoblastic Leukaemia Cell Line HSB-2 With a Combination of Anti-CD7 and Anti-CD38-Saporin Immunotoxins Performs Better Than Using Each Immunotoxin Individually

3.1 Introduction

An immunotoxin (IT) is a hybrid molecule that is comprised of a MAb conjugated to a toxin molecule. The therapeutic potency of an IT is determined in part on the Ab moiety binding to a specific cell surface target antigen, its subsequent internalisation and ultimately translocation of the toxin component from an intracellular vesicular compartment to the cytosol. Once in the cytosol, the toxin kills the cell apoptotically by catalytically inactivating ribosomes. An IT has no bystander effects since it only kills cells into which the toxin has been internalised and delivered to the cytosol. It is therefore of paramount importance that all of the leukaemia cell population is selected for and eliminated. If some cells from within the tumour population evade killing by the IT, then surviving tumour cells with growth potential continue to proliferate and eventually relapse will occur. One of the main factors that could prevent a single IT from killing all the cells within the leukaemic population is that of antigen heterogeneity. This will compromise single target IT treatment by preventing delivery of the toxin, saporin, to any of the cells that are negative or that weakly express any single target antigen.

One possible approach to overcome this obstacle is the use of combinations or "cocktails" of ITs, each IT within the cocktail specific for a different target antigen. This is based on the hypothesis that multiple or double antigen negative variant cells are likely to occur with a lower frequency than cells that are only single antigen negative. Thus, using a combination of two or more ITs would increase the probability of delivering saporin to all cells within the global tumour cell population with the added bonus of delivering more saporin to the cells that were positive for both molecules. It is also possible that factors such as direct cell signalling, and recruitment of cytotoxic host effectors (Shen *et al.*, 1994), such as complement activation and ADCC (Flavell *et al.* 1998), could work in conjunction with the toxin to

achieve an improved therapeutic effect when combinations of Ab-based treatments are utilised.

An improved therapeutic outcome when using combinations of ITs compared to the use of single ITs has been demonstrated in several studies. In severe combined immunodeficient (SCID) mice xenografted with the human Burkitt lymphoma cell line Ramos, the use of an anti-CD19 saporin IT in combination with an anti-CD38 saporin IT demonstrated a significant increase in the efficacy of selective cell killing compared with the use of each IT individually (Flavell *et al* 1995). This improvement in therapeutic effect was seen to be enhanced further by targeting the tumour with a combination of three ITs directed against CD19, CD22 and CD38 molecules on the Ramos cell surface. When these three antigens were targeted against simultaneously with three different ITs, 100% survival of the SCID-Ramos mice over a 300-day period was achieved (Flavell *et al* 1997). The same group demonstrated, both *in vitro* and *in vivo*, that using anti-CD7- and anti-CD38 saporin ITs simultaneously against the T-cell acute lymphoblastic cell line CCRF CEM resulted in a significant improvement in efficacy compared with the two ITs used singly (Flavell *et al* 2001). Other groups have also found combinations of ITs to be more effective than single IT treatments. Strong *et al* (1985) demonstrated the value of using a four-IT cocktail to purge leukaemia cells from bone marrow for transplantation, and Vooijs *et al* (1996) have shown the enhanced cytotoxicity obtained against Reed-Sternberg cell lines by the combined use of anti-CD80 and anti-CD86 ITs.

In this study a greater cytotoxic effect was demonstrated when the two ITs, HB2-saporin IT (anti-CD7) and OKT10-saporin IT (anti-CD38), were used in combination compared with their individual potencies on the T-cell ALL cell line HSB-2 both *in vivo* and *in vitro*. This is in concordance with the findings described previously with the CCRF CEM cell line and the SCID-Ramos model (Flavell *et al.*, 2001, 1997).

3.2 Methods and Experimental Design

Three different assays were used to investigate the mechanisms by which a greater therapeutic effect can be obtained by using a combination of an anti-CD7- and anti-CD38-saporin IT than when each IT is used individually.

3.2.1 Protein synthesis inhibition assay

A protein synthesis inhibition assay was performed *in vitro* to show the short term effects of the two ITs HB2-saporin IT and OKT10-saporin IT on HSB-2 cells. Specific details of the method used can be found in the Materials and Methods section 2.7. In brief, triplicate cultures of $5x10^4$ HSB-2 cells were exposed to various concentrations, ranging between 0.0001-10μg/ml (in one log intervals), of the immunotoxins HB2-saporin IT, OKT10-saporin IT and their native antibodies singly and in combination in medium. (Full details of the conditions tested by this assay are listed in table 3.1). Cultures were incubated for 48 hours in a humidified atmosphere of 5% CO_2/95% air. After this period, 1μCi ^{3}H-leucine (ICN Biomedicals, Hampshire, UK.) was added to each culture for a further 14 to 16 hours and uptake measured relative to that seen in untreated cultures grown in medium alone. Where a combination of two ITs, two antibodies, or a combination of an IT with an Ab was used, the final dose was comprised of half of each component part, for example, to give a final concentration of 1μg/ml, each IT would be present at 0.5μg/ml. This maintains a constant concentration of Ab molecules for comparison of treatments. Data was expressed as a percentage of ^{3}H-leucine incorporation relative to untreated control cultures.

3.2.2 In vitro cell proliferation assay

An *in vitro* cell proliferation study was undertaken to demonstrate the long-term effects of various IT and Ab treatments on the proliferation of HSB-2 cells. (See section 2.6 for a detailed method.) In brief, $2x10^5$ HSB-2 cells were cultured in R10 medium in T25 flasks containing given concentrations of IT, native Ab or combinations of both. The various treatments studied here are listed in Table 3.2. The final concentration of each treatment was 0.5μg/ml. When the treatment was comprised of a combination of ITs, antibodies, or both, 0.25μg/ml of each was used. Viable cell counts were conducted on the cultures at regular

intervals using trypan blue dye exclusion. Cultures were maintained until the cells had overgrown.

3.2.3 Treatment of HSB-2 leukaemia in SCID mice

A study was conducted to determine how these cytotoxic agents behave *in vivo* using a model of HSB-2 leukaemia in SCID-mice. Details of this experiment can be found in sections 2.5. Briefly, groups of SCID mice composed of nearly equal proportions of males and females (5-8 weeks old) were inoculated with two million HSB-2 cells seven days prior to receiving an i.v. bolus injection of therapy. The therapy groups are summarised in Table 3.3. The experiment was conducted over a 128-130 day period during which animals were inspected daily and any mice that were obviously unwell were killed humanely according to a Home Office Schedule 1 method. This study investigate the effects of ITs and antibodies both used individually, and in various combinations, on the survival rate of the SCID mice xenografted with HSB-2 leukaemia, relative to PBS sham treated animals.

When a combination of two ITs, two antibodies, or a combination of an IT with an Ab was used, the final dose was comprised of half of each component part, for example, to give a final concentration of 10μg per animal, each IT would be present at 5μg per animal.

3.2.4 Statistical evaluation

Statistical differences between therapy groups were evaluated by Log-rank analysis using SPSS 9.0.0 for Windows statistical software package (SPSS UK Ltd. Woking, Surrey).

3.3 Results

3.3.1 In vitro protein synthesis inhibition in HSB-2 cells treated with immunotoxins and antibodies

The dose-response curves showing protein synthesis inhibition in target HSB-2 cells following exposure to different concentrations of HB2-saporin IT and OKT10-saporin IT alone and in combination are shown in figure 3.1A. The IC_{50} values (defined as the concentration that produces a 50% inhibition of protein synthesis levels compared with untreated cultures) and the fold increase above the IC_{50} value for saporin alone (2000ng/ml)

obtained for each treatment are summarised in table 3.1. HB2-saporin IT performed marginally better against the HSB-2 cells than OKT10-saporin IT resulting in IC_{50} values of 1.5ng/ml and 2.5ng/ml respectively. Although treatment of cells with OKT10-saporin IT resulted in an 800-fold increase in cytotoxicity, it was not as efficient at inhibiting protein synthesis in target cells as HB2-saporin IT (which demonstrated a 1333-fold increase in cytotoxicity). Both ITs used in combination did not perform any better than the most potent of the two ITs, but instead displayed an intermediate effect with an achieved IC_{50} of 2.0ng/ml.

Table 3.1. *In vitro* inhibition of protein synthesis in target HSB-2 cells by immunotoxins used singly or in combination or a single immunotoxin used in combination with a single Ab.

Treatment	**IC_{50} (ng/ml)†**	**Fold-increase‡**
HB2-saporin IT	1.5	1333
HB2-saporin IT + OKT10-saporin IT	2.0	1000
OKT10-saporin IT	2.5	800
HB2-saporin IT + OKT10 Ab	5.0	400
OKT10-saporin IT + HB2 Ab	15.0	133
Saporin alone	2000	—

† The concentration that inhibits protein synthesis by 50% relative to untreated controls
‡ Calculated relative to the toxicity produced by saporin alone i.e. saporin IC_{50}/treatment IC_{50}

Neither HB2 nor OKT10 Ab used singly or in combination resulted in any significant reduction in the protein synthesis levels in HSB-2 cells (figure 3.1B). When HB2-Saporin IT was used in combination with OKT10 Ab, or a mixture of OKT10-Saporin IT with HB2 Ab was employed, a decrease in cytotoxic performance was observed compared with that produced by treatment with the relative IT alone. A 3-fold reduction of protein synthesis inhibition was obtained when HB2-Saporin IT was used in combination with OKT10 Ab compared to HB2-Saporin IT alone. A 6-fold reduction in protein synthesis inhibition resulted from the use of the combination of OKT10-Saporin IT and HB2 Ab relative to the IT alone.

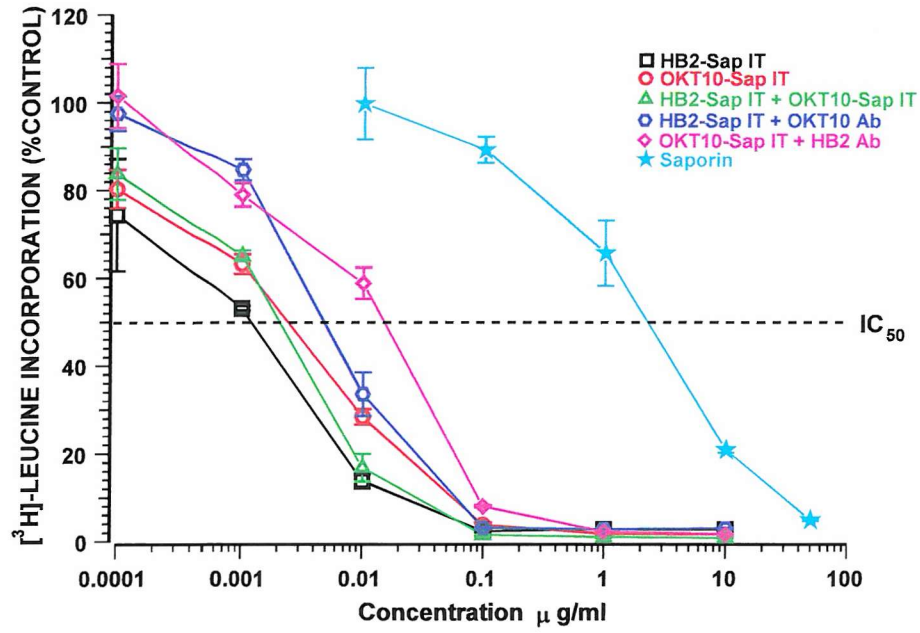

Figure 3.1A. Protein synthesis inhibition in HSB-2 cells exposed to increasing concentrations of HB2-Saporin, OKT10-Saporin, a combination of both HB2-Saporin + OKT10-Saporin, a combination of immunotoxin with Ab or saporin alone. Data points shown represent mean values of triplicate cultures; bars SD (n-1).

3.3.2 Inhibition of HSB-2 cell proliferation in vitro by immunotoxins and antibodies

Two hundred thousand HSB-2 cells were cultured in T25 flasks over a period of 50 days. The cells were continuously exposed to various IT and Ab treatments which are summarised together with their effects on cell proliferation in table 3.2. The final concentration of each treatment was 0.5μg/ml. When the treatment was comprised of a combination of ITs, antibodies or both, 0.25μg/ml of each was used.

The data shown in figure 3.2 reveals that both ITs significantly delayed the proliferation of HSB-2 T-ALL cells compared to control cells maintained in medium alone. HB2-Saporin IT delayed proliferation of HSB-2 cells by 7 days relative to medium control cells which were proliferating on the first day of cell counting (day 3). OKT10-Saporin IT inhibited the proliferation of HSB-2 cells more effectively than HB2-Saporin IT taking a further 14 days to

reach the time to outgrowth. This contrasts the findings of the protein synthesis inhibition assay described in section 3.3.1 in which HB2-Saporin IT was shown to be 1.7 times more effective at inhibiting protein synthesis in target HSB-2 cells than OKT10-Saporin IT. No living cells were detected in cultures of HSB-2 cells exposed to a combination of both ITs throughout the 50 day duration of the experiment.

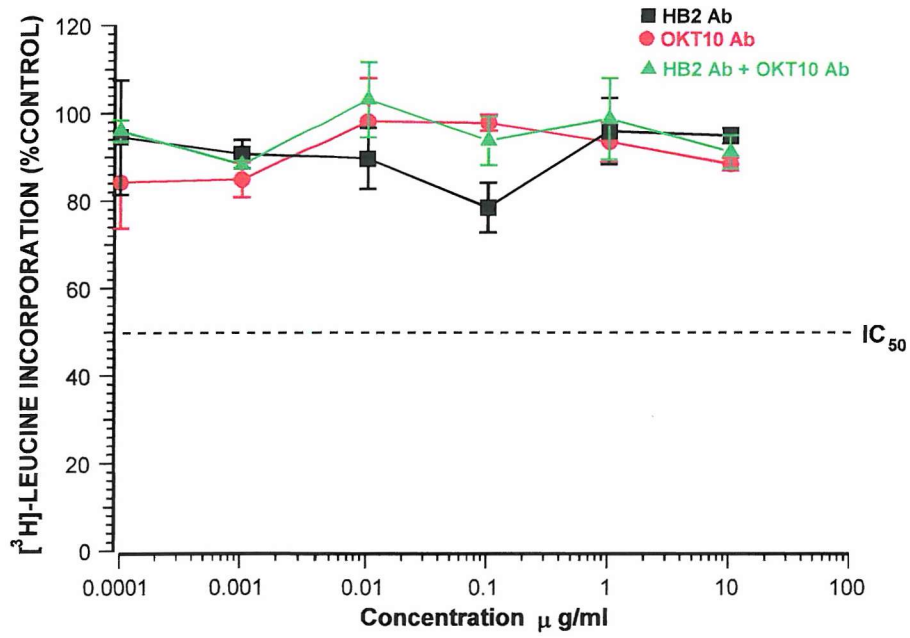

Figure 3.1B. Protein synthesis inhibition in HSB-2 cells exposed to increasing concentrations of HB2 Ab, OKT10 Ab or a combination of both HB2 + OKT10 antibodies. Data points shown represent mean values of triplicate cultures; bars SD (n-1).

HB2 or OKT10 Ab used alone or in combination had no significant effect on HSB-2 cell growth, which was similar to that seen in medium control cultures. The combination of HB2-Saporin IT with OKT10 Ab, or OKT10-Saporin IT with HB2 Ab, appeared to be equally as effective at inhibiting HSB-2 outgrowth as each IT used individually and there was therefore no advantage in including Ab in this *in vitro* assay.

Table 3.2. Summary of culture treatments and outcomes in a long-term proliferation assay.

Treatment	*Day proliferation first detected*	*Day of highest cell count*
Medium control	3	8
HB2 Ab	3	8
OKT10 Ab	3	8
HB2 Ab + OKT10 Ab	3	8
HB2-saporin IT	10	19
HB2-saporin IT + OKT10 Ab	10	17
OKT10-saporin IT	24	33
OKT10-saporin IT + HB2 Ab	26	35
HB2-saporin IT + OKT10-saporin IT	—	—

3.3.3 The effect of single and combination immunotoxin therapy in SCID mice transplanted with HSB-2 human T-ALL cells

In order to assess the therapeutic ability of various treatments, SCID mice bearing disseminated HSB-2 leukaemia were treated with ITs singly and in combination 7 days after inoculation with the leukaemia cells. The therapy groups can be found summarised in table 3.3, which also contains the data obtained from this study. The percentage of survivors and the mean survival time was calculated at day 128 or 130, depending on when the experiment was terminated. Log-rank analysis was undertaken to determine any statistically significant differences displayed between the different therapy groups and these data are displayed in table 3.4.

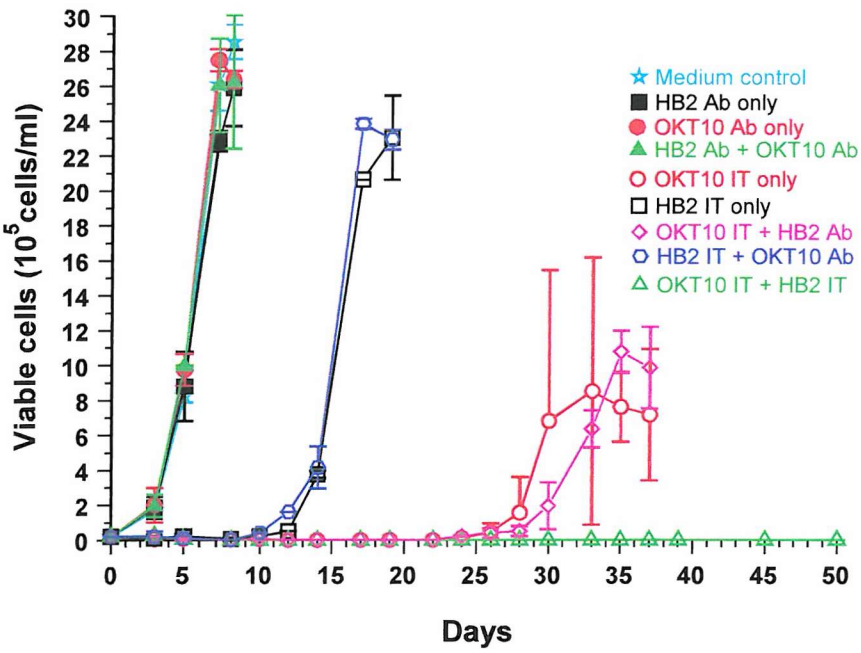

Figure 3.2. Proliferation of HSB-2 cells grown in the continuous presence of HB2-Saporin IT, OKT10-Saporin IT, a combination of both HB2-Saporin IT + OKT10-Saporin IT, HB2 Ab, OKT10 Ab or a combination of both HB2 + OKT10 antibodies, HB2-Saporin IT with OKT10 Ab, OKT10-Saporin IT with HB2 Ab, or medium control. When cultures were exposed to a single reagent the final concentration was 0.5μg/ml. When a combination of two reagents was employed, 0.25μg/ml of each reagent was combined to provide a final concentration of 0.5μg/ml.

Kaplan-Meier plots of the survival data obtained for SCID-HSB-2 mice treated with each individual IT or a combination of both ITs are shown in Figure 3.3A. In experiment 1, control animals receiving PBS sham treatment (group 4) had all died due to HSB-2 leukaemia within 66 days (Figure 3.3). HB2-saporin IT (group 1) and OKT10-saporin IT (group 2) were both found to prolong survival to a significant extent relative to the PBS sham animals (giving *p* values of 0.0052 and 0.0458 respectively). OKT10-saporin IT performed marginally better than HB2-saporin IT resulting in a 50% survival rate and mean survival of 86.4 days, compared with a 40% survival rate and mean survival of 84.6 days, although this difference in treatment efficacy was not found to be significant. Treating animals with a combination of both ITs produced the best long term survival of all the groups (with a mean survival of 110.3 days), and the greatest percentage of animals alive (66.7%) at the termination of the study on

day 128. This was highly statistically significant when compared to the survival of animals treated with PBS sham ($p = 0.0068$), but not significant when compared to HB2-Saporin IT and OKT10-Saporin IT used individually (producing p values of 0.3227 and 0.4844 respectively). This result may not have been as significant as expected due to the loss of four animals when a water bottle leaked. For this reason, the combination group was repeated in a second experiment, and even though this group performed better than before, the results were still not significant when compared to the treatment of animals with each IT individually.

Table 3.3. Summary of experimental SCID mouse groups and therapy outcomes.

Treatment numbers	***Treatment***	***Number of animals***	***% Survival ‡***	***Mean survival (days) †***
Experiment 1				
1	HB2-SAPORIN IT	10	40	84.6
2	OKT10-SAPORIN IT	10	50	86.4
3	Combination HB2-SAPORIN + OKT10-SAPORIN ITs	6	66.67	110.3
4	PBS sham	8	0	45.4
Experiment 2				
5	Combination HB2-SAPORIN + OKT10-SAPORIN ITs	8	75	117
6	HB2 Ab	8	25	78
7	OKT10 Ab	8	12.5	64
8	Combination HB2 Ab + OKT10 Ab	8	37.5	115.6
9	Combination HB2-SAPORIN + OKT10 Ab	8	50	97.4
10	Combination OKT10-SAPORIN + HB2 Ab	8	37.5	103.4
11	PBS Sham	4	0	66.8

† Mean survival calculated at termination of study at 128/130 days
‡ Percentage at 128/130 days

In a second experiment, the therapeutic effects of the native antibodies HB2 and OKT10 in the SCID-HSB-2 model were examined and these results are shown in figure 3.3B. Both HB2 (group 6) and OKT10 (group 7) Ab produced a slight improvement on survival compared with the PBS sham treatment group (11) but neither group was significant. However, when both antibodies were used simultaneously, a greatly significant prolongation of survival (resulting in a difference in mean survival of 48.9 days) was observed compared to the sham treated animals ($p = 0.0077$). Neither Ab performed as well as their respective IT although a statistical difference between the two types of therapy was not found. HB2 Ab produced a mean survival of 78 days compared with 84.6 days with HB2-Saporin IT ($p = 0.5246$). OKT10 Ab resulted in a mean survival of 64 days compared with 86.4 days with OKT10-Saporin IT ($p = 0.1900$).

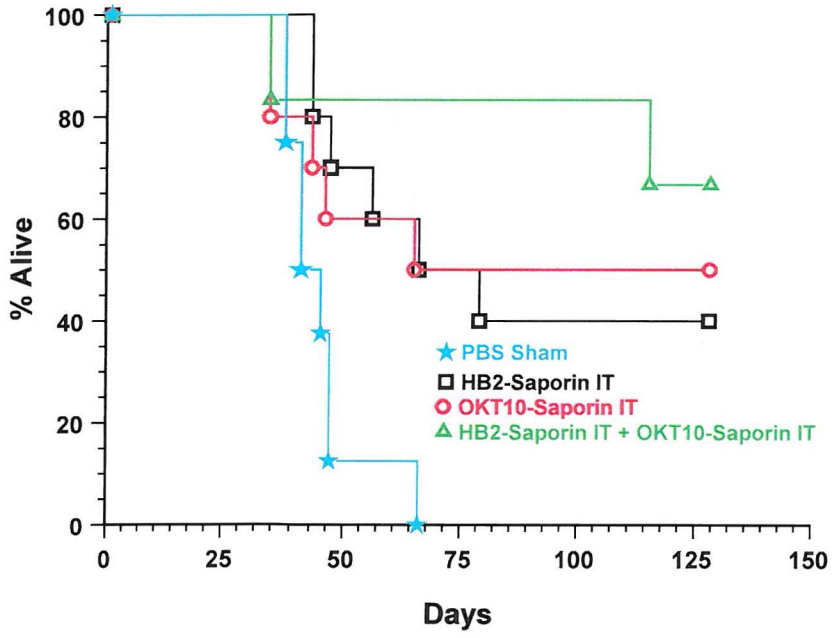

Figure 3.3A Survival of SCID-HSB-2 mice injected on day 1 with two million HSB-2 cells and treated on day 7 with 10μg of HB2-Saporin, OKT10-Saporin, a combination of both ITs (at 5μg each) or PBS sham treated.

To ascertain whether the increased benefit of using two ITs in combination was due to an additive interaction between one of the IT components and the Ab component of the second IT, studies were undertaken to compare groups of SCID-HSB-2 mice treated with an IT/Ab pair. The results are shown in figure 3.3C. A reduction in the therapeutic ability of HB2-Saporin IT + OKT10 Ab and OKT10-Saporin IT + HB2 Ab to prolong survival compared to the group treated with the combination of ITs was observed, although the differences between these groups were not statistically significant ($p = 0.3527$ and 0.1692 respectively). No notable increase in therapeutic efficacy was observed when using an IT/Ab pair compared with the use of the individual IT. A slight but not significant increase in the mean survival and the percentage survived could be seen with the HB2 IT + OKT10 Ab pair compared with HB2-Saporin IT alone (97.4 days, 50%; 84.6 days, 40% respectively).

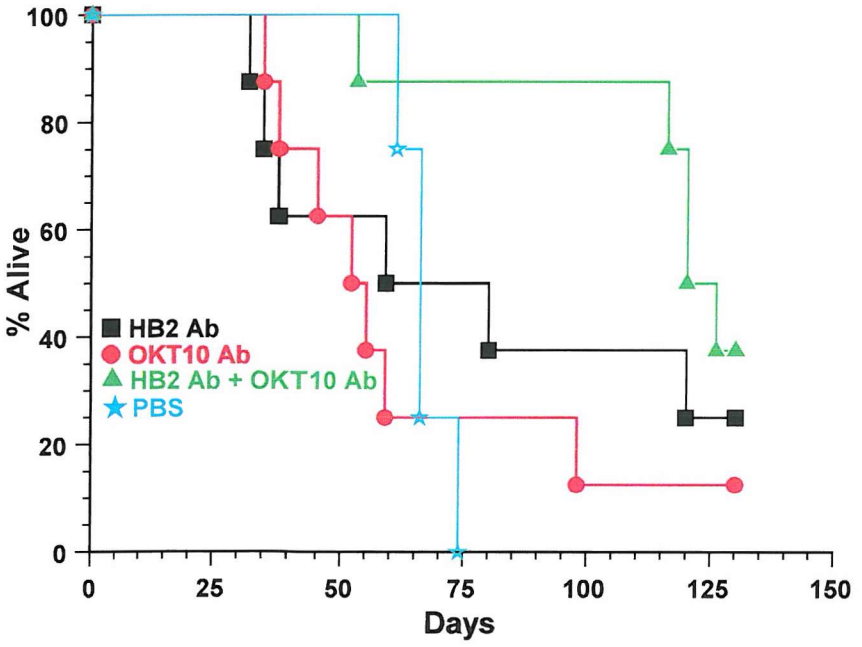

Figure 3.3B. Survival of SCID-HSB-2 mice injected on day 1 with two million HSB-2 cells and treated on day 7 with 10μg of HB2 Ab, OKT10 Ab, a combination of both antibodies (at 5μg each) or PBS sham treated.

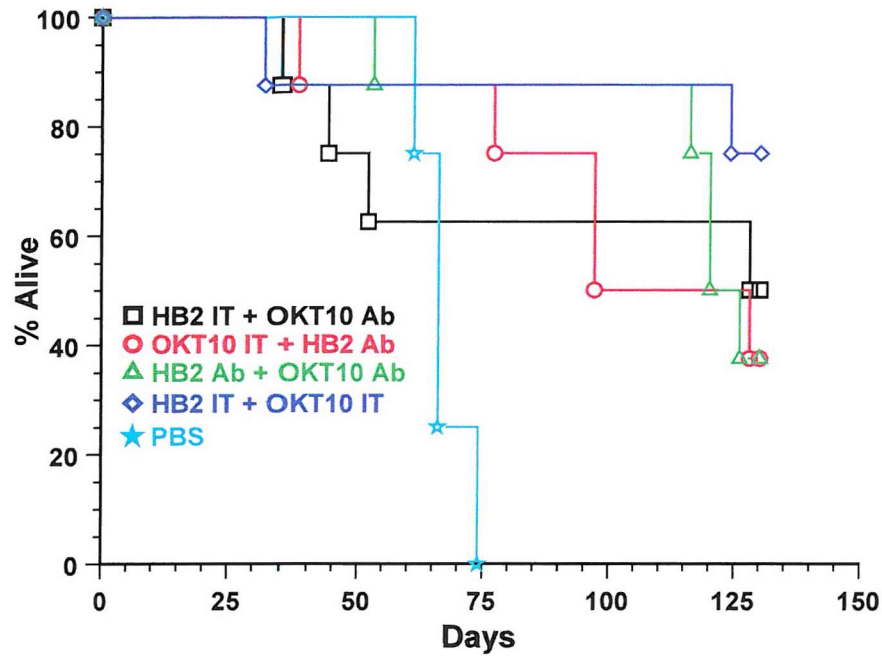

Figure 3.3C. Survival of SCID-HSB-2 mice injected on day 1 with two million HSB-2 cells and treated on day 7 with 10μg of HB2-Saporin with OKT10 Ab, OKT10-Saporin with HB2 Ab, a combination of both ITs, a combinations of both antibodies (all at 5μg each) or PBS sham treated.

3.4 Discussion

The overall results of this study strongly indicate that using two different Ab-saporin ITs to target the antigens CD7 and CD38 on the cell surface of the T- cell ALL cell line HSB-2 delivers a better therapeutic effect than using the two ITs individually. The observed increased survival rate of animals in the combination IT group in the SCID-HSB-2 model was also reflected in the long term *in vitro* proliferation study by the total lack of cell proliferation in cultures exposed to the same treatment. This was not displayed in the short term protein synthesis inhibition (PSI) assay where the combination IT therapy does not even perform as well as the most potent of the two individual ITs (HB2-saporin IT).

Table 3.4. A comparison of the mean survival and statistically significant differences displayed between the various treatment groups.

Treatment 1	*Vs*	*Treatment 2*	*Mean Survival (Days) 1 vs 2*		*P value*
1		2	84.6	86.4	0.9288
1		3	84.6	110.3	0.3227
1		4	84.6	45.4	0.0052
1		5	84.6	117	0.1507
1		6	84.6	78	0.5246
1		8	84.6	115.6	0.5860
1		9	84.6	97.4	0.7236
2		3	86.4	110.3	0.4844
2		4	86.4	45.4	0.0458
2		5	86.4	117	0.2970
2		7	86.4	64	0.1900
2		8	86.4	115.6	0.9223
2		10	86.4	103.4	0.9935
3		4	110.3	45.4	0.0068
5		6	117	78	0.0427
5		7	117	64	0.0107
5		8	117	115.6	0.1692
5		9	117	97.4	0.3527
5		10	117	103.4	0.1692
6		7	78	64	0.5104
6		8	78	115.6	0.2423
6		10	78	103.4	0.3236
6		11	78	66.8	0.4967
7		8	64	115.6	0.0251
7		9	64	97.4	0.1348
7		11	64	66.8	0.5870
8		11	115.6	66.8	0.0077
9		10	97.4	103.4	0.8020
9		11	97.4	66.8	0.2052
10		11	103.4	66.8	0.0077

Flavell *et al.*, (1994, 2001) have described how an increase in cytotoxic potency has not been exemplified in any of the PSI studies conducted of this kind, although it can be demonstrated using a combination of two bispecific antibodies targeting saporin to the same two antigens CD7 and CD38. In this case a 10-fold increase between the combination treatment and the use of individual bispecific antibodies could be detected by the protein synthesis assay (Flavell *et al.*, 1992). In the present study, the improved therapeutic effect may not be seen because the mechanism by which the combination of ITs prolongs animal survival may be a longer ongoing process than can be detected in such a short term assay.

In accordance with this work other groups have also shown that combinations of ITs produce significantly higher survival rates than the use of single ITs. Engert *et al.*, (1995) demonstrated that the simultaneous use of anti-CD30 and anti-CD25 ricin A chain ITs resulted in an improved therapeutic outcome of Hodgkin's lymphoma in nude mice than with the single agents. Another group have achieved enhanced toxicity using anti-CD7- and anti-CD38-saporin ITs in combination against the T-cell ALL cell line CCRF CEM, prolonging the mean survival time by 122 days longer than the most potent single IT, in the same SCID mouse model as used for the present study (Flavell *et al.*, 2001).

In the present study and in that performed on CCRF CEM cells, *in vitro* and *in vivo,* a clear difference between the protein synthesis inhibiting capability of the two ITs can be seen. The long term proliferation assay shows that OKT10-saporin IT can delay growth of the tumour to a significantly greater extent than HB2-saporin IT alone. This pattern is also observed in the SCID-mouse model but to a lesser extent. This difference may have become more statistically significant if the experiment had been carried on for longer and greater differences between the therapy groups obtained, as with the SCID-CEM data.

Research undertaken by Flavell *et al.*, (1998) has investigated the mechanism(s) by which the HB2 Ab and its respective IT exert their anti-leukaemia effects. Data from this work suggests that the Ab does not act by inducing complement-mediated lysis or through growth inhibitory signalling after binding of the Ab to the CD7 molecule, but is thought to induce ADCC by SCID mouse NK or NK-like cells via Fc receptors. This mechanism is exerted by HB2-saporin IT and acts in conjunction with its toxin-mediated cytotoxicity. This is also demonstrated in a chromium release assay where both OKT10 and HB2 antibodies and ITs cause ADCC lysis of CCRF CEM cells (Flavell *et al.*, 2001).

HB2 and OKT10 Ab are both of the same subclass, and so it would be expected that OKT10 Ab would also be capable of inducing ADCC. It appears that neither Ab acts through growth inhibitory signalling in these assays. Differences in the way in which the two ITs activate the ADCC process may differ and to what extent may explain why OKT10-saporin IT produces a prolonged therapeutic response compared with HB2-saporin IT. These factors could include

the affinity of the Ab to the target antigen, the number of Ab molecules bound to the target antigen, the tendency of the Ab-antigen complex to modulate or the three dimensional orientation of Fc tails, which are all known to influence the extent of ADCC (Tutt *et al.*, 1998). Even different antibodies of the same subclass and isotype can exhibit varying degrees of avidity for the Fc receptor (Dillman *et al.*, 1986).

In both the Ramos-SCID experiments and the same study conducted on CCRF CEM cells, OKT10 Ab was shown to produce a greater prolongation of animal survival than both anti-CD19 and anti-CD7 antibodies, although each Ab prolonged survival to varying degrees. As all three antibodies investigated against these antigen molecules are of the subclass IgG_1 it is uncertain as to why they vary in effect so much. The effect of OKT10 Ab on the prolongation of animal survival seen previously was not so obvious in this study, although a slight enhancement of the HB2-Saporin IT treatment can be observed when used in combination with this Ab. When animals were treated with both antibodies in combination an additive effect of both the single antibodies was observed. This was presumably attributable to the ability of both antibodies to induce ADCC.

In the present *in vitro* studies, no anti-proliferative effect can be seen to be exerted by the HB2 and OKT10 antibodies either individually or in combination which supports the evidence that these antibodies do not activate complement or act through direct growth inhibitory signals. If these antibodies do exert a growth inhibitory effect via an ADCC mechanism then this would not be expected to be observed in these *in vitro* studies, as no NK or NK-like cells were present in the systems used. It may be possible that these antibodies do activate complement, like the IgG_1 anti-CD7 murine Ab TH-69 (Baum *et al.*, 1996) but are unable to induce these components in the *in vitro* system used. This appears unlikely since Flavell *et al.*, (1998) investigated the ability of HB2 Ab to activate SCID complement and was unable to demonstrate the effects of complement.

A possible reason why OKT10-saporin IT causes a greater prolongation of animal survival may be that the topography of the CD38 antigen on the cell surface or its manner of insertion into the membrane renders the target cell more susceptible to cytolysis by ADCC directed against the molecule. The CD38 antigen may be more accessible to OKT10 Ab binding as well as for binding of the Fc fragment on the Ab molecule to the FcγRIII on the effector cell.

Work by Ghetie *et al.,* (1992) has demonstrated an increase in therapeutic efficacy of the anti-CD19- and anti-CD22-ricin A chain ITs when they were used in combination against Daudi cells in a SCID-mouse model. They found that the anti-CD19 Ab HD37 used in combination with the anti-CD22 IT RFB4-dgR was equally as effective at producing cytotoxicity as was a specificity equivalent combination of the two ITs. It was later shown that the HD37 Ab was producing an anti-proliferative signalling effect alongside the toxin-mediated cytotoxicity mediated by the anti-CD22 IT that was responsible for the therapeutic efficacy of this combination (Ghetie *et al.,* 1994). This may be the mechanism of the increased therapeutic outcome in the present study but this seems unlikely, as there was no evidence of either Ab causing an anti-proliferative signalling effect in the *in vitro* assays undertaken in this study. This is also unlikely since neither IT/Ab pair appeared to perform as well therapeutically as the combination of both ITs.

The data from the SCID-HSB-2 model does not always provide a clear indication of the differences in therapeutic efficacy between different therapy groups. If this study had been conducted over a longer time period with larger group sizes, these data may have been statistically significant.

In conclusion, it is hypothesised that the increased therapeutic effect on HSB-2 T-ALL tumour progression displayed by a combination of ITs is explained by one or all of the following reasons. Firstly, using two ITs simultaneously overcomes antigen heterogeneity, increasing the probability of targeting all the cells in the tumour population, including the cells down-regulated or negative for one of the two target molecules. Secondly, a larger and possibly more effective dose of the toxin saporin can be delivered to cells positive for both

antigen targets. Finally, ADCC mechanisms may work additively with the specific delivery of toxin by the IT and more effectively if two separate cell surface molecules are targeted. The data obtained here supports the ever growing evidence that a combination of ITs can overcome the problem of antigen heterogeneity. Most of the evidence supporting this hypothesis has been obtained from studies conducted on mice. The possibility remains that what has been observed in mice may not transfer to the human system, since most murine monoclonal antibodies have been found not to be cytocidal against neoplastic cells in humans because they only weakly activate human complement or cell-mediated cytotoxicity (Waldmann 1991). This problem may be overcome by producing chimeric antibodies consisting of murine Fab fragments which recognise the target antigen and a human Fc which can successfully activate the host effectors. Stevenson *et al.,* (1991) have already developed a mouse/human chimeric Ab to the CD38 antigen using OKT10 Fab fragments. The human IgG1/OKT10 mouse Fab chimeric Ab has demonstrated the ability to successfully mediate ADCC in preclinical trials. Even so, it is encouraging that many experiments of this nature have been performed on a system shown to produce a disseminated pattern of leukaemia similar to that seen in man (Flavell *et al.,* 1994) and have repeatedly demonstrated the proof of principle that combinations of ITs can be effective at treating haematological malignancies.

Chapter 4

Internalisation Kinetics of CD7 and CD38 Following Ligation Determined by Flow Cytometric Analysis

4.1. Introduction

The cytotoxicity studies described in chapter 3 revealed significant differences between the potency of OKT10-saporin IT and HB2-saporin IT for HSB-2 cells when used as individual reagents. It was also observed that a marked improvement in performance occurred when the two were used in combination in the *in vitro* long term cell proliferation assay as well as in the *in vivo* SCID mouse experiment. However this enhancement was not reported in the short term protein synthesis inhibition assay. The question addressed by the work conducted within this chapter is what factor(s) account for these differences in efficacy. There are several determinants that define the potency of an individual IT for target cells, among which are the affinity of the MAb for the antigen (Youle and Neville 1982, Ramakrishnan and Houston 1984), the characteristics of the target cell and antigen (Bjorn *et al.,* 1985), the rate and more importantly the route of internalisation of the bound IT (Press *et al.,* 1986, Casellas *et al.*, 1982, Lambert *et al.*, 1985, Youle *et al.*, 1986, Goldmacher *et al.*, 1989) and finally the epitope on the target antigen recognised by the Ab (Press *et al.*, 1988, May *et al.*, 1990).

It was speculated that the combination of the two ITs used recognising CD7 or CD38 exert an improved therapeutic efficacy for any one or possibly all of the following reasons: (i) that targeting against two different cell surface molecules on the tumour cell surface may help overcome the heterogeneity of antigen expression, (ii) that targeting against two different cell surface molecules with two ITs might increase the amount of toxin delivered to the target cell, or (iii) that targeting against two different cell surface antigens simultaneously may beneficially affect the internalisation and routing characteristics.

An IT has no bystander effect on surrounding cells or tissue, since the toxin will only act on a cell into which it has internalised. It has been proposed that receptor-mediated endocytosis of cell surface antigen-IT complexes is essential for their effectiveness as cytotoxic agents (Lambert *et al.,* 1985, Youle and Neville 1987, Raso and Basala 1984, Wargalla and Reisfeld 1989, Goldmacher *et al.,* 1989), particularly since ITs that fail to be

internalised are unable to kill tumour cells (Lambert *et* al., 1985). Some studies have correlated the rate of internalisation of an IT with its cytotoxic potency (Wargalla and Reisfeld 1989, Goldmacher *et al.*, 1989). It may be that variations in the internalisation kinetics of the two ITs used in this study account for the differences seen in their cytotoxic potencies. Where two different surface antigens were targeted simultaneously, the increased therapeutic effect that this delivered may be due to changes in the way in which one or both antigens are internalised and delivered to an appropriate intracellular compartment. Thus, it may be that more saporin is delivered to the ribosomes within the cytosolic compartment. There is already evidence to suggest that CD38 has physical and functional lateral associations of this kind with other cell surface molecules including CD3 in normal and tumour T lymphocytes, a complex of surface immunoglobulin (sIg) and CD2/CD19 in normal and tumour B cells, as well as the low-affinity IgG Fc receptor CD16 in NK cells (Funaro *et al.*, 1993). It is therefore plausible that a similar interaction may exist between CD7 and CD38.

In theory, only one ricin molecule and presumably other related molecules such as saporin, is required to reach the cytosol to irreversibly inhibit protein synthesis (Eiklid *et al.*, 1980). However, since ITs are usually transported through cellular compartments where the toxin may be either proteolytically cleaved or inactivated by low pH, it is necessary for many more molecules to be endocytosed to guarantee cytotoxicity. For this reason, differences in cytotoxic potency may correlate with the total number of molecules internalised.

In this chapter, a flow cytometric method was employed in an attempt to address some of these issues. Using this technique, the modulation of CD38 and CD7 molecules from the cell surface was monitored and this enabled us to determine whether there was a correlation between the characteristics and rate of internalisation and the observed cytotoxic potency of each of these two ITs. These investigations were also intended to reveal any differences that may have occurred to the internalisation characteristics of either CD7 or CD38 when both antigens were simultaneously ligated by their respective antibodies. In these studies, modulation was defined as the decrease in antigen from the surface brought about either by the shedding process which eliminates Ab-antigen complexes from the cell (Unanue and Karnovsky 1973) or the process of internalisation of the same complexes by specific endocytotic processes (Silverstein *et al.*, 1977).

The flow cytometric analysis indicated that the internalisation kinetics of an IT was not the only factor influencing its cytotoxic potency. For this reason, it was considered that information on the fate of the IT once it has entered the cell would be vital in elucidating any additional factors that affect IT potency. For example, there is data to suggest that some ITs are rapidly degraded in lysosomes within minutes of entering the cell, thus preventing the toxin from reaching target ribosomes. Other ITs have been shown to be recycled to the cell surface before the toxin can translocate to the cytosol. If OKT10-Saporin IT and HB2-Saporin IT display such differences in their intracellular routing, it might help to explain why there are differences in their cytotoxic potencies.

Directly radiolabelling the antibodies of interest with iodine-125 (I^{125}) was to be used to monitor the internalisation, degradation, recycling and shedding characteristics of the antibodies, ITs and their respective antigens. This technique enables the quantification of CD7 and CD38 levels expressed on the cell surface and the affinity of the antibodies tested for these antigens, since the flow cytometric analysis performed was qualitative but only semi-quantitative. Flow cytometry only allowed the proportion of Ab internalised to be quantified, whereas a radioisotopic technique should enable accurate quantification of the actual number of molecules internalised, degraded, recycled or shed.

The main questions addressed in this chapter were; Firstly, what are the relative numbers of antigen molecules of interest expressed on the surface of each cell, and is there a correlation between expression levels and sensitivity to ITs against these antigens? Secondly, with what affinity do the antibodies bind to the antigens CD7 and CD38? Thirdly, is there a correlation between the affinity of the antibodies and the cytotoxicity of the ITs against these antigens? Finally, when the two antigens are ligated simultaneously by their cognate antibodies, does this affect the amount or affinity of binding to these antigens? It was also intended to quantify the degradation and exocytosis rates of the two antigen markers as well as give an indication of any effect the use of combinations of antibodies may have on internalisation, degradation or exocytosis rates of CD7 and CD38.

4.2. Methods and Experimental Design

4.2.1. Flow cytometric endocytosis assay

A flow cytometric assay was employed to follow the modulation of antibodies to CD7 and CD38 alone and in combination over a 24 hour time period. Slight variations were made to the flow cytometric assay to enable the clear distinction of various aspects of the internalisation characteristics of both CD7 and CD38 when ligated individually or in combination. These variations are described below.

In the first protocol, cells were incubated with a saturating concentration (10μg/ml) of intact Ab (either HB2 Ab or OKT10 Ab) and allowed to bind at 4°C for 30 minutes. Excess unbound Ab was removed by washing twice in PBS and 0.1% azide and the cells resuspended in R10 culture medium. Cells were then incubated at 37°C and aliquots of 10^6 cells were removed at various time points. The samples were either labelled immediately with the secondary Ab (referred to hereafter as pulsed samples) or re-incubated with the primary Ab before being labelled with the secondary reagent (referred to hereafter as pulsed restain samples).

In the second protocol, cells were not pre-incubated but were continually exposed to Ab once the cells were resuspended in R10 medium containing a saturating concentration (10μg/ml) of the Ab. This was to allow the Ab to bind to the cells and maintain a steady equilibrium throughout the duration of the experiment. Samples were taken at the same time points as the pulsed samples and were either labelled immediately with the secondary Ab (referred to hereafter as continuous exposure samples) or re-incubated with the primary Ab before being labelled with the secondary reagent (referred to hereafter as continuous restain samples).

The same series of experiments were also performed with immunotoxins constructed from both native antibodies to determine if the addition of the saporin molecule to the Ab influenced the internalisation characteristics. In addition, Fab' fragments of both antibodies were investigated to determine whether or not bivalent binding was a requirement for internalisation of the antibodies used in these studies. Additionally, both antibodies were ligated simultaneously to determine if this influenced the internalisation

characteristics of either antigen and whether any associations exist, in terms of co-modulation, between the two surface molecules CD7 and CD38.

Data from these studies were plotted in duplicate as a percentage of the mean fluorescence intensity produced by control cells saturated with the primary Ab and maintained at 4°C to prevent endocytosis from occurring.

The methods described above were not able to discriminate the way in which each individual antigen behaved when co-ligated simultaneously. Both HB2-Saporin IT and OKT10-Saporin IT used to ligate CD7 and CD38 simultaneously are comprised of murine antibodies, so the anti-mouse IgG-FITC conjugate detected the combined modulation of both reagents. This method could therefore only reveal the overall effect of co-ligation on antigen modulation rather than the individual trends of each antigen. For this reason, a third approach was taken whereby one of the antigens was ligated by intact Ab while the second antigen was ligated with a $F(ab)_2$ fragment of the native Ab. The protocol was almost identical to that described above except that an Fc-specific FITC conjugated IgG secondary reagent was used to detect the intact Ab only. It was assumed that the Fc fragment on intact Ab would not influence the internalisation characteristics of HB2 Ab or OKT10 Ab on HSB-2 cells and therefore that the $F(ab)_2$ fragment while still maintaining bivalent binding would internalise in a similar manner to intact Ab.

The last modulation experiment of this type involved ligation of one antigen followed by internalisation at 37°C. Samples of cells were then removed at various time points and subjected to flow cytometric analysis. Half the samples were incubated with a FITC-conjugated secondary Ab (to the whole Ab molecule) to detect the amount of Ab remaining on the cell surface, and the other half were incubated with a MAb, directly conjugated to FITC, against the second unligated antigen. This was done to monitor surface levels of the unligated antigen to determine whether ligation of the first antigen influenced the surface expression of the other. Further details of these experiments can be found under section 2.8.3.

4.2.2 Radioiodination

The monoclonal antibodies HB2 (anti-CD7) and OKT10 (anti-CD38) and their respective ITs were radiolabelled with ^{125}I-Na using IODO-BEADS (Pierce and Warriner) according to the manufacturer's instructions. Details can be found in section 2.9.1.

4.2.3 Autoradiography

To confirm that the correct fractions eluting from the column were selected, samples of the fractions were run on a 5% non reducing sodium dodecyl sulphate polyacrylamide gel by electrophoresis (as described in section 2.4). This was also used to indicate any possible adverse effects that iodination may have had on Ab integrity. The gels were dried in a Bio-Rad Slab Dryer (Model 443), and then autoradiographed onto photographic x-ray film (Fuji). Various exposure times were used for development of the autoradiograph depending on the amount and intensity of ^{125}I incorporated into the protein.

4.2.4 Surface-bound ^{125}I-OKT10 and ^{125}I-HB2 Antibodies and Immunotoxins

The amount of surface bound material was determined by incubating 10^6 cells with various concentrations (0.1, 0.5, 1, 5 and 10μg/ml) of ^{125}I-labelled Ab. Non-specific binding was assessed by blocking the cells with a 1000-fold excess of "cold" (unlabelled) Ab 5 minutes prior to exposure of cells to the labelled Ab. The cells were incubated with ^{125}I-Ab for 30 minutes at 4°C after which time the samples were spun through phthalate oil to separate excess Ab from that bound to the cells. Cell pellets and supernatants were counted separately on a gamma counter. The number of antigen molecules per cell and Ab affinity was determined using Scatchard analysis (Scatchard 1949).

This method was also used to detect any differences in the number of molecules bound to the cell surface when both antigens were simultaneously ligated. The protocol followed was as before except this time the cells were saturated with 20μg/ml of one Ab and then incubated with various concentrations (as described above) of the second Ab (which was ^{125}I-labelled). Scatchard analysis was carried out in the same manner as before, as only one of the antibodies was radioactively labelled.

4.2.5. Proposed Endocytosis Assay

This assay was not conducted in its entirety for reasons that are explained later in this chapter, however it is described here to explain the purpose of the elution studies shown in section 4.3.8. To determine the extent of Ab internalised at various time points both as a percentage of the amount bound to the cell surface at the start of the experiment and as a number of molecules, an endocytosis assay based on a modification of that used by Press *et al.*, 1988 was designed. Cells were to be pelleted by centrifugation followed by incubation with ^{125}I-MAb. For pulsed exposure (as in the flow cytometry experiments), the cells would be incubated with radiolabelled Ab at 10μg/ml for 30 minutes at 4°C before excess Ab would be removed by washing twice with ice-cold PBS containing 1% BSA. The cells would then be resuspended in R10 medium and incubated in a flask at 37°C to allow endocytosis to occur. To monitor the effect of continuous exposure to the Ab on internalisation, the cells would be immediately resuspended in R10 medium containing 10μg/ml (a saturating concentration) of ^{125}I-Ab after centrifugation, followed by incubation at 37°C for various time intervals. To determine the extent of surface bound Ab before internalisation, samples of cells labelled with the Ab were to be kept at 4°C. At various time points from 0 to 24h, samples were to be extracted and assayed for supernatant radioactivity, membrane-bound radioactivity, and intracellular radioactivity as described below. Both the pulsed and continuous exposure samples were to be treated identically.

Cell samples were to be extracted at time intervals of 0, ½, 1, 3, 6, 9 and 24h. Cells were to be spun through phthalate oil and the radioactivity associated with the cell pellet would then be counted. Another sample of cells would be washed to remove any non-cell associated radioactivity, followed by acid treatment. The cells were then to be spun through phthalate oil and the cell associated radioactivity counted again. This count would represent the internalised molecules at this time. The absolute number of intracellular molecules would be calculated from the acid-treated cells initially incubated at 37°C after correcting for radioactivity in cells treated similarly at 4°C.

The number of molecules bound to the cell surface at any one time point was determined by subtracting the amount of intracellular radioactivity from the total radioactivity associated with the cells after incubation at 37°C.

4.2.5.1 Degradation of ^{125}I-Antibody

After incubation of the cells with radiolabelled Ab at 37°C and 4°C, cells were to be pelleted by centrifugation and the supernatant treated with 10% trichloroacetic acid (TCA). The intracellularly degraded and subsequently exocytosed Ab would be calculated by measuring the amount of radioactivity of the TCA-soluble fraction of the supernatant. The radioactivity of the soluble fraction from the cells incubated at 4°C was to be subtracted from that obtained at 37°C to remove any background radioactivity.

4.2.5.2 Internalisation of ^{125}I-antibody

Internalisation was to be defined as the total number of molecules that has crossed the cell membrane and hence was determined by the summation of the internalised Ab and the amount of Ab that had been degraded and exocytosed.

These results were all to be plot as a percentage of the surface bound material found on cells maintained at 4°C.

4.2.6 Preliminary Studies to Determine Optimum Conditions for Eluting Surface Bound Antibody

Cells saturated with ^{125}I-Ab and maintained at 4°C to prevent internalisation were treated with various acidic buffers to elute the surface-bound material from the cell surface. To determine which buffer at what pH produced the optimum condition for eluting the Ab from the surface of HSB-2 cells, the following protocol was used. One million cells were incubated with 10μg/ml ^{125}I-Ab for 30 minutes at 4°C. Excess Ab was removed by washing with PBS and 0.1% azide. The cells were then resuspended in 300μl of the elution buffer to be tested. Cells were incubated with the elution buffers for different periods of time, after which the cell suspension was spun through phthalate oil. Radioactivity associated with the cell pellet was measured. All buffers were isotonic.

To evaluate the effect of low pH on the condition of the cell, a viability assay was conducted. Briefly, 10^6 cells were pelleted by centrifugation and then resuspended in the elution buffer for the same times as in the experiments described above. The cell

suspension was then neutralised by washing the cells in PBS and 0.1% azide (pH 7.3) and the viability determined immediately using trypan blue exclusion.

4.3. Results

4.3.1. *The internalisation characteristics of CD7*

The results for CD7 internalisation on HSB-2 cells following ligation by HB2 Ab either after a pulsed or continuous exposure can be seen in figure 4.1A. The pulsed exposure data (denoted by the black line) shows that CD7 was rapidly cleared from the cell surface within the first hour of incubation at 37°C. This decrease of CD7 expression levels was also displayed in the data obtained from continuous exposure (denoted by the blue and green lines) and pulsed restain samples (as shown by the red line), indicating that the antigen had been internalised or shed from the cell surface but not re-expressed. Approximately 40% of the molecules bound to the plasma membrane at time 0 had modulated from the cell surface within an hour of incubation. After the first hour, the rate of internalisation appeared to slow, although still remained fairly rapid for the remainder of the 24 hour period. By 3 hours, 50% of the surface bound Ab at the start of the experiment have been internalised, and by 24 hours, almost all of the HB2 Ab had cleared from the surface of the HSB-2 cells.

For the first hour of the experiment, the pulsed restain samples (red line) followed the same rapid downward trend as observed with the pulsed samples, after which time the rate of CD7 clearance from the surface decreased over the following 5 hours. By 6 hours, an increase in CD7 expression levels on the cell surface was observed, which continued to increase for the remainder of the experiment. The purpose of the restain samples was to detect any unligated Ab on the surface, which may have been a result of recycling antigen or alternatively to an upregulation of CD7. During the 24 hour period of the experiment, CD7 antigen levels never reached those found at the start of the experiment.

Continuous exposure to the monoclonal Ab HB2 differed from the pulsed exposure by displaying a modulation pattern that was intermediate to the pulsed exposure and the pulsed restain. Modulation of CD7 from the cell surface was still biphasic with a rapid clearance from the surface within the first hour of incubation with Ab, but was then followed by a slower decrease in CD7 surface expression levels by three hours and beyond. It should be taken into account when interpreting these findings that the amount

of Ab detected in the continuous exposure samples represents both modulation of the antigen as well as any re-expression that may have occurred.

A

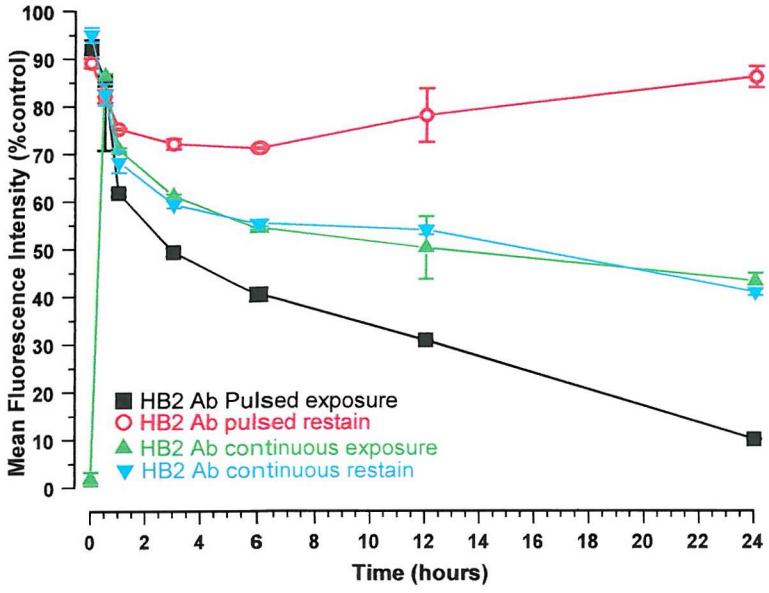

B

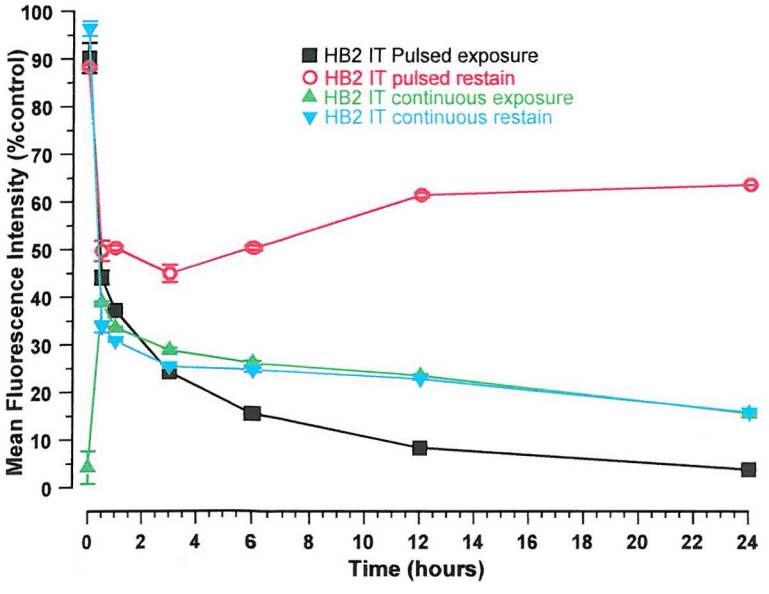

Figure 4.1 Kinetics of internalisation and re-expression of CD7 in HSB-2 cells following ligation with HB2 Ab (A) or HB2-Saporin IT (B). Data represents surface bound Ab or IT expressed as a percentage of the mean fluorescence intensity from cells saturated with the primary reagent and maintained at 4°C. Bars = SD(n-1).

C

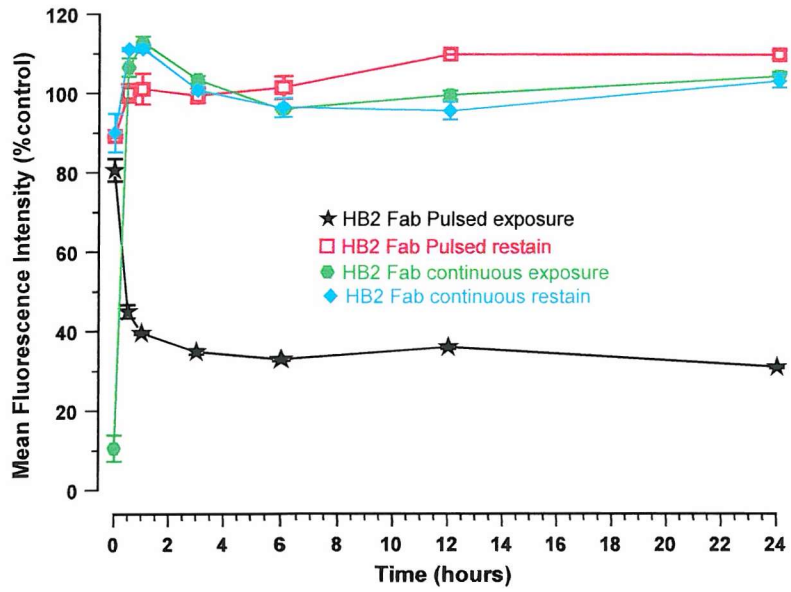

Figure 4.1C Kinetics of internalisation and re-expression of CD7 on HSB-2 cells following ligation with HB2 Fab' fragment. Data represents surface bound Fab' expressed as a percentage of the mean fluorescence intensity from cells saturated with Fab' and maintained at 4°C. Bars = SD(n-1).

The trends of internalisation seen with the Ab were also observed when the antigen was ligated by an IT comprised of the same MAb and the toxin molecule saporin (as shown in figure 4.1B). The main notable difference with the IT was that the IT appeared to modulate more rapidly and to a slightly greater extent than the native Ab.

The CD7 antigen was also ligated with the Fab' fragment of HB2 Ab to investigate the effect of univalent versus bivalent binding (and hence cross-linking) on internalisation kinetics. A distinct difference in the internalisation characteristic was observed. The same rapid decrease in CD7 expression was seen within the first hour of incubation (shown by the pulsed exposure line in figure 4.1C), as it did when ligated with intact Ab, but after this time the modulation of the antigen plateaued. Contrary to this, the pulsed restain and continuous exposure data indicated that there was no change to CD7 expression on the cell surface throughout the 24 hour duration of the experiment.

4.3.2. The internalisation characteristics of CD38

The modulation pattern of CD38 from the surface of HSB-2 T-ALL cells following ligation by OKT10 Ab (shown in figure 4.2A) was very distinct from that of CD7, although both were biphasic in their internalisation rates. When the cells were exposed to Ab for half an hour then washed, most of the modulation of CD38 occurred within the first 3 to 6 hours of incubation at 37°C, after which time the rate of CD38 internalisation plateaued at approximately 40-50% until the end of the experiment at 24 hours. This was also seen when the antigen was ligated with the respective IT (OKT10-Saporin IT) as shown in figure 4.2B. The rapid decline in CD38 surface levels observed within the first few hours was of a lesser rate than that seen with CD7. The modulation of CD38 within the first three hours was also displayed by the pulsed restain and the continuous exposure samples indicating that this was due to internalisation or shedding of the antigen. After this time an upregulation or re-expression of antigen started to occur which continued until the 6 hour time point when the surface levels of CD38 were maintained at approximately 100% of the original saturation levels. The immunotoxin was shown to behave in an identical manner to the native Ab (figure 4.2B).

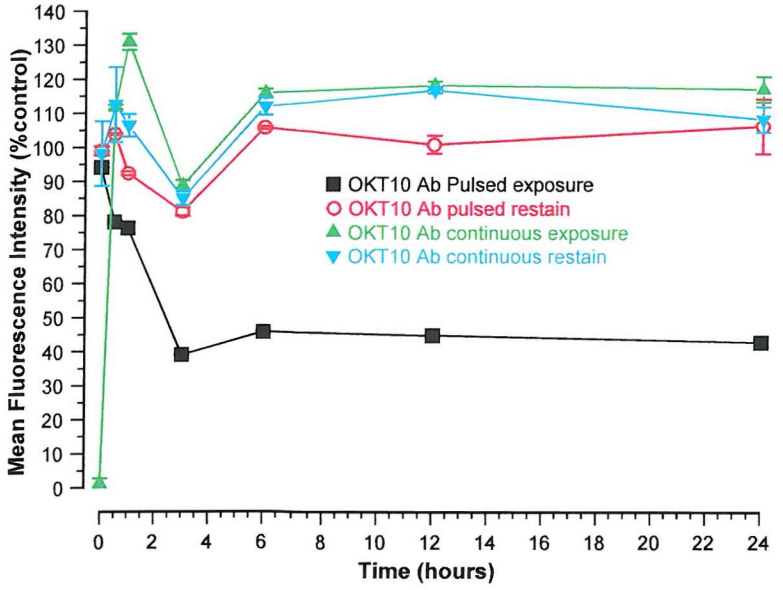

Figure 4.2A Kinetics of internalisation and re-expression of CD38 on HSB-2 cells following ligation with intact OKT10 Ab. Data represents surface bound Ab expressed as a percentage of the mean fluorescence intensity from cells saturated with Ab and maintained at 4°C. Bars = SD(n-1).

B

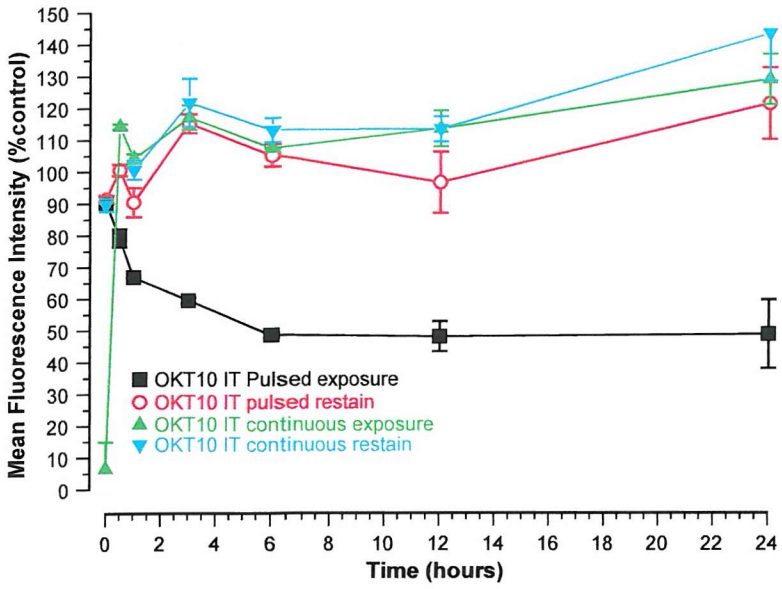

C

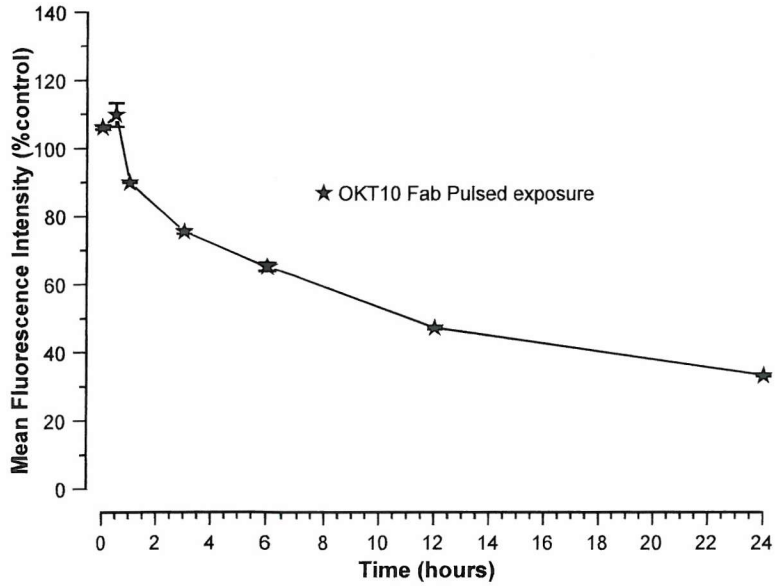

Figure 4.2 Kinetics of internalisation and re-expression of CD38 in HSB-2 cells following ligation with OKT10-Saporin IT(B) or OKT10 Fab' (C) (pulsed exposure only). Data represents surface bound IT or Fab' expressed as a percentage of the mean fluorescence intensity from cells saturated with the primary reagent and maintained at 4°C.
Bars = SD(n-1).

The effect of bivalent binding on internalisation was investigated by comparing the internalisation characteristics obtained from ligating CD38 with the Fab' fragment of OKT10 Ab with those from intact Ab (figures 4.2 C and D). An unexplained phenomenon

occurred when the Fab' fragment of OKT10 Ab was used to ligate the antigen. The pulsed samples followed a similar trend to that observed when the antigen was ligated by intact Ab (figure 4.2C), but a much greater amount of Fab' fragments were detected in the pulsed restain samples where levels of approximately 180% of saturation levels were reached (figure 4.2D). Approximately four hundred and fifty percent of saturation levels on untreated cells were observed in both the continuous samples. It was not possible to determine why this occurred with the Fab' fragment using the detection method employed, although it was possible that the fragments were aggregating on the cell surface creating more sites for the secondary reagent to bind to.

D

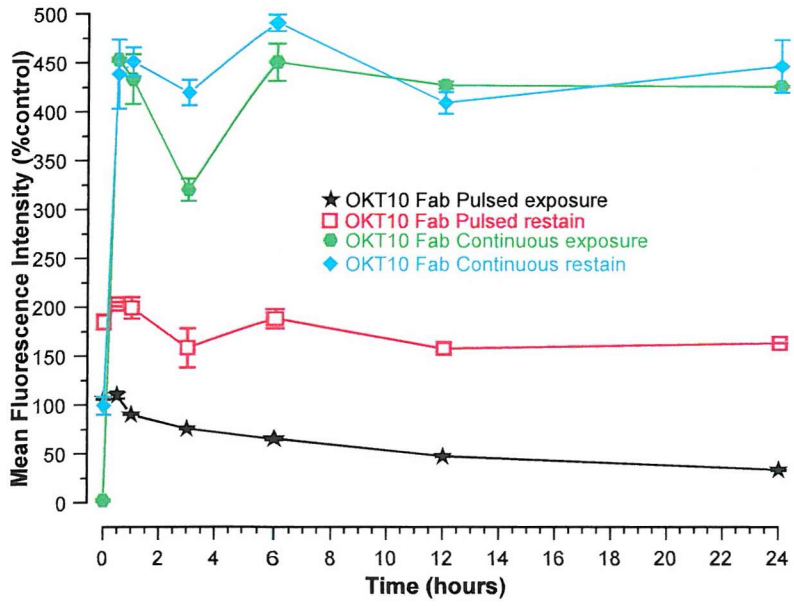

Figure 4.2D Kinetics of internalisation and re-expression of CD38 on HSB-2 cells following ligation with OKT10 Fab' Ab fragment. Data represents surface bound Fab' expressed as a percentage of the mean fluorescence intensity from cells saturated with Fab' and maintained at 4°C. Bars = SD(n-1).

4.3.3. *The internalisation characteristics of CD7 and CD38 when ligated simultaneously*

The internalisation characteristics of the two antigens when ligated simultaneously were investigated using two separate approaches. The first method involved incubating the cells with a saturating concentration of ITs against both CD7 and CD38 and then using a FITC-conjugated secondary Ab to the whole Ab molecule to detect their presence on the cell surface. This gave an overall indication of the modulation of these two antigens but

did not enable distinction between the two IT molecules. These observations are illustrated in figure 4.3.

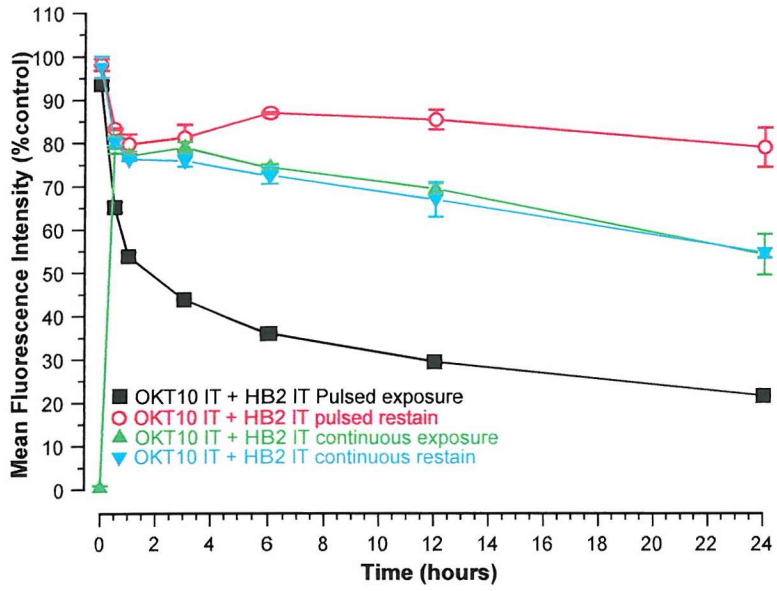

Figure 4.3 Kinetics of internalisation of CD7 and CD38 on HSB-2 cells when co-ligated by the ITs HB2 and OKT10 respectively. Data represents surface bound IT as a percentage of the mean fluorescence intensity from cells saturated with both ITs and maintained at 4°C. Bars = SD(n-1).

The internalisation profile of both antigens combined in the pulsed exposure samples displayed a steep gradient similar to that displayed by the modulation of CD7 alone within the first hour of incubation at 37°C followed by a progressively slower rate of internalisation. Over the 24 hour duration of the experiment, 75% of the total amount of IT bound to the cells was modulated. This was a much greater amount of internalisation than was observed when CD38 was ligated by OKT10 IT alone which appeared to modulate only 50% of total cell surface molecules in 24 hours. This observation might indicate that using the two ITs in combination increases the overall rate and amount of internalisation exhibited by each IT.

It appeared that the internalisation kinetics of the two antigens ligated simultaneously mainly follow the trends observed with CD7 modulation with the occasional characteristic of CD38 internalisation. The continuous exposure samples exhibited properties different from the pulsed samples which was a characteristic seen with CD7 but not CD38 when individually ligated, although these were not as distinct as with CD7 alone. The pulsed restain samples resembled the trends observed with CD38 ligation only where antigen

levels rapidly increased back up to the original levels expressed at the start of the experiment.

As explained previously, it was not possible to observe the behaviour of each antigen individually using this technique. For this reason, it was also not possible to distinguish whether these results were showing an increase in the total amount of Ab internalised or simply just an average of the two individual internalisation trends. In an attempt to determine individual internalisation characteristics when both antigens were co-ligated with their respective antibodies, a second approach was taken. This involved ligating both antigens simultaneously as before but one antigen was ligated with intact Ab and the other with a $F(ab)_2$ fragment of the appropriate Ab. This way a FITC-conjugated secondary agent specific for the Fc fragment only present on the intact Ab could be used to detect the modulation of a single antigen at a time. The data from this technique (shown in figure 4.4) indicated that the previous observations that suggested an increased internalisation rate when both antigens were co-ligated (figure 4.3) was no more than an intermediate fluorescence pattern of the two antigens. Thus, there appeared to be no effect on the rate or trends of internalisation of each of the individual antigens when co-ligated to those seen when ligated individually.

An investigation to answer whether or not any associations exist between the two antigens CD7 and CD38 was also undertaken. In this experiment, only one of the antigens was ligated at the start of the experiment to initiate modulation of the molecule. At various time points the expression level of the second antigen was determined by the use of a directly FITC labelled Ab to the antigen. The data to these experiments can be seen in figures 4.5A&B and clearly indicate that there was no apparent effect. It therefore appeared that there was no association existing between the two molecules that influenced the modulation of either antigen as there were no significant differences to the surface expression levels of either unligated antigen throughout the 24 hour duration of the experiment.

A

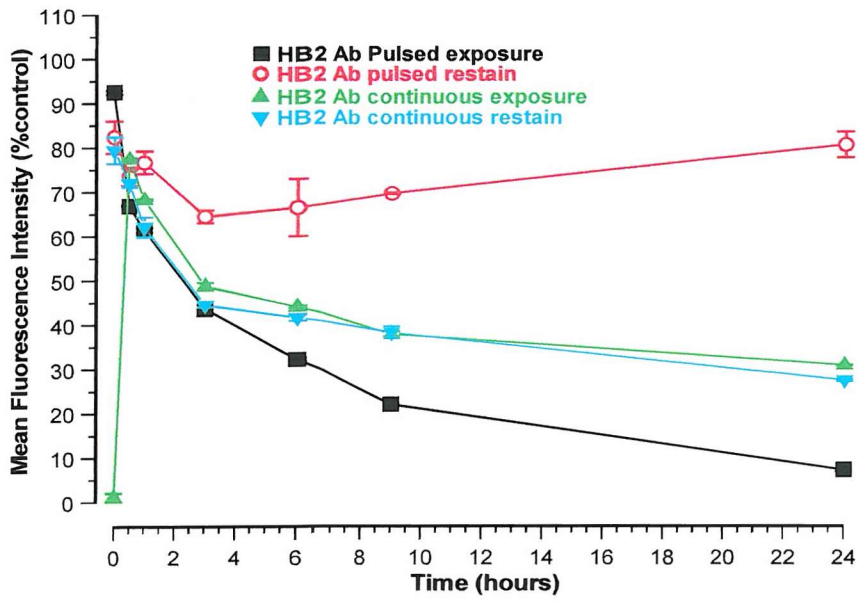

B

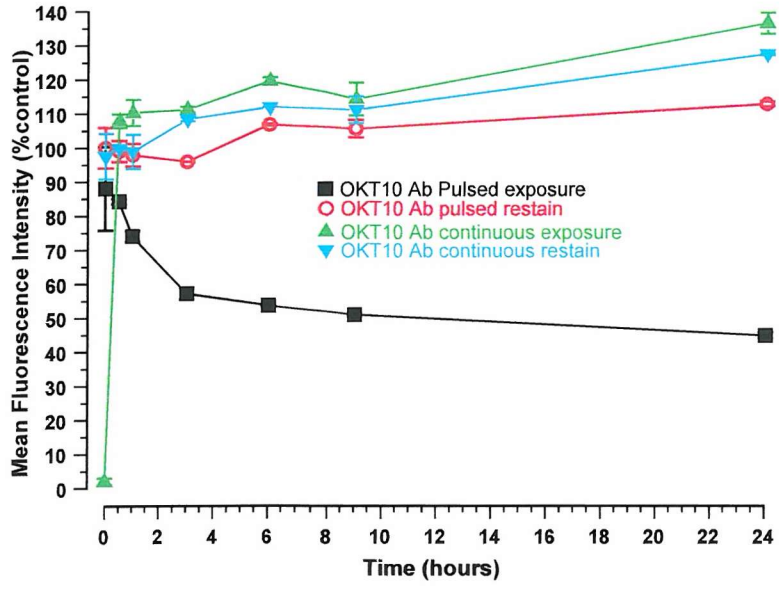

Figure 4.4 Kinetics of internalisation of CD7 (**A**) or CD38 (**B**) following ligation of the antigen by intact Ab when CD38 (**A**) or CD7 (**B**) is coligated by a $F(ab)_2$ fragment. Only intact Ab was measured by an Fc-specific FITC conjugated secondary Ab. Data represents surface bound intact Ab expressed as a percentage of cells saturated with intact Ab and $F(ab)_2$ and maintained at 4°C. Bars = SD(n-1).

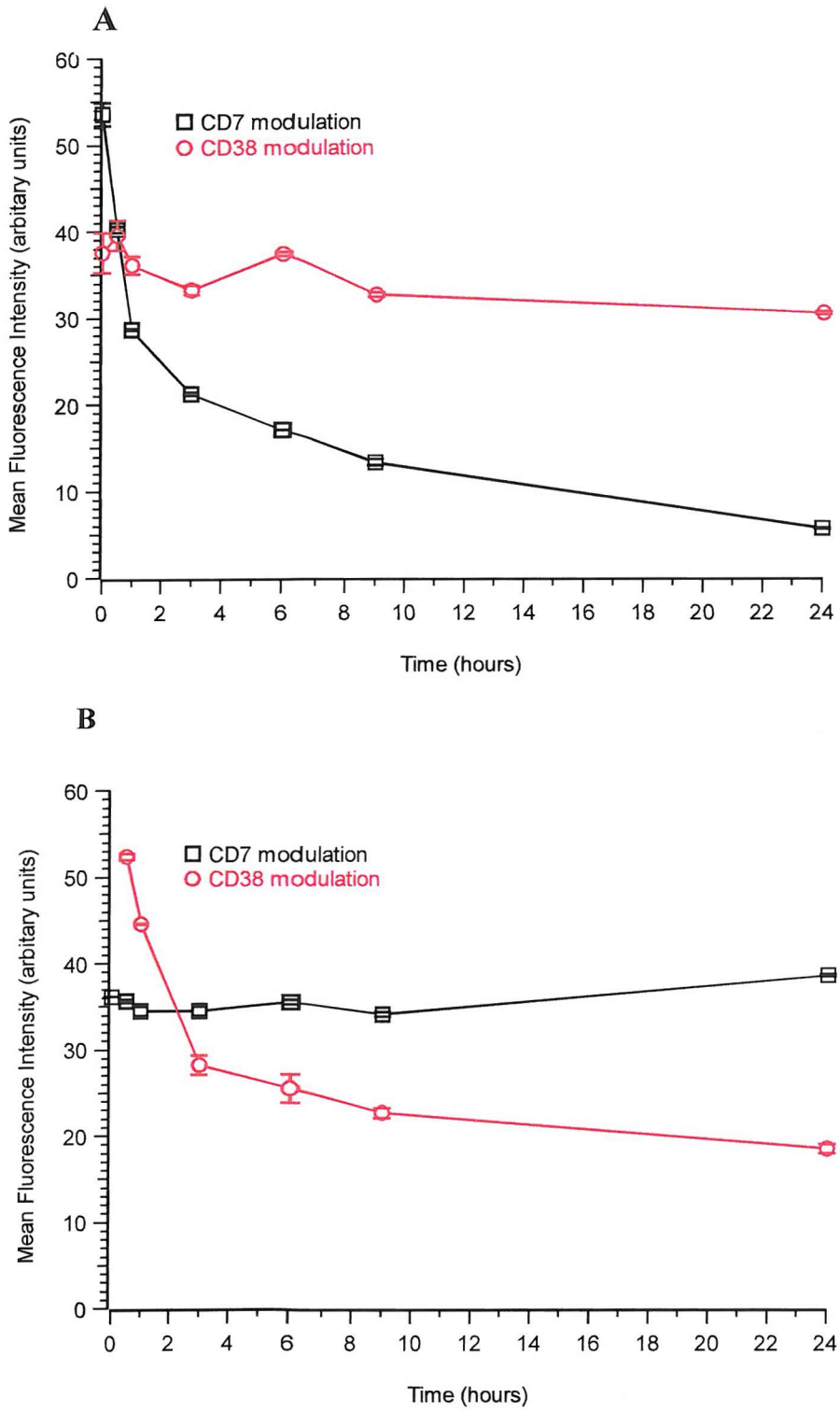

Figure 4.5. Kinetics of internalisation of CD7 (**A**) or CD38 (**B**) following ligation of the antigen by intact Ab while CD38 (**A**) and CD7 (**B**) levels were detected at each time point but were not ligated throughout the experiment. Data represents surface bound Ab expressed as the mean fluorescence intensity (arbitrary units). Bars + SD(n-1).

4.3.4 Iodination of OKT10 and HB2 Antibodies

The antibodies OKT10 (anti-CD38) and HB2 (anti-CD7) were both iodinated using ^{125}I-Na in the presence of an IODO-BEAD (Pierce and Warriner) as described by the

manufacturer (detailed in section 2.9.1). Following iodination, the antibodies were passed through a PD-10 gel filtration column (Bio-Rad) to separate iodinated Ab from free iodine-125. This process was monitored by extracting 10µl samples from each 1ml fraction collected, which were then counted on a gamma counter for counts per minute (cpm). Using the cpm data an elution profile was constructed as shown in figure 4.6. The Ab was the first peak of each trace to pass through the column. Only fractions 4 and 5 off the PD-10 column were pooled together so that only Ab with the greatest extent of ^{125}I-labelling was used for binding studies. As can be seen by the data in figure 4.6, HB2 Ab incorporated ^{125}I with a greater efficiency than OKT10 Ab.

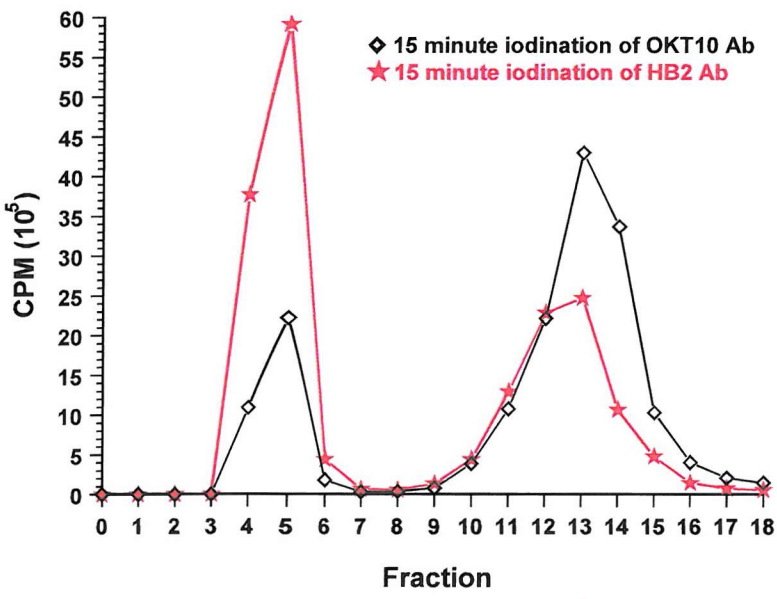

Figure 4.6 Elution profiles of iodinated HB2 Ab (☆) and OKT10 Ab (◇) from a PD-10 gel filtration column.

SDS-PAGE analysis under non-reducing conditions on a 5% separating gel was performed with samples from each peak of both iodinated antibodies to confirm which peak(s) contained the iodinated Ab. The gels were dried and autoradiographed and a representative result is shown in figure 4.7. Iodinated Ab was mainly visible in fractions 4 and 5 with a trace amount visible in fraction 6 (depending on the length of exposure to the gel). Iodinated HB2 Ab cannot be seen in lane 3 in figure 4.7(A) so as not to overexpose the other bands but was seen when the exposure was lengthened. The iodination procedure was successful for both antibodies resulting in minimal degradation products (shown in figure 4.7A and B where the Ab can be seen at 160kD). A 15 minute

incubation with ^{125}I-Na was found to be the optimum time for iodide incorporation into these proteins (data not shown).

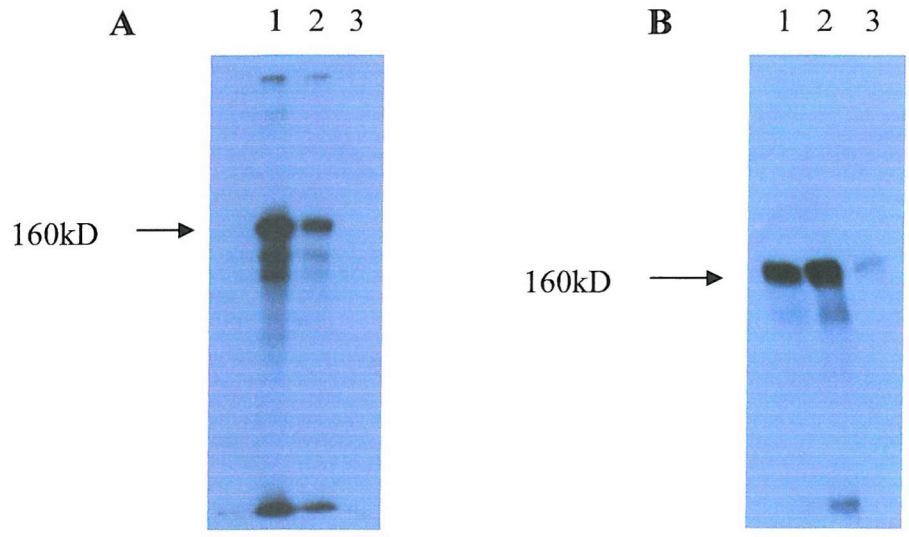

Figure 4.7 Autoradiograph of the SDS-PAGE analysis of fractions produced by the (A) HB2 Ab and (B) OKT10 Ab iodination. Samples were run on a 5% separating gel under non-reducing conditions. Ab was visible in fractions 4 (track 1), 5 (track2) and 6 (track3).

4.3.5 Iodination of OKT10- and HB2-Saporin Immunotoxins

Immunotoxins comprised of the native antibodies HB2 and OKT10 were also iodinated to determine any differences in the number of binding sites and affinity for their respective antigens that may occur after the conjugation process. An identical procedure was carried out on both OKT10- and HB2-Saporin immunotoxins as was followed for the iodination of their respective native antibodies. The iodination was carried out for 15 minutes. An elution profile of the iodinated ITs were obtained as before and are shown in figure 4.8 A and B. Native Ab was iodinated on the same occasion for comparative purposes. Whereas previously HB2 Ab appeared to iodinate with greater efficiency than OKT10 Ab, their elution profiles (figure 4.8 A & B) indicated that both ITs iodinated with similar efficiencies. Fractions 4 and 5 were pooled for both ITs to keep the iodinated proportion of IT at an optimum.

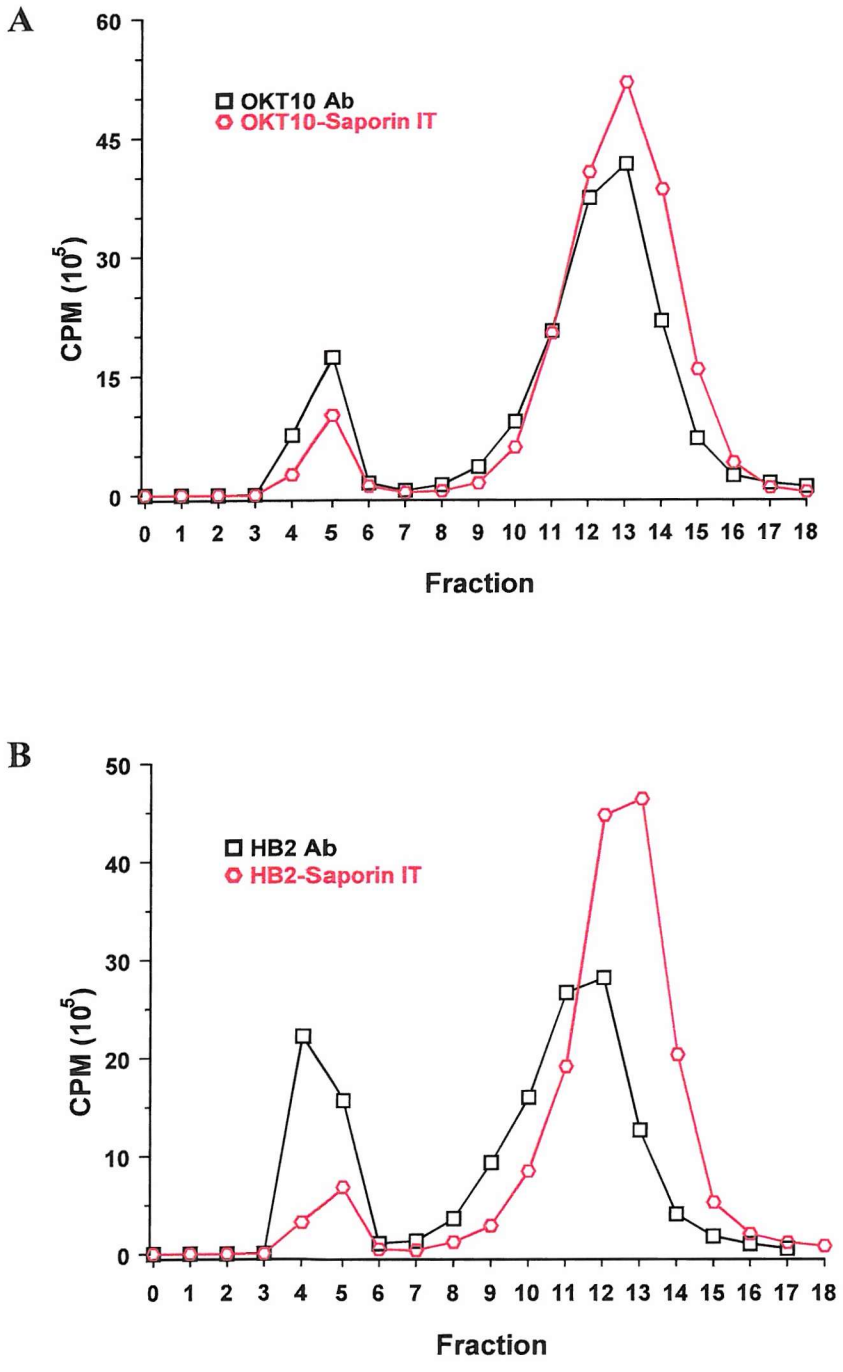

Figure 4.8 Elution profiles of (A) iodinated HB2 and (B) Ab (□) and immunotoxin (⬡) from a PD-10 gel filtration column.

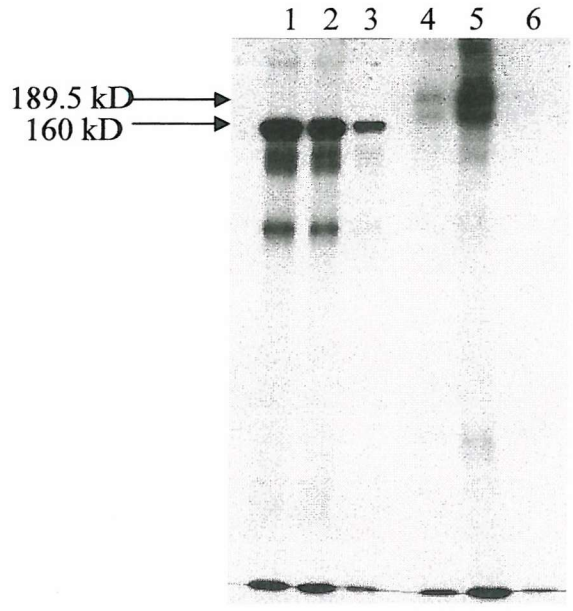

Figure 4.9 An autoradiograph of the SDS-PAGE analysis of fractions produced by the iodination of OKT10 Ab (tracks 1-3) and OKT10-Saporin IT (tracks 4-6). Samples were run on a 7.5% separating gel under non-reducing conditions. Iodinated Ab was visible in fractions 4 (track 1), 5 (track2) and 6 (track3) and iodinated immunotoxin was visible in fractions 4 (track 4), 5 (track 5) and faintly in 6 (track 6). Also visible in tracks 4 and 5 is iodinated unconjugated Ab.

SDS-PAGE analysis under non-reducing conditions on a 7.5% separating gel was performed with samples from each peak of both iodinated antibodies to confirm which peak(s) contained the iodinated Ab and immunotoxin. The gels were dried and autoradiographed (a representative example of which is shown in figure 4.9). The Ab was found as before within fractions 4, 5 and 6 with minimal degradation products. The immunotoxins were also found within fractions 4, 5 and 6. The iodination procedure was successful for both immunotoxins resulting in minimal low molecular weight degradation products (shown in figure 4.9 where the Ab can be seen at 160 kD and the IT at 189.5 kD), although there was a small proportion of unconjugated Ab that had become iodinated. This Ab may have become unconjugated during the iodination procedure.

4.3.6 CD7 and CD38 antigen density and antibody binding affinity

The binding capability of ^{125}I-labelled anti-CD7 and anti-CD38 monoclonal antibodies HB2 and OKT10 (respectively) to HSB-2 cells was determined by Scatchard analysis. A

representative example of the data that was obtained by this method is shown in figure 4.10. Table 4.1 summarises the antigen density and Ab binding affinity data derived from several separate experiments. The average number of HB2 Ab binding sites per HSB-2 cell was estimated to be $1.91x10^5$/cell with a binding affinity (represented by the dissociation constant, K_D) of 1.66nM. In contrast to this, it would appear that not only were there less CD38 molecules per cell with an average number of $1.02x10^5$/cell (which was approximately half of the number of CD7 molecules present on the surface), but OKT10 Ab also had a lower binding affinity (approximately 9.80nM) for its antigen. Both antibodies had high affinities for their respective antigens since they were both in the nanomolar range but HB2 Ab had an affinity for CD7 which was almost 6-fold greater than that of OKT10 Ab for CD38.

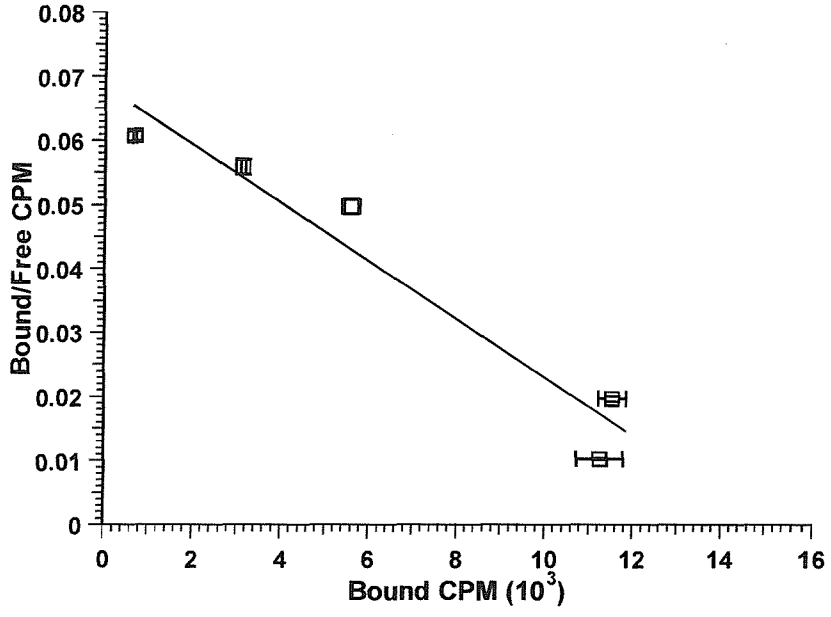

Figure 4.10 A representative Scatchard plot from a single binding study of OKT10 Ab on HSB-2 cells (r^2 of 0.93). This gives a straight line from which the binding parameters K_D and B_{max} (maximum binding sites) can be calculated. Data is represented as the mean of duplicate samples. Bars = SD(n-1).

Table 4.1 The number of binding sites and affinity of HB2 and OKT10 Ab on HSB-2 cells when bound singly or in combination as determined by Scatchard analysis. When both antibodies were bound simultaneously, one Ab was radiolabelled and the other was not (the labelled Ab is the Ab denoted in the table).

^{125}I-labelled Ab	Antigen	Single/Combination Study	No. molecules per cell	K_D
HB2	CD7	Single	191,053	1.7nM †
HB2	CD7 labelled	Combination	169,738	1.1nM
OKT10	CD38	Single	96,907	9.8nM †
OKT10	CD38	Single	120,282	9.7nM ‡
OKT10	CD38 labelled	Combination	106,084	7.7nM ‡

The data represented here is calculated from values taken from Scatchard plots all with correlation coefficients of $r^2 > 0.85$

† Data derived from three individual experiments

‡ Data derived from the same experiment for comparison between the single and combination study.

For comparative purposes, a similar analysis was performed on CCRF CEM cells (also a T-ALL cell line) with the HB2 and OKT10 antibodies (data not shown). It was found that although the antibodies maintained a similar affinity for these antigens (1.77nM and 13.21nM respectively), as on HSB-2 cells, their expression levels were very different on this cell line. CD7 was expressed at a level of 5.8×10^4/cell while there were 6×10^4 CD38 molecules expressed on the CCRF CEM cell surface. Another noticeable difference between the expression levels on these two cell lines was that CD7 and CD38 were found at similar levels on CCRF CEM cells whereas on HSB-2 cells CD7 was expressed at levels that were approximately twice as great as that of CD38.

When both antigens were ligated with one Ab radiolabelled, and the other one unlabelled, a slight decrease in the number of molecules of Ab bound to the cell surface was observed, and was accompanied by an apparent increase in the binding affinity for the antigen (table 4.1). This phenomenon was similar for both antibodies. The number of molecules of OKT10 Ab bound to the cell surface dropped from 1.20×10^5 molecules/cell to 1.06×10^5 molecules/cell with an apparent 1.25 fold increase in affinity of the Ab for the antigen. Similarly, HB2 Ab was found to bind to 1.69×10^5 molecules/cell when the antibodies were used in combination, but to 1.95×10^5 molecules/cell when the antigen was singly ligated. An apparent 1.32-fold increase in binding affinity of HB2 Ab for CD7 was observed when both antigens were ligated simultaneously.

4.3.7 Comparison of the ability of immunotoxins and antibodies to bind to HSB-2 cells

Experiments were conducted to determine the number of sites that HB2- and OKT10-Saporin ITs bound to and with what affinity (data summarised in table 4.2). These studies were done in parallel with their respective native antibodies to investigate whether the ability of the Ab (component of an IT) to bind to its antigen is reduced by the conjugation procedure, a phenomenon that has been previously demonstrated by flow cytometry (data not shown). Unexpectedly, both immunotoxins displayed an increased number of binding sites (with a 1.5 fold increase for both CD7 and CD38) compared with their respective Ab, but with reduced affinity (a 1.2 fold decrease for CD38 and 1.35 fold for CD7). The data is summarised in figure 4.11.

Table 4.2 Comparison of the number of binding sites and binding affinity of OKT10 and HB2 ITs and antibodies on HSB-2 cells as determined by Scatchard analysis.

Antigen	Antibody Binding Sites (rec/cell)	Immunotoxin Binding Sites (rec/cell)	Antibody K_D (M)	Immunotoxin K_D (M)
CD38	61431	96434	6.7×10^{-9}	8.1×10^{-9}
CD38	85653	131529	1.02×10^{-8}	1.26×10^{-8}
CD7	76188	113760	7.87×10^{-10}	1.07×10^{-9}
CD7	68711	198793	1.11×10^{-9}	1.53×10^{-9}

This experiment was carried out on two separate occasions for each antigen. Each row of the table displays the data from a single experiment.

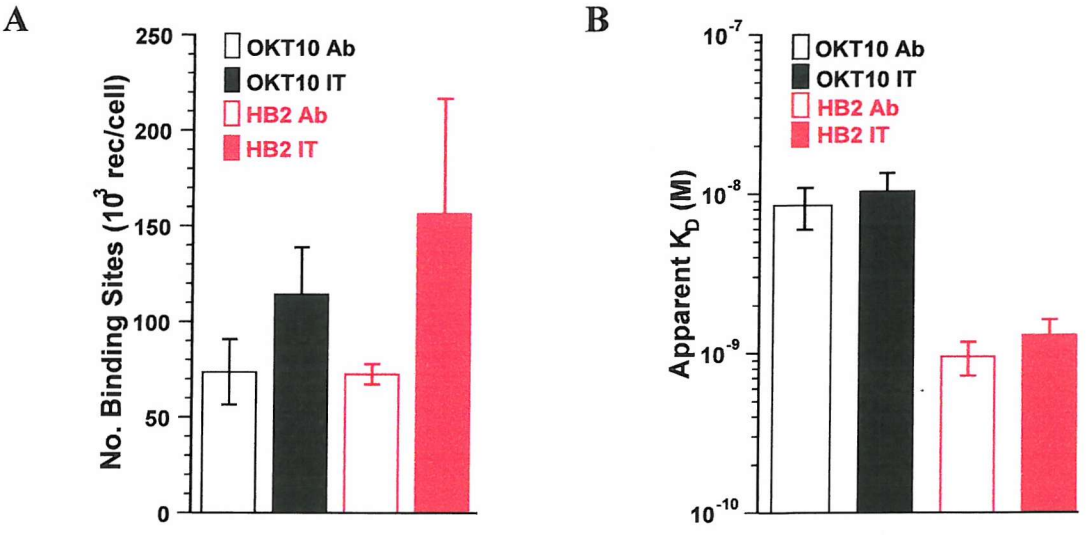

Figure 4.11 Comparison of the number of binding sites (A) and binding affinity (B) of OKT10 and HB2 ITs and antibodies on HSB-2 cells as determined by Scatchard analysis. Data is represented as the mean of data derived from two separate experiments. Bars SD(n-1).

4.3.8 Preliminary Studies to Determine the Optimum Conditions for Eluting Surface Bound Antibody

Preliminary studies were conducted to investigate which buffer and pH would provide the optimum conditions for removing surface bound radioiodinated Ab from the surface of HSB-2 cells. These conditions needed to be optimised before the proposed endocytosis assay could be performed. Acidic buffers have commonly been used for this purpose. It was necessary to find the correct conditions by which removal of the Ab from the cell surface could be achieved without compromising the integrity of the cell membrane, as this would cause the release of internalised material into the extracellular medium.

The first buffer investigated was isotonic Tris-HCl at pHs ranging from 2.2 to 7. One million cells were incubated with 300µl of this buffer at each pH for 5 minutes at 4°C following saturation of the cells with ^{125}I-MAb. Subsequent to this, the cell suspension was spun through a layer of phthalate oil and the radioactivity associated with the cell pellet was measured on a gamma counter. The data obtained from this experiment was plotted as a percentage of the Ab remaining on the cell surface relative to control samples which were incubated in PBS (pH 7.4) as shown in figure 4.12.

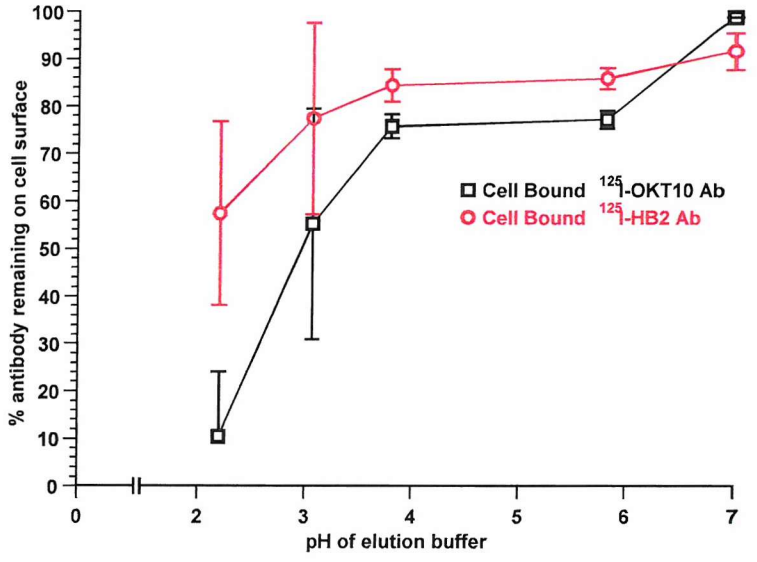

Figure 4.12 Percentage of ^{125}I-OKT10 Ab (□) and ^{125}I-HB2 Ab (○) remaining on the surface of HSB-2 cells when treated for 5 minutes at 4°C with isotonic TRIS-HCl at pH 2-7. Bars = SD(n-1).

It would appear that this buffer was capable of removing up to 90% of the surface bound ^{125}I-OKT10 Ab at pH 2.2, whereas only 43% of ^{125}I-HB2 Ab was removed when cells were exposed to the same conditions. At a pH of 3 or greater no more than 50% of either Ab was eluted. For this reason it was decided that these conditions would not be suitable for an endocytosis assay, since the results obtained using this method would be misleading and inaccurate.

The effects of an isotonic citrate-phosphate buffer on Ab elution were investigated on both antibodies to establish if this buffer performed any better at eluting Ab. After saturation with ^{125}I-MAb, the cells were incubated twice with this buffer for 5 minutes at 4°C to see if this resulted in improved elution of both antibodies. Data was obtained for the elution OKT10 and HB2 antibodies (figure 4.13 A and B respectively) when using the citrate-phosphate buffer. The data was plotted as cell associated CPM against pH (figure 4.13). It became apparent, when examining the data for both antibodies that the ability of the buffer to remove material from the cell surface was greatly reduced when the pH was increased. Only when the cells were treated with citrate-phosphate buffer pH 2.5 did the cell associated cpm reduce to background levels. Any increase in pH above a value of 2.5 resulted in a considerable amount of cell associated radioactivity especially with HB2 Ab (with counts of 11541 at pH 3.0).

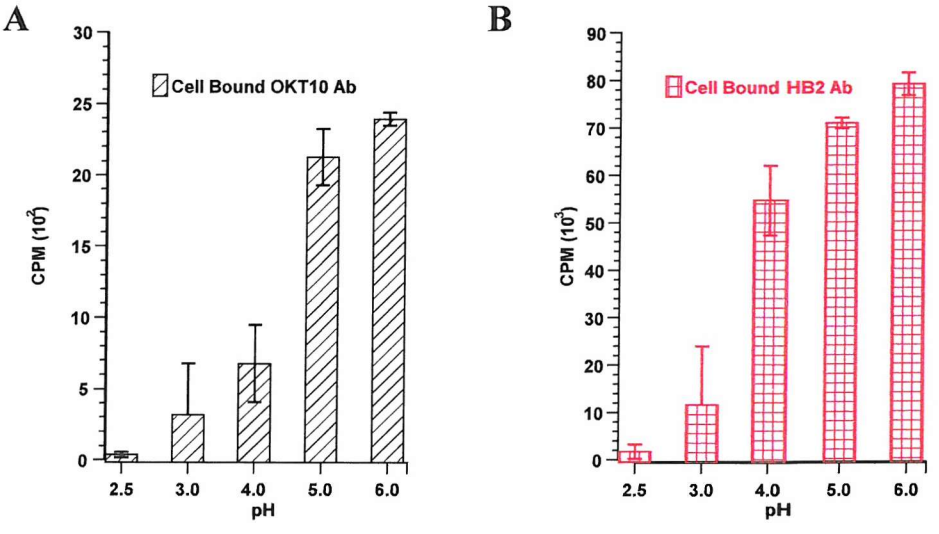

Figure 4.13 Cell bound ^{125}I-OKT10 Ab (A) and ^{125}I-HB2 Ab (B) on the surface of HSB-2 cells after cells were treated twice for 5 minutes at 4°C with isotonic Citrate-Phosphate at pH 2.5-6. Bars = SD(n-1).

A cell viability assay was conducted to examine the effect of a 5 minute incubation (at 4°C) of the citrate-phosphate buffer on the integrity of the cell membrane. This was performed using trypan blue exclusion and data obtained from this work is summarised in table 4.3. Incubating cells with the citrate-phosphate buffer at pH 2.5 resulted in a complete loss of cell viability (i.e. 0% of viable cells). Non-viable cells are less likely to pellet efficiently through the phthalate oil, which may account for the low level of cell-associated radioactivity observed in the cells exposed to this condition. The cell viability greatly increased when cells were treated at pH 3.0, but this pH did not provide the optimum conditions for elution of the Ab from the cell surface.

Table 4.3 A Summary of the cell viabilities of HSB-2 cells treated with Citrate-phosphate and Glycine-HCl at various pHs for different lengths of time.

Buffer	pH	Condition	% viable ∞
Citrate-phosphate	2.5	5 minutes at 4°C	0
Citrate-phosphate	3.0	5 minutes at 4°C	87
Citrate-phosphate	4.0	5 minutes at 4°C	97
Citrate-phosphate	5.0	5 minutes at 4°C	96
Citrate-phosphate	6.0	5 minutes at 4°C	92
Glycine-HCl	2.0	5 minutes at 4°C	0
Glycine-HCl	3.0	5 minutes at 4°C	95
Glycine-HCl	4.0	5 minutes at 4°C	92
Citrate-phosphate	2.5	2 x 5 minutes at 4°C	3
Citrate-phosphate	2.6	2 x 5 minutes at 4°C	2.4
Citrate-phosphate	2.7	2 x 5 minutes at 4°C	0
Citrate-phosphate	2.8	2 x 5 minutes at 4°C	4.6
Citrate-phosphate	2.9	2 x 5 minutes at 4°C	11
Citrate-phosphate	3.0	2 x 5 minutes at 4°C	41.1
Glycine-HCl	2.5	2 x 5 minutes at 4°C	0
Glycine-HCl	2.6	2 x 5 minutes at 4°C	0
Glycine-HCl	2.7	2 x 5 minutes at 4°C	0
Glycine-HCl	2.8	2 x 5 minutes at 4°C	0
Glycine-HCl	2.9	2 x 5 minutes at 4°C	0
Glycine-HCl	3.0	2 x 5 minutes at 4°C	66

∞ % viable calculated by dividing the no. of viable cells by the total cell count (viable + non-viable) and multiplying by 100.

Isotonic glycine-HCl was tested in the same way as the citrate-phosphate buffer by incubating the cells twice with each pH for 5 minutes at 4°C, but only at pH 2.0-4.0 (figure 4.14). Glycine-HCl at pH 2.0 appeared better at eluting both OKT10 and HB2 Ab (figure 4.14 A and B respectively) from the cell surface than pH3.0 or 4.0. As seen before, OKT10 Ab appeared to be efficiently eluted from the cell surface at pH 3.0 whereas HB2 Ab still displayed a large amount of cell associated radioactivity at this pH.

The cell viability assay indicated that a viability of 0% was obtained by exposing the cells to this buffer at pH 2.0, but by increasing the pH to 3.0 a viability of 95% was maintained.

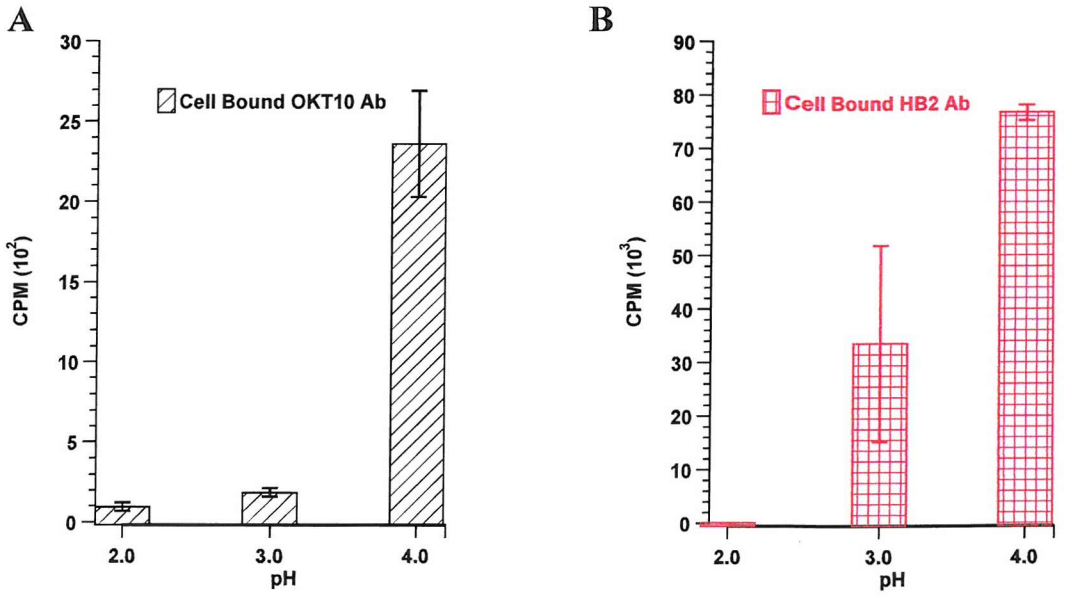

Figure 4.14 Cell bound ^{125}I-OKT10 Ab (A) and ^{125}I-HB2 Ab (B) on the surface of HSB-2 cells after cells were treated twice for 5 minutes at 4°C with isotonic Glycine-HCl at pH 2-4. Bars = SD(n-1).

Since optimum conditions suitable for the elution of both antibodies were required for the endocytosis assay, the next progression was to investigate whether a pH between 2.5 and 3.0 of either of the two buffers would enable the efficient release of surface bound Ab without disrupting the cell. Citrate-phosphate and glycine-HCl buffers were both tested at pHs of 0.1 increments between 2.5 and 3.0 by incubating the cells twice for 5 minutes at 4°C. Although the data from these experiments (figures 4.15A&B) looked promising, an observation made during the experimentation indicated to the contrary. It was observed that when the cell suspension was spun through phthalate oil (after incubation with the elution buffers), that the cells were not pelleted efficiently and the appearance of a white substance, presumably lipids, was noticed on the surface of the oil. This occurred in all the conditions tested with both buffers except those of pH 3.0 and above. This phenomenon made it difficult to draw any accurate conclusions from this data.

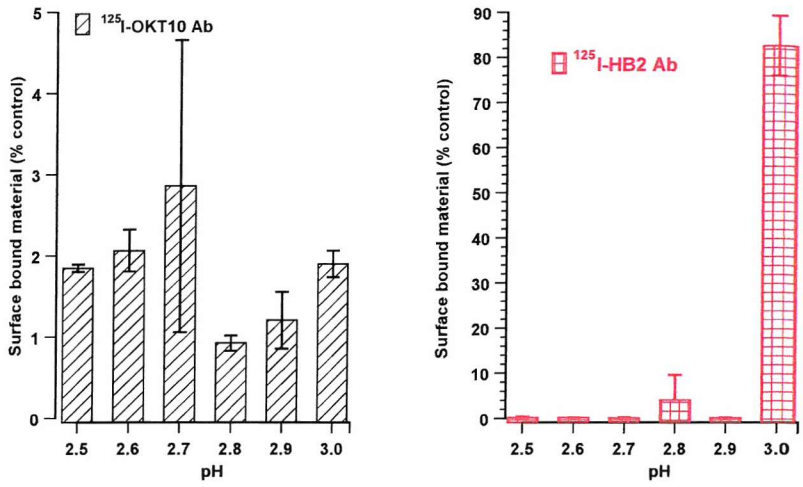

Figure 4.15 Cell bound ^{125}I-OKT10 Ab (A) and ^{125}I-HB2 Ab (B) on the surface of HSB-2 cells. Cells were treated twice for 5 minutes at 4°C with isotonic (A) Citrate-phosphate or (B) Glycine-HCl. Bars = SD(n-1).

Cell viability data was also obtained for cells exposed to either glycine-HCl or citrate-phosphate buffer at pHs ranging between 2.5 to 3.0 (table 4.3). This data confirmed the poor viability of cells exposed to glycine-HCl between 2.5 and 2.9. Although the viability of the cells was considerably increased when they were exposed to pH 3.0, it was still low enough for there to be a possibility of misleading results, especially if the membrane of a proportion of the cells had become leaky, since internalised Ab may have been able to escape into the extracellular medium. The use of citrate-phosphate buffer resulted in similar findings. Even when the buffer was used at pH 3.0 the viability was still below 50%.

The use of proteolytic enzymes was investigated to determine the efficiency of cleaving the Ab from the cell surface. Various concentrations of trypsin, ranging between 0.05mg/ml and 0.5mg/ml (in half logs), were used at a neutral pH. The cells were exposed to trypsin (in the presence of EDTA) for 30 minutes at 37°C. Subsequent to this the cell suspension was spun through phthalate oil and the data obtained was plot as the percentage of surface bound material relative to controls incubated in PBS against concentration of trypsin. As can be seen in figure 4.16, none of the dilutions of trypsin tested on HSB-2 cells were found suitable for the removal of a sufficient amount of either HB2 or OKT10 Ab from the cell surface. In fact, the most effective dose of trypsin was 0.5mg/ml which at the most, only appeared to strip 70% of the surface bound Ab.

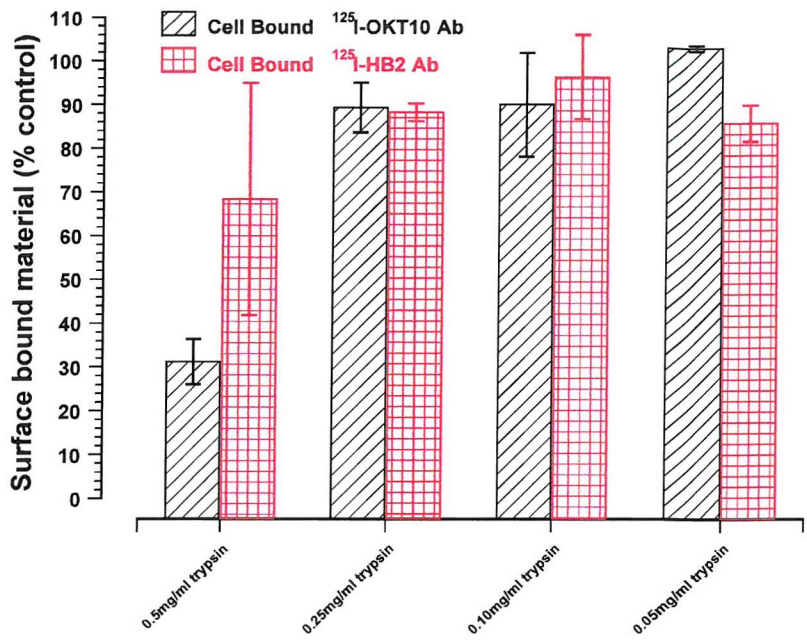

Figure 4.16 Cell bound ^{125}I-OKT10 Ab (black) and ^{125}I-HB2 Ab (red) on the surface of HSB-2 cells after treatment with trypsin at various concentrations between 0.05 and 0.5mg/ml at 37°C for 30 minutes. Bars = SD(n-1).

Pepsin is an enzyme well documented for its ability to produce $F(ab)_2$ fragments when incubated with intact Ab and can go on further to produce the smaller Fab' fragments. As this enzyme is found in the gut, acidic pHs produce the optimum conditions for pepsin to work in. The cells were incubated with glycine-HCl at pHs ranging from 2.7 to 3.3 containing 5mg/ml of pepsin for 5 minutes at 4°C following saturation with either ^{125}I-OKT10 or ^{125}I-HB2 Ab. The results obtained (shown in figure 4.17) indicated that at pH 2.7 and pH 3.0 this buffer may have removed a large proportion of the radiolabelled Ab from the cell surface, but the cells were disrupted by these conditions and did not pellet efficiently through the oil until the pH was increased to 3.3 or above. Unfortunately, there was still a large amount of radioactive material associated with the cells at this pH (figure 4.17), making it unsuitable for use in the endocytosis assay.

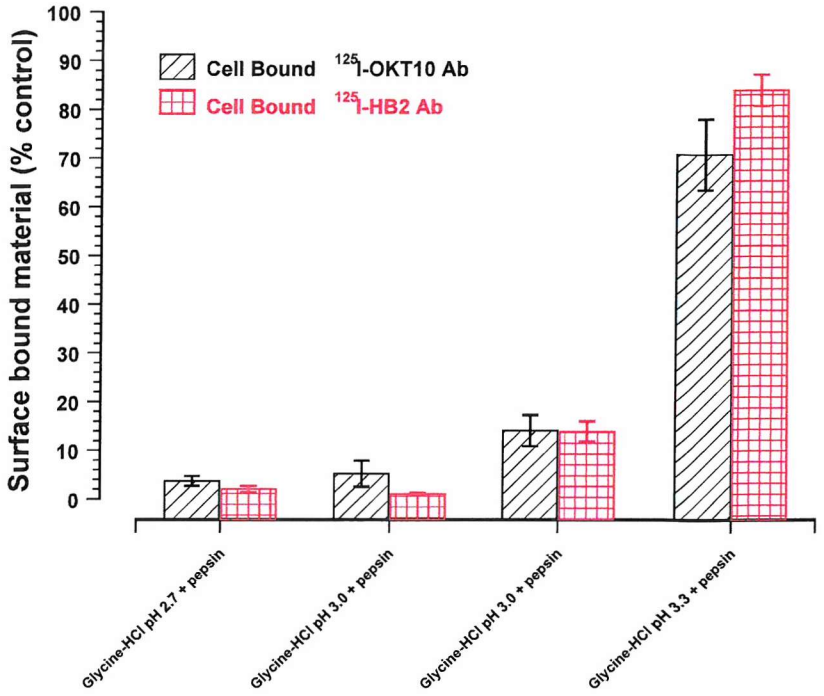

Figure 4.17 Percentage of ^{125}I-OKT10 Ab (black) and ^{125}I-HB2 Ab (red) on the surface of HSB-2 cells treated with pepsin at 5mg/ml in Glycine-HCl ranging between 2.7 and 3.3 at 4°C for 5 minutes. Bars = SD(n-1).

4.4. Discussion

The main observation to be taken from this data was how two potent immunotoxins have very distinct internalisation characteristics. CD7 modulated very rapidly from the cell surface within the first hour of incubation at 37°C and continued to internalise, albeit at a slower rate, for the rest of the 24 hour time course. In contrast to this, CD38 modulated from the surface rapidly to start with over a period of 3 to 6 hours, after which time this process appeared to plateau. This was either due to an equilibrium between the two processes of internalisation and re-expression being reached, or because no more antigen modulated from the cell surface.

Many different groups (Carriere *et al.*, 1989, Suzuki *et al.*, 1991, Akbar *et al.*, 1991) have also reported on the rapid modulation of CD7 antigen from the surface of T cells as has been observed in the studies presented here. Baum *et al.*, (1996) monitored the internalisation of an anti-CD7 mAb (TH-69) of the IgG_1 subclass using ^{131}I directly labelled Ab over a total period of 4 hours on the T-ALL cell line CEM. Their data showed a very similar rate of internalisation to that displayed by our Ab with only 34% of the total surface CD7 remaining after four hours. This group also found the rapid modulation of

CD7 to be reproducible in an *in vivo* nude mice model. This suggests that *in vitro* studies can provide a good representation of the behaviour of these agents *in vivo.*

Carriere *et al.,* (1989) reported that in 30 minutes CD7 modulated 50% of original surface levels on the CEM cell line, whereas Tonevitsky *et al.,* (1993) states that 70% of CD7 was internalised during this time. These groups have also found that CD7 completely modulated from the surface in just a matter of a few hours. Although this data is in agreement with the findings here that CD7 internalises very rapidly and eventually modulates completely from the cell surface, our findings show that this process can take between 12 to 24 hours. The discrepancies observed between data from different groups may be attributable to the relative sensitivities of the assays undertaken, since most investigations of this kind are done using radiolabelled antibodies as opposed to measuring surface fluorescence levels as was done here. If the aforementioned studies were performed using antibodies of a lower affinity or avidity for the antigen than the one used for this work, then this may have resulted in losses of Ab from the surface of these cells during washing procedures giving a false indication of surface expression levels. Much of the data on the internalisation kinetics of CD7 have been obtained on T cell lines of a similar nature to HSB-2 cells such as CEM cells which may behave slightly differently to the same conditions, hence may also account for some of the slight variations seen in the results obtained.

In this study, it was found that CD38 had a very distinct modulation pattern from CD7. The internalisation kinetics of this antigen were biphasic with rapid modulation within the first few hours of incubation followed by a plateau. Funaro *et al.,* (1998) have studied the endocytosis of the human CD38 molecule in normal lymphocytes and in various leukaemia- and lymphoma derived cell lines. This group described the kinetics of CD38 internalisation as similar to that of CD23 on B cells (Grenier-Brossette *et al.*, 1992) which is slower than the ligand induced internalisation of many other membrane proteins (Marano *et al.*, 1989). This work supports that statement when the internalisation of CD38 is compared with that of CD7.

Also in agreement with our observations is that of Funaro *et al.*, (1998) who found that CD38 internalisation never involved the entire amount of surface molecules. In fact, the internalised fraction appeared to represent an almost constant percentage (of 30-40%) of the total amount of surface molecules. Similarly, it was found that on HSB-2 cells up to 50% of surface CD38 was internalised over a 24 hour period. This plateau in internalisation kinetics appeared to occur after 6 hours and after this time the amount of Ab on the surface of the cell appeared to remain constant. There are several possible explanations for this phenomenon. It may suggest the existence of two pools of CD38 molecules on the cell surface, one of which may undergo internalisation upon Ab ligation and the other which may not. An example of a surface molecule with this property is CD22 (Shan and Press 1995). The two pools of antigen may also differ in structural conformation, which is supported by evidence of a high molecular weight form of CD38 (Umar *et al.*, 1996). It may be possible that if two pools of CD38 exist that the two may differ in their interactions with other still unknown membrane proteins affecting their internalisation characteristics.

The CD38 molecule has been cloned and sequenced. This work revealed that CD38 has a very short cytoplasmic tail which lacks the conventional signals and potential phosphorylation sites involved in internalisation (Jackson and Bell 1990). It is thought that the modulation of CD38 from the cell surface may depend on interactions with other surface molecules which may be co-internalised or exhibit lateral interactions with CD38 (Funaro *et al.*, 1993). Such interactions would have to be of submembrane localisation and harbour the signal and regulation domains that are lacking in the molecule itself.

The cytotoxicity assays described in chapter 3 demonstrated how both anti-CD7 and anti-CD38 immunotoxins act as potent cytotoxic agents against the T-ALL leukaemia cell line *in vitro* and *in vivo*, even though they differed greatly in their internalisation kinetics. This was an indication that there was not a direct correlation between internalisation and cytotoxic potency unlike the findings of Wargalla *et al.*, (1989) which stated that there was a direct correlation. The short term protein synthesis inhibition assay (in chapter 3) suggested that HB2-saporin (anti-CD7) performed marginally better than OKT10-saporin

(anti-CD38), whereas in both the long-term outgrowth assay and the *in vivo* SCID mice experiment the reverse appeared to be true. These differences may be a result of the kinetics of internalisation. HB2-saporin IT may be much faster acting as it internalises at a much faster rate and to a greater extent than CD38, but this action may be shorter lived if the IT is more readily degraded. This is discussed by Tonevitsky *et al.*, (1993) when it is suggested that the cytotoxic effect of ITs against receptors with a high internalisation rate may be lower than the value expected, due to recycling of the antigen to the cell surface. This is because a high rate of antigen recycling may lead to a situation when the receptor returns to the surface with IT still attached so that the toxin has not reached the cytoplasm. It was also discussed that these ITs with rapid internalisation kinetics have a good probability of reaching lysosomes to be enzymatically degraded (Tonevitsky *et al.*, 1993). These are likely explanations for the discrepancies in the potencies of each IT between the different cytotoxicity assays.

The potent cytotoxic capability of OKT10-saporin IT may be explained by saporin delivered toxicity as a result of the internalised proportion of IT in addition to any ADCC mediated action on the cell surface by the fraction remaining bound to the non-internalised molecules of CD38. This may also be the mechanism used by HB2-saporin but less IT remains on the surface to activate ADCC mediated killing. The fact that internalisation kinetics do not correlate directly to cytotoxic potency may also indicate that intracellular routing may play a more important role in determining the potency of individual ITs. The fact that CD38 does not internalise as much and as rapidly as CD7 may also explain why in a short term assay such as the PSI this IT does not appear to act as well as HB2-saporin, and the observation that OKT10-saporin IT can remain bound to the cell surface for at least 24 hours may also help to explain why its actions are slower but longer lived.

When considering these ITs as possible therapeutic agents against such diseases as leukaemia and lymphoma it is important to try to assess the possible down regulation of the target antigens after exposure to therapy. If this phenomenon was to occur the therapy would be of no use after the initial dose. The pulsed restain and continuous exposure

samples were used to investigate the possible downregulation of CD7 and CD38 once exposed to their respective antibodies.

It would appear that CD7 began to downregulate as the antigen was internalised but re-emerged on the surface after a period of 6 hours and continued to increase in expression levels for the rest of the 24 hour duration. CD7 expression levels did not reach their original saturation levels by this time but looked to be continuing to increase, as this process did plateau. When CD7 was continually exposed to Ab a slightly different effect on re-expression of the molecule was observed. The overall expression of CD7 decreased throughout the 24 hour period of the experiment although it was expected that some re-expression would occur as the decrease in CD7 levels detected were not as low as those receiving a pulsed exposure to Ab and then allowed to internalise.

The re-expression of CD38 was slightly different from that of CD7. This antigen molecule progressively decreased in number on the cell surface up until 3 hours after which time the surface antigen expression levels increased rapidly to levels similar to those seen at the beginning of the experiment. This may be due to either recycling of the antigen or *de novo* synthesis of the molecule or replacement of antigen by an intracellular store. An interesting observation that can be made from the continuous exposure data of CD38 was that there was no difference in the effect of continuous or pulsed exposure of the antigen to the Ab, unlike with CD7. This work provided an encouraging indication that neither antigen downregulates to the extent whereby further IT treatment would become redundant.

The effect of univalent binding on internalisation was investigated by incubating the cells with the Fab' fragment of the intact antibodies studied, followed by incubation at 37°C. After cells were pulsed for half an hour with the Fab' fragment of the anti-CD7 Ab HB2, there was a gradual decrease in antigen surface levels for the first 3 to 6 hours. A plateau in expression levels followed this, at least until 24 hours. There are two possible explanations for this, the first being that the antigen was internalised. If this occurred then

the plateau in internalisation kinetics and the steady state reached in the pulsed restain and continuous samples may be explained by the very rapid process of recycling of antigen to the cell surface which may not be seen between the half hour gap between time points. The other explanation, which may be implied by lack of change to detection levels in the pulsed restain and continuous exposure samples, is that the Fab' fragment was not internalised. If this was the case then the decrease noted in the pulsed samples may be due to the reduced avidity of this fragment compared to the intact Ab which resulted in the fragment dissociating from the antigen. Alternatively, it may suggest that cross-linking is necessary for the internalisation of CD7 since the Fab' fragment would not be able to cross-link the antigen.

Mellman and colleagues (Mellman *et al.*, 1984, Mellman and Plutner 1984) have shown that monovalent Fab' fragments with specificity directed against membrane receptors were recycled although the corresponding polyvalent IgG induced transport toward the lysosomes. Some investigators found that univalent Fab' or Fab' fragments directed against surface immunoglobulin (sIg) internalise poorly (Karnovsky and Unanue 1973), whereas others demonstrated that Fab' fragments internalise as well as (or better than) bivalent antibodies (Mellman *et al.*, 1984, Goud and Antoine 1984). Pauza *et al.*, (1997) investigated the use of single-chain Fv (sFv) immunotoxins as therapeutic agents against human T cell malignancies. Their work described how no significant differences to the extent of internalisation were discovered between the bivalent intact Ab and the monovalent sFv fragment targeted against CD7 within a given cell line. This work and some of the work mentioned above would indicate that cross-linking is not a requirement for internalisation of the CD7 antigen. This is probably what was demonstrated by the data displayed here, although further studies would be needed to determine that the modulation from the cell surface of Fab' was internalisation and not shedding or dissociation of the fragment from the antigen.

The effect of monovalent binding was also investigated on CD38. Again looking at the pulsed samples it would appear that CD38 still managed to internalise to a similar if not a better extent than the intact Ab when ligated by Fab', indicating that cross-linking is not a requirement for the modulation of CD38. This decrease in the detection of the Fab'

fragment on the surface may also have been due to the fragment dropping off as a result of low avidity for the antigen, but as it was so similar to the intact Ab it seemed likely that the majority of this drop was a result of modulation of the antigen. In this experiment there appeared to be a significant increase in CD38 expression when the pulsed samples were restained and an even greater one when the cells were continuously exposed to the fragment. This was likely to be due to aggregation of the Fab' fragment on the cell surface or some other unexplained phenomenon. One method that could confirm whether or not either of the Fab' fragments still internalised efficiently would be to make immunotoxins with these fragments and see if they are still cytotoxic. An alternative approach would be to label a Fab' fragment with fluorescence or gold particle and then try to visualise them within the cell using confocal microscopy.

CD38 has been shown to have associations with other surface molecules such as CD3, CR2/CD19 and CD16 (Funaro *et al.*, 1993), whereas CD7 has been associated with both CD3 and CD45 (Lazarovits *et al.*, 1994). There appears to be no evidence of any associations between CD7 and CD38, which was supported by these studies since when one of the antigens was ligated and allowed to modulate, the other antigen did not change its expression levels on the cell surface. This data indicated that there is no association between the two molecules when only one was ligated. We also investigated whether any association existed between these antigens when both were ligated by their respective IT. When both ITs were detected simultaneously it had appeared that more antigen was internalised as a result of co-ligation as more than 50% had disappeared from the surface. This value was an increase to the amount of CD38 internalised when ligated individually. When this was studied further by ligating one antigen by intact Ab and the other with the $F(ab)_2$ fragments of the Ab and detected by an Fc-specific FITC labelled secondary agent, it could be clearly seen that there was no significant effect of co-ligation on the internalisation kinetics of either of the two antigens.

It may be argued that using $F(ab)_2$ fragments to ligate the second antigen would not necessarily mimic the internalisation characteristics of the intact Ab but it was assumed that $F(ab)_2$ Ab should in theory internalise in an identical fashion to intact Ab, since it has two antigen-binding sites and so can crosslink antigenic determinants. However, there is

one possible important exception to this where Fc binding by FcγRII (CD32) may cause multiple crosslinking and induce a greater downregulation of the ligated antigen as with CD19 on Daudi cells (Vervoordeldonk *et al.,* 1994). CD32 is found on mononuclear phagocytes, neutrophils, eosinophils, platelets and B cells, but not on T cells such as those used in these experiments, therefore it would be unlikely that this event would occur.

In addition to studies implying that ligating both antigens simultaneously with antibodies does not affect their internalisation characteristics, investigations were also conducted with ^{125}I-MoAb to determine the effects of co-ligation on the binding capability of both antibodies. These studies demonstrate that there was no increase in the binding capacity of these two antibodies. In fact, the number of sites that each Ab bound to decreased but only very marginally.

Scatchard analysis determined that HB2 Ab bound with greater affinity for its antigen compared with OKT10 Ab for CD38 and bound to twice as many sites per cell. This in combination with the internalisation studies indicates that much more HB2 Ab is delivered into the cell interior and yet in the long term is not as potent as an IT comprised of OKT10 Ab. This may indicate that the intracellular routing of HB2 Ab within the cell is an inefficient process and the Ab or IT is prone to degradation. In contrast to this, only a relatively small number of OKT10 Ab molecules are taken up by the cell, which suggests that once inside the cell this molecule is more efficiently routed to the cytosol, and less rapidly degraded.

Studies to investigate the effect of conjugation of the toxin molecule to the Ab on the binding capacity of the Ab did not confirm the data obtained by flow cytometry. The gel data would suggest that the iodination procedure had resulted in a small proportion of unconjugated Ab which may have lead to misleading results in the Scatchard analysis. This may explain why the ITs obtained a higher binding capacity than their respective antibodies, since this did not agree with repeated studies on flow cytometry which without exception show a reduction in binding capacity of ITs in comparison with their respective Ab.

Unfortunately the endocytosis assay was not established. This was to be used to inform us more about the fate of the IT or Ab once within the cell as well as to confirm and quantify the internalisation data. It would confirm or dispute the hypothesis that HB2 Ab is rapidly degraded and CD38 is not. The cell line HSB-2 which was used for these studies, may have been more sensitive to acidic pHs then other cell lines that have successfully been used for this purpose. As a result the next chapters investigated other methods that would provide us with information of the fate of these two antibodies after internalisation.

The work in this chapter all leads to the conclusion that co-ligation of the two antigens CD7 and CD38 does not interfere with the internalisation kinetics in such a way as to bring about the increase in the therapeutic effect of using two ITs against these molecules in combination. What this data has shown is that the internalisation kinetics may help to explain some of the slight differences observed between the cytotoxic characteristics of the two ITs. Since this work has not elucidated the mechanism(s) behind the improved therapeutic effect of using two ITs in combinations investigations need to be done into other possible factors such as intracellular routing, recycling, and degradation of the ITs when used individually and in combination. Maybe these studies will determine what characteristic or property of one IT will make it more potent than the next and how these factors are influenced when more than one antigen is ligated at once to provide an increased therapeutic outcome.

CHAPTER 5

The Effects of Brefeldin A on Immunotoxin Cytotoxicity

5.1 Introduction

Immunotoxins have promising potential as therapeutic agents for cancer especially leukaemias and lymphomas and have shown to have marked activities in clinical trials (Vitetta *et al.*, 1991, Amlot *et al.*, 1993, Grossbard *et al.*, 1993). There are a multitude of factors that can affect the potency of an IT and severely limit its therapeutic value. These include isotype, affinity (van Oosterhout *et al.*, 1994) of the antibody moiety, and proximity of the target antigen epitope to the plasma membrane (May *et al.*, 1991), all of which affect the internalisation capability of an IT. The intracellular trafficking of an IT determines the efficiency with which the IT is delivered to an appropriate intracellular compartment to translocate to the cytosol. The flow cytometric studies in chapter 4 demonstrate that the internalisation characteristics of an IT can greatly influence the cytotoxic potency of an IT but they also show that it is not the only factor that determines the therapeutic ability of an IT. For this reason it was considered important to elucidate the features of the intracellular pathways of the anti-CD38 IT OKT10-Saporin and the anti-CD7 IT HB2-Saporin. Determination of the intracellular trafficking of these two ITs might explain why ITs against CD7 and CD38 are both very potent reagents even though they have different internalisation characteristics and how they may provide a greater cytotoxic response when the two ITs are used in combination. A considerable amount of work has been done to establish the pathways by which ricin and antibody-ricin ITs reach the cytosol to intoxicate the cell (Calafat *et al.*, 1988, Carriere *et al.*, 1985, van Deurs *et al.*, 1986, Raso *et al.*, 1987, Wales *et al.*, 1993, Sandvig *et al.*, 1999, Simpson *et al.*, 1999). A vital tool in these investigations has been the drug brefeldin A.

Brefeldin A is a fungal isoprenoid antibiotic which has been noted for its inhibitory effects on anterograde protein transport beyond the Golgi (Misumi *et al.*, 1986; Oda *et al.*, 1987), the rapid disassembly of the Golgi complex (Lippincott-Schwartz *et al.*, 1989), and the retrieval of resident and itinerant Golgi proteins to the ER. The cis, medial and trans cisternae of the Golgi complex redistribute to the ER rapidly after addition of BFA, but removing BFA from the culture media can rapidly reverse these effects. BFA inhibits nucleotide exchange onto ADP-ribosylation factor (ARF), a GTP binding protein

(Donaldson *et al.*, 1992) preventing assembly of cytosolic coat proteins (which include COP I components) onto target membranes (Orci *et al.*, 1991). At the same time, extensive retrograde transport of Golgi tubules occurs with BFA, which leads to the complete loss of Golgi structure (Lippincott-Schwartz *et al.*, 1990). Since retrograde transport of proteins from the Golgi back to the ER is not disturbed by BFA (Pelham 1991) it has been suggested that transport into the ER induced by BFA simply shows enhanced trafficking through the retrograde pathway as a result of non-selective transport into it of Golgi protein and lipid (Klausner *et al.*, 1992; Lippincott-Schwartz 1993). (For more details about the action of BFA refer to section 1.6.4.)

Redistribution of the components of the Golgi apparatus to the ER results in complete inhibition of ricin toxicity in a number of different cell types (Yoshida *et al.*, 1991). This inhibition can also be demonstrated with the toxins Pseudomonas exotoxin and Shiga toxin but not Diphtheria toxin as this reaches the cytosol by escaping from an acidic intracellular compartment.

Sandvig *et al.*, (1991) showed that a direct correlation between the effects of BFA on Golgi structure and toxic effect of ricin exists. In MDCK cells in which BFA does not perturb the Golgi apparatus, no protection against ricin toxicity was observed. Upon the addition of BFA, the Golgi stacks in cells which were protected against ricin, rapidly transformed into a tubulo-vesicular reticulum connected to the ER, however, the TGN in these cells remained intact. Ricin could be found localised in the TGN both in cells when the BFA was added before and after the toxin, but it was found not to be transported back to the ER once treated by the drug. These effects of BFA treatment on ricin toxicity indicate that the toxin must traverse the Golgi stack to reach the ER before translocation to the cytosol occurs. Other evidence has since become apparent that confirms that ricin is modified in the Golgi before reaching the ER (Rapak *et al.*, 1997). Tyrosine sulphation was used as a labelling procedure as this process takes place in the Golgi apparatus. Only molecules that had been retrogradely transported to the Golgi complex would be labelled. Sulphated ricin A chain was found in the cytosol implying that it was transported retrogradely, through the Golgi stacks to the ER, and then translocated to the cytosol.

Since saporin inactivates protein synthesis by causing release of adenine 4324 from the 28S rRNA of the large subunit of eukaryotic ribosomes in the same way as ricin, we were interested to determine whether BFA could inhibit saporin toxicity as it does with ricin. If so, this would indicate that saporin too must traverse the Golgi stacks and would enlighten us to some of its intracellular pathway. This chapter aims to establish a system in which BFA could be used to disrupt the Golgi apparatus in HSB-2 cells in order to determine whether it may or may not protect the cells from saporin cytotoxicity. Before a system could be developed it was essential to determine the effects of BFA alone on HSB-2 cells. A protein synthesis inhibition assay was conducted to determine the effects of BFA on protein synthesis and also to give an indication the toxicity of the drug to HSB-2 cells. To reinforce this data, electron microscopy studies were undertaken to demonstrate the toxic nature of BFA and to give an indication of the time course over which changes to organelle morphology occur. Since HSB-2 cells cannot be exposed to BFA for prolonged periods of time before the cells undergo apoptosis, a protein synthesis inhibition assay was conducted to demonstrate the kinetics of the protein synthesis inhibition by continuous exposure to ITs. The aim of this was to determine when the cells should be exposed to BFA to potentially protect the cells from the cytotoxic effects of the ITs.

5.2 Methods and Experimental Design

5.2.1 *The effects of brefeldin A on protein synthesis*

To investigate the effects of BFA on protein synthesis, a protein synthesis inhibition assay was conducted (as described in section 2.7 except where stated otherwise). Firstly, the effects of a pulsed exposure of HSB-2 cells to four different concentrations (0.05, 0.5, 5 and 50μg/ml) of BFA was investigated. Cells were incubated with BFA at the four different concentrations for 30 minutes at 37°C, after which excess drug was removed by two 5 minute washes at 1500rpm with PBS. Cells were then resuspended in fresh R10 medium without BFA and incubated at 37°C for either 24 or 48 hours, after which the cultures were pulsed with ^{3}H-leucine for an hour and then harvested. Additionally, the effects of continuous exposure to various concentrations of BFA were investigated. Cells were incubated in R10 medium containing various concentrations of BFA for ½, 1 ½, 3, 6, 12, and 24hrs after which they were pulsed for an hour and harvested. Data were plotted as the percentage of ^{3}H-leucine incorporated by the cells relative to untreated control cultures that were exposed to an equivalent amount of methanol (since BFA was reconstituted as a stock of 5mg/ml in methanol).

5.2.2 The effects of Brefeldin A on Organelle Morphology

To be able to investigate the effects of BFA on IT cytotoxicity it was important to know firstly that the HSB-2 T-ALL cell line was sensitive to the agent and secondly the kinetics of the changes to cell morphology. It is known that the effects of BFA on cell morphology can be rapidly reversed once the drug has been removed from cells. Cells that had been exposed to the drug for 30 minutes before it was removed were fixed and processed to determine how long the effects of the drug lasted after its removal.

HSB-2 cells were either exposed to 50μg/ml of BFA for 30 minutes at 37°C before excess drug was removed by two washes with PBS and the cells were then resuspended in medium without BFA for various periods of time, or the cells were resuspended in R10 medium containing 50μg/ml BFA and incubated at 37°C for the same time intervals. At the following times intervals of 0, 2h, 24h and 48h cells were taken from the cultures, washed twice and then prepared for electron microscopy as described in section 2.11.1.

5.2.3 Kinetics of IT action

The kinetics of protein synthesis inactivation in HSB-2 cells of the anti-CD7 IT (HB2-saporin), and the anti-CD38 IT (OKT10-saporin) when used singly or in combination, were determined in 96 well microcultures of cells. The kinetics of unconjugated saporin was also investigated. Triplicate cultures of HSB-2 cells were exposed to various different molar concentrations of each IT alone and in combination (with final concentrations with one log intervals ranging between 10^{-13}M and 10^{-7}M) or saporin (10^{-9}M – 10^{-7}M) for 3, 6, 11.5, 24, 34, and 48h. Cultures were pulsed with 1μCi ^{3}H-leucine for 1h and then harvested. Data obtained from these cultures were expressed as a percentage of the amount of ^{3}H-leucine incorporated by untreated cultures maintained in medium for the same time intervals. Regression analysis of the percentage of ^{3}H-leucine incorporation against the length of incubation with the IT(s) and saporin was undertaken for each of the concentrations investigated. The time taken for protein synthesis levels to reduce by one log is defined as the t_{10} and was obtained from the point where the line of regression intercepted the 10% protein synthesis level.

5.3 Results

5.3.1 The effect of brefeldin A on protein synthesis

The effects on protein synthesis of a 30 minute pulsed exposure of HSB-2 cells to four different concentrations (0.05, 0.5, 5, 50μg/ml) of BFA at times intervals of 0, 24 and 48 hours after the removal of the drug can be seen in Figure 5.1. The data is represented as a percentage of ^{3}H-leucine incorporation by untreated cells against time after exposure. No prolonged effect was produced by the 30 minute exposure to the drug over the 48 hr duration of this experiment. This observed result was for all concentrations of BFA used. The extent of ^{3}H-leucine incorporation remained fairly constant for each concentration of BFA. It is also notable that there was no correlation between the extent of ^{3}H-leucine incorporation and the concentration of BFA the cells had been exposed to. Since there appears to be no substantial alteration to protein synthesis over 48 hours after the removal of BFA, it would suggest that a 30 minute incubation with BFA did not produce any prolonged toxicity to HSB-2 cells.

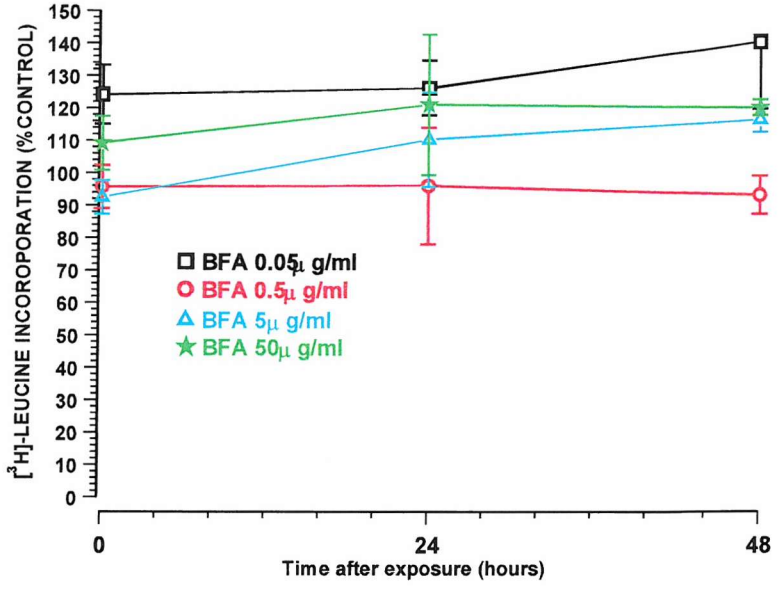

Figure 5.1 The effect of BFA on protein synthesis of HSB-2 cells after a 30 minute pulsed exposure. HSB-2 cells were exposed to four different concentrations (0.05, 0.5, 5 and 50μg/ml) BFA for 30 minutes at 37°C, excess drug was then removed and the cells incubated as microcultures in 96 well plates and pulsed with ^{3}H-leucine for an hour, immediately (time = 0), 24 hours or 48 hours later. Data were represented as a percentage of ^{3}H-leucine incorporation relative to control cultures. Data points shown represent mean values of sextuplet cultures; bars SD (n-1).

5.3.2 The effects of Brefeldin A on Organelle Morphology

In this study, the effect of BFA on the organisation of the Golgi complex was examined ultrastructurally in the cell line HSB-2. Cells were incubated in culture medium R10 containing 50μg/ml for the following periods of time; 0h, 2h, 24h and 48h before the samples were fixed and processed for viewing with an electron microscope. Cells grown in culture medium without BFA were fixed and processed to provide a comparison to highlight any changes to organelle morphology.

In control cells it was possible to see the presence of Golgi stacks, the occasional rough ER, regularly shaped mitochondria with stable membranes, a large lobed nucleus and a large amount of vesicular material (Figure 5.2). Similarly, no substantial changes to organelle morphology were observed in cells resuspended in medium containing BFA and fixed immediately (Figure 5.3A). The cells contained healthy, normal looking mitochondria, the ER appeared unaffected, the cells were intact and there was the occasional small vesicle.

After two hours of BFA exposure, cells were dramatically different in appearance (Figure 5.3B). The ER had become highly dilated (especially in the perinuclear area), the mitochondria were becoming more elongated in shape and there were a large number of electron lucent vesicles that were much greater in size than those seen in control cells.

By 24 hours, cells exposed to BFA appeared to have lysed and some of the alginate matrix the cells were set in had entered the cell interior. Since the cells were fixed before being set in the matrix, the cells could not have actively taken up the alginate. In most of the cells exposed to BFA for this length of time, it was not possible to see many, if any, internal organelles. Most cells contained dark clumps of condensed chromatin (shown in Figure 5.4), which is characteristic of a cell undergoing apoptosis. This indicated that after 24 hours of exposure to BFA, the drug had irreversibly damaged the cell structure.

After 48 hours of continuous exposure to BFA, there were cells which contained a significant amount of condensed chromatin, indicating that cells were still undergoing apoptosis. Figure 5.5 showed an example of a cell in which the Golgi apparatus and ER had become greatly distorted during this lengthy incubation with BFA. The alginate

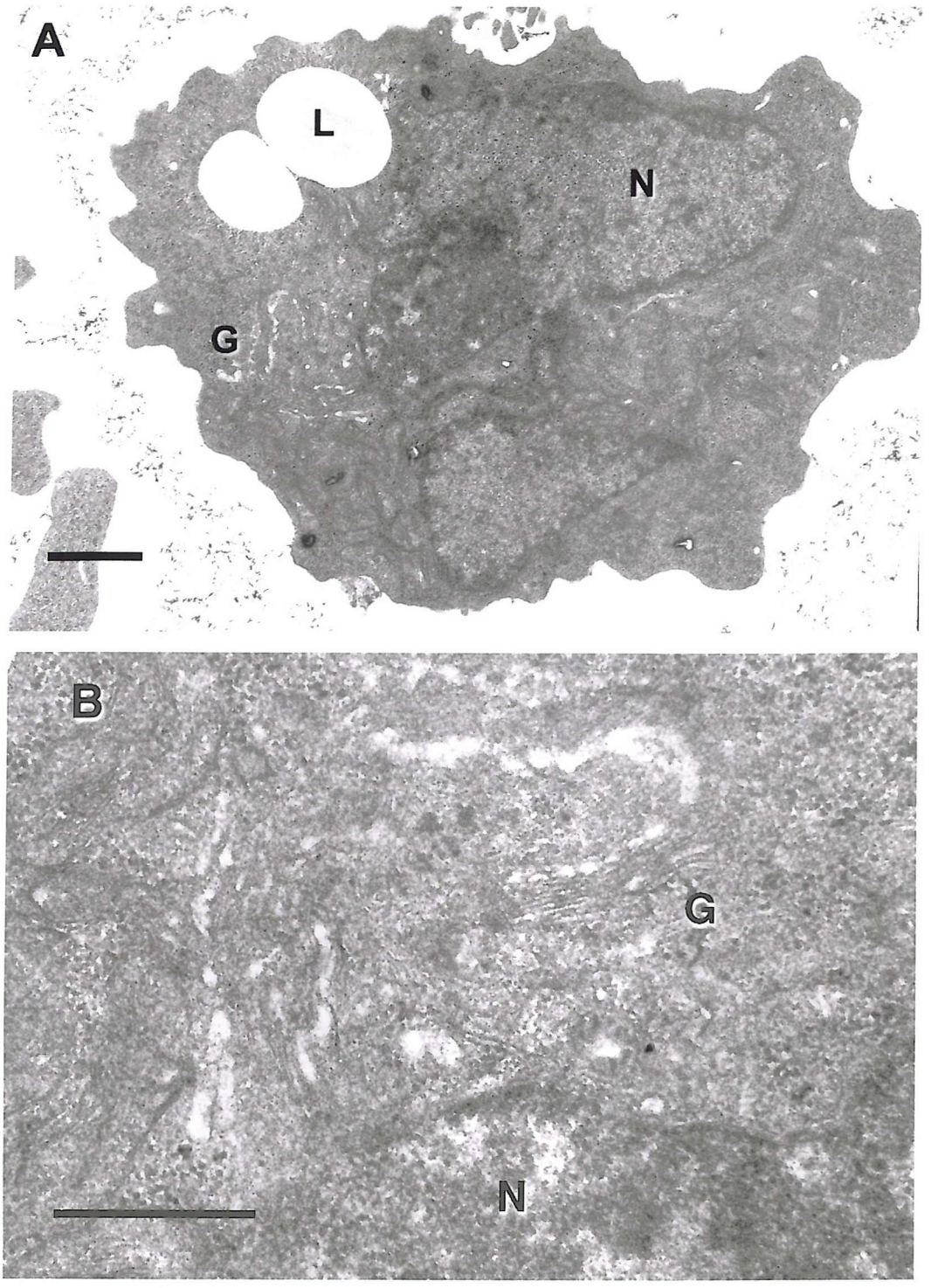

Figure 5.2. The organisation of internal organelles in untreated HSB-2 ALL leukaemia cells. Untreated HSB-2 cells were fixed and prepared for electron microscopy as described in section 5.2.2. (A) A low magnification micrograph of an untreated cell; scale bar = 1µm. (B) A high magnification micrograph of an untreated cell; scale bar = 0.5µm. G, Golgi apparatus; L, lipid droplet; N, nucleus.

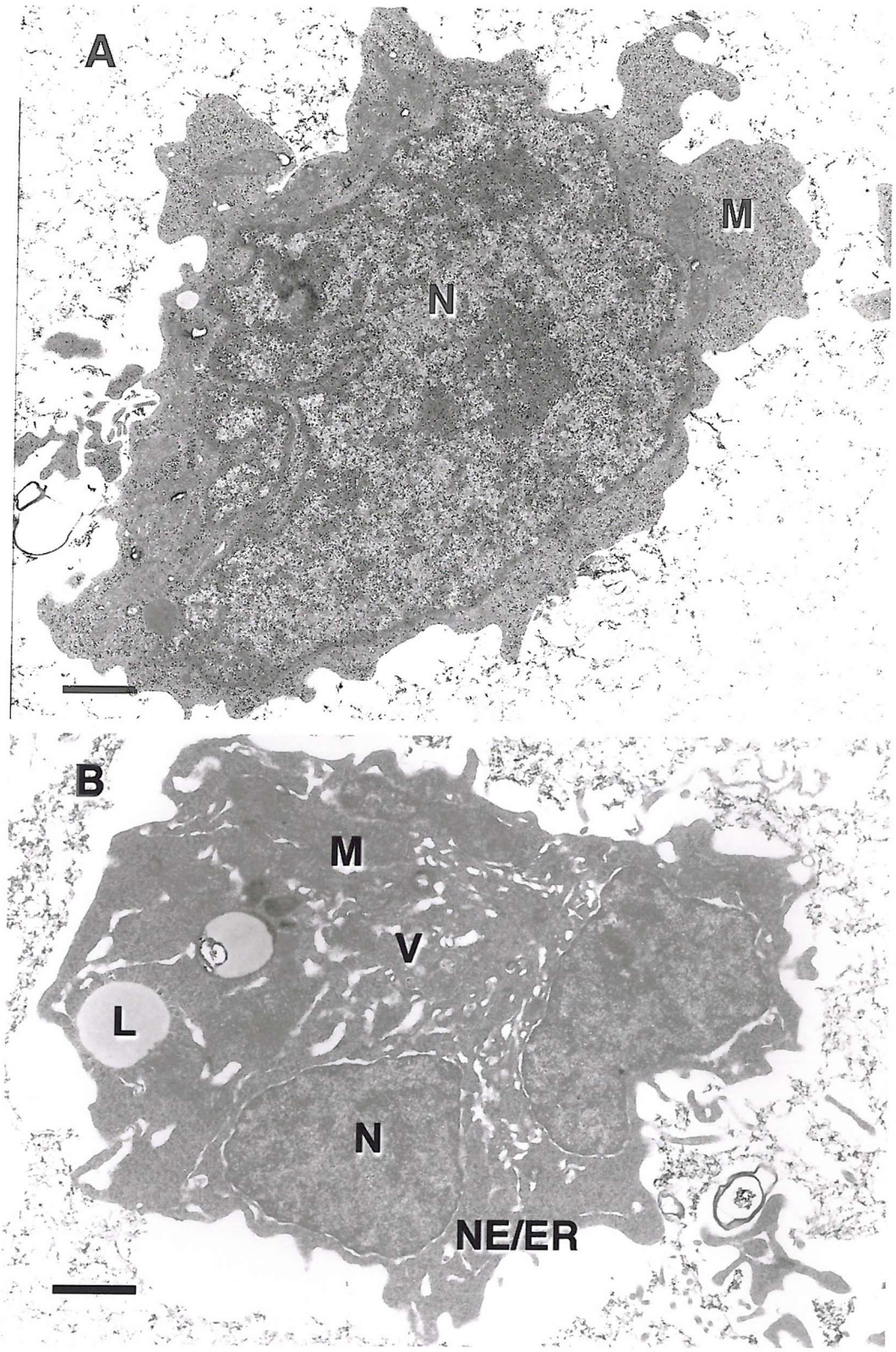

Figure 5.3. Changes in organelle morphology after a short incubation with BFA. Cells were resuspended in R10 medium containing 50µg/ml of BFA and either (A) fixed immediately; scale bar 1µm or (B) incubated at 37°C for 2 hours and then fixed and prepared for the electron microscope; scale bar = 1µm. N, nucleus; M, mitochondria; L, lipid droplet; NE/ER, nuclear envelop/endoplasmic reticulum; V,

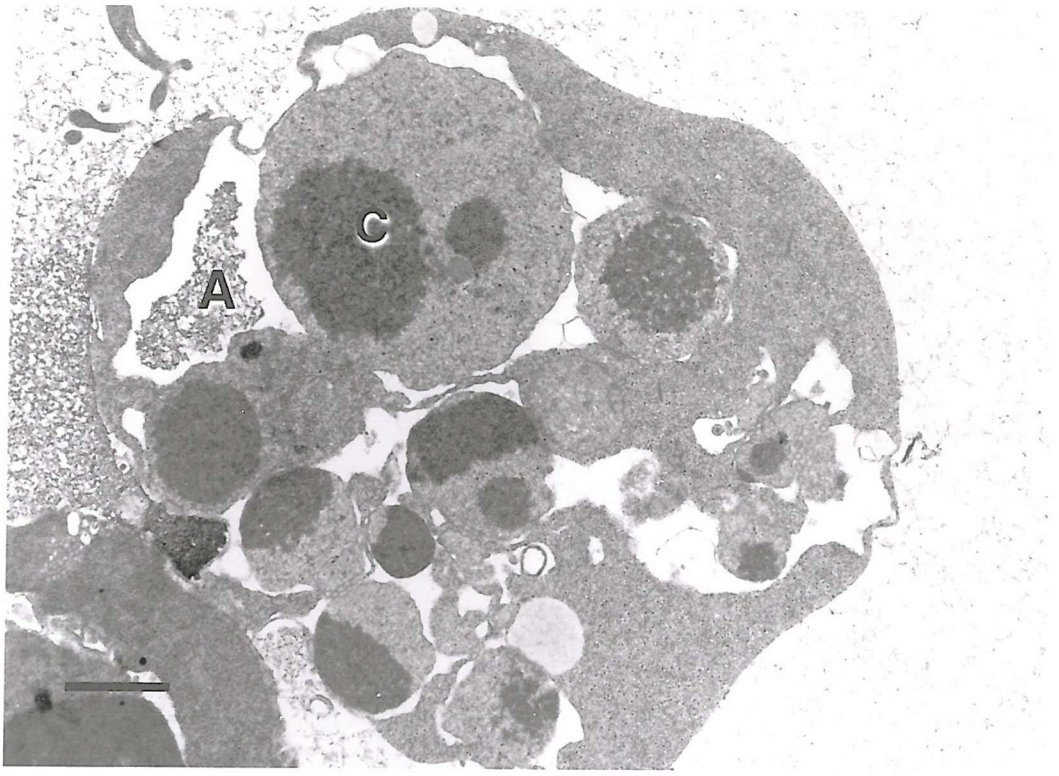

Figure 5.4. Changes in organelle morphology after sustained incubation with BFA. Cells were resuspended in R10 medium containing 50µg/ml of BFA, incubated at 37°C for 24 hours, fixed then processed for viewing under an electron microscope. This shows an example of a cell undergoing BFA-induced apoptosis; scale bar = 1µm. C, condensed chromatin; A. sodium alginate matrix.

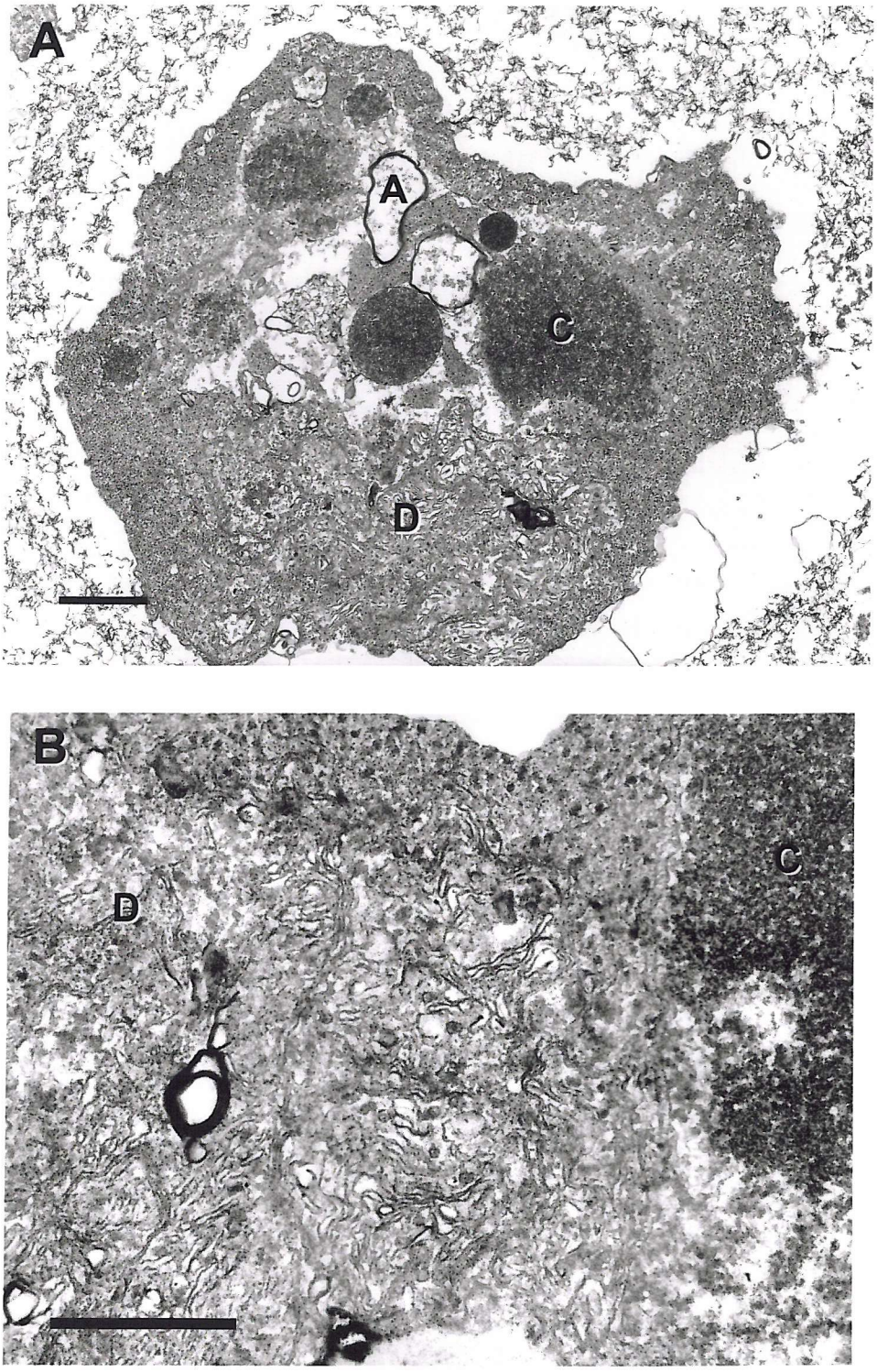

Figure 5.5. Changes in organelle morphology after a prolonged incubation with BFA. Cells were resuspended in R10 medium containing 50µg/ml of BFA, incubated at 37°C for 48 hours, fixed and then prepared for examination under an electron microscope. (A) A low magnification micrograph of a cell after 48 hours of continuous exposure to BFA; scale bar = 1µm. (B) A high magnification micrograph of a cell after 48 hours of exposure to BFA; scale bar = 0.5µm. C, condensed chromatin; A, sodium alginate matrix; D, distorted organelle.

matrix had once again been found within the middle of the cell. The cells no longer contained any internal viable organelles and were not considered functional or viable.

The BFA-induced transformation of Golgi stacks and disruption of the internal organelles were demonstrated to be reversible when cells were first incubated for 30 minutes in the presence of BFA, washed and then incubated without BFA. In cells fixed immediately after the removal of BFA (Figure 5.6), there was a slight enlargement of the perinuclear area, which was presumably due to the effect of the drug on the ER. The presence of large vesicles was also observed within the cytoplasm. These may have resulted from vesiculation of the Golgi stacks, although they did not differ greatly in appearance from vesicles found in control cells. After 2 hours of incubation in fresh medium, no signs of BFA treatment were apparent (Figure 5.7). The mitochondria appeared normal and healthy, the ER and nuclear envelope were clearly defined as in the control cells and in the higher magnification pictures typical Golgi stacks with surrounding vesicles could be observed. This reassembly of the Golgi stacks and reversal of the effects of BFA were also demonstrated in cells incubated for 24 and 48 hours in fresh medium, although there was the occasional cell that had not successfully recovered from the BFA treatment (Figure 5.8 and 5.9). In these cells there was an enlarged ER, a large amount of vesicular material and elongated mitochondria. This may be a result of the effects of BFA treatment not having reversed in these cells, or that the drug may not have been removed from all the cells successfully.

5.3.3 Kinetics of IT action

Experiments were conducted to determine the rate at which seven different concentrations (of final concentrations with one log intervals ranging between 10^{-7} and 10^{-13}M) of HB2-Saporin IT and OKT10-Saporin IT, when used individually or in combination, inhibited protein synthesis in HSB-2 T-ALL cells compared with native saporin. Determination of the kinetics of IT action was used to indicate when these reagents first inhibited protein synthesis to enable us to define the optimum time for the addition of BFA to cell cultures in order to block the cytotoxic actions of the ITs. The rate slopes (determined by regression analysis) were expressed as a percentage of protein synthesis relative to untreated control cultures, and can be seen in figures 5.10 A-D.

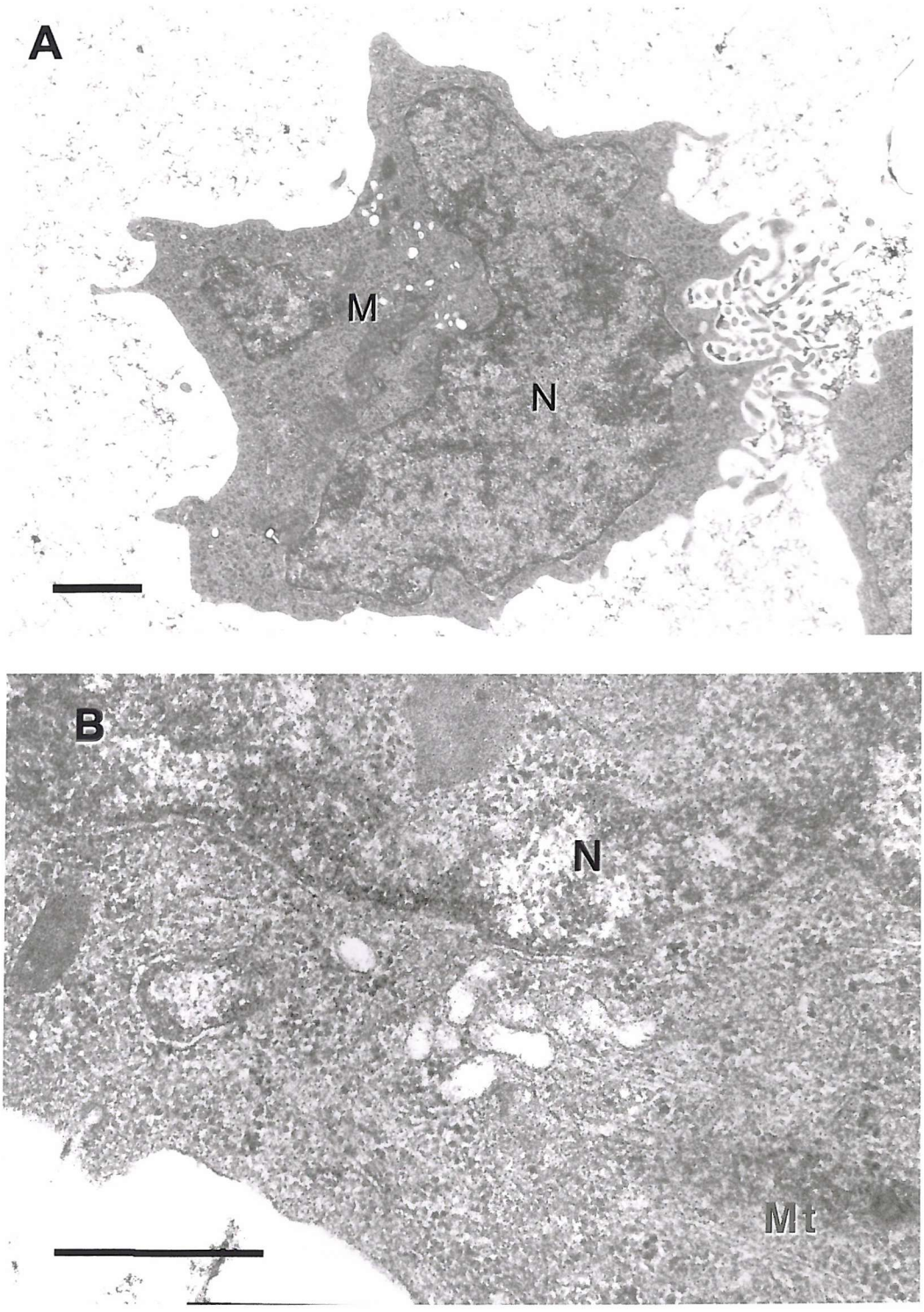

Figure 5.6. Effects of a 30 minute pulsed exposure to BFA. Cells were resuspended in R10 medium containing 50µg/ml of BFA and incubated for 30 minutes at 37°C. Following this the drug was removed and the cells were cultured in fresh R10 medium without BFA. Cells were fixed immediately after a 30 minute incubation with BFA and prepared for an electron microscope. (A) A low magnification micrograph of a treated cell; scale bar = 1µm. (B) A high magnification micrograph of a BFA treated cell; scale = 0.5µm. N, nucleus; Mt, microtubules; M, mitochondria.

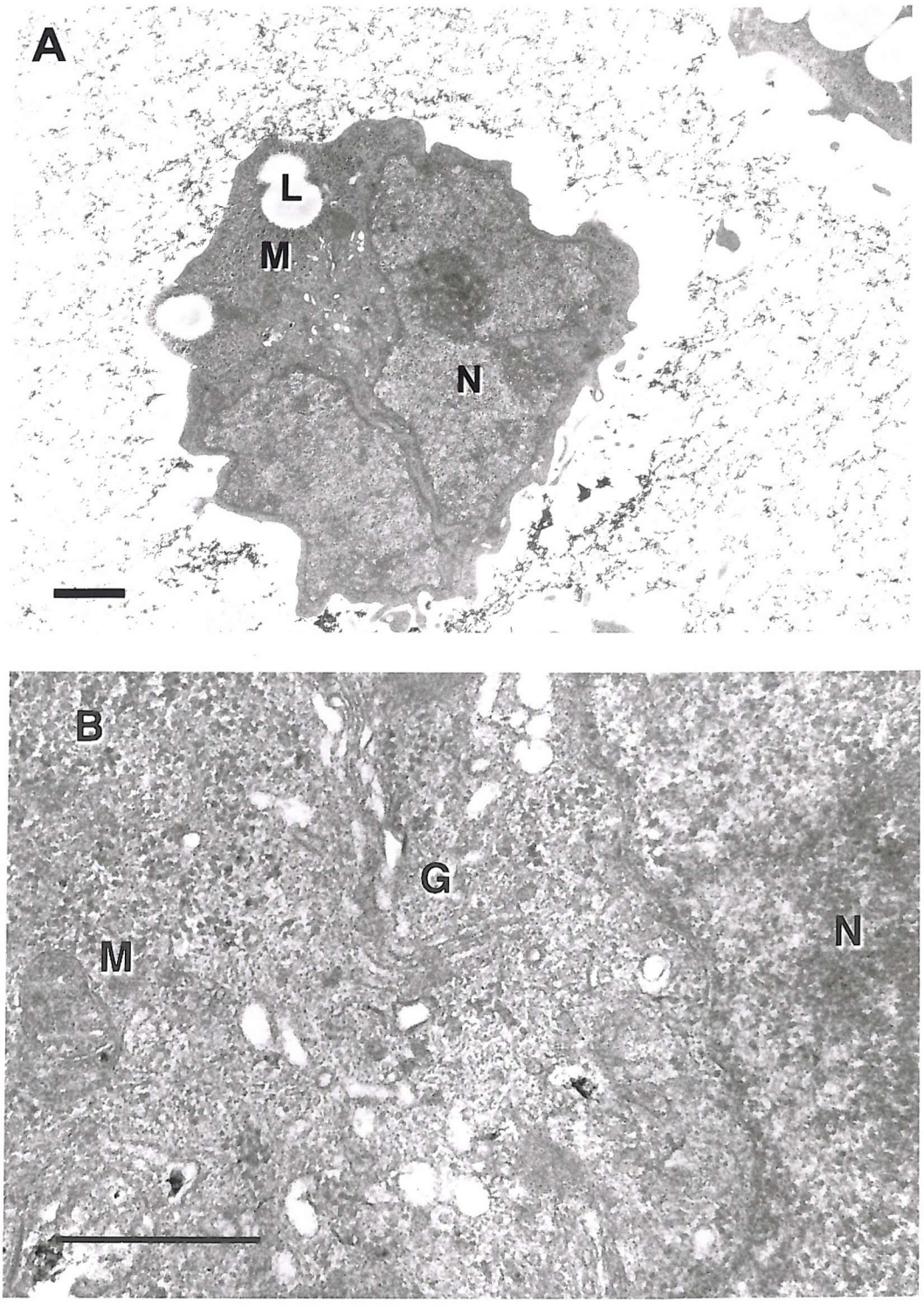

Figure 5.7. Prolonged effects of a 30 minute exposure to BFA. Cells were resuspended in R10 medium containing 50µg/ml of BFA and incubated for 30 minutes at 37^{o}C. Following this the drug was removed and the cells were cultured in fresh R10 medium without BFA. Cells were incubated for a further 2 hours before they were fixed and prepared for electron microscopy. (A) Low magnification; scale bar = 1µm. (B) High magnification; scale bar = 0.5µm. L, lipid droplet; M, mitochondria; N, nucleus; G, Golgi apparatus.

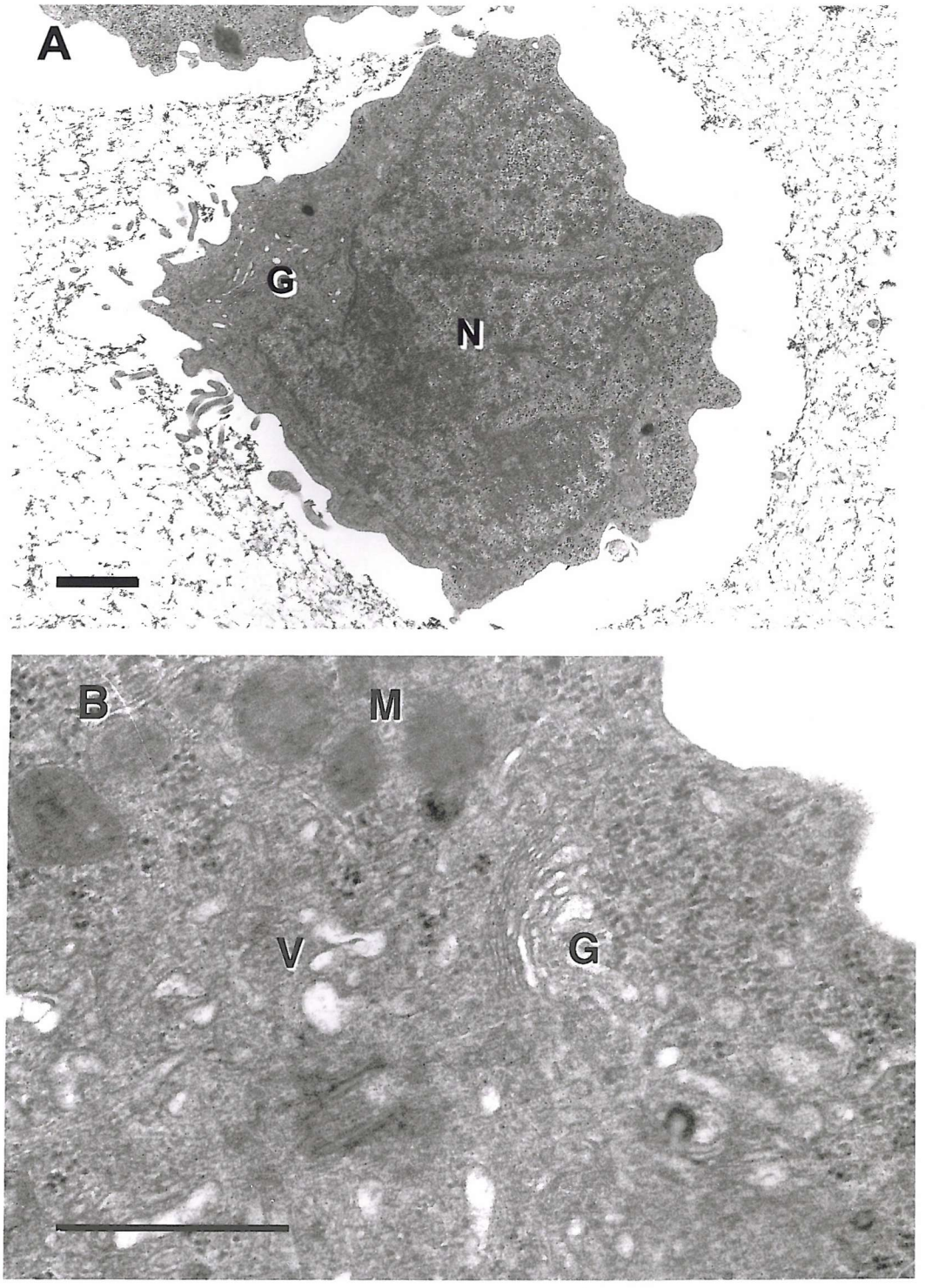

Figure 5.8. Prolonged effects of a 30 minute exposure to BFA. Cells were resuspended in R10 medium containing 50µg/ml of BFA and incubated for 30 minutes at 37°C. Following this the drug was removed and the cells were cultured in fresh R10 medium without BFA. Cells were incubated at 37°C for a further 24 hours before they were fixed and processed for electron microscopy. (A) A low magnification of a cell that has not fully recovered from the effects of BFA; scale bar = 1µm. (B) A high magnification micrograph of a cell fully recovered from the effects of BFA; scale bar = 0.5µm. N, nucleus; M, mitochondria; L, lipid droplet; V, endocytic vesicles; G, Golgi apparatus.

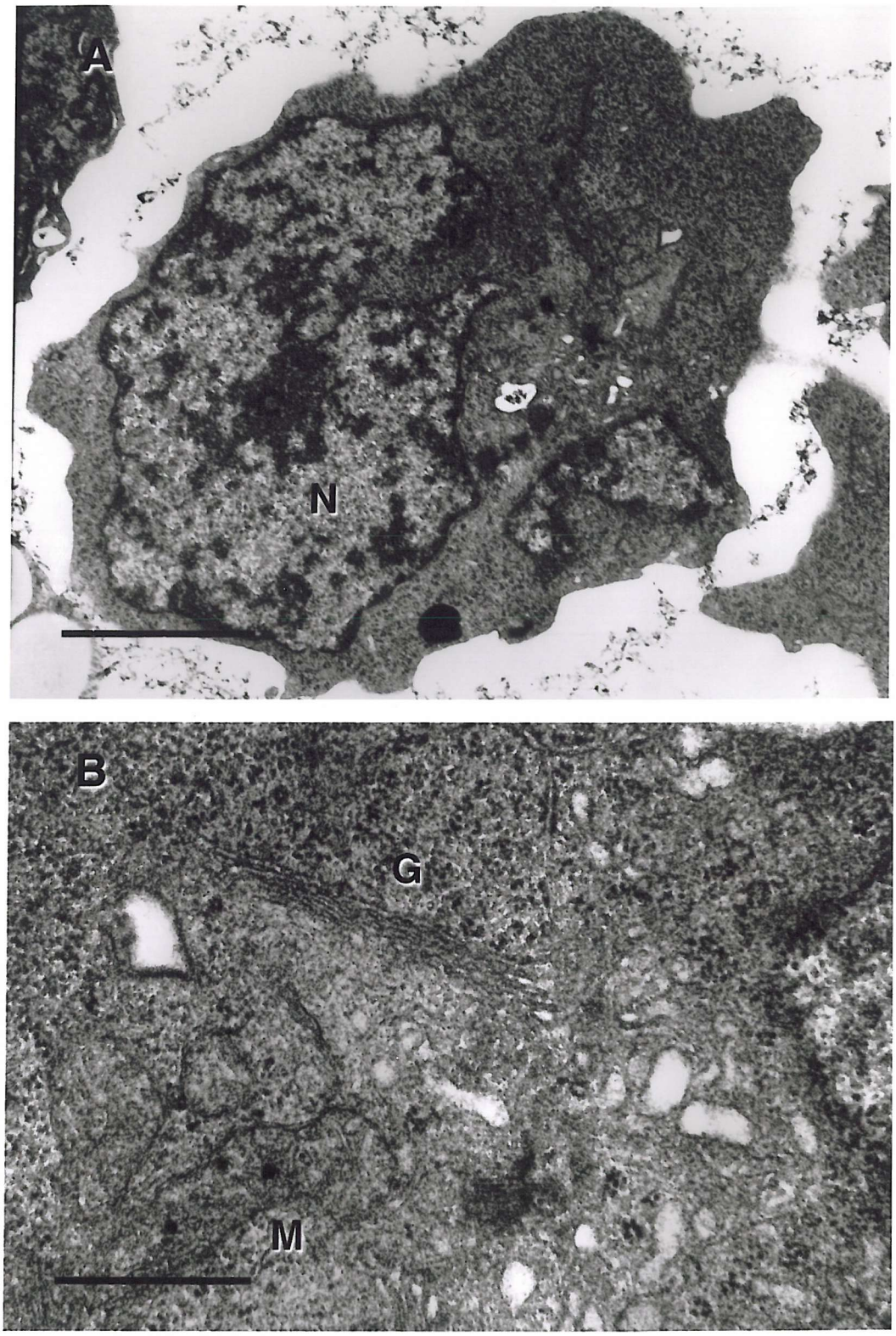

Figure 5.9. Prolonged effects of a 30 minute exposure to BFA. Cells were resuspended in R10 medium containing 50µg/ml of BFA and incubated for 30 minutes at 37°C. Following this the drug was removed and the cells were cultured in fresh R10 medium without BFA. Cells were incubated at 37°C for a further 48 hours before they were fixed and processed for electron microscopy. (A) Low magnification; scale bar = 1µm. (B) High magnification; scale bar = 0.5µm. N, nucleus; M, mitochondria; G, Golgi apparatus.

The time taken for an inhibition of protein synthesis of one log compared with untreated control cultures is referred to as the t_{10} value. This value for each reagent was plotted against concentration as shown in figure 5.10 E. Of the two ITs, the anti-CD7 IT HB2-Saporin clearly inactivates protein synthesis more rapidly than the anti-CD38 IT OKT10-Saporin when each reagent was used individually between the concentrations 10^{-9} and 10^{-13}M. Interestingly, the two ITs used in combination did not act any faster than HB2-Saporin IT alone and moreover, seemed to inhibit protein synthesis at a slower rate at low concentrations (10^{-11}-10^{-13}M). Inactivation of protein synthesis was more rapid with the combination of two ITs than with the use of OKT10 Saporin IT alone. Between 10^{-12} and 10^{-13}M both ITs individually and in combination were relatively ineffective. Native saporin was only toxic at high concentrations (10^{-5}-10^{-7}M) and required at least a 2-log greater concentration than either of the two ITs to produce the same rate of toxicity as the ITs at 10^{-7}M. Between the concentrations of 10^{-13} and 10^{-10}M for HB2-Saporin and 10^{-13} and 10^{-9}M the rate of protein synthesis inactivation was dose-dependent. Increasing the concentration of ITs past 10^{-10} or 10^{-9}M did not seem to have any greater effect on the rate of inhibition produced. This was true for both ITs individually and in combination. From the individual rate slopes it was decided that the first signs of cytotoxicity appeared after 12 hours of continuous incubation of cells with the ITs.

5.3.4 The effect of continuous exposure of cells to Brefeldin A

The effect of continuous exposure of HSB-2 cells to the drug BFA over various periods of time was determined by a protein synthesis inhibition assay. Cell cultures were exposed to BFA at concentrations of 0.025, 0.25, 2.5 and 25μg/ml for the time points 30 minutes, 1 ½ and 3 hours and 0.05, 0.5, 5 and 50μg/ml for the time points 6, 12 and 24hr. At each time point the cultures were pulsed with ^{3}H-leucine for 1hr, then harvested for counting incorporation levels on a scintillation counter. Data were represented in figure 5.11 as a percentage of ^{3}H-leucine incorporated into treated cultures relative to untreated cultures. A decrease in ^{3}H-leucine incorporation indicated a drop in the amount of protein synthesis which at the later time points may have resulted from a decrease in the number of viable, metabolically active cells.

Inhibition of protein synthesis of HSB-2 cells after continuous exposure to BFA was shown to be time-dependent. Curiously, the effects of BFA on protein synthesis did not appear to be dependent on concentration after the first three hours of exposure to the drug,

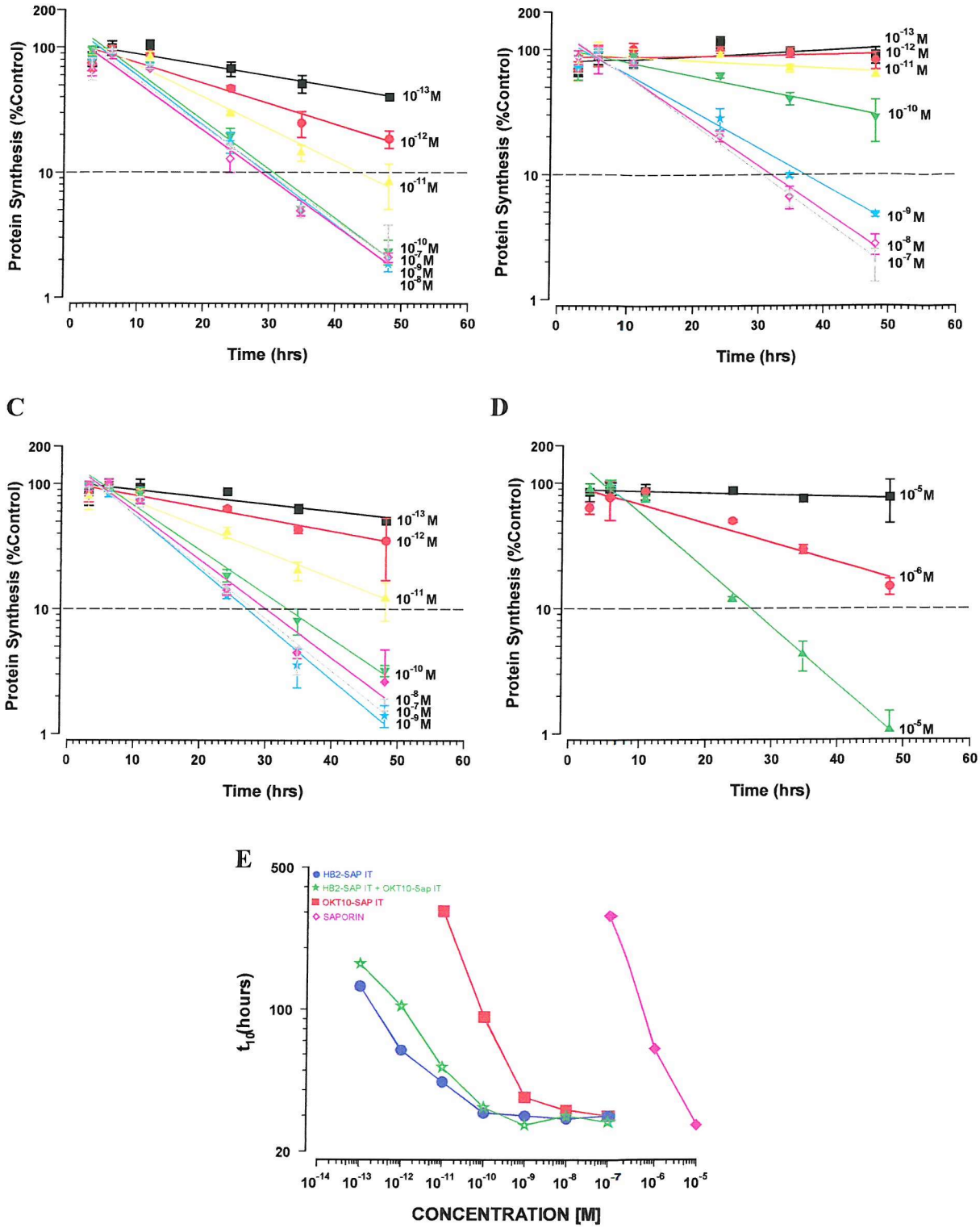

Figure 5.10. Kinetics of protein synthesis inhibition in HSB-2 T-ALL cells after exposure to HB2-Saporin IT (A), OKT10-Saporin IT (B), a combination of both ITs (C), at various concentrations ranging from 10^{-13} to 10^{-7} M and native saporin (D) at concentrations between 10^{-9} and 10^{-7} M. Where necessary, the regression line was extrapolated beyond the final time point to obtain a value for t_{10}. The regression coefficients were as follows: A, HB2-Saporin IT r = 0.950 (10^{-13} M), r = 0.963 (10^{-12} M), r = 0.988 (10^{-11} M), r = 0.991 (10^{-10} M), r = 0.989 (10^{-9} M), r = 0.983 (10^{-8} M), r = 0.981 (10^{-7} M). B OKT10-Saporin IT r = 0.527 (10^{-13} M), r = 0.156 (10^{-12} M), r = 0.738 (10^{-11} M), r = 0.947 (10^{-10} M), r = 0.982 (10^{-9} M), r = 0.991 (10^{-8} M), r = 0.988 (10^{-7} M). C IT Combination r = 0.920 (10^{-13} M), r = 0.960 (10^{-12} M), r = 0.959 (10^{-11} M), r = 0.942 (10^{-10} M), r = 0.993 (10^{-9} M), r = 0.985 (10^{-8} M), r = 0.935 (10^{-7} M). D Saporin r = 0.819 (10^{-7}M), r = 0.919 (10^{-6} M), r = 0.927 (10^{-5} M). E The t_{10} values obtained from graphs A-D where the line of regression intercepts the 10% level of protein synthesis were plotted against concentration for HB2-Saporin IT, OKT10-Saporin IT, both ITs in combination and saporin.

at least not at the concentrations used for these experiments. There was little change to protein synthesis over the first three hours of exposure with only a 30% decrease at the highest dose of BFA. Following this, at 6 hours there was a considerable decrease in the extent of ^{3}H-leucine uptake by the cell cultures, with a maximum reduction in protein synthesis of 43%. Over the subsequent 6 hours of exposure to the drug the protein synthesis levels continued to decrease but only to 35% of control levels. By 24 hours the amount of ^{3}H-leucine taken up by the cultures was minimal (16%) and most of the cell cultures were considered to be non-viable by this time.

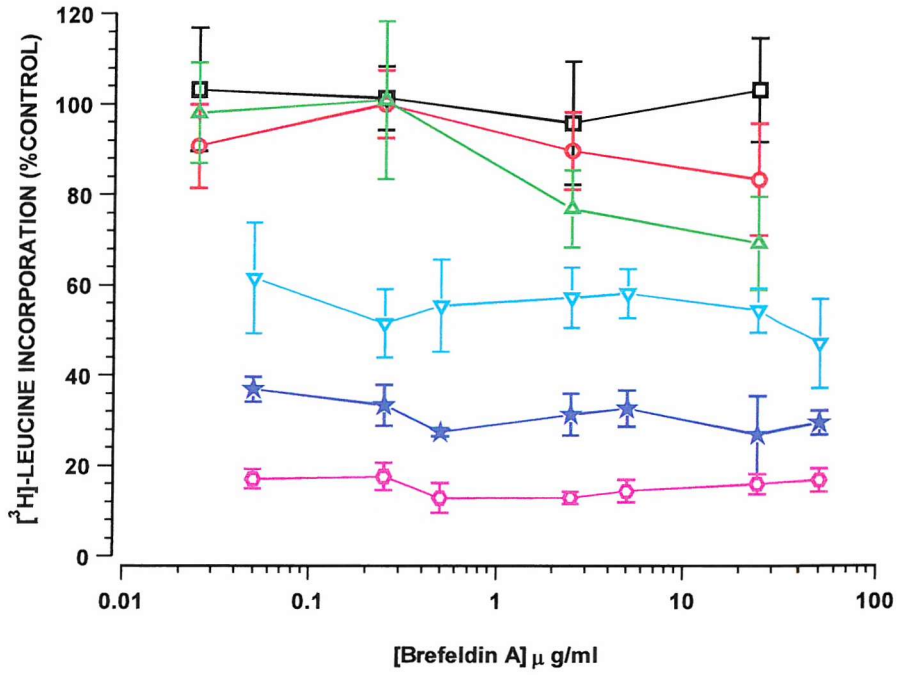

Figure 5.11. The effect of continuous exposure of HSB-2 cells to various concentrations of BFA for 30 minutes (black square), 1 ½ hr (red circle), 3hr (green triangle), 6hr (cyan triangle), 12 hr (blue star) and 24hr (magenta hexagon). For time points of 30-3hr concentrations between 0.025 and 25μg/ml were used and for 6-24hr 0.05 - 50μg/ml were investigated. Data were represented as a mean of sextuplet cultures with SD(n-1) error bars.

From this data it was decided that 6 hours was likely to be the longest exposure to BFA that the cells would withstand before the damage produced was irreversible. To confirm this, cells were exposed to BFA for 6 hours, fixed and then processed for electron microscopy. The images produced can be seen in figure 5.12. After 6 hours of BFA exposure the ER was frequently found highly dilated especially in the perinuclear area and subtle changes in the morphology of mitochondria had become apparent. They appeared to be longer and more elongated than those seen in the control cells. There were also a greater number of electron lucent vesicles visible in BFA treated cells that were much

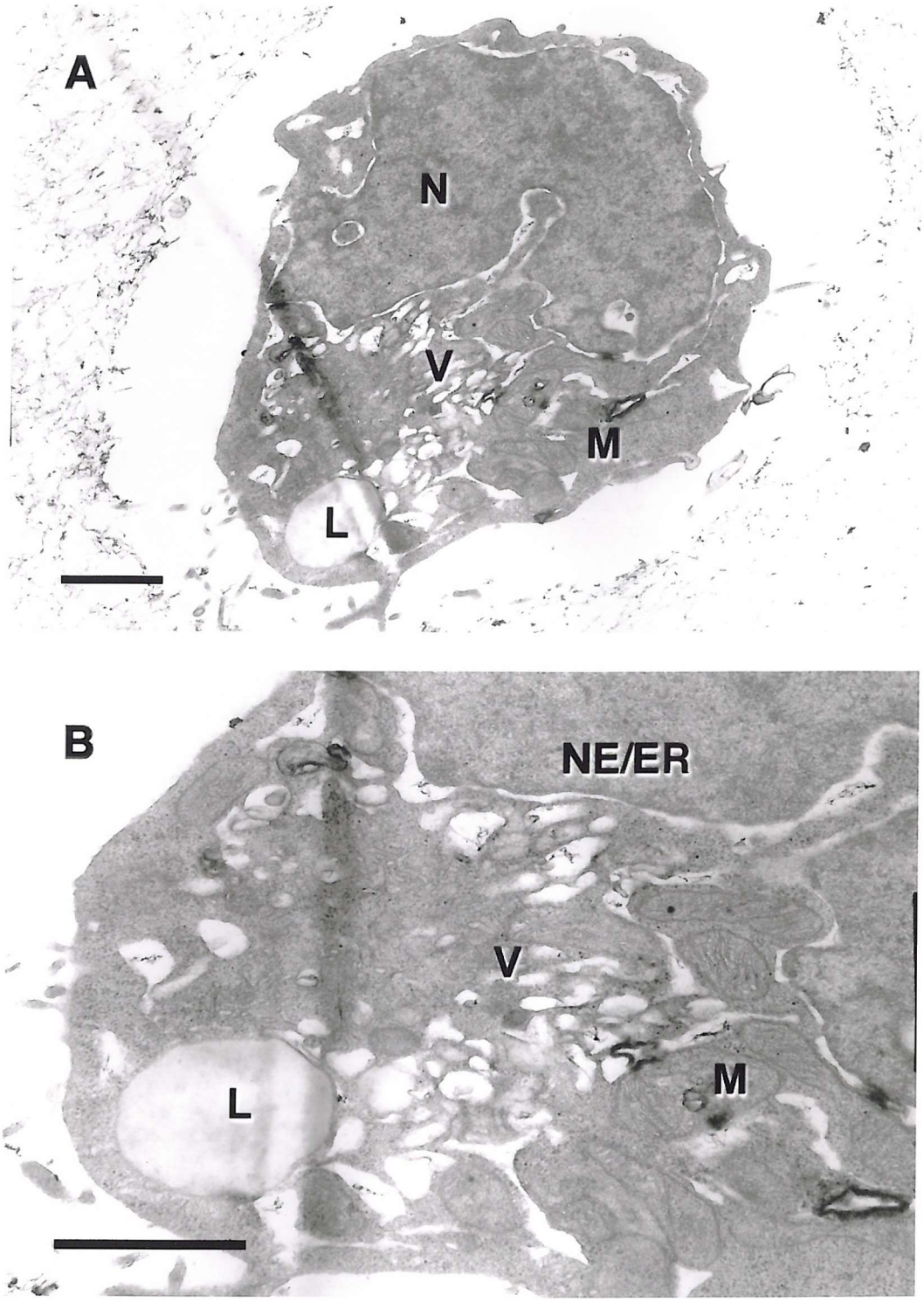

Figure 5.12. Changes in organelle morphology after a six hour incubation with BFA. Cells were resuspended in R10 medium containing 50µg/ml of incubated at 37°C for 6 hours, fixed then processed for viewing under an electron microscope. (A) A low magnification micrograph of a cell after 6 hours of continuous exposure to BFA; scale bar = 1µm. (B) A high magnification micrograph of a cell after 6 hours of exposure to BFA; scale bar = 0.5µm. N, nucleus; M, mitochondria; L, lipid droplet; NE/ER, nuclear envelop/endoplasmic reticulum.

larger in size than in controls and were in close proximity of each other. These vesicles may have formed from the disruption of the Golgi stacks and the ER. These cells appeared relatively healthy compared to those exposed to BFA for periods of 12 hours or more since they did not contain condensed chromatin and did not appear to be undergoing apoptosis. The plasma membrane and the double membrane of the mitochondria were left intact, indicating that the cell was likely to recover from the treatment.

5.3.5 The effect of BFA treatment on immunotoxin potency

From the data on IT kinetics and the information gained about the effects of continuous exposure to BFA, a protein synthesis inhibition assay was designed to determine the effect of disrupting the Golgi apparatus using BFA on IT potency. If the ITs used here needed to pass through the Golgi stacks to reach the ER and translocate to the cytosol before inactivating the ribosomes, a decrease in the cytotoxic potency would have been expected when BFA was added to the cell cultures. The initial signs of toxicity to cultures induced by the ITs were observed after 12 hours of exposure to the IT. This was the time chosen for the addition of BFA to the cell cultures with the expectation that if the IT translocates to the cytosol via this route that a reduction in the potency may have been observed. Cultures were set up as normal for a protein synthesis inhibition assay and were left to incubate in the presence of IT for 12 hours, after which time 20µl of a 20µg/ml (final concentration) of BFA or medium (for cultures exposed to HB2-Saporin IT, OKT10-Saporin IT, a combination of both ITs or saporin alone) was added to the wells. This was left for a further 6 hours, then pulsed with ^{3}H-leucine for an hour and harvested. The results from this experiment can be found in figure 5.13. Studying the data obtained from this experiment it was clear to see, that over the time scales chosen, there was no significant effect on the potency of the HB2-Saporin IT, OKT10-Saporin IT, a combination of both ITs or the native saporin in the presence of BFA.

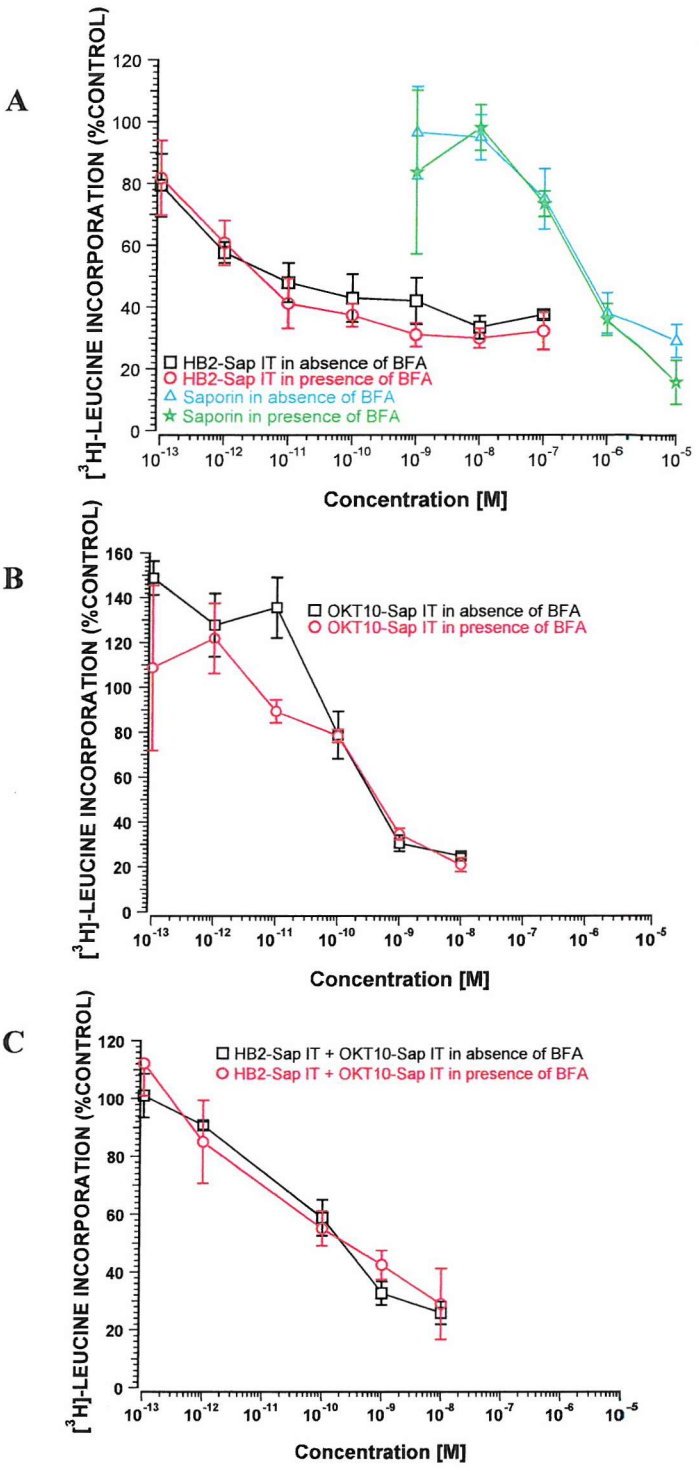

Figure 5.13. The effect of BFA on IT and native saporin cytotoxicity. HSB-2 cells were incubated with HB2-Saporin (A), OKT10-saporin (B), a combination of both ITs (C) or native saporin (A) for 12 hours before addition of 20µg/ml BFA. The cells were incubated with IT or toxin and the BFA for a further 6 hours before the cultures were pulsed with ^{3}H-leucine and harvested. Data were represented as a percentage of ^{3}H-leucine incorporation relative to control cultures. Data points shown represent mean values of triplicate cultures; bars SD (n-1).

5.4 Discussion

All immunotoxins must bind to cell surface receptors or antigens which are subsequently endocytosed via coated and/or uncoated pits and vesicles. The endocytosed material is generally found within endosomes. Once in endosomes the IT may be transported back to the plasma membrane, to the lysosome where it will be degraded, or to the trans-Golgi network (TGN). The exact location from which the toxin moiety translocates to the cytosol is not always known. Diphtheria toxin has been shown to enter the cytosol directly from acidified endosomes or lysosomes, whereas ricin may enter the cytosol from the TGN, the Golgi stacks or the endoplasmic reticulum. The route an IT takes to the cytosol is an important factor that influences the efficiency of the therapy. By gaining a greater understanding of the intracellular pathways of ITs it may be possible to find ways of influencing and enhancing this process so that less IT gets degraded and more IT reaches its target, the ribosome.

There has been a great deal of work investigating the intracellular routing of the toxin ricin and to a lesser extent ricin A-chain ITs. BFA has been an essential tool in these studies. Experiments have shown that there is a lag period for the inhibition of protein synthesis by ricin of approximately 60-90 minutes at 37°C (Yoshida *et al.*, 1991). Ricin has been visualised in the Golgi stacks around this time. Using this information, Yoshida *et al.*, (1991) exposed cells to BFA at various times relevant to the incubation of Vero cells with ricin for an hour. Pre-treatment of cells with BFA did not protect them from ricin which was presumably because of the rapid reversibility of the effects of BFA on the Golgi stacks once the drug was removed. Coincubation of cells with BFA and ricin simultaneously, significantly reduced the cytotoxicity of ricin but BFA was most effective at inhibiting ricin cytotoxicity when added 30 minutes after removal of ricin from the culture medium.

The main question we were attempting to answer, at least in part, was what intracellular pathway do the anti-CD7 and anti-CD38- saporin ITs follow to reach the cytosol? In this chapter, we have concentrated on the question; does the intracellular pathway of either or both ITs involve entering the Golgi apparatus as with ricin in a retrograde pathway? This work aimed to determine whether or not the drug BFA would protect HSB-2 cells from the cytotoxicity of immunotoxins. If so, it would be possible to infer that the saporin-ITs used here require the Golgi stacks in some way to translocate to the cytosol. To be able to

determine this, many different parameters needed investigation. It was necessary to demonstrate that the HSB-2 cell line was sensitive to BFA in such a way as to disrupt the Golgi apparatus. This was important to know since there is evidence to suggest that some cells are resistant to the Golgi disruptive effects of BFA. MDCK is an example of such a cell line (Hunziker *et al.*, 1991). Another important determinant was the concentration of BFA that would induce disruption of the Golgi apparatus, but to cause as little damage to the cells as possible.

The first issue addressed was what concentration of BFA should be used to induce disruption of the Golgi apparatus while avoiding toxicity to the cells. Many different doses have been used by various groups ranging between 1μg/ml and 10μg/ml (Yoshida *et al.*, 1991, Ippoliti *et al.*, 1995, Sandvig *et al.*, 1991 and Wood *et al.*, 1991). The reason for such a wide range of concentrations was probably due to the differing sensitivities of each of the different cell lines investigated. The protein synthesis inhibition assays conducted to show the effect of BFA on protein synthesis indicated that after the first three hours of exposure to the drug, increasing the concentration of BFA no longer increased the inhibition of protein synthesis. From the electron microscopy images produced after exposure of cells to 50μg/ml BFA, it was possible to see that this concentration was capable of disrupting the Golgi apparatus to varying degrees over the different time periods.

The effects of BFA have also been found to be rapidly reversed once the drug is removed from the cells, so this was a factor that needed consideration, especially since the inhibitory actions of both ITs occur over such a long time period (at least 12 hours). If the use of continuous exposure to BFA was necessary to sustain disruption of the Golgi apparatus long enough to see a response, then the toxicity to the cell and the effects this would have on cellular functions were also necessary considerations.

It was clearly demonstrated by the electron micrographs that once the drug had been removed from the cells, any changes to organelle morphology and structure that had occurred were rapidly reversed. Cells that were only exposed to BFA for 30 minutes did not display any significant difference in morphology compared with control cells, although it was still possible to see an enlargement of the ER and some possible

vesiculation of the Golgi stacks. This lack of change to the intracellular organelles may be due to a slight reversal of the drug's effects taking place during processing procedures or it might indicate that a longer incubation time was necessary with this cell line for the effects to take place. Since there are reports to indicate that many of the effects of BFA treatment can be observed within 15 minutes of incubation, the former is more likely (Hess *et al.*, 2000). The majority of cells exposed to BFA for 30 minutes and then incubated for substantial periods of time in the absence of the drug showed signs of recovery from the treatment. The effects of the drug on the organelles of these cells appeared to have successfully reversed and the cells did not display any differences in appearance compared to control cells.

Another point that was made obvious from these investigations was that HSB-2 cells could only be exposed to BFA for a limited period of time before its effects become irreversible and fatal. By 24 hours and beyond, the cells appeared to be undergoing apoptosis or cell lysis and did not appear to be recoverable. This data was supported by that obtained from the protein synthesis inhibition assay showing that the extent of protein synthesis undertaken by HSB-2 cells continuously exposed to BFA had fallen to 35% of original levels by 24 hours and then down to under 20% by 48 hours. This indicated that most of the cells had stopped undergoing protein synthesis, had reduced the extent of protein synthesis or were non-viable. This data suggested that HSB-2 cells should not be exposed for times greater than 6 hours in any future assay undertaken so a not to lead to misleading results.

Shao *et al.*, (1996) have described the induction of apoptosis by BFA in different human cancer cell lines similar to those seen in the electron microscopy studies described here. The main feature observed in this study was DNA fragmentation as a characteristic of apoptosis. The kinetics of BFA-induced DNA fragmentation were found to vary between the cells, manifesting after 15 hours in HL60 (a leukaemia cell line) and between 48-72 hours in K562 leukaemia and HT-29 colon carcinoma cells. Signs of apoptosis in HSB-2 cells, due to prolonged exposure to BFA, were first observed after 24 hours of incubation with BFA. The cells did not display any evidence of DNA fragmentation or any other characteristic of apoptosis at the 6 hour time period, therefore it must occur between 6-24 hours of continuous incubation with BFA. This was in concordance with the findings of Shao *et al.*, (1996).

Unlike ricin, which has been shown to be toxic to Vero cells as soon as 90 minutes after incubation with the toxin (Yoshida *et al.*, 1991), saporin does not contain a binding domain and so therefore binds non-specifically to cells. In ricin the B chain is also believed to aid transport of ricin A chain through the cell to the cytosol. For this reason, it takes a relatively high concentration of saporin to be toxic to the cells and this process is considerably slower than with the ricin, taking up to 12 hours to show the first indications of toxicity. To make this process more specific and efficient, the toxin has been conjugated to carrier molecules such as antibodies to CD molecules expressed on the surface of tumour cells. The advantage of using a carrier molecule to deliver saporin to the cytosol, is that it enables lower doses of IT to be used than those used with saporin alone, but as demonstrated by the protein synthesis inhibition experiments which were used to define the kinetics of IT toxicity, the first significant signs of cytotoxicity was after 12 hours of incubation with either or both of the ITs. A similar rate slope for HB2-Saporin against the HSB-2 cell line was also observed previously by Flavell *et al.*, (1997). It is not known whether the delay in cytotoxicity is due to a slow, inefficient routing process to the site of translocation, or if there is a lag phase produced by the translocation process itself. It is also perceivable that there may be a delay in the detection of protein synthesis inactivation by this method.

No great difference in the rate of cytotoxicity was observed between the HB2-Saporin used alone or in combination with OKT10-Saporin IT, although it is very clear that OKT10-Saporin IT is much slower in its rate of inactivation. This would correlate with the differences in the internalisation kinetics observed between the two ITs.

To overcome the toxic effects of BFA on HSB-2 cells whilst investigating the effects of BFA on IT toxicity, an assay was designed to enable the IT to pass its lag phase before the addition of BFA to the cultures for the subsequent 6 hours to try to block the IT's intracellular pathway. It would appear that BFA does not influence the intracellular routing of either HB2-Saporin IT, OKT10-Saporin IT, a combination of both ITs or native saporin in such a way as to alter their cytotoxic potency. Indeed, this may have been a result of adding BFA to the cultures at an irrelevant time for Golgi disruption, since it has been demonstrated with ricin that the timing of such an event is crucial (Yoshida *et al.*, 1991). It is possible that most of the IT and saporin had reached the Golgi apparatus and

passed through this region by the time of BFA addition, hence making it too late to influence their cytotoxicity. With ricin, there is a much shorter lag time which makes it a lot easier to determine the best time to use BFA to block intoxication pathways. This data also indicates that ligating the cells with a combination of both ITs does not alter the intracellular routing of either of the ITs in a way that routes them though the Golgi apparatus.

It appears unlikely that passing through the Golgi apparatus is a component part of the intracellular routing for these ITs or indeed saporin. From the data shown here, it is not possible to rule out the Golgi apparatus as an essential organelle to the cytotoxicity of these ITs. What can be stated is that when the Golgi is disrupted 12 hours into incubation with IT, it does not affect the toxicity of either ITs or native saporin. In order to confirm whether or not these ITs pass through the Golgi apparatus, a study was undertaken to visualise these components within the cell.

Chapter 6

Monitoring the Internalisation and Intracellular Routing of CD7 and CD38 Using Confocal Laser Scanning and Electron Microscopy

6.1 Introduction

Immunotoxins, comprised of antibodies coupled to a toxin or ribosome inactivating protein (saporin in the case of the immunotoxins described in this thesis), exert a cytotoxicity which is directed to its site of action within the cell by the specificity of the MAb (Casellas *et al.*, 1984, Jansen *et al.*, 1982). The studies in chapter 3 and 4 were conducted to investigate the relationship between MAb-induced modulation and cytotoxic potency of the corresponding IT in order to identify the internalisation characteristics needed for good IT activity. Both properties depend on the nature of the target antigen. Previous results on other models have indicated that antibodies that internalised efficiently made better ITs than those that did not (Pirker *et al.*, 1985). To the contrary, Carriere *et al.*, (1989) showed that although monoclonal antibodies directed against CD4 and 150kD antigens internalised efficiently, the endocytosis of these antibodies was inefficient for IT activity. This suggested that good internalisation is not the only factor necessary to achieve effective protein synthesis inhibition in the target cell. The internalisation characteristics of HB2 and OKT10 antibodies and their respective ITs as determined by flow cytometry were described in chapter 4. These observations did not fully explain the differences in cytotoxic potencies of these two ITs displayed in chapter 3. OKT10 Ab internalised more slowly than HB2 Ab, and over a 24 hour time period much less OKT10 Ab was internalised. This data lead one to expect a large difference in cytotoxic potencies between the two ITs, but this was not observed in a protein synthesis inhibition assay. In fact, in the long term cell outgrowth assay and the *in vivo* study, OKT10-Saporin IT appears to be more potent than HB2-Saporin IT. From this data it is obvious that factors other than internalisation must have an important role in determining the cytotoxic potency of an Ab-directed IT.

Therefore, the purpose of the work described in this chapter was to confirm the observations regarding internalisation from the cell surface of these two antibodies made by flow cytometric analysis and then to investigate the intracellular pathways followed by these molecules using confocal laser scanning microscopy. Monitoring the internalisation

of CD7 and CD38 when ligated by their respective antibodies enabled us to see that the modulation of these molecules from the cell surface was due to internalisation and not to shedding. Co-localisation assays were then conducted to determine whether the anti-CD38 Ab, OKT10, and the anti-CD7 Ab, HB2, influenced the internalisation and/or the intracellular routing characteristics of either of these individual molecules when both were simultaneously co-ligated. Following this, both OKT10 and HB2 Abs were incubated with cells in medium containing transferrin-TRITC to provide us with an indication as to what kind of endocytic compartments these molecules travelled in. To follow up studies in the previous chapter, which indicate that neither IT passed through the Golgi compartment, a trans-Golgi network marker was employed to determine whether these molecules entered this tubular network. This is important in terms of how saporin is delivered to ribosomes when conjugated to these two antibodies. Finally, transmission electron microscopy was employed to identify which compartments were involved in the intracellular pathway of HB2 Ab.

6.2 Methods and experimental design

6.2.1 Preparation of fluorescein-conjugated antibodies

Fluorescein was conjugated to both HB2 and OKT10 antibodies according to the protocol described in section 2.3.6. These conjugates were used to follow the internalisation and intracellular pathway taken by these two antibodies.

6.2.2 Preparation of Alexa Fluor ™ 568-conjugated antibodies

The Alexa Fluor™ 568 Protein Labeling Kit (Molecular Probes Europe BV, Leiden, The Netherlands) was used to conjugate this dye to both antibodies according to the manufacturer's instructions described in section 2.3.7. These conjugates were used to follow the internalisation and intracellular pathway taken by these two antibodies.

6.2.3 Competitive Binding Studies

In competitive binding studies, HSB-2 cells were incubated with fluorophore-labelled Ab at a concentration of 20μg/ml in the presence or absence of a 10- or 100-fold mass excess (of the concentration of labelled Ab) of: 1) the same unconjugated Ab, or 2) an Ab irrelevant for the antigen but relevant for the cell line, or 3) an Ab irrelevant for the antigen and the cell line. This was performed for 30 minutes at 4°C (to prevent

endocytosis) before the cells were fixed in paraformaldehyde. All antibodies were of the same isotype (IgG_1). This assay was used to demonstrate the specificity of the conjugated Ab for the antigen and the lack of interaction between the fluorochrome and the cells. Full details of this method can be found in section 2.10.1.

***6.2.4** Endocytosis of HB2 and OKT10 Ab monitored by Confocal microscopy*

The cells were labelled with antibodies directly conjugated to fluorophores and incubated at 37°C to allow internalisation of the Ab and its position within the cell to be monitored using confocal laser scanning microscopy.

To follow the internalisation of each individual Ab the cells were incubated with fluorophore labelled Ab at 4°C (to prevent endocytosis). Samples were taken and fixed to show the distribution of the Ab on the cells before endocytosis occurred. Following this cells were incubated at 37°C and samples were taken from the flask, fixed and viewed under the confocal microscope at 30 mins, 1hr, 3hr, 6hr and 24hr. This enabled the intracellular distribution of the Ab to be observed once internalisation had occurred in order to determine what proportion of the Ab had been taken up by the cell. The cells were counterstained with toluidine blue (0.5% v/v in 0.5% borax) which weakly stains the cytoplasm and strongly stains the nucleus making it useful for defining the cell perimeter. Full details of this experiment can be found in section 2.10.2.

***6.2.5** Co-localisation of OKT10 and HB2 antibodies*

For studies investigating the extent of co-localisation between OKT10 and HB2 Ab, the same protocol was followed except that no counterstain was used. For this work, HB2 Ab was directly conjugated to Alexa Fluor™ 568 dye and OKT10 Ab was directly conjugated to FITC. In this experiment both antibodies were added simultaneously. A co-localisation analysis program (Leica, UK) was used to analyse the exact location of both probes. Details of this method can be found in section 2.10.3.

Additional studies were undertaken whereby an Ab that was directly conjugated to FITC ligated one antigen and an unlabelled Ab ligated the other antigen. This was done for both possible permutations. The method was followed as described for tracing the pathway of the individual antibodies.

6.2.6 Co-localisation of OKT10 Ab- and HB2 Ab-FITC with transferrin-TRITC

To take these investigations further and elucidate the intracellular routing of these two antibodies, either OKT10 Ab-FITC or HB2 Ab-FITC was incubated simultaneously with transferrin-TRITC (a generous gift from Dr Rodolfo Ippoliti, Rome). The cells were incubated at 37°C for endocytosis to occur and samples were taken from the flask at 0, 15, 30, 45, 60, 90 and 120 minutes. Two channel analysis was undertaken to establish the location of both probes throughout the cell followed by co-localisation analysis. This study was undertaken to help elucidate which intracellular pathway was followed by each Ab and in which compartments they localised in. (Full details of this experiment can be found in section 2.10.4.)

6.2.7. Co-localisation of CD7 and CD38 with human TGN46

The TGN and Golgi apparatus has been speculated to be an important part of the intracellular routing of some toxins such as ricin and possibly immunotoxins. In order to visualise whether or not either or both OKT10 or HB2 Ab was transported through the TGN a co-localisation study was conducted with these antibodies and a TGN marker TGN46. Cells were incubated with either HB2 Ab-AF568 or OKT10 Ab-AF568 at 37°C and samples taken at time 0, 30, 60, 90 120, 240 and 360 minutes. The TGN was then stained by an Ab to human TGN46 followed by a FITC-conjugated secondary Ab. The cells were then viewed under the confocal microscope for both the FITC and the AF568 staining. A full description of this method can be found in section 2.10.5. By determining the routing of each of the ITs it was hoped to bring a greater understanding as to how these two ITs work synergistically.

6.2.8 Preparation of cells for electron microscopy studies

To provide additional details of the compartments involved in the intracellular pathways of the HB2 IT, electron microscopy studies were employed.

6.2.8.1 Post-fixation method

HSB-2 cells were incubated with a saturating concentration of HB2 (anti-CD7) Ab and then transferred to 37°C to allow endocytosis to occur. Cells were taken at 0, 30 or 60 minutes and prepared for cryosectioning as described in section 2.11.2.1. Ultrathin cryosections were cut in a cryo chamber (as described in section 2.11.4), collected onto carbon coated, formvar EM grids and stored on gelatine plates. The grids were

immunolabelled with a 1:20 dilution of anti-mouse IgG-gold conjugate (10nm) as described in section 2.11.5. Following this, the grids were embedded in methyl cellulose and uranyl acetate (described in section 2.11.6). The grids were viewed on a Hitachi H7000 transmission electron microscope.

6.2.8.2 Pre-fixation method

An alternative technique for the visualisation of the Ab within the cell was the pre-fixation method. The cells were incubated with HB2 Ab at 4°C as described in section 6.2.8.1., but in this method the secondary gold conjugate was incubated with the cells prior to internalisation of the primary Ab. Cells were incubated for 0, 30 minutes and 1 hour before they were embedded in to agarose as described in section 2.11.3. Blocks were cryosectioned, and sections collected onto grids were post fixed in 1% glutaraldehyde prior to embedding in methyl cellulose and uranyl acetate (section 2.11.6). Cells were viewed on a Hitachi H7000 transmission microscope. Full details of this method were described in section 2.11.2.2.

Both methods can result in non-specific binding and uptake of the secondary gold conjugate and so by comparing images produced by both methods it is easier to distinguish specific from non-specific binding.

6.3 Results

6.3.1 Competitive Binding Studies

6.3.1.1 Direct labelling of CD38 with OKT10 Ab-FITC

Cells were incubated with 20μg/ml OKT10 Ab directly conjugated to FITC either in the presence or absence of a 10-fold or 100-fold excess of the concentration of the OKT10 Ab-FITC of unlabelled relevant or irrelevant Ab. Figure 6.1 shows the widespread distribution of CD38 over the entire surface of HSB-2 cells, observed immediately after ligation at 4°C. The fluorescence occasionally displayed partial patching in limited regions of the cell membrane. Since these cells were maintained at 4°C, no internalisation should have taken place and therefore most of the fluorescence is expected to be limited to the plasma membrane and not within the cell.

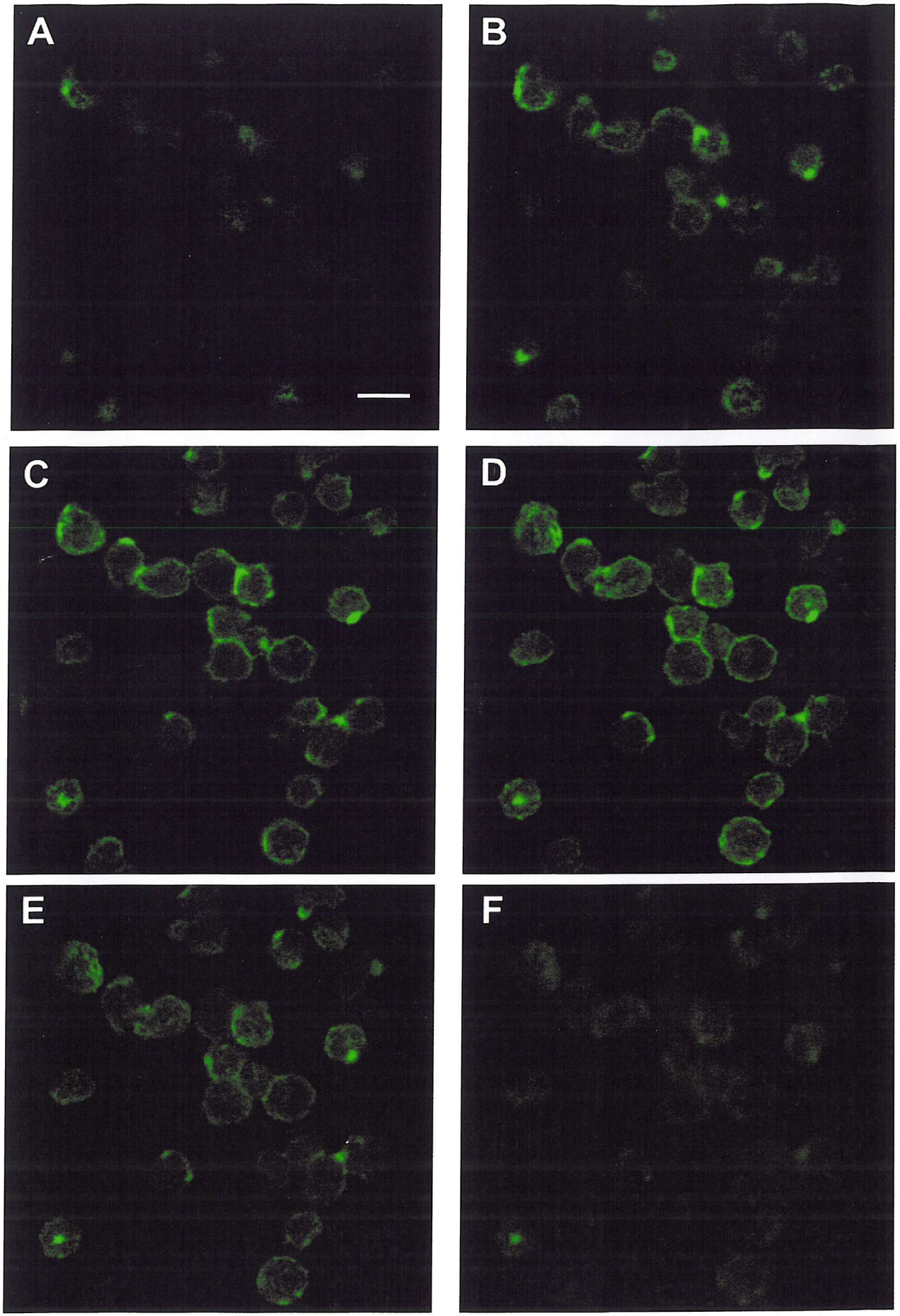

Figure 6.1. Alternate 1μm slices (A-F) through the z-plane of a sample after cells were incubated with OKT10-FITC at 4°C for 30 minutes.
Scale Bar 20μm.

In figure 6.2 it can be clearly seen that a 100-fold excess of relevant unlabelled competing Ab blocked the binding of the fluorophore labelled Ab since fluorescence was reduced to background levels (figure 6.2B). The same result was observed when a 10-fold excess of OKT10 Ab was used.

When a 100-fold excess of unlabelled HB2 Ab (relevant for CD7 on HSB-2 cells but not CD38) was added, the fluorescence pattern displayed in control cells was maintained (figure 6.2C). There was no alteration to the peripheral staining displayed by cells labelled with the OKT10 Ab-FITC alone. The presence of patching was also detected. As expected, no change was observed when only a 10-fold excess of unlabelled Ab was used. No alteration to the binding of OKT10 Ab-FITC was found when the cells were incubated with the conjugate in the presence of a 100-fold excess of unlabelled BU12 Ab (irrelevant for both CD38 and the HSB-2 cell line). This demonstrates that it requires a specific Ab for the CD38 antigen, as opposed to just an excess of Ab, to block the binding of OKT10 Ab-FITC.

6.3.1.2 Direct labelling of CD38 with OKT10 Ab-AF568

The pattern of staining produced by incubating HSB-2 cells with 20μg/ml of OKT10Ab-AF568 can be seen in figure 6.3. As with OKT10 Ab-FITC there was a widespread distribution of this molecule across the whole cell surface with occasional patching on the cell membrane. One main observation was that the fluorescence intensity was not as great as that displayed by OKT10 Ab-FITC.

When the cells were incubated with OKT10 Ab-AF568 in the presence of a 100-fold excess of unconjugated OKT10 Ab, all that could be seen was autofluorescence, since the cells appeared no different from control cells with no fluorescence bound to them (data not shown), indicating that the binding of OKT10 Ab-AF568 was specifically blocked by this Ab (figure 6.4B). Addition of either a 10- or 100-fold excess of either HB2 Ab or BU12 Ab (shown in figures 6.4C and 6.4D respectively) did not alter the pattern of staining of OKT10 Ab-AF568 shown on control cells (figure 6.4A).

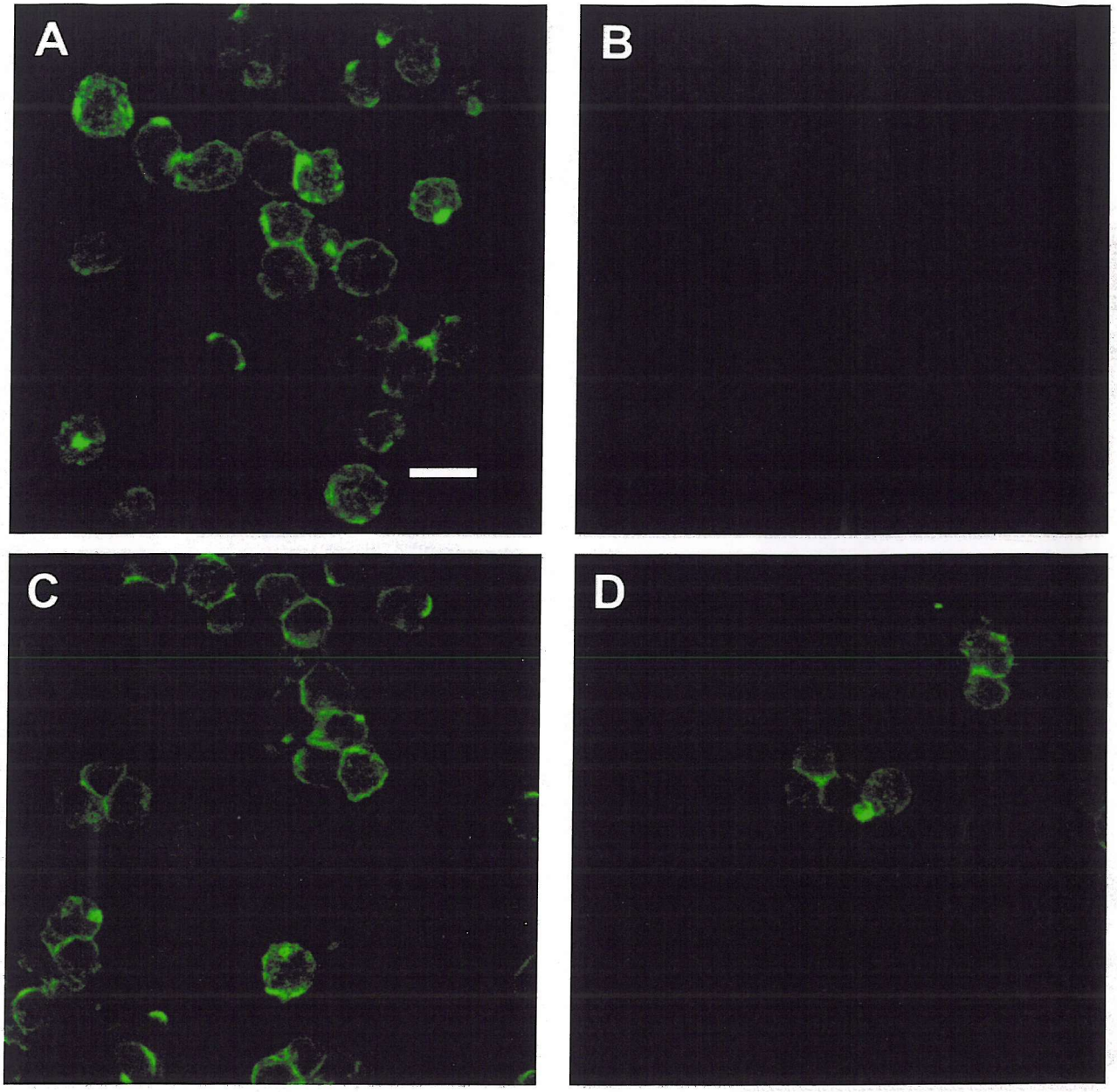

Figure 6.2. Competitive binding of OKT10-FITC on HSB-2 cells: (A) cells incubated with OKT10-FITC alone; (B) cells incubated with OKT10-FITC in the presence of 100-fold excess of OKT10 Ab; (C) cells incubated with OKT10-FITC in the presence of 100-fold excess of HB2 Ab; (D) cells incubated with OKT10-FITC in the presence of 100-fold excess of BU12 Ab. Images are 3D topographical constructs of 15 sections of 1μm each.
Scale Bar 20μm.

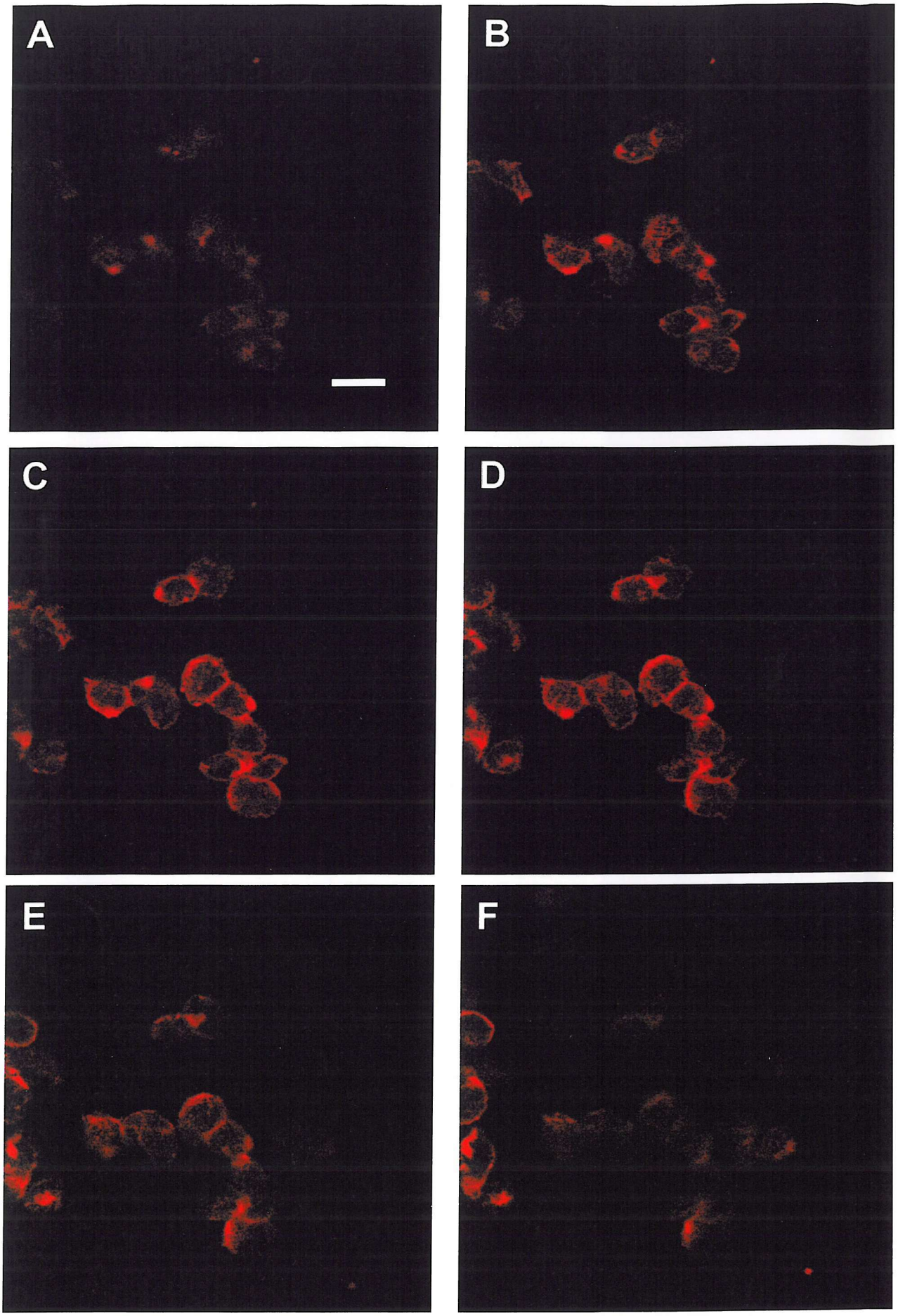

Figure 6.3. Alternate 1μm slices (A-F) through the z-plane of a sample after cells were incubated with OKT10-AF568 at 4°C for 30 minutes.
Scale Bar 20μm.

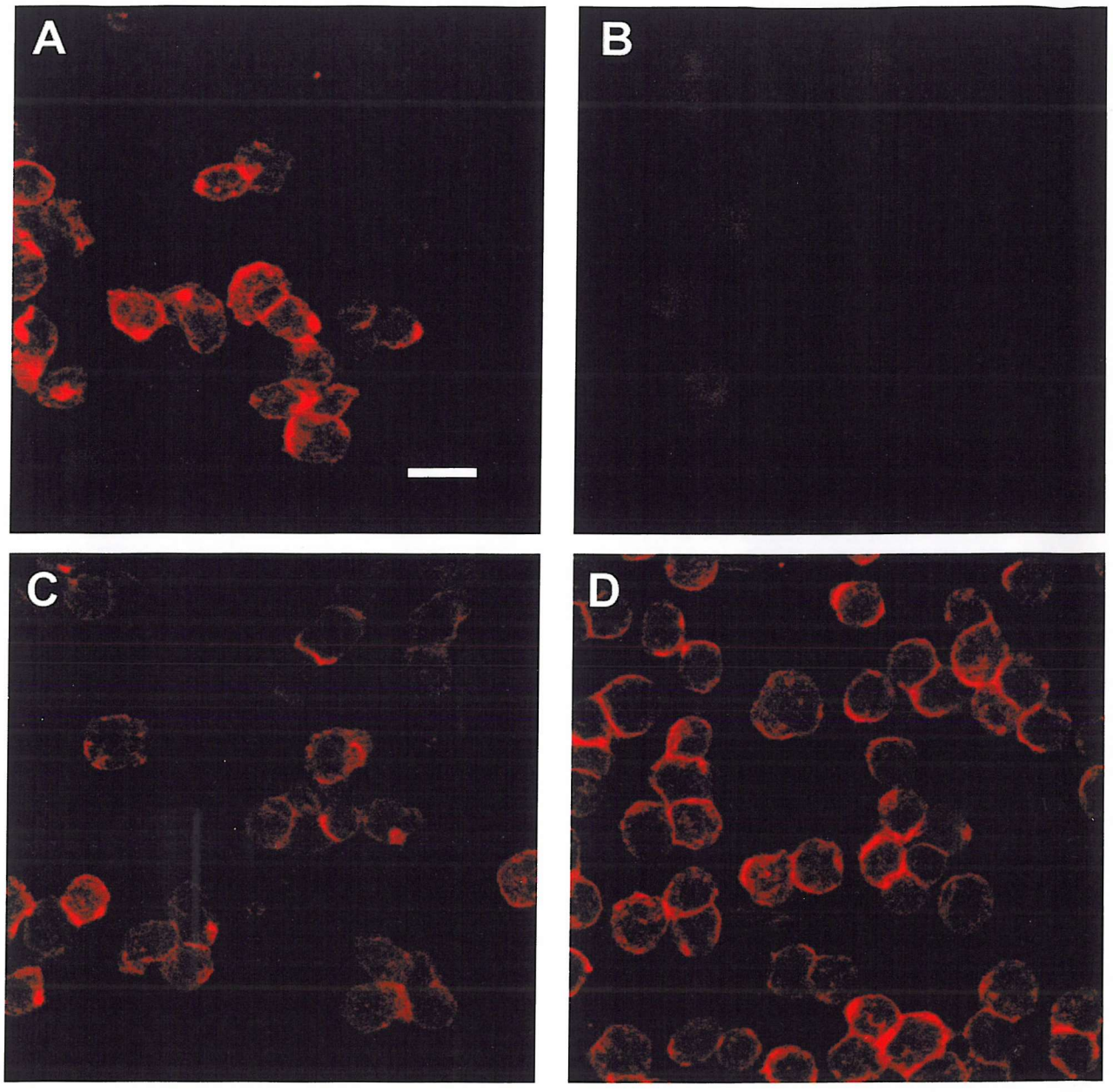

Figure 6.4. Competitive binding of OKT10-AF568 on HSB-2 cells: (A) cells incubated with OKT10-AF568 alone; (B) cells incubated with OKT10-AF568 in the presence of 100-fold excess of OKT10 Ab; (C) cells incubated with OKT10-AF568 in the presence of 100-fold excess of HB2 Ab; (D) cells incubated with OKT10-AF568 in the presence of 100-fold excess of BU12 Ab. Images are 3D topographical constructs of 15 sections of 1μm each.
Scale Bar 20μm.

6.3.1.3 Direct labelling of CD7 with HB2 Ab-FITC

In figure 6.5 CD7 was distributed across the whole surface of the cell, but in this experiment had also become patched on the surface. On some of the cells, HB2 Ab-FITC had concentrated in a limited region of the cell surface. This distribution of the Ab suggested that the cells had not been constantly maintained at 4°C and that the antigen had already started undergoing patching of the CD7 or even internalisation.

A 100-fold excess of unlabelled HB2 Ab greatly reduced the extent of HB2 Ab-FITC binding, although some FITC was still found bound to the cells (figure 6.6B).

The pattern of HB2 Ab-FITC binding was not altered or reduced significantly by the addition of a 100-fold excess of OKT10 Ab (relevant for CD38 on HSB-2 cells but not for CD7) or BU12 Ab (irrelevant Ab for the antigen and cell line) as shown in figure 6.2C and 6.2D respectively. The same was observed when a 10-fold excess of either Ab was added.

6.3.1.4 Direct labelling of CD7 with HB2 Ab-AF568

HB2 Ab-AF568 displayed the same patches of fluorescence as was displayed by the HB2 Ab-FITC in this experiment (figure 6.7). When the HB2 Ab was directly conjugated to AF568 the fluorescence intensity was greatly reduced compared to that produced by the Ab conjugated to FITC. For this reason, the labelling pattern of this Ab conjugate was less obvious and appeared to be less extensive within the cells compared to that seen with the FITC conjugated Ab.

Incubating the cells with HB2 Ab-AF568 and a 100-fold excess of HB2 unlabelled Ab blocked all the binding of HB2 Ab-AF568 (figure 6.8B). The image appears noisy due to the use of a high gain in an attempt to display the presence of cells by means of their autofluorescence. The binding fluorescence pattern of HB2 Ab-AF568 was not altered by the addition of an excess of either OKT10 Ab or BU12 Ab (figure 6.8C and 6.8D respectively).

6.3.4 Analysis of CD38 internalisation

Internalisation of membrane CD38 inside the T-ALL tumour line HSB-2 was investigated over a time course of 24 hours by confocal laser scanning microscopy (figure 6.9). This method enabled differentiation between fluorescent signals from the plasma membrane

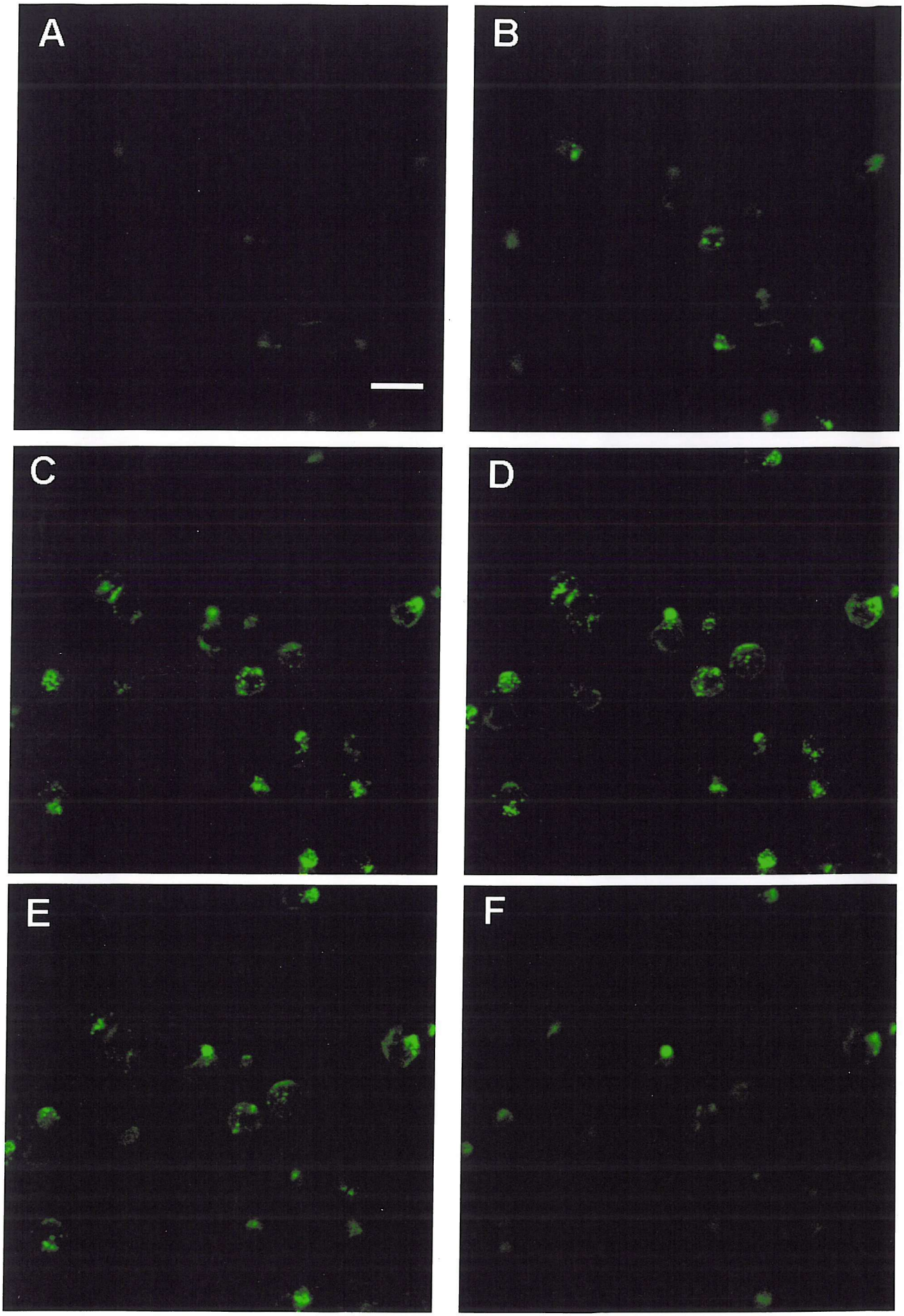

Figure 6.5. Alternate 1μm slices (A-F) through the z-plane of a sample after cells were incubated with HB2-FITC at 4°C for 30 minutes.
Scale Bar 20μm.

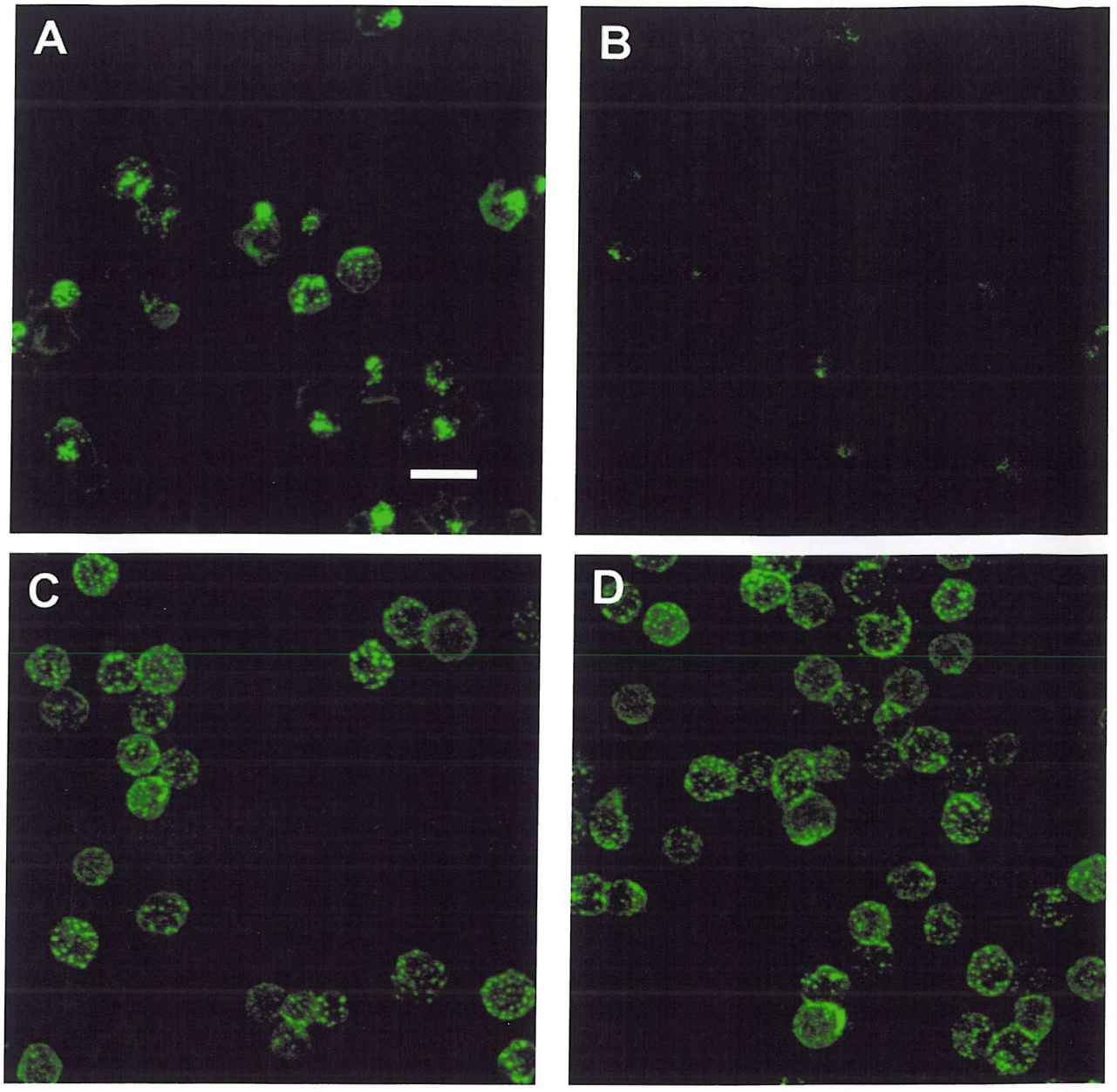

Figure 6.6. Competitive binding of HB2-FITC on HSB-2 cells: (A) cells incubated with HB2-FITC alone; (B) cells incubated with HB2-FITC in the presence of 100-fold excess of HB2 Ab; (C) cells incubated with HB2-FITC in the presence of 100-fold excess of OKT10 Ab; (D) cells incubated with HB2-FITC in the presence of 100-fold excess of BU12 Ab. Images are 3D topographical constructs of 15 sections of 1μm each. Scale Bar 20μm.

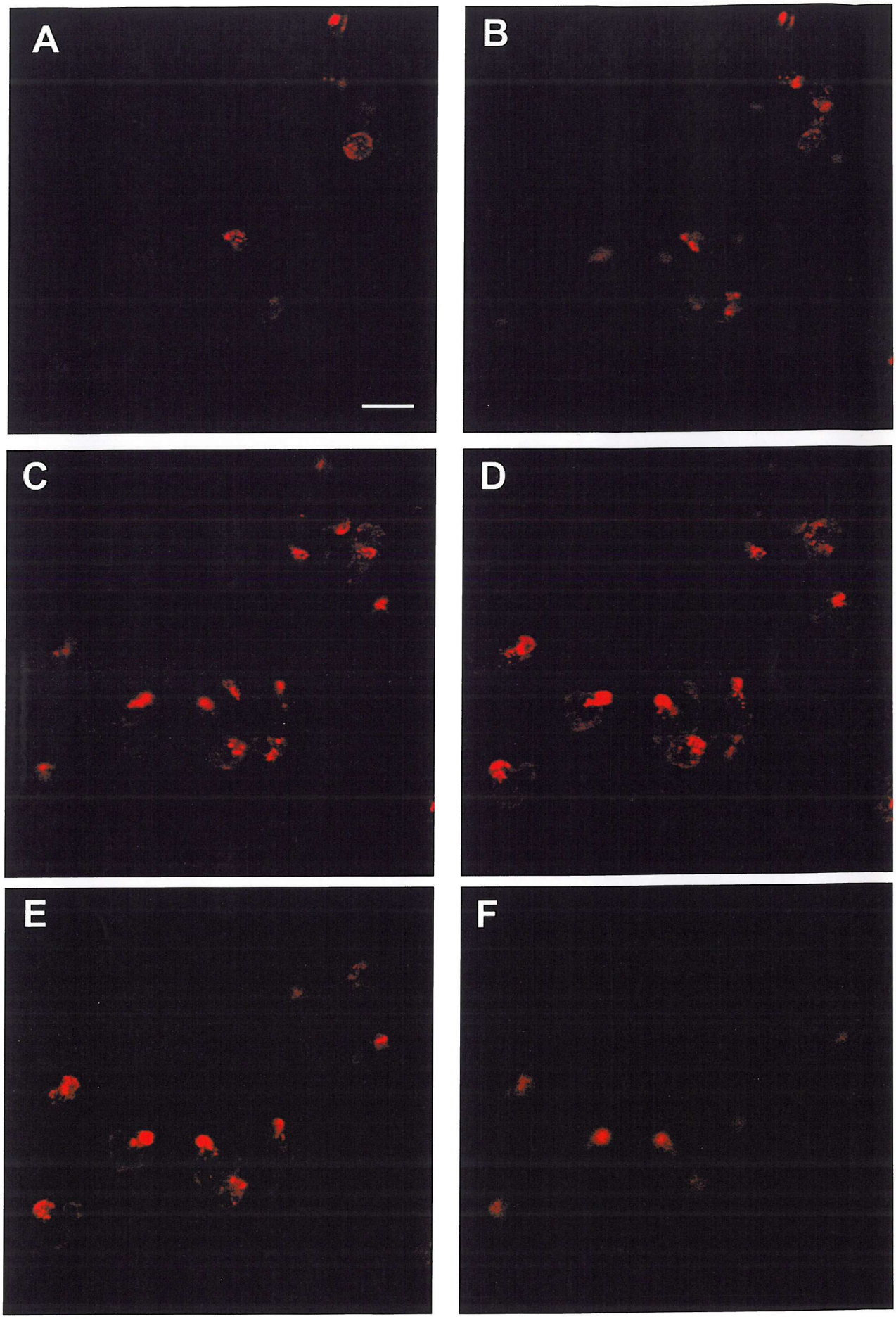

Figure 6.7. Alternate 1μm slices (A-F) through the z-plane of a sample after cells were incubated with HB2-AF568 at 4°C for 30 minutes.
Scale Bar 20μm.

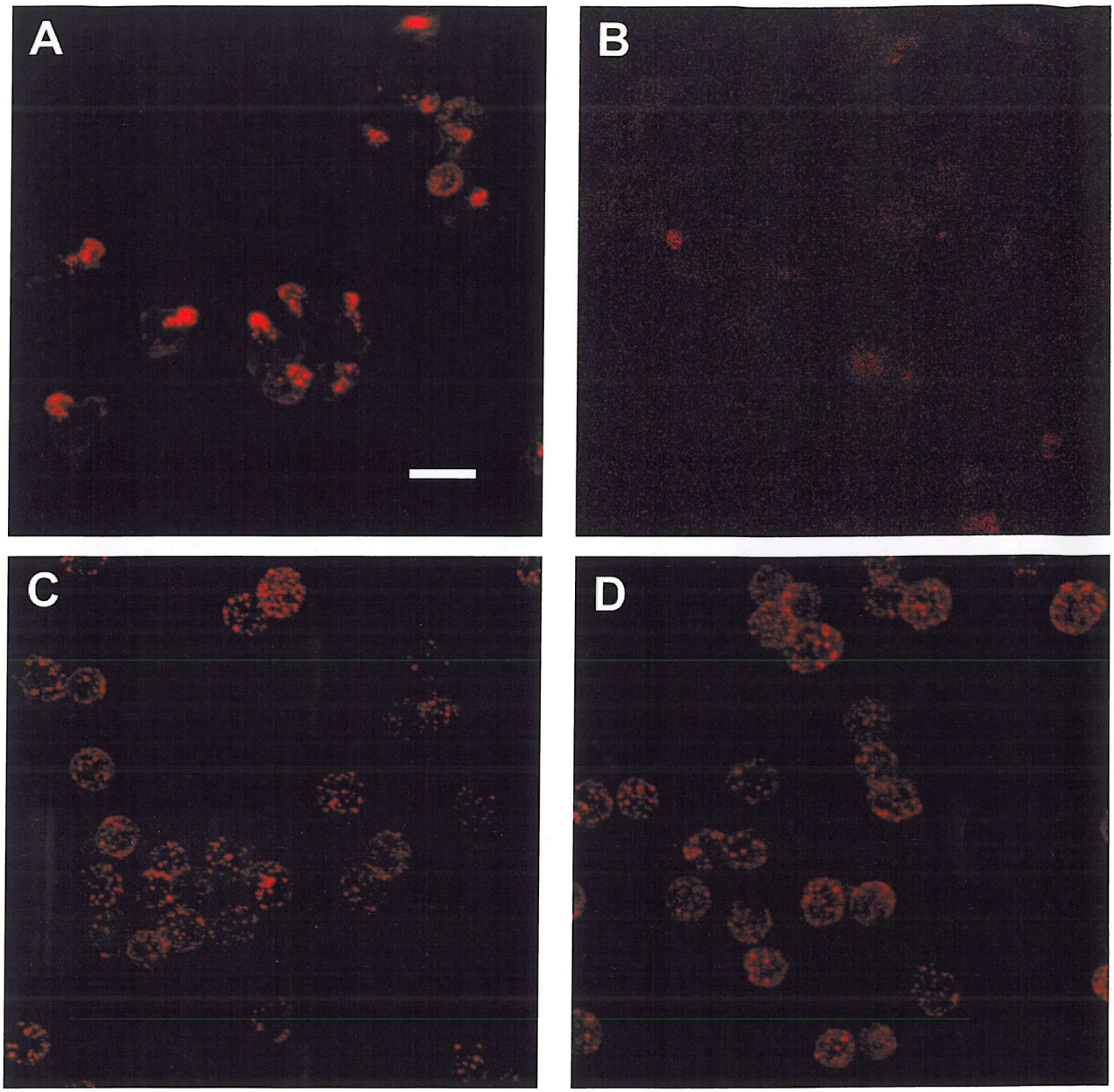

Figure 6.8. Competitive binding of HB2-AF568 on HSB-2 cells: (A) cells incubated with HB2-AF568 alone; (B) cells incubated with HB2-AF568 in the presence of 100-fold excess of HB2 Ab; (C) cells incubated with HB2-AF568 in the presence of 100-fold excess of OKT10 Ab; (D) cells incubated with HB2-AF568 in the presence of 100-fold excess of BU12 Ab. Images are 3D topographical constructs of 15 sections of 1μm each.
Scale Bar 20μm.

and those from the cytoplasm and gave an approximate indication of the intracellular location of the molecule within the cell. HSB-2 cells were incubated with saturating amounts of OKT10 Ab-FITC (anti-CD38 MAb) for 30 minutes at 4°C, successively incubated at 37°C for different intervals, washed and fixed with 4% (w/v) paraformaldehyde.

Cells maintained at 4°C (at time 0) were generally homogeneously stained over the entire membrane area, although a few cells showed the labelled Ab concentrated in patches on the cell surface. After 30 minutes of incubation in medium at 37°C, the Ab was less evenly distributed across the cell membrane and had become concentrated in one small region of the cell surface (i.e. capping had occurred). Some fluorescence was observed within the cytoplasm of the cell indicating that a small amount of Ab had internalised into the cytoplasm and to a much lesser extent into the perinuclear region of the cell. The majority of the fluorescence appeared to be on the cell membrane 1 hour after the start of incubation at 37°C. Although there was still a small amount of capping present on the cells, Ab was still found surrounding the whole cell. There was a trace amount of internalised Ab at this time, most of which was found in the submembrane region of the cell. This pattern of Ab staining was maintained in the cells studied for the rest of the time points. At 24 hours there was still very strong peripheral staining with only a trace amount of internalised Ab detectable.

6.3.5 Analysis of CD7 internalisation

The internalisation of membrane CD7 inside HSB-2 cells was investigated by ligating the antigen with an anti-CD7 MAb directly conjugated to fluorescein (HB2 Ab-FITC) and its movement through the cells followed as described above. Images from this experiment can be found in figure 6.10. At time 0 (when cells had been maintained at 4°C), the majority of labelling with this Ab could be seen to be peripheral and was presumably on the cell membrane. Generally the Ab was evenly distributed over the whole cell surface and patches of the Ab in concentrated regions of the membrane had only occurred on a few of the cells studied. Within 30 minutes of incubation at 37°C, patching had occurred whereby the Ab was concentrated along one region of the cell membrane. This appeared to constitute most of the Ab that was found bound to the surface at time 0. After 30 minutes there had been a considerable degree of internalisation of the Ab, most of which was found in the submembrane region of the cell (as determined by the toluidine blue

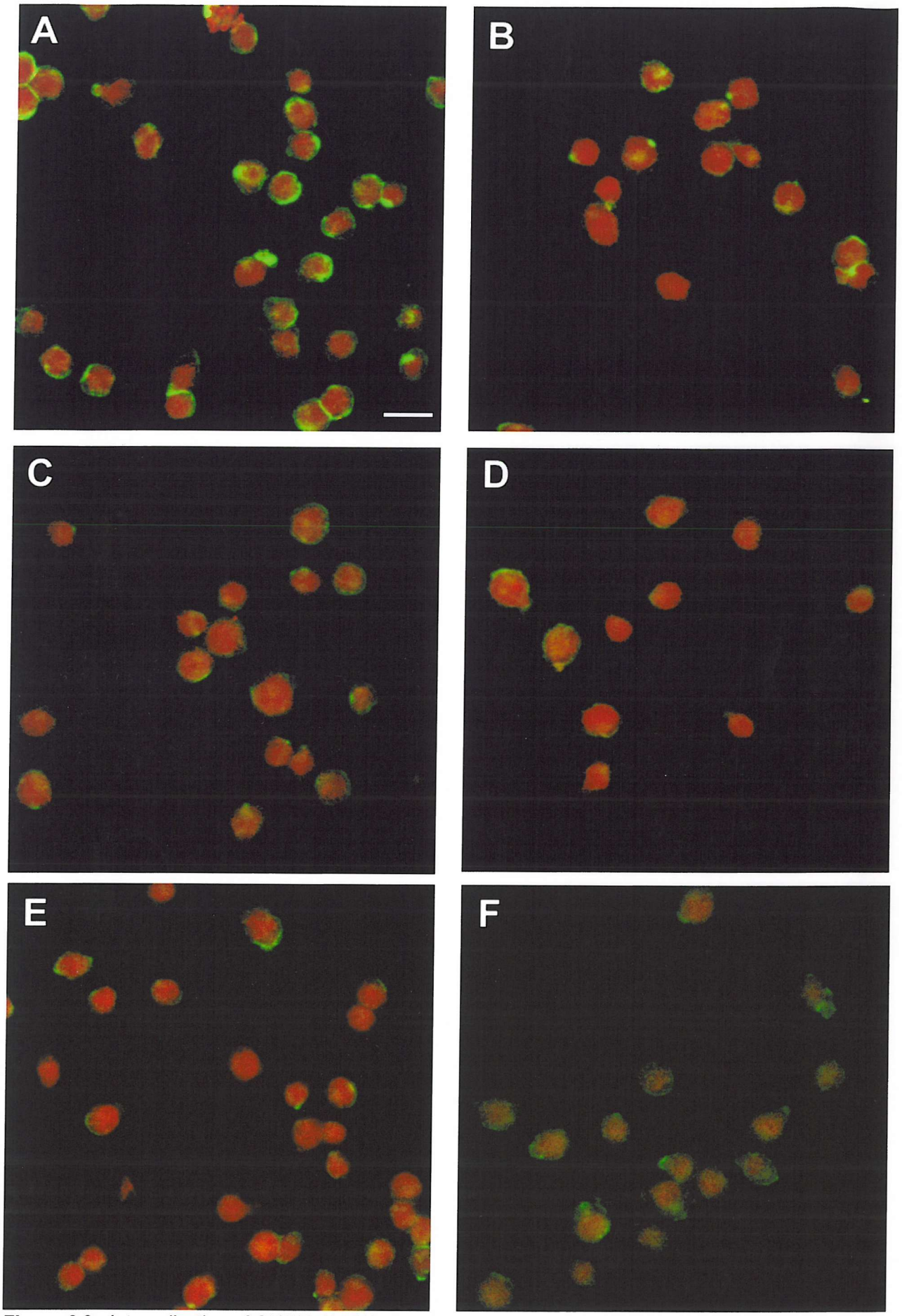

Figure 6.9. Internalisation of OKT10 Ab: (A) visualised after staining at 4°C (at time 0); (B) visualised after subsequent warming to 37°C for 30 minutes; (C) after 1hour at 37°C; (D) after 3 hours at 37°C; (E) after 6 hours at 37°C; (F) after 24 hours at 37°C. Images are 3D topographical constructs from 15 sections of 1μm each.
Scale Bar 20μm.

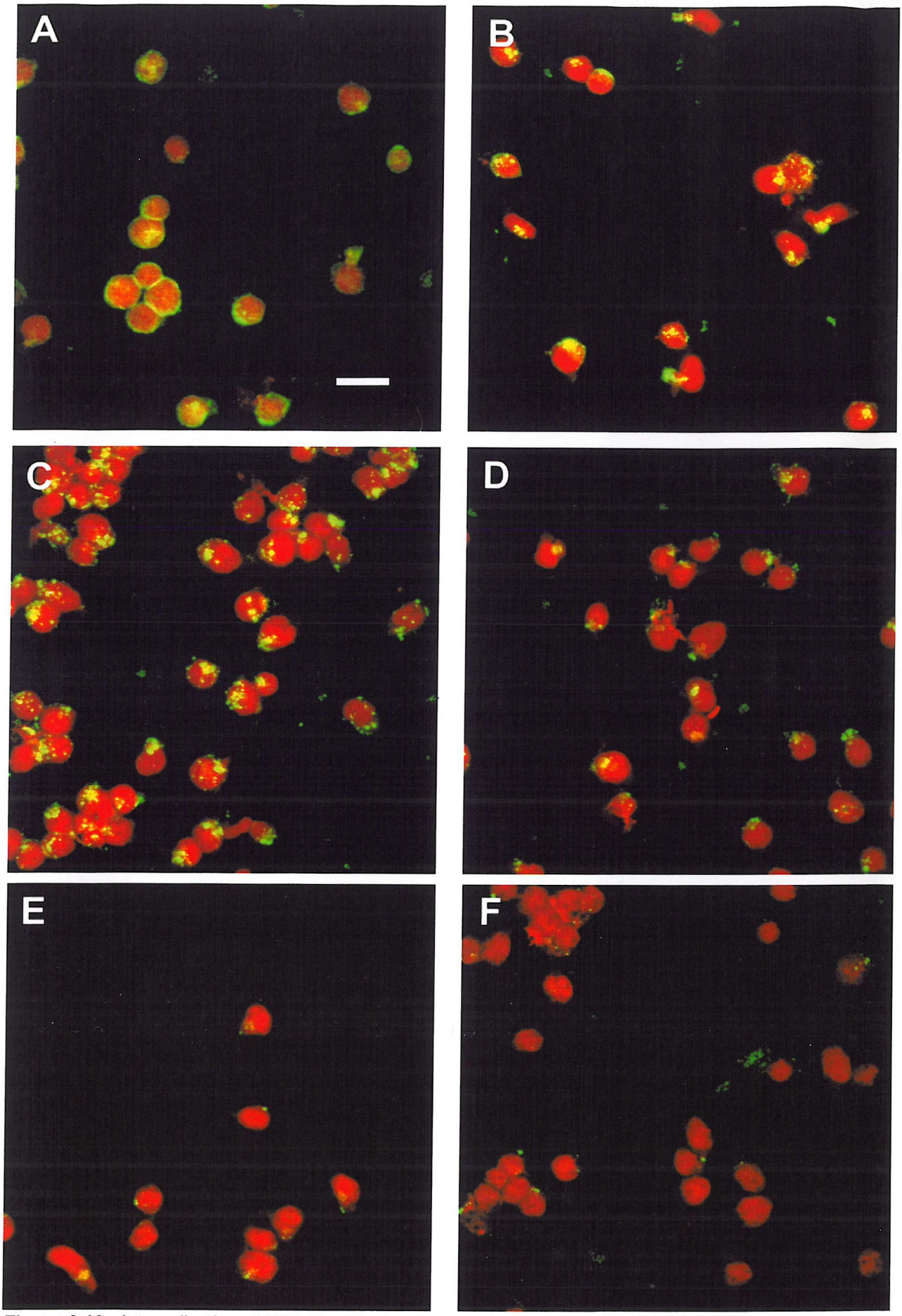

Figure 6.10. Internalisation of HB2 Ab: (A) visualised after staining at 4°C (at time 0); (B) visualised after subsequent warming to 37°C for 30 minutes; (C) after 1 hour at 37°C; (D) after 3 hours at 37°C; (E) after 6 hours at 37°C; (F) after 24 hours at 37°C. Images are 3D topographical constructs from 15 sections of 1μm each.
Scale Bar 20μm.

staining), although a small proportion of the internalised Ab was found in the perinuclear region. By 1 hour, a large proportion of the Ab that was originally bound to the cell surface had entered the cell interior, although patching was still found at the plasma membrane. By this time the fluorescence was spread across the cytoplasm to the perinuclear region. From 3 hours onwards the amount of Ab detected within the cell diminished greatly. At 3 hours, there was still some Ab remaining on the cell surface in capped areas as well as some in the perinuclear region. By 6 hours there was virtually no fluorescence detectable inside the cell. All that remained after 24 hours was some Ab concentrated on a small region on the cell surface.

6.3.6 Co-localisation of HB2 Ab and OKT10 Ab

A study was undertaken to determine whether or not HB2 Ab and OKT10 Ab co-localised when both ligated their respective antigens. For this, CD7 of HSB-2 cells was ligated with HB2 Ab-AF568 (red) and CD38 was ligated with OKT10 Ab-FITC (green). The cells were then transferred to medium at 37°C and the antibodies allowed to internalise for the same time intervals as studied previously, fixed and then analysed. A co-localisation analysis program was used to compare pixel by pixel the location of each probe and indicate the degree by which the two were co-localised. A graded colour scale denoted the extent of co-localisation. Areas denoted by purple/blue were areas of low co-localisation or in most cases co-localisation of stain in the red channel with autofluorescence detected in the green channel. Green/yellow denotes an intermediate level of co-localisation and red/pink shows areas of considerable co-localisation.

Using this method, it can be seen (in figures 6.11 and 6.12) that both antibodies were present on the cell membrane at the start of the experiment. Patching and capping on the cell membrane was observed by both antibodies at time 0 (figure 6.11A) and these were the regions (in green) on the cell surface where co-localisation was at its uppermost. A greater proportion of HB2 Ab had internalised after 30 minutes incubation compared with OKT10 Ab of which the majority was still seen on the plasma membrane (data not shown). Only a trace amount of OKT10 Ab was detected within the cytoplasm. As the amount of HB2 Ab still bound to the membrane decreased throughout the time course, the amount of co-localisation with OKT10 Ab decreased. By 24 hours there was no significant co-localisation of the two antibodies (figure 6.12B).

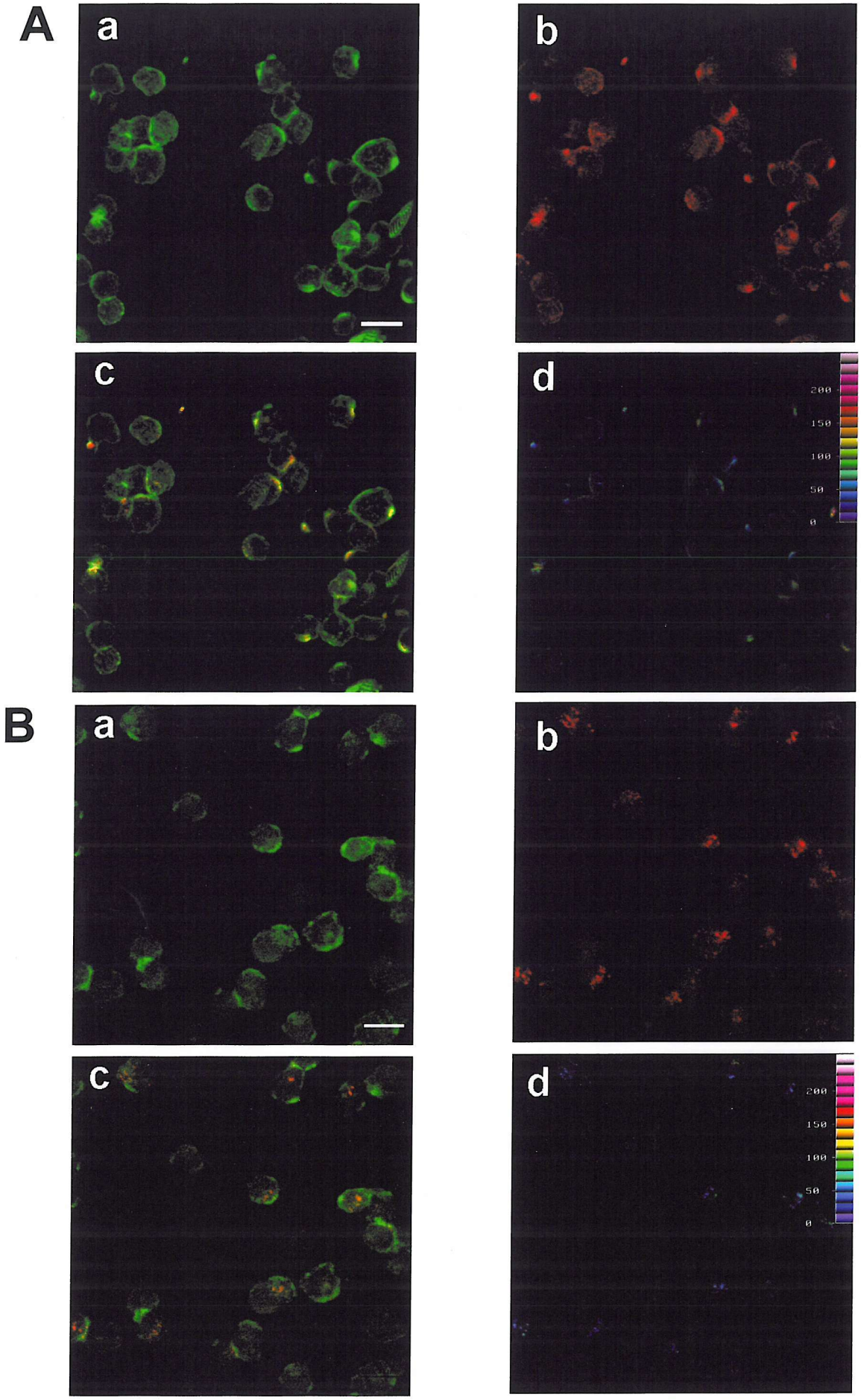

Figure 6.11. Co-localisation of CD7 and CD38 when ligated by HB2 Ab-AF568 (red) and OKT10 Ab-FITC (green) respectively. Cells visualised at time 0 (A) and 1 hour (B): (a) OKT10 Ab-FITC; (b) HB2 Ab-AF568; (c) OKT10 Ab-FITC and HB2 Ab-AF568; (d) co-localisation analysis. Images are 3D topographical constructs of 15 sections of 1μm each.
Scale Bar 20μm.

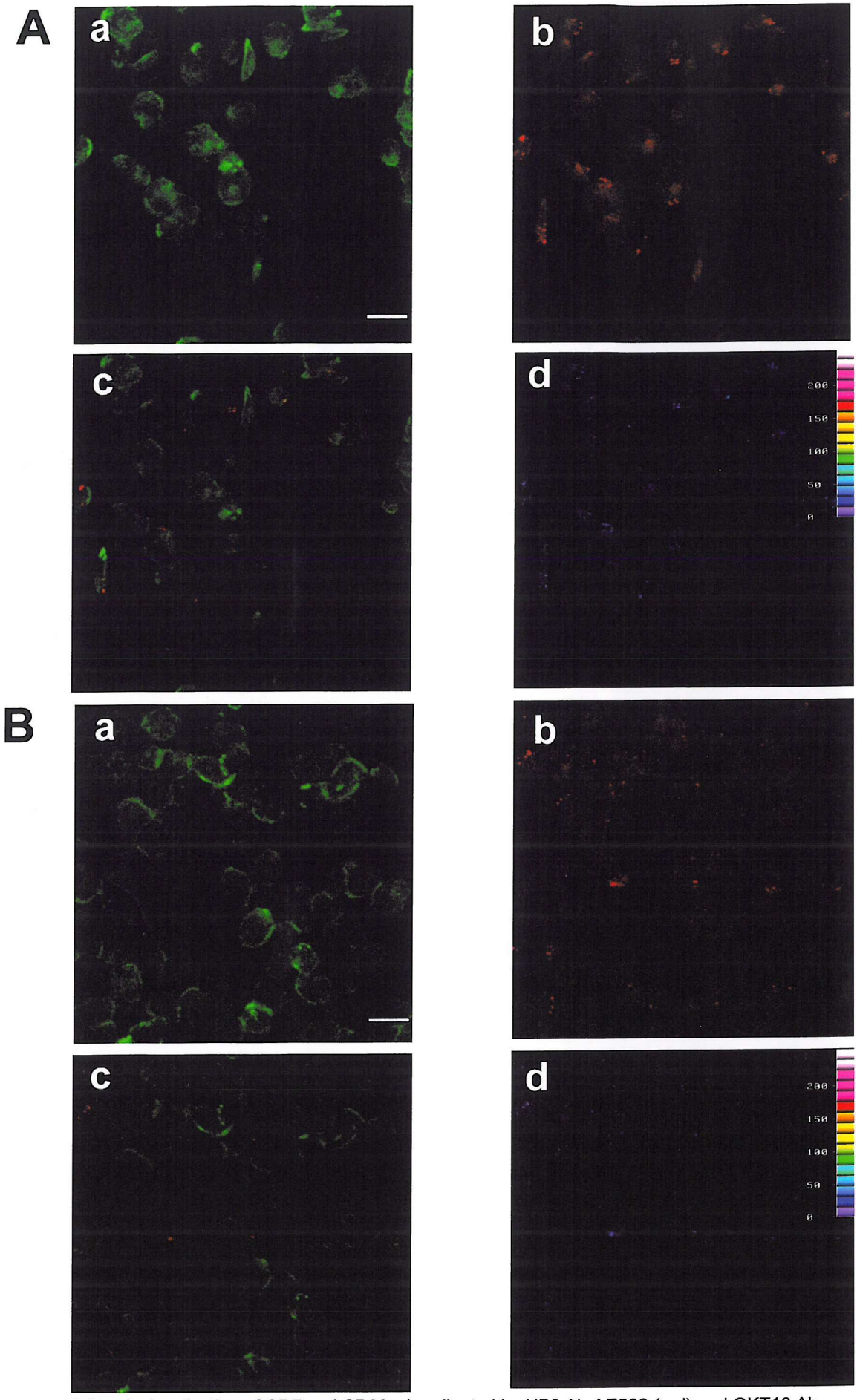

Figure 6.12. Co-localisation of CD7 and CD38 when ligated by HB2 Ab-AF568 (red) and OKT10 Ab-FITC (green) respectively. Cells visualised at 6 hours (A) and 24 hours (B): (a) OKT10 Ab-FITC; (b) HB2 Ab-AF568; (c) OKT10 Ab-FITC and HB2 Ab-AF568; (d) co-localisation analysis. Images are 3D topographical constructs of 15 sections of 1μm each.
Scale Bar 20μm.

6.3.7 The effect of co-localisation on internalisation and intracellular routing

An experiment was conducted to determine if when one Ab conjugated to a fluorescent probe was bound to its antigen and the second unlabelled Ab was bound to its antigen, could a difference in the pattern of internalisation be detected compared to that when only a single antigen was ligated. When CD7 was ligated with HB2 Ab-FITC and CD38 was ligated with unlabelled OKT10 Ab no substantial differences to their intracellular pathways were observed compared to the Ab staining produced when each antigen was ligated singly (as shown by figure 6.13 D-F). There was still a strong peripheral staining at the start of the experiment, with a large amount of capping and internalisation within the first 30 minutes, which increased until 3 hours, when a significant fall in the amount of Ab detected inside the cell was first observed. By 6 hours, almost all of the Ab had disappeared.

No apparent change to the internalisation of CD38 was observed when it was ligated with OKT10 Ab-FITC and CD7 was ligated by unlabelled HB2 Ab (figure 6.13 A-C). CD38 displayed a strong peripheral staining on the cell membrane at the start of the experiment as it did when ligated singly. This was followed over consecutive time points by capping of the Ab in limited regions of the membrane and a slight but gradual increase in the extent of internalisation just as when the antigen was ligated singly.

6.3.8. Co-localisation of OKT10 Ab- and HB2 Ab-FITC with transferrin-TRITC

Cells were incubated with either OKT10 Ab- or HB2 Ab-FITC for 30 minutes at 4°C, and then transferred to medium containing 20μg/ml of transferrin-TRITC to allow both the Ab and transferrin to internalise for the following time intervals: 0, 15, 30, 45, 60, 90 and 120 minutes. This was done to determine whether these antibodies shared the same intracellular compartments and pathway as transferrin to help elucidate the routing of these molecules.

Figure 6.14 shows 3D topographical constructs for the three time intervals of 0 minute, 45 minute and 2 hours of both OKT10-FITC and transferrin-TRITC. Adjacent to each of these images are the co-localisation analysis images for the respective time points. At time 0, there was very little transferrin-TRITC bound to the cells as it had only just been introduced to the culture medium. OKT10 Ab-FITC stained the periphery of the cell with

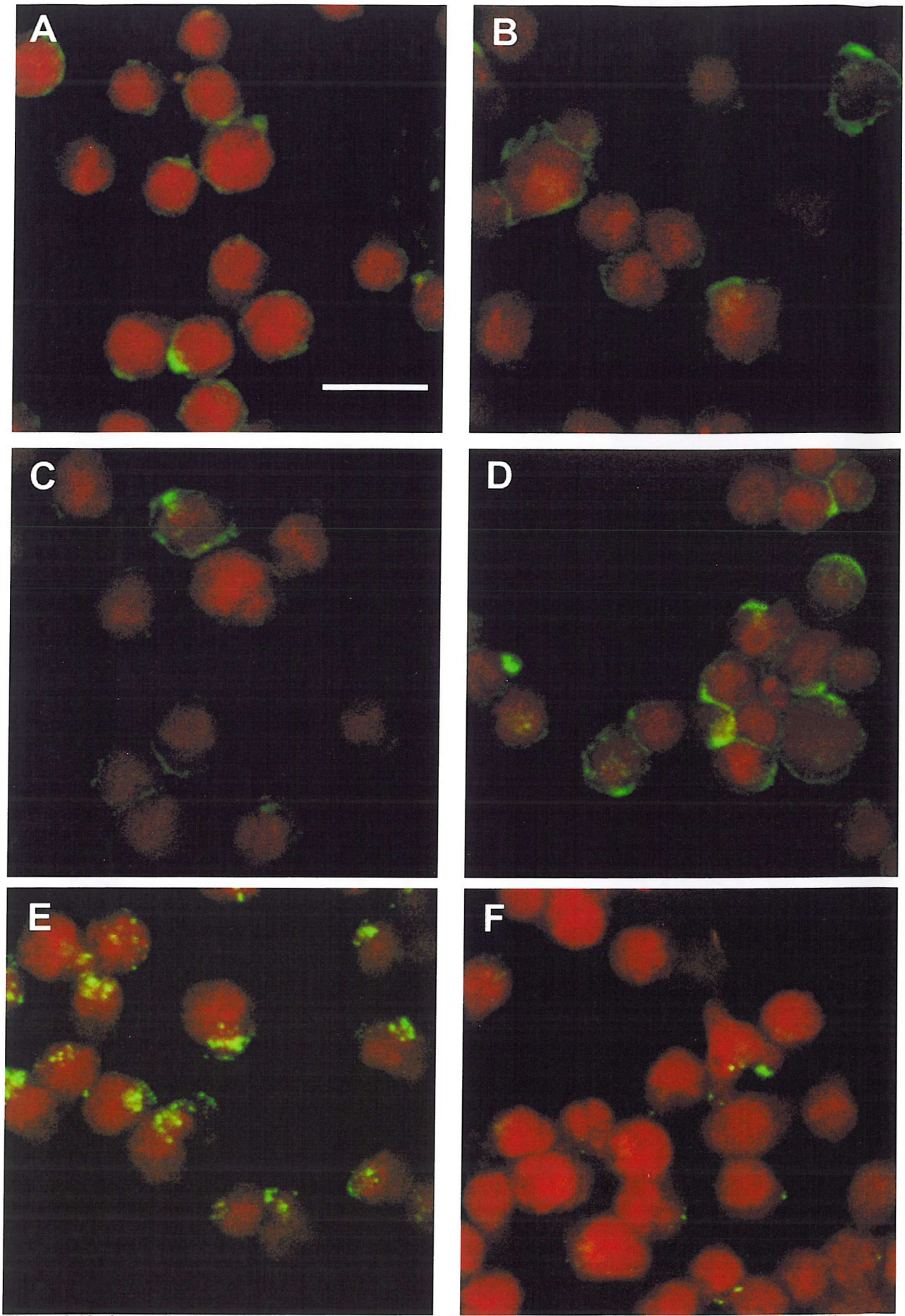

Figure 6.13. Internalisation of CD38 when it is ligated by OKT10 Ab-FITC and CD7 is ligated by HB2 Ab: (A) visualised after staining at 4°C (at time0); (B) after 1hour at 37°C; (C) after 3 hours at 37°C. Internalisation of CD7 when it is ligated by HB2 Ab-FITC and CD38 is ligated by OKT10 Ab: (D) visualised after staining at 4°C (at time 0); (E) after 1 hour at 37°C; (F) after 6 hours at 37°C. Images are 3D topographical constructs from 15 sections of 1μm each.
Scale Bar 20μm.

slight patching along one edge of many of the cells shown (figure 6.14A). Since there was so little transferrin-TRITC bound to the cells at this point there was no significant co-localisation (denoted by the small amount of blue signal in the co-localisation analysis image in figure 6.14B).

From 15 minutes onwards it was clear that the internalisation and routing of OKT10 Ab-FITC and transferrin-TRITC differed greatly (demonstrated by the lack of co-localisation displayed in figure 6.14D at time 45 minutes). OKT10 Ab-FITC remained mostly on the cell membrane with only a small proportion visible within the cell interior whereas transferrin-TRITC was rapidly internalised within specific condense compartments which entered the cell from one specific region of the membrane (as demonstrated at 45 minutes in figure 6.14C). There was virtually no TRITC staining on the cell membrane after 15 minutes. Even after 2 hours where more OKT10 Ab-FITC had been internalised, no significant amount of co-localisation was seen (as shown in figures 6.14E and F by the blue shading).

This was greatly contrasted by the significant amount of co-localisation seen when cells were incubated with both HB2 Ab-FITC and transferrin-TRITC. As before at time 0 (figure 6.15A) there was very little transferrin-TRITC bound to the plasma membrane, but the small proportion that had bound appeared to be co-localised with HB2 Ab-FITC also on the cell surface, especially in regions where the Ab had begun to concentrate (denoted by the red/orange signal in the co-localisation analysis image). By 15 minutes both HB2 Ab-FITC and transferrin-TRITC had internalised. There was still a significant amount of HB2 Ab-FITC remaining on the cell membrane, whereas the transferrin-TRITC was mostly found within the cell interior. It was clear that much of the Ab and transferrin-TRITC had co-localised within the same intracellular compartments. From this point onwards it became obvious that both reagents were internalised from the same region of the cell membrane as demonstrated at time 45 minutes in figure 6.14C. The co-localisation analysis image shows a significant amount of pink signal demonstrating the large extent of co-localisation observed. This co-localisation reached a peak before 1 hour, after which time the amount of HB2 Ab-FITC staining within the cell interior began to reduce as not all the Ab was internalised by within this short study, and so by 2 hours the amount of co-localisation between these two reagents reduced accordingly (figure 6.15E

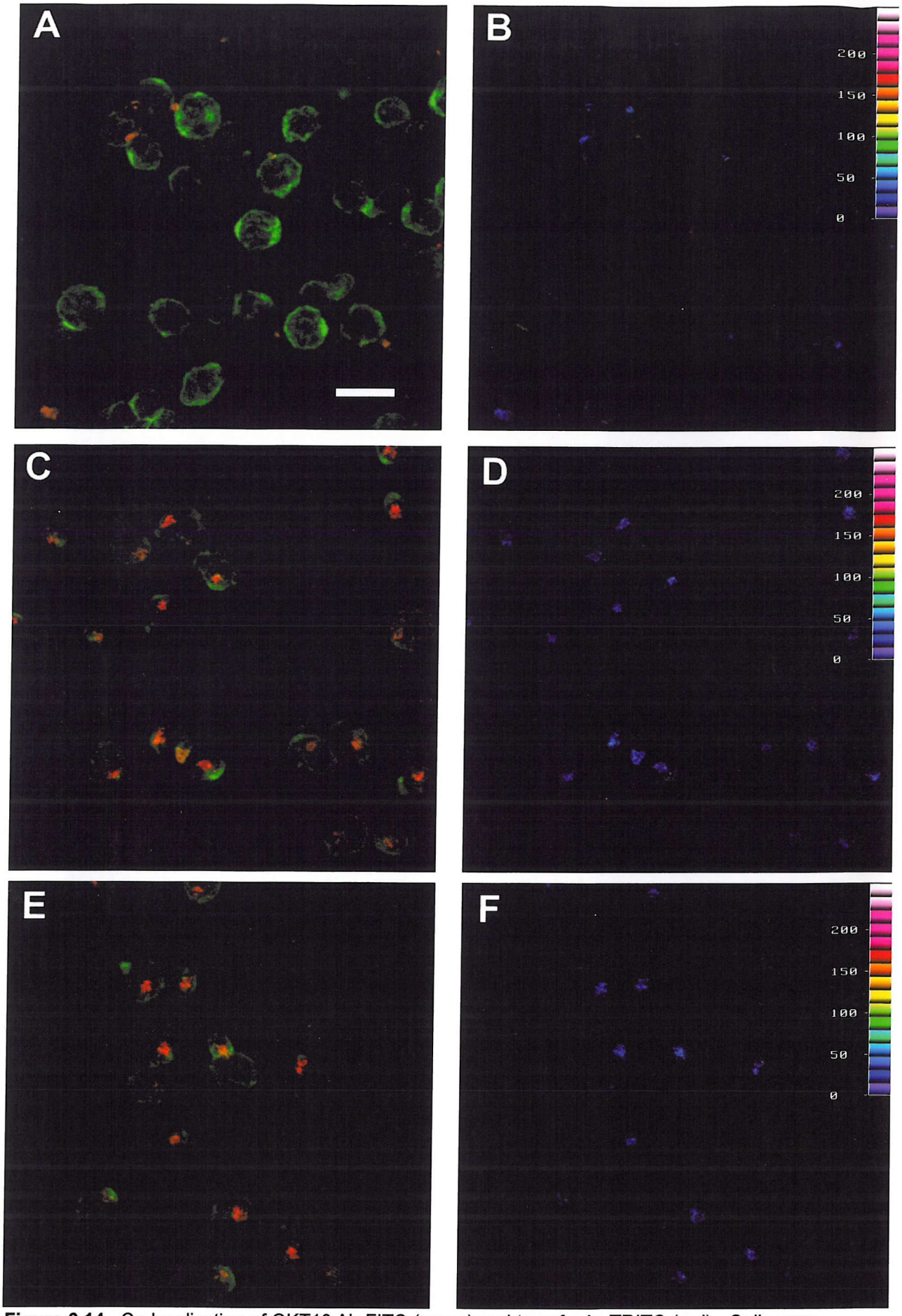

Figure 6.14. Co-localisation of OKT10 Ab-FITC (green) and transferrin-TRITC (red). Cells were visualised at time 0 (A), 45 minutes (C) and 2 hours (E) after incubation at 37°C. Images are 3D topographical constructs of 15 sections of 1μm each. Images B, D and F show the co-localisation analysis of each time point.
Scale Bar 20μm.

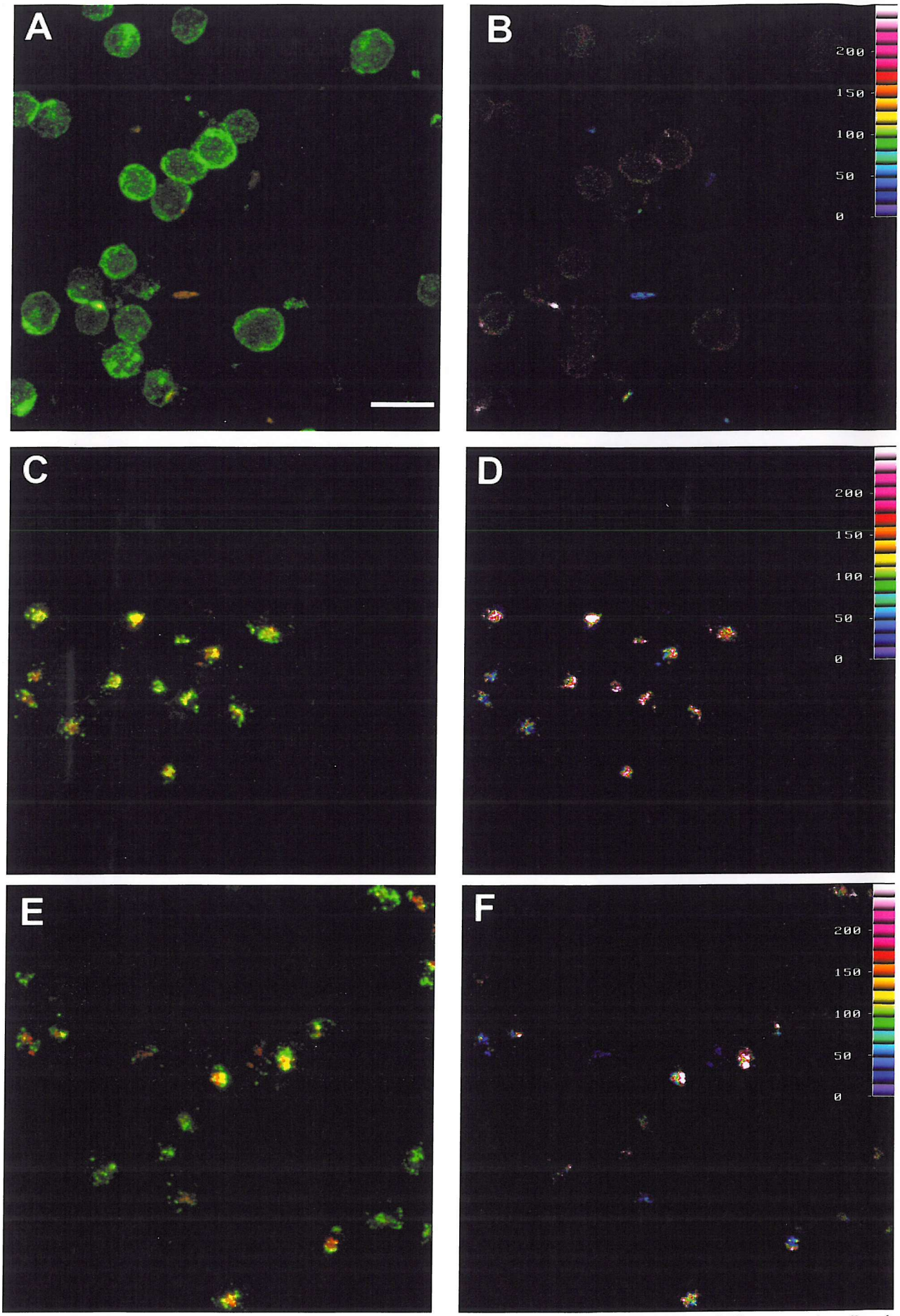

Figure 6.15. Co-localisation of HB2 Ab-FITC (green) and transferrin-TRITC (red). Cells were visualised at time 0 (A), 45 minutes (C) and 2 hours (E) after incubation at 37°C. Images are 3D topographical constructs of 15 sections of 1μm each. Images B, D and F show the co-localisation analysis of each time point.
Scale Bar 20μm.

and F). At no point was either all the TRITC co-localised with the FITC or all the FITC co-localised with the TRITC.

6.3.9. Staining the Golgi apparatus

The studies to determine if OKT10 Ab- and HB2 Ab-FITC co-localised with transferrin-TRITC were used to follow the early stages of the endocytic pathway of these antibodies. To help elucidate the compartments involved in the later stages of endocytosis we needed to fluorescently stain the Golgi apparatus. Three different methods of staining were tested to stain the Golgi apparatus before any co-localisation assay could be carried out. Firstly, 1-acyl-2-(N-4-nitrobenzo-2-oxa-1,3-diazole)aminocaproyl sphingosine (C_6-NBD-Ceramide) was used. This green fluorescent compound is known to produce selective staining of the Golgi complex. The molecular basis for this labelling is not yet fully understood but could be due to interaction of the fluorescent ceramide with specific proteins or lipids in the Golgi apparatus, or to a physical property of the membrane of this organelle (for example the phase state of its lipids) (Pagano 1989). C_6-NBD-Ceramide is considered to be actively taken up by cells via endocytosis since endocytosis inhibitors such as azide can block internalisation of this stain (Sleight and Pagano 1984).

Originally this compound was tested by incubating 10^6 cells with 100µl of C_6-NBD-ceramide at 10µg/ml in the form of a bovine serum albumin (BSA) complex (recommended for labelling cells with this compound) for 30 minutes at 37°C. Following this the cells were washed, cytospun, coverslipped and viewed under the confocal microscope. Figure 6.16A shows the diffuse staining pattern obtained by this protocol. The image was very noisy and the staining was poorly defined. It appeared to stain a large proportion of the plasma membrane and produced a crescent shaped pattern of staining along one edge of the cytoplasm. It was likely that this molecule had stained the plasma membrane since it has been described to travel between there and the Golgi apparatus. This compound was then further tested by incubating the cells with concentrations of 2.5, 5 and 10µM for 10, 30 and 45 minutes at 37°C to see if these factors would improve the staining of the Golgi apparatus. No image was produced that bore a greater resemblance to the Golgi apparatus than that in figure 6.16A. In fact, when the cells were treated as

described above they appeared to decrease in size and the staining appeared even more diffuse (data not shown).

The TGN46 glycoprotein is the human equivalent of the rat *trans*-Golgi network marker TGN38. It is localised primarily to the TGN which made it a good marker for TGN in the investigations undertaken. A sheep Ab against this marker was tested at two concentrations of 0.1 and 1μg/ml and detected by a donkey anti-sheep FITC conjugated secondary Ab at two dilutions of 1:100 and 1:200. All conditions tested produced a clearly defined pattern of staining in the perinuclear region of the cell which was characteristic of the Golgi apparatus. Figure 6.16B shows cells stained by using 1μg/ml of the primary Ab followed by a 1:200 dilution of the FITC conjugated secondary Ab. This combination produced the clearest, strongest fluorescent staining pattern compared with the other conditions tested. However the image appears noisy which was considered to be debris on the slide from the washing procedures as it only appeared on the last sections visualised.

Figures 6.16C and D show the staining produced by a primary Ab (a rabbit polyclonal) to the beta prime subunit of COP I, known as BSTR. COP I is a coat protein that coats vesicles involved in vesicular trafficking in the early secretory pathway. This protein is found on Golgi membranes. The primary Ab was tested at dilutions of 1:500 and 1:1000 followed by an anti-rabbit TRITC or FITC conjugated secondary (in figures 6.16C and 6.16D respectively) at either a 1:20 or 1:40 dilution. A similar pattern of staining was produced by both secondary antibodies but was much clearer and of greater intensity when a FITC conjugate was used. The staining was mostly in the perinuclear region which was characteristic of Golgi like staining and was very similar to the pattern produced by the anti-TGN46 Ab. In figure 6.16D it was also possible to see the punctate peripheral structures that are also labelled with BSTR. Figure 6.16C shows cells stained with a 1:500 dilution of BSTR followed by 1:40 dilution of the TRITC conjugate, and figure 6.16D displays cells stained by a 1:500 dilution of BSTR followed by 1:20 dilution of the FITC conjugate. These were the best images produced by these reagents.

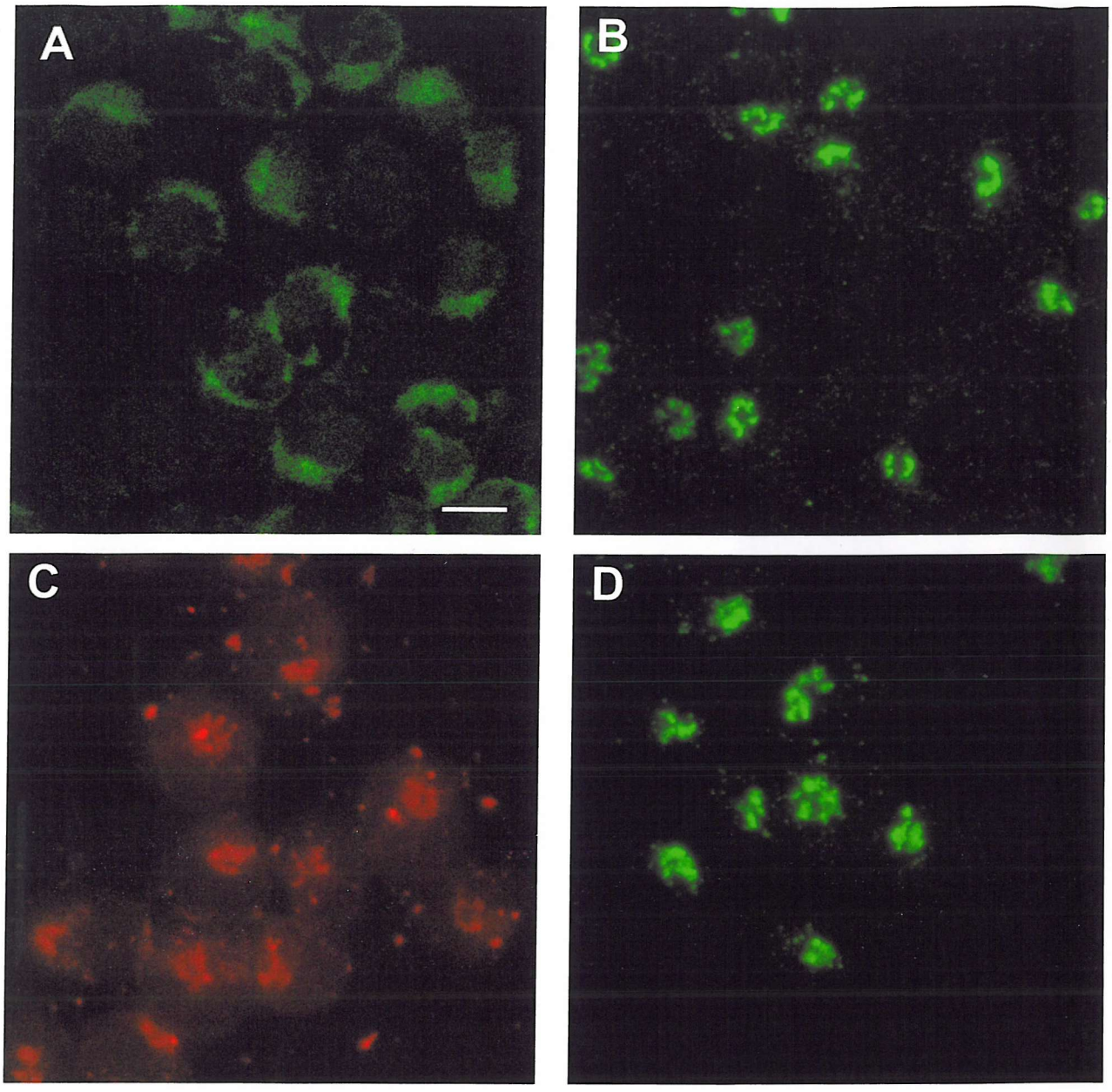

Figure 6.16. Staining the Golgi apparatus. Cells were stained with C6-NBD-ceramide for 30 minutes at 37°C (A), with an anti-TGN46 Ab detected by a FITC conjugated secondary antibody (B) or with BSTR detected by either a TRITC conjugated secondary antibody (C) or a FITC conjugated secondary antibody (D). Images are 3D topographical constructs of 15 sections of 1μm each.
Scale Bar 20μm.

The TGN marker gave more consistently clearer images of greater fluorescent intensity than BSTR with less staining of peripheral structures. For this reason, TGN46 was the marker used for the co-localisation assays.

6.3.10. Co-localisation of CD38 and CD7 with human TGN46

Ten million cells were incubated with a saturating concentration (20μg/ml) of OKT10 Ab-AF568 or HB2 Ab-AF568 and incubated at 37°C to allow these antibodies to internalise. At various time points, 10^6 cells were sampled from the flask, fixed and stained for the Golgi apparatus using an Ab against the TGN marker TGN46. Figure 6.17 shows 3D topographical constructs of four of the time intervals studied of the internalisation and routing of OKT10 Ab-AF568. At time 0, OKT10 Ab-AF568 was found widely distributed across the whole cell membrane. There was no Ab found internalised at this point, hence as expected there was no co-localisation of this Ab with the Golgi apparatus. By 30 minutes into the internalisation of OKT10 Ab-AF568 virtually no stain was visible, which indicated that the dye was being photobleached. This was supported by the presence of peripheral staining along with a small proportion of internalised Ab on cells that were stained with the OKT10 Ab-AF568 alone. The staining of TGN46 at the 1 hour time point was very intense and had crossed over into the red channel. This was why there appeared to be co-localisation of the Ab with the Golgi stacks in figure 6.17C. In an attempt to compensate for the cross-over, the signal that had overlapped into the FITC channel was measured on control cells that were only stained for TGN46 and then this was subtracted from the overall FITC signal on the sample stained for both molecules. By doing this all Ab signal was lost. Control samples containing OKT10 Ab-AF568 alone at time 1 hour did not show any pattern of staining that was similar to the Golgi stain. Figure 6.17E shows the TGN46 stain in the green channel and figure 6.17F displays the stain in the red channel where there should be no stain to demonstrate the amount of crossover observed. By 90 minutes, there was some peripheral staining of OKT10 Ab-AF568 but most of the signal displayed was due to the crossover from the green channel, autofluorescence and the Golgi-like stain.

In contrast, HB2 Ab-AF568 produced a much more intense, better defined pattern of staining. There was still less staining when compared with the pattern of fluorescence produced from earlier time studies conducted, which suggested that photobleaching was

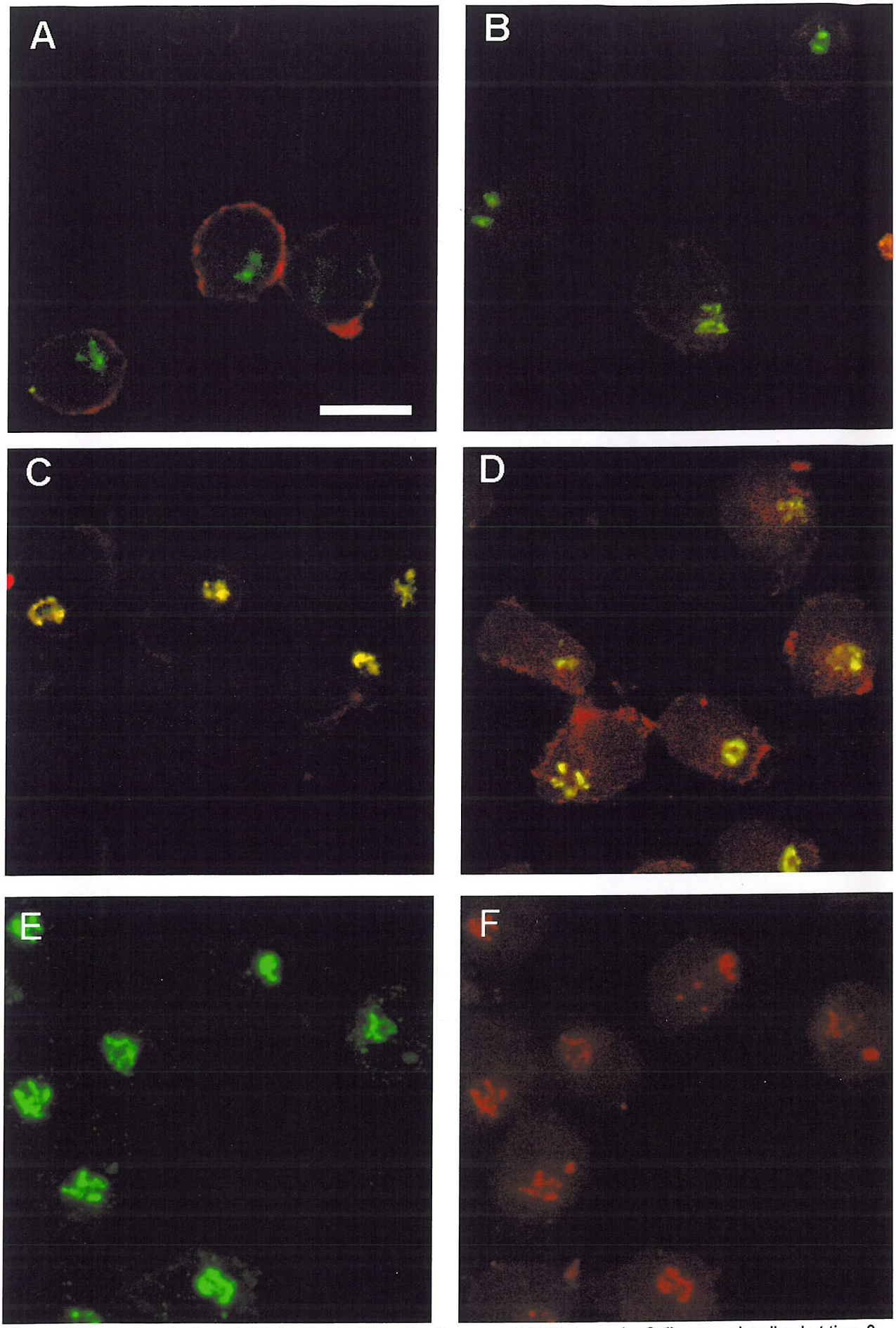

Figure 6.17. Co-localisation of OKT10 Ab-AF568 (red) with human TGN46 (green). Cells were visualised at time 0 (A), 30 minutes (B), 1 hour (C) and 90 minutes (D) after incubation at 37°C. The staining pattern of TGN46 in the green channel (E) and the red channel (F). Images are 3D topographical constructs of 15 sections of 1μm each. Scale Bar 20μm.

occurring with this dye during the staining of the Golgi apparatus. Figure 6.18 shows a single representative section through cells at time 0, 30, 45 60 and 90 minutes after the start of incubation at 37°C. Adjacent to these images are the respective co-localisation analysis images of the 3D topographical constructs of each time point. At time 0, all the Ab was distributed evenly on the cell membrane and there was no evidence of any internalisation (figure 6.18A and B). For this reason, there was no co-localisation with the TGN. By 15 minutes, the Ab had internalised into vesicular-like compartments which were not in the region of the TGN (data not shown). From 30 minutes onwards, most of the internalised Ab appeared close to the TGN marker and it became difficult to determine whether the two were co-localised, but looking at the co-localisation analysis images it would appear that there was not a significant amount of co-localisation between this Ab and TGN46 (figures 6.18C-H) as denoted by the blue/green signal in the co-localisation analysis images.

6.3.11 *Endocytosis of HB2 (anti-CD7) antibody at the ultrastructural level*

At time 0, gold labelled Ab was found evenly distributed across the cell membrane (as displayed in figure 6.19A). There was no evidence of Ab congregating or clustering in any particular region of the cell membrane nor was there any sign of gold label within the cell interior. This was to be expected since the cells had been maintained at 4°C to prevent endocytosis of the Ab. After 1 hour at 37°C, the gold label had started to appear in compartments of multivesicular-like structure varying in size between 0.25 and 0.6μm in diameter (figure 6.19B). Some gold label was still present on the plasma membrane but most of the Ab that was visible was found within the cell at this time. There was evidence of some non-specific binding within the cell interior and on the spaces between cells (as the gold conjugate was able to bind non-specifically anywhere on the grid). This made it difficult to discriminate between the specific and non-specific labelling and so a direct immunogold method was conducted to confirm the presence of Ab in the structures described above.

As with the post-fixation method, gold label was observed widely spread across the whole of the cell membrane with no obvious clumping or patching when fixed at time 0 (data not shown). After 30 minutes, Ab was found entering the cell in what appears to be an

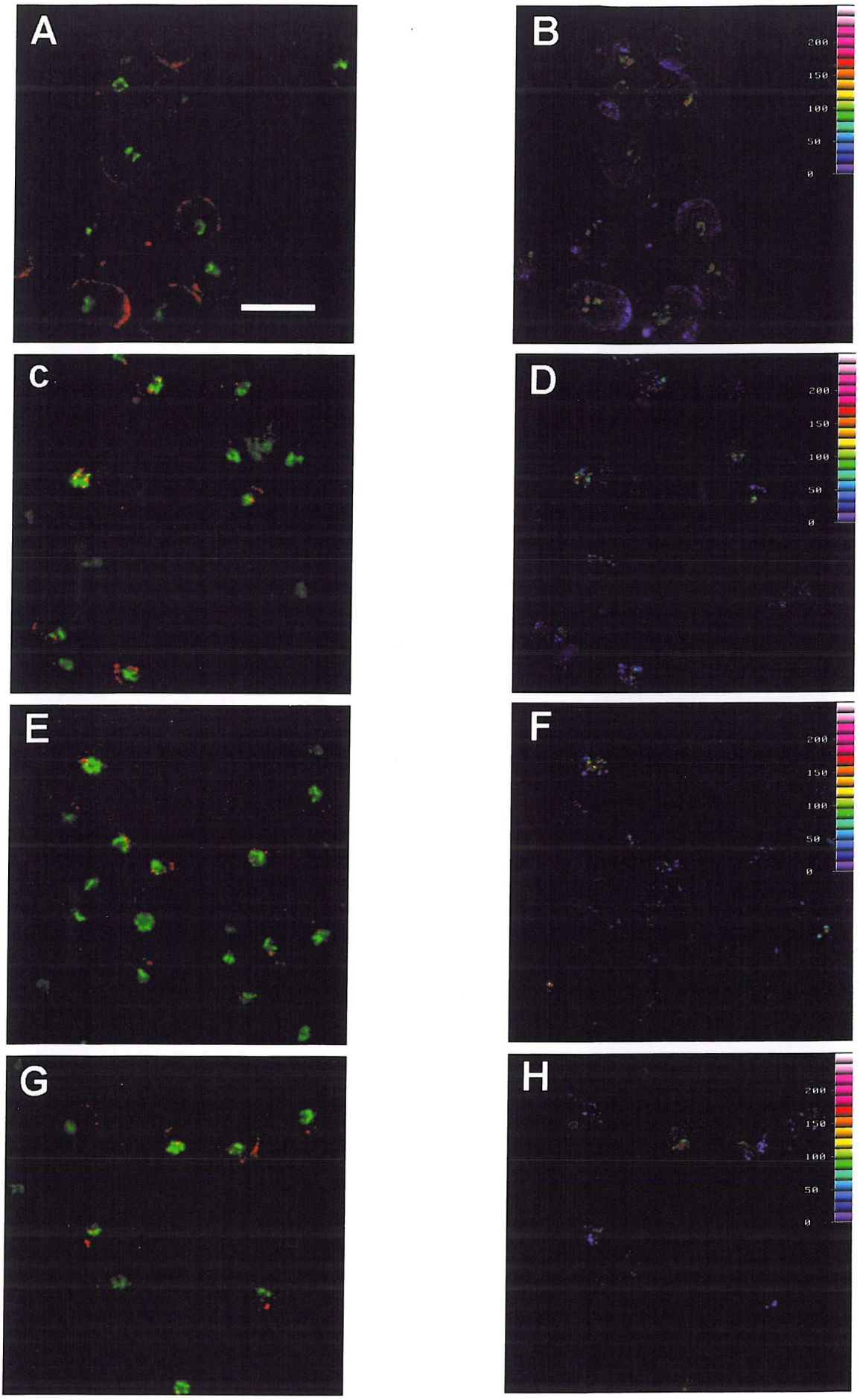

Figure 6.18. Co-localisation of HB2 Ab-AF568 (red) with human TGN46 (green). Cells were visualised at time 0 (A), 30 minutes (C), 1 hour (E) and 90 minutes (G) after incubation at 37°C. Images are a representative section from each time point. Images B, D, F and H show the co-localisation analysis of each time point. Co-localisation analysis was conducted on 3D topographical constructs of 15 sections of 1μm each.
Scale Bar 20μm.

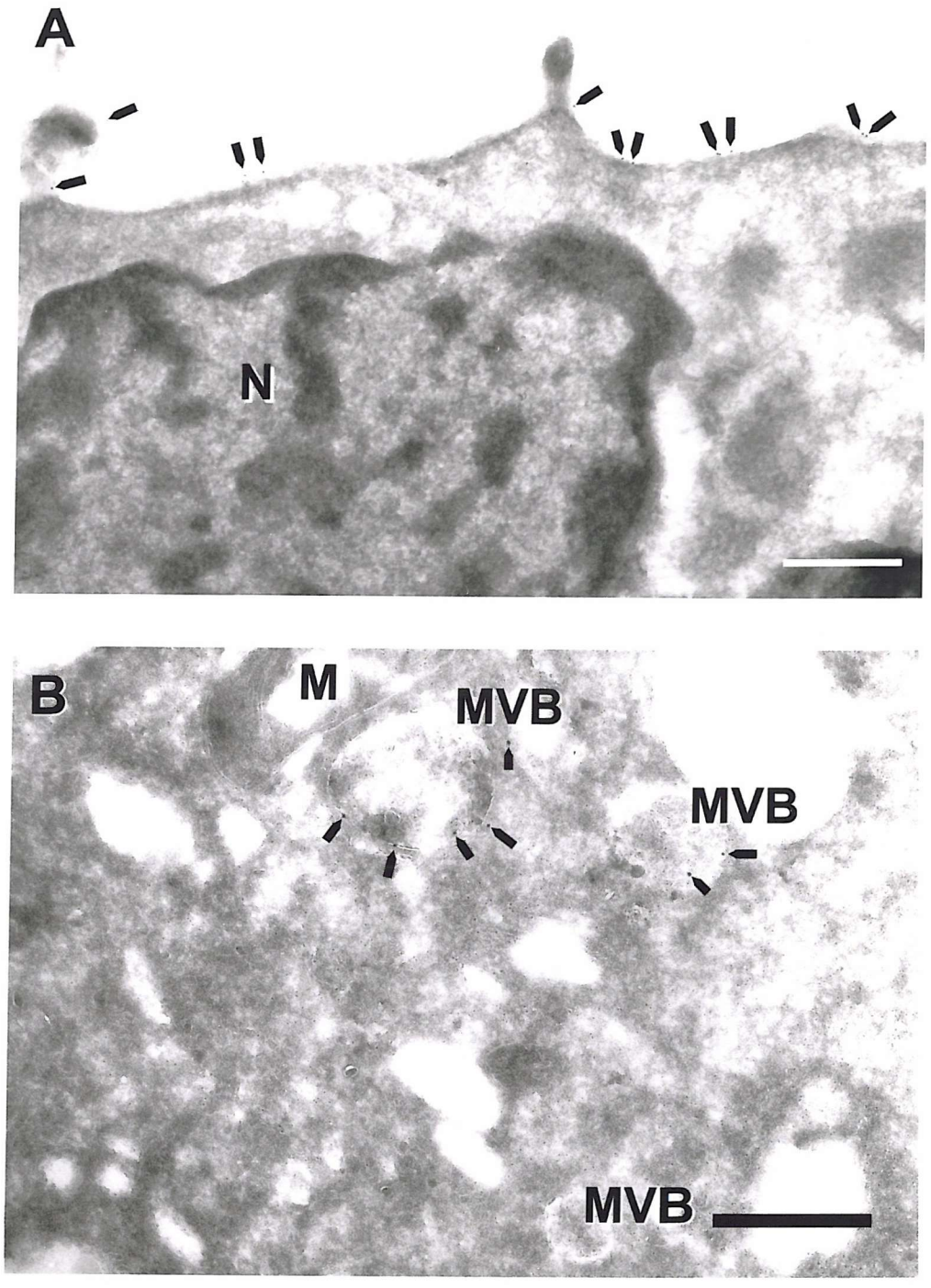

Figure 6.19 Endocytosis of HB2 Ab at the ultrastructural level using the post-fixation method. (A) Membrane labelling at time 0. Scale Bar 1μm. (B) Internalised Ab found within multivesicular bodies (MVB) at 1hr. Scale Bar 0.5μm. N, nucleus; M, mitochondrion

invagination formed by part of the plasma membrane (figure 6.20A). Gold label was also found in the multivesicular bodies described above throughout the cytoplasm (in figure 6.20B). At 30 minutes there was virtually no labelling of the cell membrane, but this does not mean that there was not any Ab on the membrane at this time. HB2 Ab was still found entering the cells at 1 hour and was seen in small vesicles (figure 6.21A) and multivesicular bodies further into the cytoplasm (figure 6.21B). In figure 6.21A it was possible to see a Golgi complex and at this time point it was clear that no gold label was found in this organelle.

6.4 Discussion

The aim of this study was to investigate the intracellular pathway that the anti-CD7 Ab HB2 and the anti-CD38 Ab OKT10 take. A better understanding of these mechanisms might enable optimisation of the actions of ITs conjugated from these antibodies. The questions I set out to address in these studies were as follows: Do the pathways followed by these two antibodies involve entering the Golgi apparatus as with ricin i.e. in a retrograde pathway? In what intracellular compartments do the ITs travel through the cell? And does attacking a leukaemia cell with two ITs simultaneously affect the intracellular routing of the individual ITs in a way that enhances their cytotoxic abilities? Through this work, answers to many of these questions were proposed.

Figure 6.22 shows the various models of endocytosis, processing and translocation that an IT or native toxin can undergo to enable it to inhibit protein synthesis. ITs bind to the cell surface (1) via the targeting moiety and are generally internalised by receptor-mediated endocytosis (2). Ricin and PE are routed to the *trans*-Golgi network (4) via endosomes (3), and DT is routed to an acidified endosome (4). Some ITs may be recycled directly to the plasma membrane at this point (3). From the Golgi apparatus the IT may travel retrogradely through the stacks to the ER. From the ER or the acidified endosome the IT translocates to the cytosol where it inhibits protein synthesis either by damaging 28S rRNA or by inactivating EF-2 (5). Alternatively the ITs may be transported into lysosomes whereby they will be rapidly degraded (5). These are the various intracellular pathways that these ITs may follow.

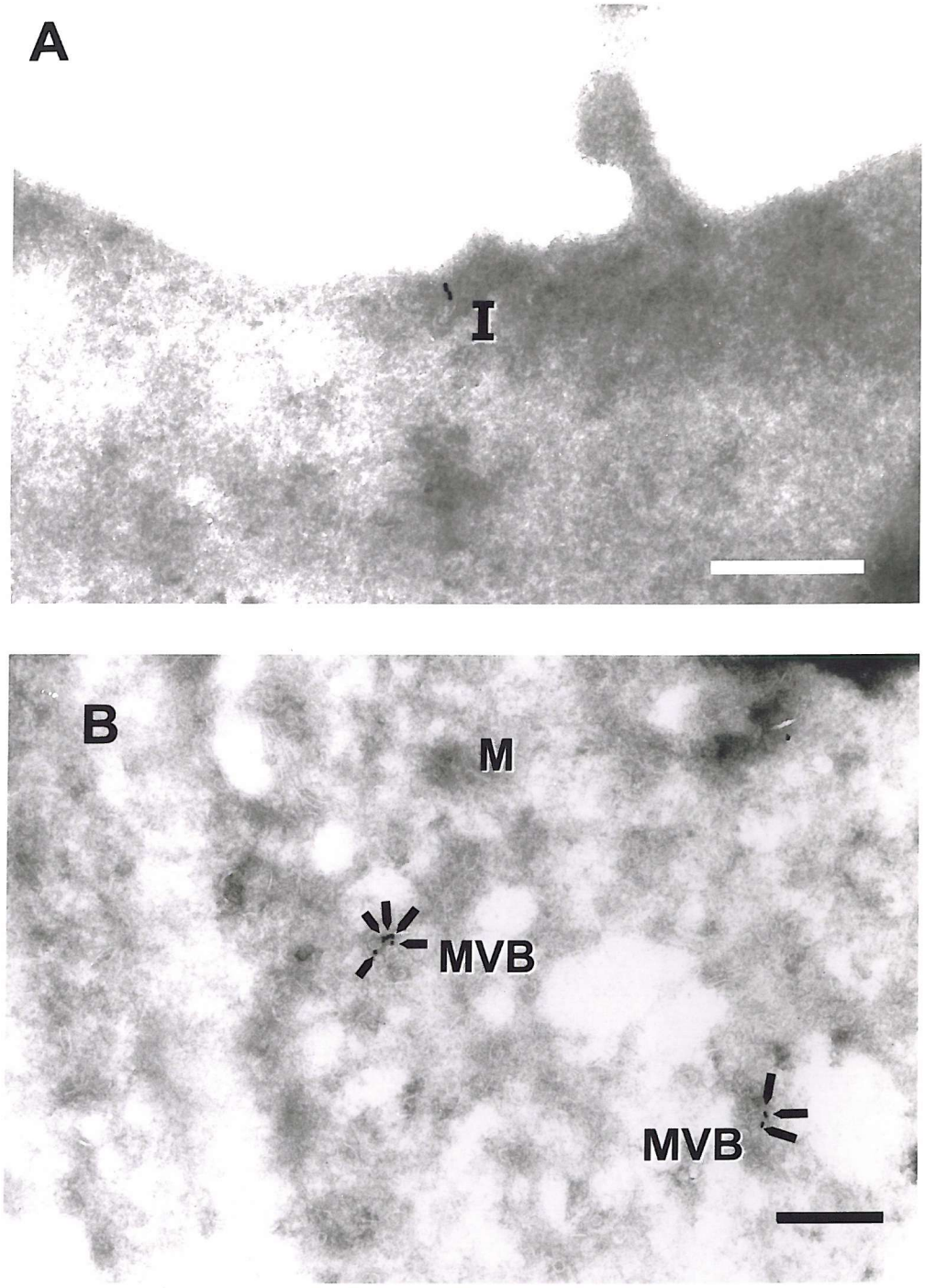

Figure 6.20 Endocytosis of HB2 Ab at the ultrastructural level using the pre-fixation method. (A) Entry of HB2 Ab into the cell via invagination (I) of the plasma membrane after 30 minutes at 37°C. (B) Internalised Ab found within multivesicular bodies (MVB) at 30 minutes. M, mitochondrion
Scale Bar 0.5μm.

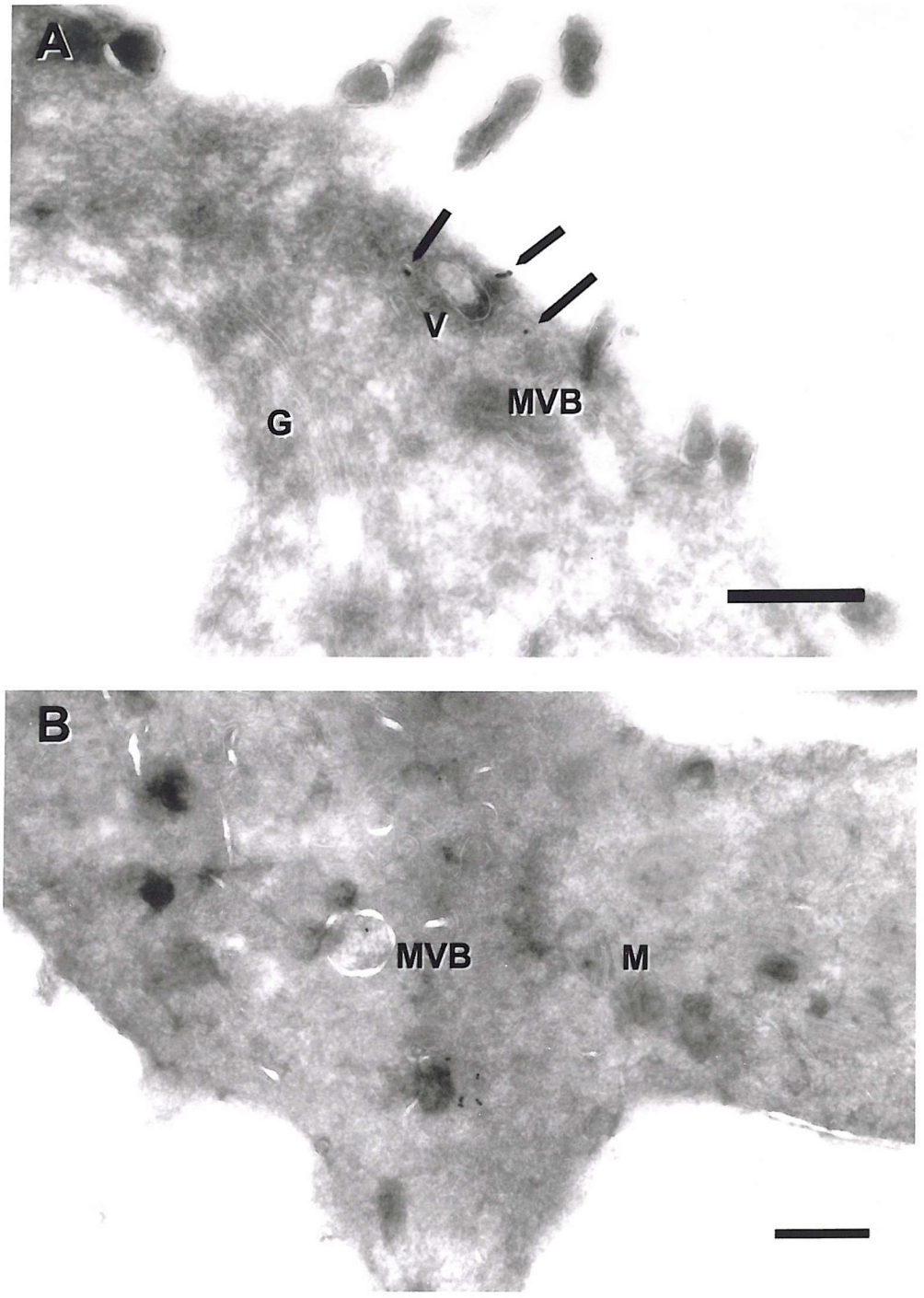

Figure 6.21 Endocytosis of HB2 Ab at the ultrastructural level using the pre-fixation method at 1hr. (A) Ab entering the cells can be seen delivered in concise compartments but not in the Golgi apparatus (G). (B) shows the presence of HB2 Ab in multivesicular bodies (MVBs). M, mitochondria.
Scale Bar 0.5μm.

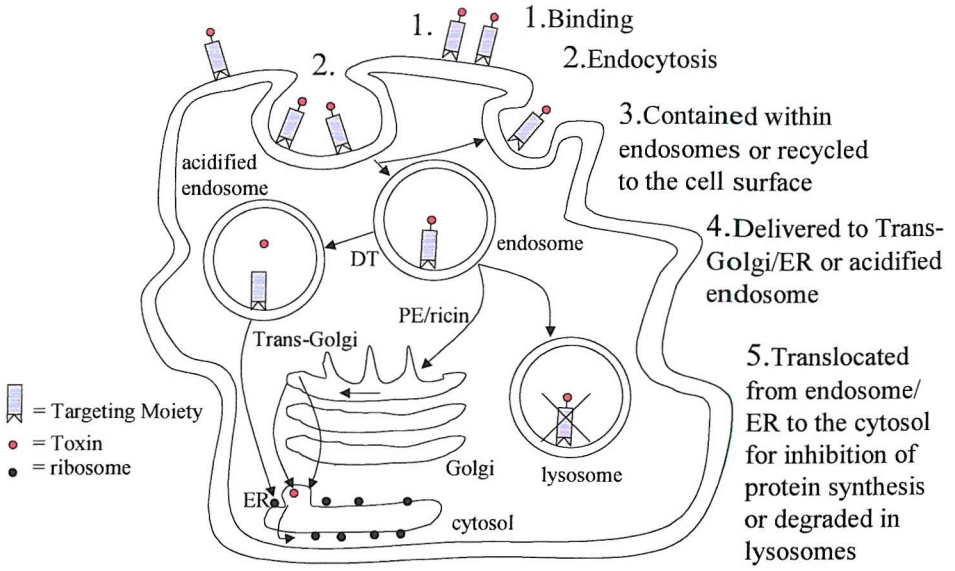

Figure 6.22 Mode of action of ITs, PE, ricin or DT. ITs bind to the cell surface via the targeting moiety and are internalised by receptor-mediated endocytosis. Some ITs are routed to the *trans*-Golgi network via endosomes whereas DT is routed to acidified endosomes. ITs can be degraded in lysosomes or translocated from the endosome or ER to the cytosol for inhibition of protein synthesis.

These studies correlate well with the findings in the flow cytometric investigations (chapter 4) and clearly highlight the differences in both the rates and characteristics of internalisation of the two antigen-Ab complexes. The immunofluorescence studies demonstrate the rapid modulation of CD7 within the first hour of incubation at 37°C observed by flow cytometry and then how the antigen-Ab complex concentrates (probably within vesicles) inside the cell before gradually disappearing probably as a result of degradation of the Ab. Electron microscopic studies on CEM cells (also a T-ALL cell line) by Carriere *et al.*, (1989) have described the same diffuse binding of an Ab against CD7 on the plasma membrane as displayed here whilst the cells were maintained at 4°C. This was followed, in their studies, by internalisation via clathrin-coated structures of the plasma membrane or via non-coated macroinvaginations after 15 minutes at 37°C as determined by immunogold electron microscopy. It was also observed in their studies that between 15 minutes and 4 hours the anti-CD7 Ab was seen in different intracellular compartments such as endocytic vacuoles, tubulovesicular structures and lysosomes. This would correlate with the distribution of the Ab in the cells studied here, since HB2 Ab can be seen throughout the cytoplasm and the extent of labelling within the cell interior during

the later time points drops significantly. This was probably a result of the decrease in pH within intracellular compartments causing a reduction in the intensity of the FITC signal or it may have been because most of the fluorescent label had been degraded by this time in lysosomes. It was most likely that it was targeted to lysosomes since other groups have found that the majority of Ab is rapidly targeted towards this structure (Carriere *et al.*, 1989). Another group has reported the presence of vesicles containing CD7 in the proximity of the Golgi apparatus (Boulad *et al.*, 1993). Since there was a significant amount of Ab internalised to the perinuclear region in HSB-2 cells this is consistent with what was seen in our cells. This was also supported by the co-localisation studies with TGN46. The TGN46 glycoprotein is primarily localised within the *trans* Golgi network and to a certain extent in the trans cisternae of the Golgi stacks. It was not clear whether or not the HB2 Ab was visualised in exactly the same compartment as this stain but it was obvious that the Ab was found in the immediate vicinity of this protein as was found by Boulad *et al.*, (1993). This region of the cell may have contained the tubulovesicular structures described by Carriere *et al.*, (1989).

The finding that HB2 Ab was co-internalised with transferrin showed HB2 Ab in the early endocytic pathway suggesting the presence of HB2 Ab in endosomes. Transferrin has been shown to enter cell lines in coated vesicles and once endocytosed can be found in tubular structures adjacent to the Golgi complex (Geuze *et al.*, 1983; Yamashiro *et al.*, 1984). Since only a proportion of the HB2 Ab was found co-localised with transferrin-TRITC it may suggest that the Ab is internalised in both clathrin-coated and non-coated vesicles (as described by Carriere *et al.*, 1989). It is also in accordance with the implication that HB2 Ab may be found in tubulovesicular structures adjacent to the Golgi complex. The confocal studies did not show any significant co-localisation of either of the two antibodies with a Golgi marker. This would indicate that they do not pass through this route. The alternative explanation could be that most ITs are routed to lysosomes and only a small amount may escape this route to enter the Golgi. If this was the case then it may be below the sensitivity of the assay to detect such small amounts in the Golgi complex. It must also be remembered that TGN46 only stained the TGN and the *trans* cisternae of the Golgi complex, so the Ab may have been in part of the Golgi complex which was not stained with TGN46. If HB2 Ab was to follow the same route as transferrin as suggested here, it would suggest again that it does not pass through the

Golgi apparatus. Ippoliti *et al.*, (1995) have shown that a transferrin-Saporin conjugate does not accumulate in the Golgi apparatus.

My hypothesis about the endocytic pathway of the anti-CD7 Ab based on the studies described here is as follows:

a) The Ab binds to CD7 on the plasma membrane;
b) Following binding, the Ab clumps in regions of the cell membrane possibly where invaginations of the plasma membrane have started to form;
c) Endocytosis is triggered and small endocytic vesicles are formed;
d) The HB2 Ab-CD7 complex is accumulated in punctate structures (possibly endosomes) and then larger structures (presumably multivesicular bodies);
e) Most of the Ab is likely to be degraded in lysosomes (since the fluorescence rapidly disappeared from the cell interior and gold label was seen in MVBs which are commonly considered to be a pre-lysosomal compartment), but it is possible that somewhere along this pathway, the Ab escapes from the vesicles into the cytoplasm as in chapter 3 it was shown that HB2-Saporin IT is cytotoxic and must reach ribosomes in the cytosol.

It is known that when saporin is conjugated to HB2 Ab, at least part of this conjugate must reach the cytosol for the IT to be cytotoxic. Whether this is just the toxin or part of the toxin or if it is the whole conjugate is unknown.

In contrast to CD7, CD38 has a much slower rate of internalisation (demonstrated by both flow cytometry and confocal microscopy) and does not concentrate in the cell interior as HB2 Ab does. Funaro *et al.*, (1998) have described the same homogeneous distribution described here of surface CD38 on Supt-1 cells (another T-ALL cell line) immediately after saturation with the Ab. This was followed by an increasing incidence of capping, which occurred within the first 15 minutes and a significant extent of internalised Ab within the cytoplasm two hours later. This corresponds quite clearly to what has been seen in this study. As confirmed by the flow cytometry study, not all of the surface bound CD38 was internalised, demonstrated by the large proportion of peripheral staining detected throughout the 24 hour duration of the investigation.

Funaro *et al.*, (1998) have shown that treatment of cells with lysosomotropic agents increased the internalised fraction of the CD38/MAb complex. Therefore, it is plausible that membrane CD38 on T cells undergoes internalisation followed, at least partially, by recycling and re-expression on the cell membrane. This would explain why OKT10 Ab is not found concentrated within the cell and may account for the re-expression detected in the flow cytometry work. Since the amount of CD38 expressed on the surface of HSB-2 cells did not increase above 100% of original saturation levels in the flow cytometry experiments, it would suggest that this re-expression of CD38 was mainly due to recycling antigen as opposed to *de novo* synthesis and exocytosis of new antigen.

Electron microscopy studies by Funaro *et al.*, (1998) describe how CD38 displays a uniform surface distribution immediately after binding the MAb IB4. Following ligation and incubation at 37°C, CD38 rapidly clustered in specialised regions of the cell membrane morphologically similar to coated pits. The electron microscopy work of Funaro *et al.*, (1998) describes how CD38 is taken up into endocytic vesicles and follows a very specific pathway before a proportion of it is recirculated to areas of the plasma membrane where CD38 is already present at a high density. Capping in HSB-2 cells ligated with OKT10 Ab was present with a great intensity throughout the whole duration of the time study and if the Ab was recycled to such areas this would explain why the intensity is maintained for so long.

When both antigens were ligated with their respective labelled Ab, co-localisation of the two molecules was mainly restricted to the cell membrane where the antigens patched or capped. As the antigens internalised the amount of co-localisation reduced greatly. This suggested that when both antigens were ligated by Ab simultaneously they did not internalise via the same endocytic vesicles/compartments as each other. Much of the co-localisation detected by the analysis program was so low that it was likely to be detecting co-localisation with the autofluorescence given off by the cells (this was denoted by the dark blue region of the scale).

The co-localisation assay with both antibodies labelled and the study following the pathway of one Ab at a time while both antigens were ligated clearly demonstrated the lack of association between the two antigens regarding internalisation. This work also gave a clear indication that these two antigens internalise independently of each other and

neither Ab appeared to influence the internalisation of the other. This was also demonstrated by the flow cytometric modulation experiments where no substantial difference to the modulation of either antigen could be observed when both were ligated simultaneously. The increased internalisation of one antigen as a result of the second antigen was one of the possible explanations for the increased cytotoxicity observed when both antigens were ligated with ITs, therefore there must be some factor(s) other than rate and extent of internalisation responsible for this effect. There does not appear to be any significant difference in the intracellular pathways followed by the two antibodies when the antigens are co-ligated, indicating that it is not an influence that one Ab has on the intracellular routing of the other Ab that was producing the increased cytotoxicity observed when the two ITs were used in combination.

Carriere *et al.*, (1989) discovered that internalisation of monoclonal antibodies via coated structures seems to be a favourable entry route for IT activity. In that particular study, an IT against CD7 which is intensely internalised via such coated structures, is 100 times more effective in a protein synthesis inhibition assay than the IT against CD5 which was found in coated structures to a lesser extent. This may explain why HB2-Saporin IT performs marginally better than OKT10-Saporin IT in the protein synthesis inhibition assay.

This work was conducted using antibodies directly conjugated to either FITC or the Alexa Fluor™ 568 (referred to as AF568). It could be argued that directly conjugating fluorophores to antibodies could interfere with the internalisation and routing of these molecules. However, the binding pattern of fluorescence and that found within the cell after internalisation appeared to be the same irrespective of the fluorophore attached to the Ab. The competitive binding studies have demonstrated that these conjugated antibodies still bound effectively to the cells and that binding was only blocked by an excess of unlabelled Ab for the antigen targeted. This indicated that these antibodies bound specifically to the relevant antigen. A clean signal was produced by these conjugates indicating that non-specific binding of the antibodies was minimal. There was some staining still present on cells incubated with HB2 Ab-FITC in the presence of excess unlabelled HB2 Ab, but this could have been a result of internalised Ab (before binding had been blocked), or it may have indicated that a greater concentration of unlabelled Ab

was required to block all of the binding of HB2 Ab-FITC. The alternative approach to using directly labelled antibodies would be to fix the cells, permeabilise them and use a secondary fluorescent reagent to detect the whereabouts of the Ab of interest. This in itself has many problems such as the need to permeabilise effectively, the possibility of non-specific binding of the secondary reagent and the possible loss of antigenicity during the fixation process. Some of these problems were avoided by the directly conjugated approach taken.

Two approaches were undertaken for the ultrastructural studies to determine which intracellular compartments HB2 Ab passed through. These were preliminary studies and were limited to just three early time points. The first approach involved internalising HB2 Ab followed by fixation then staining whole cryo-sections with a secondary gold Ab. Since the gold conjugate had uniform access it was able to label any part of the section. This resulted in some non-specific labelling of the grids particularly in regions between cells, the nucleus and mitochondria, which prompted the use of the second approach. This involved binding HB2 Ab to the cells and then binding the secondary gold conjugated Ab to that. This complex was then internalised. Since these were preliminary studies the correct concentration of secondary conjugate had not been fully determined. Further studies of this type would benefit from the titration of this secondary reagent. These studies showed that using this technique for determining the intracellular routing of these antibodies was promising and that if these studies had been carried out further many more components of these pathways may be elucidated.

I am aware that I have only tested the intracellular routes of unconjugated antibodies. This was due to the technical problems encountered when trying to visualise both components of the IT simultaneously. This is important to know as it is uncertain as to whether both components reach the cytosol or if it is just the toxic component that crosses into the cytosol. If the latter was the case it would be important to follow both components at once. In support of our findings providing a good indication of the majority of the IT pathway is the work of Ippoliti *et al.,* (1995) who have shown that it is the carrier that affects the routing the most at least in the early stages before the translocation event.

In all the studies conducted in this and previous chapters, it has become increasingly clear that there is no direct correlation between internalisation, intracellular routing and

cytotoxic potency. Each IT can display different cytotoxic potencies depending on the type of assay used, for example, OKT10-Saporin IT did not perform the best in the protein synthesis inhibition assay, although it clearly performed better in the longer outgrowth assay and the *in vivo* study. A rapidly internalising IT such as HB2-Saporin IT appears to inhibit protein synthesis sooner than a slower internalising IT, such as OKT10-Saporin IT, but its actions appear to be a lot shorter lived. This is presumably because HB2-Saporin IT is routed more readily to lysosomes, which may be a result of its fast rate of internalisation. In contrast, OKT10-Saporin is a lot less readily internalised but its effects are prolonged. Using a combination of ITs against CD7 and CD38 simultaneously may act well together as one IT would inhibit protein synthesis cells fairly rapidly and any that were missed by that IT may be attacked by the second IT that has a slower but prolonged mechanism of inhibition. The main indication from these studies is that the cytotoxic potency of an IT cannot be determined by one factor alone. The rate of internalisation will affect how quickly the IT will perform but it is the intracellular routing of the IT that determines the amount of the internalised IT that reaches the ribosome and how prolonged the cytotoxic activity is.

Chapter 7

General Discussion

The use of a combination of two or more ITs has repeatedly been shown to produce a greater and more selective cytotoxicity against a variety of human cancers than single Ab or IT therapy (Flavell *et al.*, 1992; Engert *et al.*, 1995; Flavell *et al.*, 2001; Ghetie *et al.*, 1992). In this study it was demonstrated that a combination of HB2-Saporin (anti-CD7) IT and OKT10-Saporin (anti-CD38) IT was much more effective against the leukaemia cell line HSB-2 (developed from the cells from the peripheral blood of a child with T-ALL) than either of the ITs used individually (chapter 3). This was clearly demonstrated in both *in vitro* and *in vivo* assays. The *in vitro* long term outgrowth assay in which cells were continuously exposed to one or other of the two individual ITs and a combination of the two ITs showed no growth of the cells exposed to both ITs over the 50-day period. Although each IT used individually did delay growth of leukaemia cells in culture, the cells did eventually outgrow, even in cultures that were exposed to a combination of IT and antibody. This indicates that the increase in therapeutic ability of the IT combination was not simply due to the effect of the additional antibody molecule. The evidence was not quite so pronounced in the *in vivo* model, but it still demonstrated an increase in the percentage of mice surviving 128 days compared to either IT used alone or in combination. In a different *in vitro* assay, cells were continuously exposed to both ITs individually or in combination for a period of 48 hours following which protein synthesis was measured. This data did not demonstrate any increased protein synthesis inhibitory ability of the combination therapy. These results indicate that cells need to be exposed to combination therapy for more than 48 hours for the enhanced cytotoxicity to be observed. In concurrence with this study is the work of Flavell *et al.*, (2001) in which the actions of the same two ITs used in combination have been shown to be far more potent than the use of either IT individually against the T-ALL cell line CEM. These two studies together indicate the value this combination of two ITs might have when used for the treatment of T-ALL.

Although several studies have shown that a combination of ITs is more therapeutically effective at killing tumour cells than single target IT therapy, there has been little

investigation into the mechanisms by which this phenomenon occurs. A number of mechanisms for this increase in cytotoxicity have been speculated and are as follows:

1) The binding of one antibody may cause an increase in the binding ability of the second antibody moiety to the cell surface and hence increase the amount of IT bound to the cell.
2) Co-ligation of target antigens may affect the rate or extent of internalisation of one or both of the ITs in such a way that increases selective cytotoxicity.
3) Co-ligation of target antigens may affect the intracellular fate or routing of either or both ITs in a way that increases the likelihood of saporin translocation to the cytosol and subsequent increase in ribosome inactivation.
4) The use of combination IT therapy may overcome the problem that antigen heterogeneity imposes on single antigen therapy.

To test some of these hypotheses a series of experiments were conducted. The endocytosis and intracellular trafficking of CD7 and CD38 following ligation with the monoclonal antibodies HB2 and OKT10 (respectively) were investigated using a variety of techniques in order to determine both the rate and routing of ITs when used individually or in combination.

The sensitivity of cells to IT killing is dependent, at least in part, on the number of bound toxin molecules and this directly correlates with the density of target antigen expression on the cell surface (Rihova *et al.*, 1998). The affinity of the antibody and consequently the affinity of the IT must be sufficient to mediate specific binding to tumour cells at concentrations that can be reached in human serum without producing toxic side effects in the patient. A high density of cell surface receptors permits a high concentration of effector molecules to be directed to the target cells and consequently deliver a greater pharmacological effect (Press *et al.*, 1989). However, the effect of antigen density is substantially influenced by the rate of antigen internalisation and by delivery of IT to a compartment(s) from which it is able to translocate from to the cytosol and exert its toxic effects through ribosome inactivation (Matthay *et al.*, 1989). When using ITs constructed with ricin against the CD30 molecule, the affinity and hence avidity of antibodies rather than the epitope they recognise is the primary determinant of their potency as ricin A-containing ITs (Engert *et al.*, 1990). However, it is the particular cell surface antigen that provides the target for antibody-directed cytotoxic therapy that is of prime importance in

determining the subsequent fate of the toxin conjugate after it has bound to the cell surface (Manetti *et al.*, 1995).

For these reasons, the number of binding sites for these two antibodies expressed on the surface of HSB-2 cells and their respective affinities for these antigens were investigated. The anti-CD38 antibody OKT10 had only half as many binding sites on HSB-2 cells (and a lower binding affinity for the CD38 antigen) as the anti-CD7 antibody HB2. The OKT10-Saporin IT was more cytotoxic in both of the long term assays described in chapter 3, therefore in this instance there was not a good correlation between antigen density and cytotoxicity. The internalisation data described in chapter 4 also indicated that a smaller amount of this IT was actually taken up into the cell. This finding therefore indicates that toxin delivery via the CD38 molecule is more efficient, probably as a consequence of intracellular routing to a more appropriate compartment.

The effect of co-ligation of both antigens with antibody was also studied to determine what effect this might have on the binding capabilities of either antibody. Both antibodies displayed a slight reduction in the number of sites they bound to on the HSB-2 cells. This apparent reduced binding following co-ligation was most likely a consequence of steric hindrance.

It is accepted that internalisation via receptor-mediated endocytosis of cell surface antigen-IT complexes is an essential property for their effectiveness as cytotoxic agents (Lambert *et al.*, 1985, Youle and Neville 1987, Raso and Basala 1984, Wargalla and Reisfeld 1989, Goldmacher *et al.*, 1989). Some studies have correlated the rate of internalisation of an IT with its cytotoxic potency (Wargalla and Reisfeld 1989, Goldmacher *et al.*, 1989). Since this appears to be an important factor in the cytotoxicity of ITs, the endocytosis of both CD7 and CD38 following ligation by monoclonal antibody was monitored using both flow cytometry (described in chapter 4) and confocal laser scanning microscopy (described in chapter 6). Both techniques highlighted the marked differences in internalisation rate and in the overall extent of endocytosis between these two potent ITs. Surprisingly, the IT that internalised more rapidly and to a greater extent over a 24 hour period was HB2-Saporin which did not prove to be the IT that performed best in the two long-term assays described in chapter 3. However, it did display a greater cytotoxic ability than OKT10-Saporin IT in the short-term PSI assay which indicates that

it acts more rapidly than OKT10-Saporin IT but that its actions are shorter lived. This contradicts other studies that suggested that the efficacy of an IT correlates with the rate of internalisation (Wargella and Reisfield 1989; Preijers *et al.*, 1988) since in the present study the reverse appeared to be true. This does not necessarily dispute that internalisation is an important factor to IT cytotoxicity since an IT that fails to internalise is incapable of killing tumour cells (Lambert *et al.*, 1985), but would simply imply that intracellular routing has a greater influence on an IT's cytotoxic ability, as has been found by many others (van Horssen *et al.*, 1995; May *et al.*, 1991).

Between 40%-50% of HSB-2 cell surface CD38 molecules did not appear to modulate or shed from the cell surface over a 24 hour period and the possible reasons for this were discussed in chapter 4, but the fact that so many molecules remained ligated by antibody or IT on the surface of the tumour cells may have enabled better recruitment of NK or NK-like cells to induce ADCC than the CD7 antibody or IT. Flavell *et al.*, (1998) have demonstrated that HB2 antibody (anti-CD7) is capable of inducing ADCC via recruitment of NK cells that bind through FcγIII to the Fc domain of the IT. However, since CD7 is rapidly modulated from the cell surface of HSB-2 cells, with approximately 50% modulated within the first 3 hours and 90% internalised by 24 hours, HB2 antibody or IT is likely to be less efficient than OKT10 IT at eliciting ADCC.

Some studies have implied that a high rate of endocytosis leads to rapid delivery of the IT to lysosomes (Tonevitsky *et al.*, 1993). CD19 and CD22 are both examples of antigens that are rapidly taken up by the cell and degraded following ligation by antibody (Press *et al.*, 1989). The high rate of endocytosis and the work by Carriere and colleagues that describe the rapid routing of CD7 to lysosomes may suggest that HB2-Saporin IT was more rapidly degraded than OKT10-Saporin IT. This would leave less of the IT available for routing to the cytosol. The slow and maybe inefficient internalisation of CD38 may have resulted in a less rapidly degraded IT providing a greater opportunity for the IT to translocate to the cytosol.

Press and colleagues have also shown using cellular radioimmunoassay and immuno-electron microscopy that the two ricin immunotoxins against CD2, 35.1-A and RFT11-A, were both rapidly endocytosed by T-cells, but their intracellular fates were very different.

The more toxic RFT11-A IT was retained for longer periods of time inside endocytic vesicles (receptosomes, endosomes) and was more slowly degraded than the less effective IT 35.1-A which was rapidly transported to lysosomes, digested and expelled (Press *et al.*, 1988). Again this work demonstrates the importance of intracellular routing on IT cytotoxicity.

The ^{125}I-endocytosis assay described in chapter 4 was to be used to determine the degradation rates of both antibodies or ITs but for the reasons described previously this was not possible. The data gained from those studies would have helped confirm or dispute the above hypothesis. The EM studies it was hoped would illustrate the predominant pathway of these ITs but the work described in chapter 6 was preliminary and was incapable of visualising large numbers of antibody molecules in lysosomes, although HB2 antibody was observed predominantly in multivesicular-like structures suggesting that routing to lysosomes may have occurred at later time points. In order to confirm this, further work is necessary and lies outside the timescale of this thesis.

Antigens expressed on the cell surface of malignant cells are at times shed into the circulation (Bachier and LeMaistre 1995). Soluble antigen shed from tumour cells can act as antigenic sinks which act to decrease the delivery of the IT to the tumour. This aspect of CD7 and CD38 was not investigated in this study due to the problems experienced developing the ^{125}I-endocytosis assay discussed in chapter 4. Shedding of antigen from tumour cells was to be determined by measuring the TCA precipitable proportion of ^{125}I-label found in the culture supernatant. Since it was not feasible to conduct this assay, it was not possible to categorically state that all of the modulation of CD7 or CD38 antigen from the cell surface in the flow cytometric endocytosis assay (in chapter 4) was due to endocytosis of these molecules.

It is however likely that modulation of CD7 from the cell surface was due to internalisation since there is no evidence in the literature suggesting that shedding of this molecule occurs. Investigations by Carriere and colleagues (1989) went as far as to mention that no shedding was detected of CD7 in their assays from the T-ALL cell line CEM. In accordance with this the confocal scanning laser microscopy studies did not show a reduction in the overall immunofluorescence within the first hour or so of the investigation, although some of the fluorescence had transferred from the cell perimeter to

the cell interior. At later time points such as 6 hours onwards there was an observed decrease in the overall immunofluorescence, but this was believed to be a result of the localisation of the antibody in highly acidic intracellular compartments, possibly lysosomes causing the dramatic fall in fluorescence either by the acidity affecting the intensity of the fluorophore, quenching of the fluorophore through close interactions between the dye molecules or through degradation.

A soluble form of the transmembrane CD38 molecule has been described which is a 39kD protein consisting of the extracellular portion of the transmembrane protein (Funaro *et al.*, 1996). This soluble molecule is thought to be shed from the transmembrane molecule. From the data in this study it was not possible to determine the extent to which shedding of this molecule may have occurred. Since OKT10-Saporin IT was a very potent cytotoxic agent even though only 50-60% of the bound antibody was internalised, this suggests that the majority of the antibody that was modulated from the surface was due to internalisation rather than shedding.

Tumour cells can modulate the expression of surface antigens. Initial exposure to antibody can downregulate antigen expression, making cells resistant to further therapy. For this reason, the effect of antibody exposure was investigated. CD38 was only downmodulated transiently while antibody was internalised with rapid recycling or re-expression of the molecule within a few hours. This does not disagree with the work of Funaro *et al.,* (1998) when they suggested that CD38 may undergo recycling or re-expression after increasing the internalised fraction following treatment of the cells with lysosomotropic agents. Lysosomotropic agents, such as ammonium chloride and chloroquine, which are both weak amines, are known to increase pH in acidic intracellular compartments including endosomes, thus perturbing vesicular traffic and inhibiting both recycling and lysosomal degradation of internalised molecules (Ippoliti *et al.,* 1998). A similar effect was observed with pulsed exposure of CD7 to antibody whereby The CD7 molecule was downregulated for the first 6 hours before the antigen was re-expressed on the surface of the HSB-2 cells. In contrast to this, continuous exposure of CD7 to antibody for 24 hours caused a moderate downregulation of antigen. Even so, 30-40% of the original expression levels of CD7 still remained on the cell surface. The advantage of combination therapy may be that if downregulation of this antigen did occur after the

initial treatment, the second IT would help compensate and attack cells that are low or negative for the first target antigen.

Ultimately, none of the assays conducted in this study indicated the existence of any physical associations between CD7 and CD38 leading to an increase in the internalisation rate or intracellular routing or either antibody or IT. This was investigated in a number of ways. Firstly, the modulation of each antigen was followed using a flow cytometric method where each antigen ligated individually or simultaneously. This did not highlight any marked differences in internalisation kinetics or characteristics from those shown by either antigen when ligated individually. Since it has been shown that some antigens modulate when exposed to antibodies directed against unrelated antigens (Poste and Kirsch 1983) an alternative method was used to monitor any alterations that may occur to the expression levels of the first antigen when only the second antigen was ligated by antibody. There was no marked difference of the expression levels of the unligated antigen when the second antigen was ligated by antibody over 24 hours. Co-ligation of these two antigens with their respective antibodies did not appear to alter the intracellular pathways followed by either molecule when visualised by confocal microscopy. The two antibodies HB2 and OKT10 did not co-localise to the same intracellular vesicles. If there was any co-localisation this was beyond the sensitivity of the assay. All the data presented here would suggest that CD7 and CD38 internalise and traffic independently of each other.

In an attempt to gain a better understanding of the intracellular mechanisms of HB2-Saporin, EM studies were conducted to follow the routing of this IT within the cell. The EM studies (described in chapter 6) were limited in determining only very limited portions of the intracellular trafficking pathways. Since this work elucidated some of the main components involved in the early stages of the IT's pathway, it has been demonstrated that this could be a valid method for tracing these elements. This technique may require optimisation first to increase the sensitivity of the investigation. A similar technique using resin blocks may provide a greater resolution of intracellular organelles which is often reduced when using cryosections. Gold particles of varying sizes conjugated to the two ITs would enable the tracking of both molecules independently.

The tracing of the intracellular pathways taken by both the toxin (saporin) and antibody moiety of the IT within the cell was not directly addressed by this work. It is possible that the saporin and the antibody components become separated from one another at a key stage in the intracellular pathway. It is also likely that the antibody moiety is the determining factor for the early stages of routing (Ippoliti *et al.*, 1995) but then the saporin molecule becomes predominantly important in the latter stages during which translocation to the cytosol takes place. It may be that saporin alone translocates to the cytosol in which case this event would be missed by the protocols followed here. It can be concluded therefore that it is important to trace both components of the IT in order to reach firm conclusions. This could be done in several ways. Firstly, an IT could be followed by two colour analysis using confocal microscopy. The toxin and antibody components of the IT could be labelled with two different fluorochromes that emit at different wavelengths, enabling both components to be followed. Alternatively, electron microscopy using two different size gold conjugates may provide a better indication of the intracellular location.

In summary, the mechanisms by which enhanced therapeutic benefit of using two ITs over one are discussed here, based on the data presented above. Firstly, it does not appear to be due to an increase in the ability of binding, an alteration of the internalisation kinetics/characteristics of either IT or by influencing the intracellular routing. The most likely reason for the increased therapeutic ability of combination IT treatment is probably due to the overcoming of antigen heterogeneity exhibited by the global leukaemia cell population. By doing so, fewer of the leukaemia cell population are likely to evade targeting by the ITs. Combination therapy may also overcome problems that may occur if one of the antigens becomes downregulated within the population. The two ITs OKT10-Saporin and HB2-Saporin work together well since one is fast acting and may destroy many tumour cells in a relatively short period of time possibly through the mechanism of PSI, whereas the second IT seems longer lived and may continue to clear the remaining tumour cells after the HB2-Saporin has been degraded. OKT10-Saporin may still act by inhibiting protein synthesis, but the data here suggests a considerable amount remains on the surface of the tumour cells and so implies that an extensive proportion of its cytotoxicity may be apportioned to its ability to induce ADCC and other antibody mediated immune responses. Since the predominant mechanism of benefit to using two ITs appears to be the overcoming of antigen heterogeneity it would imply that there is a lot of value in investigating other combinations which do have associations such as CD7 and

CD3 or combinations of 3 or more ITs as has been done by Flavell *et al.,* (1997) with 3BIT.

References

Adams, R. A., L. Pothier, A. Flowers, H. Lazarus, S. Farber, G. E. Foley. 1970. The question of stemlines in human acute leukemia. Comparison of cells isolated *in vitro* and *in vivo* from a patient with acute lymphoblastic leukemia. *Experimental Cell Research.* 62: 5-10

Akbar, A. N., P. L. Amlot, C. Hawkins, W. Newsholme, S. Delaney, N. Borthwick, G. Janossy. 1991. The effect of a chimeric mouse-human CD7 antibody on human T, natural killer, and lymphokine-activated killer cell activity in vitro. *Transplantation.* 52: 325-330

Alami, M., M. P. Taupiac, B. Beaumelle. 1997. Ricin-binding proteins along the endocytic pathway: the major endosomal ricin-binding protein is endosome-specific. *Cell Biology International.* 21: 145-150.

Alessio, M., S. Roggero, A. Funaro, L. B. De Monte, L. Peruzzi, M. Geuna, F. Malavasi. 1990. CD38 molecule: structural and biochemical analysis on human T lymphocytes, thymocytes, and plasma cells. *The Journal of Immunology.* 145: 878-84

Allured, V. S., R. J. Collier, S. F. Carroll, D. B. McKay. 1986. Structure of exotoxin A of *Pseudomonas aeruginosa* at 3.0 Angstrom resolution. *Proceedings of the National Academy of Sciences USA.* 83: 1320-1324

Amlot, P. L., M. J. Stone, D. Cunningham, J. Fay, J. Newman, R. Collins, R. May, M. McCarthy, J. Richardson, V. Ghetie, et al. 1993. A phase I study of an anti-CD22-deglycosylated ricin A chain immunotoxin in the treatment of B-cell lymphomas resistant to conventional therapy. *Blood.* 82: 2624-2633.

Anderson, R. G., J. L. Goldstein, M. S. Brown. 1976. Localization of low density lipoprotein receptors on plasma membrane of normal human fibroblasts and their absence in cells from a familial hypercholesterolemia homozygote. *Proceedings of the National Academy of Sciences USA.* 73: 2434-8.

Anderson, R. G., M. S. Brown, J. L. Goldstein. 1977. Role of the coated endocytic vesicle in the uptake of receptor-bound low density lipoprotein in human fibroblasts. *Cell.* 10: 351-64.

Aridor, M., J. Weissman, S. Bannykh, C. Nuoffer, W. E. Balch. 1998. Cargo selection by the COPII budding machinery during export from the ER. *The Journal of Cell Biology.* 141: 61-70.

Aruffo, A., B. Seed. 1987. Molecular-Cloning Of 2 CD7 (T-Cell Leukemia Antigen) cDNAs By A Cos Cell Expression System. *EMBO Journal.* 6: 3313-3316

Assaraf, Y. G., R. T. Schimke. 1987. Identification of methotrexate transport deficiency in mammalian cells using fluoresceinated methotrexate and flow cytometry. *Proceedings of the National Academy of Sciences USA.* 84: 7154-7158.

Ausiello, C. M., A. la Sala, C. Ramoni, F. Urbani, A. Funaro, F. Malavasi. 1996. Secretion of IFN-gamma, IL-6, granulocyte-macrophage colony-stimulating factor and IL-10 cytokines after activation of human purified T lymphocytes upon CD38 ligation. *Cellular Immunology.* 173: 192-197

Bachier, C. R., C. F. LeMaistre. 1995. Immunotoxin therapy of cancer: rationale for development and future potential. *Clinical Immunotherapeutics.* 3: 450

Bainton, D. F. 1981. The discovery of lysosomes. *The Journal of Cell Biology.* 91: 66s-76s.

Baliga, B. S., H. N. Munro. 1972. Evidence Of Formation Of A Complex Between GTP And Elongation Factor Two And The Binding Of The Complex To A Specific Site On Mammalian Ribosomes. *Biochimica et Biophysica Acta* 277: 368-383

Baluna, R., V. Ghetie, N. Oppenheimer-Marks, E. S. Vitetta. 1996. Fibronectin inhibits the cytotoxic effect of ricin A chain on endothelial cells. *International Journal of Immunopharmacology.* 18: 355-361

Baluna, R., J. Rizo, B. E. Gordon, V. Ghetie, E. S. Vitetta. 1999. Evidence for a structural motif in toxins and interleukin-2 that may be responsible for binding to endothelial cells and initiating vascular leak syndrome. *Proceedings of the National Academy of Sciences USA*. 96: 3957-3962.

Barbieri, L., G. M. Aron, J. D. Irvin, F. Stirpe. 1982. Purification and partial characterization of another form of antiviral protein from the seeds of *Phytolacca americana* L. (Pokeweed). *Biochemical Journal*. 203: 55-59

Barclay, A. N., M. L. Birkeland, M. H. Brown, A. D. Beyers, S. J. Davies, C. Somoza, A. F. Williams, eds. 1993. *The Leucocyte Antigen Facts Book*. 1 ed. Academic Press Factsbook Series. London: Academic Press

Barlowe, C. 1998. COPII and selective export from the endoplasmic reticulum. *Biochimica et Biophysica Acta*. 1404: 67-76.

Baum, W., H. Steininger, H.-J. Bair, W. Becker, T. E. Hansen-Hagge, M. Kressel, E. Kremmer, J. R. Kalden, M. Gramatzki. 1996. Therapy with CD7 monoclonal antibody TH-69 is highly effective for xenografted human T-cell ALL. *British Journal of Haematology*. 95: 327-338

Benson, S., S. Olsnes, A. Pihl, J. Skorve, A. K. Abraham. 1975. On the mechanism of protein-synthesis inhibition by abrin and ricin. Inhibition of the GTP-hydrolysis site on the 60-S ribosomal subunit. *European Journal of Biochemistry*. 59: 573-580

Besterman, J. M., R. B. Low. 1983. Endocytosis: a review of mechanisms and plasma membrane dynamics. *Biochemical Journal*. 210: 1-13.

Bjorn, M. J., D. Ring, A. Frankel. 1985. Evaluation of monoclonal antibodies for the development of breast cancer immunotoxins. *Cancer Research*. 45: 1214-1221

Blakey, D. C., G. J. Watson, P. P. Knowles, P. E. Thorpe. 1987. Effect of chemical deglycosylation of ricin A chain on the in vivo fate and cytotoxic activity of an immunotoxin composed of ricin A chain and anti-Thy 1.1 antibody. *Cancer Research.* 47: 947-952.

Blakey, D. C., D. N. Skilleter, R. J. Price, G. J. Watson, L. I. Hart, D. R. Newell, P. E. Thorpe. 1988. Comparison of the pharmacokinetics and hepatotoxic effects of saporin and ricin A-chain immunotoxins on murine liver parenchymal cells. *Cancer Research.* 48: 7072-7078

Blewitt, M. G., L. A. Chung, E. London. 1985. Effect of pH on the conformation of diphtheria toxin and its implications for membrane penetration. *Biochemistry.* 24: 5458-5464

Bleyer, W. A., D. G. Poplack. 1985. Prophylaxis and treatment of leukaemia in the central nervous system and other sancturies. *Seminars in Oncology.* 12: 131-148

Boquet, P., A. M. P. Jr. 1976. Interaction of diphtheria toxin with mammalian cell membranes. *The Journal of Biological Chemistry.* 251: 5770-5778

Boulad, F., D. Fishwild, S. F. Carroll, H. Shio, N. A. Kernan. 1993. Endocytosis and intracellular routing of three anti T cell immunotoxins by resting and activated T cells. *Antibody, immunoconjugates and radiopharmaceuticals.* 6: 221-237

Bourrie, B. J. P., P. Casellas, H. E. Blythman, F. K. Jansen. 1986. Study Of The Plasma-Clearance Of Antibody Ricin-A-Chain Immunotoxins - Evidence For Specific Recognition Sites On The A-Chain That Mediate Rapid Clearance Of The Immunotoxin. *European Journal Of Biochemistry.* 155: 1-10

Bretscher, M. S., B. M. Pearse. 1984. Coated pits in action. *Cell.* 38: 3-4.

Broder, S., P. A. B. Jr. 1980. Cutaneous T-Cell Lymphomas. *Seminars in Oncology.* 7: 310-331

Brown, M. S., J. L. Goldstein. 1979. Receptor-mediated endocytosis: insights from the lipoprotein receptor system. *Proceedings of the National Academy of Sciences USA*. 76: 3330-7.

Brown, M. S., R. G. Anderson, J. L. Goldstein. 1983. Recycling receptors: the round-trip itinerary of migrant membrane proteins. *Cell*. 32: 663-7.

Calafat, J., C. Molthoff, H. Janssen, J. Hilkens. 1988. Endocytosis and intracellular routing of an antibody-ricin A chain conjugate. *Cancer Research*. 48: 3822-3827

Caron, P. C., D. A. Scheinberg. 1994. Immunotherapy for acute leukemias. *Current Opinions in Oncology*. 6: 14-22

Carpenter, G., S. Cohen. 1976. 125I-labeled human epidermal growth factor. Binding, internalization, and degradation in human fibroblasts. *The Journal of Cell Biology*. 71: 159-71.

Carpenter, G., S. Cohen. 1979. Epidermal growth factor. *Annual Review of Biochemistry*. 48: 193-216

Carpentier, J. L., P. Gorden, R. G. Anderson, J. L. Goldstein, M. S. Brown, S. Cohen, L. Orci. 1982. Co-localization of 125I-epidermal growth factor and ferritin-low density lipoprotein in coated pits: a quantitative electron microscopic study in normal and mutant human fibroblasts. *The Journal of Cell Biology*. 95: 73-7.

Carrel, S., S. Salvi, F. Rafti, M. Favrot, C. Rapin, R. P. Sekaly. 1991. Direct Involvement Of CD7 (Gp40) In Activation Of TCR-Gamma/Delta + T-Cells. *European Journal Of Immunology*. 21: 1195-1200

Carrera, A. C., M. Rincon, F. Sanchezmadrid, M. Lopezbotet, M. O. Delandazuri. 1988. Triggering Of Co-Mitogenic Signals In T-Cell Proliferation By Anti-Lfa-1 (CD18, CD11a), Lfa-3, And CD7 Monoclonal-Antibodies. *The Journal of Immunology*. 141: 1919-1924

Carriere, D., P. Casellas, G. Richer, P. Gros, F. K. Jansen. 1985. Endocytosis of an antibody ricin A-chain conjugate (Immuno-A-toxin) adsorbed on colloidal gold Effects of ammonium chloride and monensin. *Experimental Cell Research.* 156: 327-340

Carriere, D., J. M. Arcier, J. M. Derocq, C.Fontaine, G.Richer. 1989. Antigenic modulation induced by four monoclonal antibodies adsorbed on gold particles (specifically anti-CD4, anti-CD5, anti-CD7, and anti-150-kDa antigen): relationship between modulation and cytotoxic activity of immunotoxins. *Experimental Cell Research.* 182: 114-128

Carroll, S. F., R. J. Collier. 1984. NAD binding site of diphtheria toxin: Identification of a residue within the nicotinamide subsite by photochemical modification with NAD. *Proceedings of the National Acadamy of Sciences USA.* 81: 3307-3311

Carroll, S. F., R. J. Collier. 1987. Active site of Pseudomonas aeruginosa exotoxin A. Glutamic acid 553 is photolabelled by NAD and shows functional homology with glutamic acid 148 of diphtheria toxin. *The Journal of Biological Chemistry.* 262: 8707-8711

Casellas, P., J. P. Brown, O. Gros, P. Gros, I. Hellstrom, F. K. Jansen, P. Poncelet, R. Roncucci, H. Vidal, K. E. Hellstrom. 1982. Human melanoma cells can be killed in vitro by an immunotoxin specific for melanoma-associated antigen p97. *International Journal of Cancer.* 30: 437-443.

Casellas, P., B. J. P. Bourrie, P. Gros, F. K. Jansen. 1984. Kinetics of cytotoxicity induced by immunotoxins. Enhancement by lysomotropic amines and carboxylic ionophores. *The Journal of Biological Chemistry.* 259: 9359

Chan, A., P. J. Reynolds, Y. Shimizu. 1994. Tyrosine Kinase-Activity Associated With The CD7 Antigen - Correlation With Regulation Of T-Cell Integrin Function. *European Journal Of Immunology.* 24: 2602-2608

Chaudhary, V. K., Y. Jinno, D. FitzGerald, I. Pastan. 1990. Pseudomonas exotoxin contains a specific sequence at the carboxyl terminus that is required for cytotoxicity. *Biochemistry*. 87: 308-312

Cheng, S., F. R. Maxfield, J. Robbins, M. C. Willingham, I. H. Pastan. 1980. Receptor-mediated uptake of 3,3',5-triiodo-L-thyronine by cultured fibroblasts. *Proceedings of the National Academy of Sciences USA*. 77: 3425-6.

Chessels, J. M. 2000. Recent advances in management of acute leukaemia. *Archives of Disease in Childhood*. 82: 438-442

Chiron, M. F., C. M. Fryling, D. J. FitzGerald. 1994. Cleavage of pseudomonas exotoxin and diphtheria toxin by a furin-like enzyme prepared from beef liver. *The Journal of Biological Chemistry*. 269: 18167-18176.

Chuang, D. M., H. Weissbach. 1972. Studies on elongation factor II from calf brain. *Archives of Biochemistry and Biophysics*. 152: 114-124

Cotner, T., H. Mashimo, P. C. Kung, G. Goldstein, J. L. Strominger. 1981. Human T Cell Surface Antigens Bearing A Structural Relationship To HLA Antigens. *Proceedings of the National Academy of Sciences USA*. 78: 3858-3862

Courtoy, P. J. 1993. Analytical subcellular fractionation of endosomal compartments in rat hepatocytes. *Subcellular Biochemstry*. 19: 29-68

Crist, W., J. Boyett, M. Roper, J. Pullen, R. Metzgar, J. v. Eys, A. Ragab, K. Starling, T. Vietti, M. Cooper. 1984. Pre-B cell leukemia responds poorly to treatment: a pediatric oncology group study. *Blood*. 63: 407-414

Crist, W. M., C. E. Grossi, D. J. Pullen, M. D. Cooper. 1985. Immunologic markers in childhood acute lymphocytic leukemia. *Seminars in Oncology*. 12: 105-121

Crist, W., J. Pullen, J. Boyett, J. Falletta, J. v. Eys, M. Borowitz, J. Jackson, B. Dowell, L. Frankel, F. Quddus, e. al. 1986. Clinical and biologic features predict a poor prognosis in acute lymphoid leukemias in infants: a Pediatric Oncology Group Study. *Blood.* 67: 135-140.

Curt, G. A., J. Jolivet, D. N. Carney, B. D. Bailey, J. C. Drake, N. J. Clendeninn, B. A. Chabner. 1985. Determinants of the sensitivity of human small-cell lung cancer cell lines to methotrexate. *Journal of Clinical Investigation.* 76: 1323-1329.

Dautry-Varsat, A., A. Ciechanover, H. F. Lodish. 1983. pH and the recycling of transferrin during receptor-mediated endocytosis. *Proceedings of the National Academy of Sciences USA.* 80: 2258-62.

Day, P. J., S. R. Ernst, A. E. Frankel, A. F. Monzingo, J. M. Pascal, M. C. Molina-Svinth, J. D. Robertus. 1996. Structure and activity of an active site substitution of ricin A chain. *Biochemistry.* 35: 11098-103.

Day, P. J., S. R. Owens, J. Wesche, S. Olsnes, L. M. Roberts, J. M. Lord. 2001. An interaction between ricin and calreticulin that may have implications for toxin trafficking. *The Journal of Biological Chemistry.* 276: 7202-7208

Dillman, R. O., D. E. Johnson, D. L. Shawler. 1986. Immune interferon modulation of in vitro murine anti-human T cell monoclonal antibody-mediated cytotoxicity. *The Journal of Immunology.* 136: 728-31.

Dinndorf, P. A., G. H. Reaman. 1986. Acute lymphoblastic leukemia in infants: evidence for B cell origin of disease by use of monoclonal antibody phenotyping. *Blood.* 68: 975-978.

DiPaola, M., F. R. Maxfield. 1984. Conformational changes in the receptors for epidermal growth factor and asialoglycoproteins induced by the mildly acidic pH found in endocytic vesicles. *The Journal of Biological Chemistry.* 259: 9163-71.

Doms, R. W., G. Russ, J. W. Yewdell. 1989. Brefeldin A redistributes resident and itinerant golgi proteins in the endoplasmic reticulum. *The Journal of Cell Biology.* 109: 61-72

Doms, R. W., R. A. Lamb, J. K. Rose, A. Helenius. 1993. Folding and assembly of viral membrane proteins. *Virology.* 193: 545-62.

Donaldson, J. G., J. Lippincott-Schwartz, G. S. Bloom, T. E. Kreis, R. D. Klausner. 1990. Dissociation of a 110-kD peripheral membrane protein from the Golgi apparatus is an early event in brefeldin A action. *The Journal of Cell Biology.* 111: 2295-306.

Donaldson, J. G., D. Finazzi, R. D. Klausner. 1992. Brefeldin A inhibits Golgi membrane-catalysed exchange of guanine nucleotide onto ARF protein. *Nature.* 360: 350-352.

Dunphy, W. G., R. Brands, J. E. Rothman. 1985. Attachment of terminal N-acetylglucosamine to asparagine-linked oligosaccharides occurs in central cisternae of the Golgi stack. *Cell.* 40: 463-72.

Edwards, M. J., B. T. Heniford, E. A. Klar, K. W. Doak, F. N. Miller. 1992. Pentoxifylline inhibits interleukin-2-induced toxicity in C57BL/6 mice but preserves antitumor efficacy. *Journal of Clinical Investigation.* 90: 637-641.

Eiklid, K. 1980. Entry of Lethal Dose of Abrin, Ricin and Modeccin into the Cytosol of HeLa cells. *Experimental Cell Research.* 126: 321-326

Endo, Y., I. G. Wool. 1982. The site of action of alpha-sarcin on eukaryotic ribosomes. The sequence at the alpha-sarcin cleavage site in 28 S ribosomal ribonucleic acid. *The Journal of Biological Chemistry.* 257: 9054-9060

Endo, Y., K. Mitsui, M. Motizuki, K. Tsurugi. 1987a. The mechanism of action of ricin and related toxic lectins on eukaryotic ribosomes. *The Journal of Biological Chemistry.* 262: 5908-5912

Endo, Y., K. Tsurugi. 1987b. RNA N-glycosidase activity of ricin A-chain. Mechanism of action of the toxic lectin ricin on eukaryotic ribosomes. *The Journal of Biological Chemistry*. 262: 8128-8130

Endo, Y., A. Gluck, I. G. Wool. 1991. Ribosomal RNA identity elements for ricin A-chain recognition and catalysis. *Journal of Molecular Biology*. 221: 193-207.

Engert, A., F. Burrows, W. Jung, P. L. Tazzari, H. Stein, M. Pfreundschuh, V. Diehl, P. Thorpe. 1990. Evaluation of ricin A chain-containing immunotoxins directed against the CD30 antigen as potential reagents for the treatment of Hodgkin's disease. *Cancer Research*. 50: 84-88.

Engert, A., C. Gottstein, H. Bohlen, U. Winkler, G. Schoen, O. Manske, R. Schnell, V. Diehl, P. Thorpe. 1995. Cocktails of ricin A-chain immunotoxins against different antigens on Hodgkin and Sternberg-Reed cells have superior anti-tumor effects againt H-RS cells in vitro and solid Hodgkin tumors in mice. *International Journal Of Cancer*. 63: 304-309

Epstein, R. J. 1988. Topoisomerases in human disease. *Lancet*. 1: 521-524.

Esworthy, R. S., D. M. N. Jr. 1984. A comparative study of ricin and diphtheria toxin-antibody-conjugate kinetics on protein synthesis inactivation. *The Journal of Biological Chemistry*. 259: 11496-11504.

Fando, J. L., I. Alaba, C. Escarmis, J. L. Fernandez-Luna, E. Mendez, M. Salinas. 1985. The mode of action of restrictocin and mitogillin on eukaryotic ribosomes. Inhibition of brain protein synthesis, cleavage and sequence of the ribosomal RNA fragment. *European Journal of Biochemistry*. 149: 29-34

Farquhar, M. G., G. E. Palade. 1998. The Golgi apparatus: 100 years of progress and controversy. *Trends in Cell Biology*. 8: 2-10.

FitzGerald, D. J., I. S. Trowbridge, I. Pastan, M. C. Willingham. 1983. Enhancement of toxicity of antitransferrin receptor antibody-Pseudomonas exotoxin conjugates by adenovirus. *Proceedings of the National Academy of Sciences USA.* 80: 4134-4138.

FitzGerald, D., I. Pastan. 1989. Targeted toxin therapy for the treatment of cancer. *Journal of the National Cancer Institute.* 81: 1455-1463

Flavell, D. J., S. Cooper, B. Morland, R. French, S. U. Flavell. 1992. Effectiveness of combinations of bispecific antibodies for delivering saporin to human acute T-cell lymphoblastic leukaemia cell lines via CD7 and CD38 as cellular target molecules. *British Journal of Cancer.* 65: 545-551

Flavell, D. J., D. Boehm, L. Emery, S. U. Flavell. 1994. Improved Therapeutic Effectiveness of Cocktails of Saporin Immunotoxins Against Human Leukaemia Cell Lines. *Proceedings of the American Association for Cancer Research* 35: 508

Flavell, D. J., D. A. Boehm, L. Emery, A. Noss, A. Ramsay, S. U. Flavell. 1995. Therapy of human B-cell lymphoma bearing SCID mice is more effective with anti-CD19 and anti-CD38-saporin immunotoxins used in combination than with either immunotoxin used alone. *International Journal of Cancer.* 62: 337-344

Flavell, D. J., A. Noss, K. A. F. Pulford, N. Ling, S. U. Flavell. 1997. Systemic Therapy with 3BIT, a triple combination cocktail of anti-CD19, -CD22, and -CD38-Saporin Immunotoxins, is curative of human B-cell lymphoma in severe combined immunodeficient mice. *Cancer Research.* 57: 4824-4829

Flavell, D. J., S. Warnes, A. Noss, S. U. Flavell. 1998. Host-Mediated Antibody Dependent Cellular Cytotoxicity (ADCC) Contributes to the *in vivo* Therapeutic Efficacy of an Anti-CD7-Saporin Immunotoxin in a SCID Mouse model of Human T-ALL. *Cancer Research.* 58: 5787-5794

Flavell, D. J., D. A. Boehm, A. Noss, S. L. Warnes, S. U. Flavell. 2001. Therapy of human T-cell acute lymphoblastic leukaemia with a combination of anti-CD7 and anti-CD38-SAPORIN immunotoxins is significantly better than therapy with each individual immunotoxin. *British Journal of Cancer*. 84: 571-578.

Foley, B. T., J. M. Moehring, T. J. Moehring. 1995. Mutations in the elongation factor 2 gene which confer resistance to diphtheria toxin and Pseudomonas exotoxin A. Genetic and biochemical analyses. *The Journal of Biological Chemistry*. 270: 23218-23225

Franco, M., P. Chardin, M. Chabre, S. Paris. 1996. Myristoylation-facilitated binding of the G protein ARF1GDP to membrane phospholipids is required for its activation by a soluble nucleotide exchange factor. *The Journal of Biological Chemistry*. 271: 1573-8.

Frankel, A. E., L. L. Houston, B. F. Issell. 1986. Prospects for immunotoxin therapy in cancer. *Annual Review of Medicine*. 37: 125-142

Frankel, A. E., E. P. Tagge, M. C. Willingham. 1996. Clinical trials of targeted toxins. *Cancer Biology*. 6: 307

Frankel, A. E., J. H. Laver, M. C. Willingham, L. J. Burns, J. H. Kersey, D. A. Vallera. 1997. Therapy of patients with T-cell lymphomas using an anti-CD7 monoclonal antibody-ricin A chain immunotoxin. *Leukaemia & Lymphoma*. 26: 287-298

Freeman, A. I., V. Weinberg, M. L. Brecher, B. Jones, A. S. Glicksman, L. F. Sinks, M. Weil, H. Pleuss, J. Hananian, E. O. B. Jr, G. S. Gilchrist, T. Necheles, M. Harris, F. Kung, R. B. Patterson, H. Maurer, B. Leventhal, L. Chevalier, E. Forman, J. F. Holland. 1983. Comparison of intermediate-dose methotrexate with cranial irradiation for the post-induction treatment of acute lymphocytic leukemia in children. *New England Journal of Medicine*. 308: 477-484

Frei, E., S. E. Sallan. 1978. Acute lymphoblastic leukaemia: Treatment. *Cancer*. 42: 828-838

Friend, D. S. 1969. Cytochemical staining of multivesicular body and golgi vesicles. *The Journal of Cell Biology*. 41: 269-79.

Fuchs, R., S. Schmid, I. Mellman. 1989. A possible role for Na+,K+-ATPase in regulating ATP-dependent endosome acidification. *Proceedings of the National Academy of Sciences USA*. 86: 539-43.

Fulton, R. J., D. C. Blakey, P. P. Knowles, J. W. Uhr, P. E. Thorpe, E. S. Vitetta. 1986. Purification of Ricin A_1, A_2, and B Chains and Characterization of Their Toxicity. *The Journal of Biological Chemistry*. 261: 5314-5319

Fulton, R. J., J. W. Uhr, E. S. Vitetta. 1988a. In vivo Therapy Of The Bcl1 Tumor - Effect Of Immunotoxin Valency And Deglycosylation Of The Ricin-A Chain. *Cancer Research*. 48: 2626-2631

Fulton, R. J., T. F. Tucker, E. S. Vitetta, J. W. Uhr. 1988b. Pharmacokinetics Of Tumor-Reactive Immunotoxins In Tumor-Bearing Mice - Effect Of Antibody Valency And Deglycosylation Of The Ricin-A Chain On Clearance And Tumor-Localization. *Cancer Research*. 48: 2618-2625

Funaro, A., G. C. Spagnoli, C. M. Ausiello, M. Alessio, S. Roggero, D. Delia, M. Zaccolo, F. Malavasi. 1990. Involvement of the multilineage CD38 molecule in a unique pathway of cell activation and proliferation. *The Journal of Immunology*. 145: 2390-2396

Funaro, A., L. B. De Monte, U. Dianzani, M. Forni, F. Malavasi. 1993. Human CD38 is associated to distinct molecules which mediate transmembrane signalling in different lineages. *European Journal of Immunology*. 23: 2407-2411.

Funaro, A., A. L. Horenstein, F. Malavasi. 1995. Human CD38: a versatile leukocyte molecule with emerging clinical prospectives. *Fundamental and Clinical Immunology.* 3: 101-113

Funaro, A., A. L. Horenstein, L. Calosso, M. Morra, R. P. Tarocco, L. Franco, A. D. Flora, F. Malavasi. 1996. Identification and characterisation of an active soluble form of human CD38 in normal and pathological fluids. *International Immunology.* 8: 1643-1650

Funaro, A., M. Reinis, O. Trubiani, S. Santi, R. D. Primio, F. Malavasi. 1998. CD38 Functions Are Regulated Through an Internalisation Step. *The Journal of Immunology.* 160: 2238-2247

Gagescu, R., N. Demaurex, R. G. Parton, W. Hunziker, L. A. Huber, J. Gruenberg. 2000. The recycling endosome of Madin-Darby canine kidney cells is a mildly acidic compartment rich in raft components. *Molecular Biology of the Cell.* 11: 2775-91.

Galloway, C. J., G. E. Dean, M. Marsh, G. Rudnick, I. Mellman. 1983. Acidification of macrophage and fibroblast endocytic vesicles in vitro. *Proceedings of the National Academy of Sciences USA.* 80: 3334-8.

Gasperi-Campani, A., L. Barbieri, E. Lorenzoni, L. Montanaro, S. Sperti, E. Bonetti, F. Stirpe. 1978. Modeccin, the toxin of Adenia digitata. Purification, toxicity and inhibition of protein synthesis in vitro. *Biochemical Journal.* 174: 491-496

Gasperi-Campani, A., L. Barbieri, M. G. Battelli, F. Stirpe. 1985. On The Distribution Of Ribosome-Inactivating Proteins Amongst Plants. *Journal of Natural Products.* 48: 446-454

George, S. L., D. J. Fernbach, T. J. Vietti, M. P. Sullivan, D. M. Lane, M. E. Haggard, D. H. Berry, D. Lonsdale, D. Komp. 1973. Factors influencing survival in pediatric acute leukemia. The SWCCSG experience, 1958-1970. *Cancer.* 32: 1542-1553

Gessner, S. L., J. D. Irvin. 1980. Inhibition of elongation factor 2-dependent translocation by the pokeweed antiviral protein and ricin. *The Journal of Biological Chemistry.* 255: 3251-3253.

Geuze, H. J., J. W. Slot, G. J. Strous, H. F. Lodish, A. L. Schwartz. 1983. Intracellular site of asialoglycoprotein receptor-ligand uncoupling: double-label immunoelectron microscopy during receptor-mediated endocytosis. *Cell.* 32: 277-87.

Geuze, H. J., J. W. Slot, G. J. Strous, J. Peppard, K. von Figura, A. Hasilik, A. L. Schwartz. 1984. Intracellular receptor sorting during endocytosis: comparative immunoelectron microscopy of multiple receptors in rat liver. *Cell.* 37: 195-204.

Ghetie, M. A., J. Richardson, T. Tucker, D. Jones, J. W. Uhr, E. S. Vitetta. 1991. Antitumor activity of Fab and IgG-anti-CD22 immunotoxins in disseminated human B-cell lymphoma grown in mice with severe combined immunodeficiency disease:effect on tumor cells in extranodal sites. *Cancer Research.* 51

Ghetie, M.-A., K. Tucker, J. Richardson, J. W. Uhr, E. S. Vitetta. 1992. The Antitumour Activity of an Anti-CD22 Immunotoxin in SCID Mice With Disseminated Daudi Lymphoma in Enhanced by Either an Anti-CD19 Antibody or an Anti-CD19 Immunotoxin. *Blood.* 80: 2351-2320

Ghetie, A.-M., L. J. Picker, J. A. Richardson, K. Tucker, J. W. Uhr, E. S. Vitetta. 1994. Anti-CD19 Inhibits the Growth of Human B Cell Tumor Lines *in vitro* and of Daudi Cells in SCID Mice by Inducing Cell Cycle Arrest. *Blood.* 83: 1329-1336

Goldie, J. H., A. J. Coldman. 1983. Quantitative model for multiple levels of drug resistance in clinical tumors. *Cancer Treatment Reports.* 67: 923-931.

Goldmacher, V. S., C. F. Scott, J. M. Lambert, G. D. McIntyre, W. A. Blattler, A. R. Collinson, J. K. Stewart, L. D. Chong, S. Cook, H. S. Slayter, E. Beaumont, S. Watkins. 1989. Cytotoxicity of gelonin and its conjugates with antibodies is determined by the extent of their endocytosis. *Journal of Cellular Physiology.* 141: 222-234

Goldstein, J. L., M. S. Brown. 1974. Binding and degradation of low density lipoproteins by cultured human fibroblasts. Comparison of cells from a normal subject and from a patient with homozygous familial hypercholesterolemia. *The Journal of Biological Chemistry*. 249: 5153-62.

Goldstein, J. L., R. G. Anderson, M. S. Brown. 1979. Coated pits, coated vesicles, and receptor-mediated endocytosis. *Nature*. 279: 679-85.

Goud, B., J. C. Antoine. 1984. Emergence of a surface immunoglobulin recycling process during B lymphocyte differentiation. *The Journal of Cell Biology*. 98: 1238-1246

Gray, G. L., D. H. Smith, J. S. Baldridge, R. N. Harkins, M. L. Vasil, E. Y. Chen, H. L. Heyneker. 1984. Cloning, nucleotide-sequencing, and expression in Escherichia coli of the exotoxin-A structural gene of Pseudomonas aeruginosa. *Proceedings of the National Academy of Sciences USA*. 81: 2645-2649

Greenberg, S., K. Burridge, S. C. Silverstein. 1990. Colocalization of F-actin and talin during Fc receptor-mediated phagocytosis in mouse macrophages. *Journal of Experimental Medicine*. 172: 1853-6.

Greenfield, L., M. J. Bjorn, G. Hron, D. Fong, G. A. Buck, R. J. Collier, D. A. Kaplan. 1983. Nucleotide sequence of the structural gene for diphtheria toxin carried by Cornebacteriophage-beta. *Proceedings of the National Academy of Science USA*. 80: 6853-6857

Greenfield, L., V. G. Johnson, R. J. Youle. 1987. Mutations in Diphtheria Toxin Separate Binding from Entry and Amplify Immunotoxin Selectivity. *Science*. 238: 536-539

Grenier-Brossette, N., I. Bourget, C. Akoundi, J. Y. Bonnefoy, J. L. Cousin. 1992. Spontaneous and ligand-induced endocytosis of CD23 (Fc epsilon receptor II) from the surface of B lymphocytes generates a 16-kDa intracellular fragment. *European Journal of Immunology*. 22: 1573-1577

Griffiths, G., S. Pfeiffer, K. Simons, K. Matlin. 1985. Exit of newly synthesized membrane proteins from the trans cisterna of the Golgi complex to the plasma membrane. *The Journal of Cell Biology.* 101: 949-64.

Griffiths, G., K. Simons. 1986. The trans Golgi Network: Sorting at the exit site of the Golgi complex. *Science.* 234: 438-443

Griffiths, G. 1996. On vesicles and membrane compartments. *Protoplasma.* 195: 37-58

Griffiths, G. 2000. Gut thoughts on the Golgi complex. *Traffic.* 1: 738-45.

Grossbard, M. L., O. W. Press, F. R. Appelbaum, I. D. Bernstein, L. M. Nadler. 1992. Monoclonal antibody-based therapies of leukemia and lymphoma. *Blood.* 80: 863-878

Grossbard, M. L., J. M. Lambert, V. S. Goldmacher, N. L. Spector, J. Kinsella, L. Eliseo, F. Coral, J. A. Taylor, W. A. Blattler, C. L. Epstein. 1993. Anti-B4-blocked ricin: a phase I trial of 7-day continuous infusion in patients with B-cell neoplasms. *Journal of Clinical Oncology.* 11: 726-737.

Grossbard, M. L., L. M. Nadler. 1994. Immunotoxin therapy of lymphoid neoplasms. *Seminars in Hematology.* 31: 88-97

Gruenberg, J., G. Griffiths, K. E. Howell. 1989. Characterization of the early endosome and putative endocytic carrier vesicles in vivo and with an assay of vesicle fusion in vitro. *The Journal of Cell Biology.* 108: 1301-16.

Haghbin, M., C. T. Tan, B. D. Clarkson, V. Mike, J. H. Burchenal, M. L. Murphy. 1975. Treatment of acute lymphoblastic leukemia in children with "prophylactic" intrathecal methotrexate and intensive systemic chemotherapy. *Cancer Research.* 35: 807-811

Haigler, H. T., J. A. Mckanna, S. Cohen. 1979. Rapid Stimulation Of Pinocytosis In Human Carcinoma Cells A-431 By Epidermal Growth Factor. *The Journal of Cell Biology*. 83: 82-90

Hale, G., M. J. Dyer, M. R. Clark, J. M. Phillips, R. Marcus, L. Riechmann, G. Winter, H. Waldmann. 1988. Remission induction in non-Hodgkin lymphoma with reshaped human monoclonal antibody CAMPATH-1H. *Lancet*. 2: 1394-1399

Hammond, D., H. Sather, M. Nesbit, D. Miller, P. Coccia, A. Bleyer, J. Lukens, S. Siegel. 1986. Analysis of prognostic factors in acute lymphoblastic leukemia. *Medical and Pediatric Oncology*. 14: 124-134

Hansen, S. H., K. Sandvig, B. Van-Deurs. 1991. The Pre-endosomal Compartment Comprises Distinct Coated And Noncoated Endocytic Vesicle Populations. *The Journal of Cell Biology*. 113: 731-741

Hanson, M. R., J. J. Mulvihill. 1980. Epidemiology of childhood cancer. In *Cancer in the young*, ed. A. S. Levine, 3-12. New York: Mason

Happe, S., P. Weidman. 1998. Cell-free transport to distinct Golgi cisternae is compartment specific and ARF independent. *The Journal of Cell Biology*. 140: 511-23.

Harding, C., J. Heuser, P. Stahl. 1983. Receptor-mediated endocytosis of transferrin and recycling of the transferrin receptor in rat reticulocytes. *The Journal of Cell Biology*. 97: 329-39.

Haynes, B. F., G. S. Eisenbarth, A. S. Fauci. 1979. Human Lymphocyte Antigens: Production Of A Monoclonal Antibody That Defines Functional Thymus-Derived Lymphocyte Subsets. *Proceedings of the National Academy of Sciences USA*. 76: 5829-5833

Haynes, B. F., D. L. Mann, M. E. Hemler, J. A. Schroer, J. H. Shelhamer, G. S. Eisenbarth, J. L. Strominger, C. A. Thomas, H. S. Mostowski, A. S. Fauci. 1980. Characterization Of A Monoclonal Antibody That Defines An Immunoregulatory T Cell Subset For Immunoglobulin Synthesis In Humans. *Proceedings of the National Academy of Sciences USA*. 77: 2914-2918

Haynes, B. F., R. S. Metzgar, J. D. Minna, P. A. Bunn. 1981. Phenotypic Characterization Of Cutaneous T-Cell Lymphoma - Use Of Monoclonal-Antibodies To Compare With Other Malignant T-Cells. *New England Journal Of Medicine*. 304: 1319-1323

Haynes, B. F., S. E. Miller, T. J. Palker, J. O. Moore, P. H. Dunn, D. P. Bolognesi, R. S. Metzgar. 1983. Identification Of Human T-Cell Leukemia-Virus In A Japanese Patient With Adult T-Cell Leukemia And Cutaneous Lymphomatous Vasculitis. *Proceedings Of The National Academy Of Sciences USA*. 80: 2054-2058

Haynes, B. F., S. M. Denning, K. H. Singer, J. Kurtzberg. 1989. Ontogeny Of T-Cell Precursors - A Model For The Initial Stages Of Human T-Cell Development. *Immunology Today*. 10: 87-91

Helenius, A., I. Mellman, D. Wall, A Hubbard. 1983 *Trends in Biochemical Sciences*. 8:245-250

Henriksen, O., E. A. Robinson, E. S. Maxwell. 1975. Interaction Of Guanosine Nucleotides With Elongation Factor 2. I. Equilibrium Dialysis Studies. *The Journal of Biological Chemistry*. 250: 720-724

Hess, M. W., M. Muller, P. L. Debbage, M. Vetterlein, M. Pavelka. 2000. Cryopreparation provides new insight into the effects of brefeldin A on the structure of the HepG2 Golgi apparatus. *Journal of Structural Biology*. 130: 63-72.

Higgins, C. F., M. M. Gottesman. 1992. Is the multidrug transporter a flippase? *Trends in Biochemical Sciences*. 17: 18-21.

Hoch, D. H., M. Romero-Mira, B. E. Ehrlich, A. Finkelstein, B. R. DasGupta, L. L. Simpson. 1985. Channels formed by botulinum, tetanus, and diphtheria toxins in planar lipid bilayers: relevance to translocation of proteins across membranes. *Proceedings of the National Academy of Sciences USA*. 82: 1692-1696

Honjo, T., Y. Nishizuka, O. Hayaishi. 1968. Diphtheria toxin-dependent adenosine diphosphate ribosylation of aminoacyl transferase II and inhibition of protein synthesis. *The Journal of Biological Chemistry*. 243: 3553-3555.

Honjo, T., Y. Nishizuka, I. Kato, O. Hayaishi. 1971. Adenosine diphosphate ribosylation of aminoacyl transferase II and inhibition of protein synthesis by diphtheria toxin. *The Journal of Biological Chemistry*. 246: 4251-4260

Hopkins, C. R., I. S. Trowbridge. 1983. Internalization and processing of transferrin and the transferrin receptor in human carcinoma A431 cells. *The Journal of Cell Biology*. 97: 508-21.

Hopkins, C. R., A. Gibson, M. Shipman, K. Miller. 1990. Movement of internalized ligand-receptor complexes along a continuous endosomal reticulum. *Nature*. 346: 335-9.

Hsu, V. W., L. C. Yuan, J. G. Nuchtern, J. Lippincott-Schwartz, G. J. Hammerling, R. D. Klausner. 1991. A recycling pathway between the endoplasmic reticulum and the Golgi apparatus for retention of unassembled MHC class I molecules. *Nature*. 352: 441-4.

Hunziker, W., J. A. Whitney, I. Mellman. 1991. Selective Inhibition of Transcytosis by Brefeldin A in MDCK cells. *Cell*. 67: 617-627

Hwang, J., D. J. Fitzgerald, S. Adhya, I. Pastan. 1987. Functional Domains Of Pseudomonas Exotoxin Identified By Deletion Analysis Of The Gene Expressed In Escherichia-Coli. *Cell*. 48: 129-136

Iglewski, B. H., D. Kabat. 1975. NAD-dependent inhibition of protein synthesis by Pseudomonas aeruginosa toxin. *Proceedings of the National Academy of Sciences USA*. 72: 2284-2288

Ippoliti, R., E. Lendaro, A. Bellelli, M. Brunori. 1992. A ribosomal protein is specifically recognised by saporin, a plant toxin which inhibits protein synthesis. *FEBS Letters*. 298: 145-148

Ippoliti, R., E. Lendaro, I. D'Agostino, M. L. Fiani, D. Guidarini, S. Vestri, P. A. Benedetti, M. Brunori. 1995. A chimeric saporin-transferrin conjugate compared to ricin toxin: role of the carrier in intracellular transport and toxicity. *FASEB Journal*. 9: 1220-1225

Ippoliti, R., P. Ginobbi, E. Lendaro, I. D'Agostino, D. Ombtres, P. A. Benedetti, M. Brunori, G. Citro. 1998. The effect of monensin and chloroquine on the endocytosis and toxicity of chimeric toxins. *Cellular and Molecular Life Sciences*. 54: 866-875

Jackson, D. G., J. I. Bell. 1990. Isolation of a cDNA encoding the human CD38 (T10) molecule, a cell surface glycoprotein with an unusual discontinuous pattern of expression during lymphocyte differentiation. *The Journal of Immunology*. 144: 2811-2815

Jackson, M. R., T. Nilsson, P. A. Peterson. 1993. Retrieval of transmembrane proteins to the endoplasmic reticulum. *The Journal of Cell Biology*. 121: 317-33.

Jansen, F. K., H. E. Blythman, D. Carriere, P. Casellas, O. Gros, P. Gros, J. C. Laurent, F. Paolucci, B. Pau, P. Poncelet, G. Richer, H. Vidal, G. A. Voisin. 1982. Immunotoxins: hybrid molecules combining high specificity and potent cytotoxicity. *Immunology Reviews*. 62: 185-216

Jansen, B., D. A. Vellera, W. B. Jaszcz, D. Nguyen, J. H. Kersey. 1992. Successful treatment of human acute T-cell leukaemia in SCID mice using the anti-CD7-deglycosylated ricin A-chain immunotoxin DA7. *Cancer Research*. 52: 1314-1321

Jinno, Y., M. Ogata, V. K. Chaudhary, M. C. Willingham, S. Adhya, D. Fitzgerald, I. Pastan. 1989. Domain-Ii Mutants Of Pseudomonas Exotoxin Deficient In Translocation. *The Journal of Biological Chemistry.* 264: 15953-15959

Jung, L. K. L., S. M. Fu, T. Hara, N. Kapoor, R. A. Good. 1986. Defective Expression Of T-Cell-Associated Glycoprotein In Severe Combined Immunodeficiency. *Journal Of Clinical Investigation.* 77: 940-946

Jung, L. K. L., A. K. Roy, H. R. Chakkalath. 1992. CD7 Augments T-Cell Proliferation Via The Interleukin-2 Autocrine Pathway. *Cellular Immunology.* 141: 189-199

Kagan, B. L., A. Finkelstein, M. Colombini. 1981. Diphtheria toxin fragment forms large pores in phospholipid bilayer membranes. *Proceedings of the National Academy of Sciences USA.* 78: 49

Kalwinsky, D. K., P. Roberson, G. Dahl, J. Harber, G. Rivera, W. P. Bowman, C. H. Pui, J. Ochs, M. Abromowitch, M. E. Costlow. 1985. Clinical relevance of lymphoblast biological features in children with acute lymphoblastic leukemia. *Journal of Clinical Oncology.* 3: 477-484

Karnovsky, M. J., E. R. Unanue. 1973. Mapping and migration of lymphocyte surface macromolecules. *Federal Proceedings.* 32: 55-59

Katz, F., S. Povey, M. Parkar, C. Schneider, R. Sutherland, K. Stanley, E. Solomon, M. Greaves. 1983. Chromosome Assignment Of Monoclonal Antibody-Defined Determinants On Human-Leukemic Cells. *European Journal Of Immunology.* 13: 1008-1013

Katzin, B. J., E. J. Collins, J. D. Robertus. 1991. Structure Of Ricin A-Chain At 2.5-A. *Proteins-Structure Function And Genetics.* 10: 251-259

Kaul, P., J. Silverman, W. H. Shen, S. R. Blanke, P. D. Huynh, A. Finkelstein, R. J. Collier. 1996. Roles of Glu 349 and Asp 352 in membrane insertion and translocation by diphtheria toxin. *Protein Science*. 5: 687-692

Kielian, M. C., Z. A. Cohn. 1980. Phagosome-lysosome fusion. Characterization of intracellular membrane fusion in mouse macrophages. *The Journal of Cell Biology*. 85: 754-65.

Klausner, R. D., G. Ashwell, J. van Renswoude, J. B. Harford, K. R. Bridges. 1983. Binding of apotransferrin to K562 cells: explanation of the transferrin cycle. *Proceedings of the National Academy of Sciences USA*. 80: 2263-6.

Klausner, R. D., J. G. Donaldson, J. Lippincott-Schwartz. 1992. Brefeldin A: insights into the control of membrane traffic and organelle structure. *The Journal of Cell Biology*. 116: 1071-1080.

Kloppstech, K., R. Steinbeck, F. Klink. 1969. Characteristics of the reaction between diphtheria toxin, pyridine coenzymes and the GTP-splitting transfer factor FI. *Hoppe Seylers Z Physiol Chem*. 350: 1377-1384

Kornfeld, S., I. Mellman. 1989. The biogenesis of lysosomes. *Annual Review of Cell Biology*. 5: 483-525

Kounnas, M. Z., R. E. Morris, M. R. Thompson, D. J. FitzGerald, D. K. Strickland, C. B. Saelinger. 1992. The α-macroglobulin receptor/low density lipoprotein receptor-related protein binds and internalises Pseudomonas exotoxin A. *The Journal of Biological Chemistry*. 267: 12420-12423

Kreitman, R. J. 1999. Immunotoxins in cancer therapy. *Current Opinion in Immunology*. 11: 570-578

Kronke, M., E. Schlick, T. A. Waldman, E. S. Vitetta, W. C. Greene. 1986. Selective Killing of Human T-Lymphotropic Virus-I Infected Leukemic T-Cells by Monoclonal Anti-Interleukin 2 Receptor Antibody-Ricin A Chain Conjugates: Potentiation by Ammonium Chloride and Monensin. *Cancer Research*. 46: 3295-3298

Ktistakis, N. T., H. A. Brown, M. G. Waters, P. C. Sternweis, M. G. Roth. 1996. Evidence that phospholipase D mediates ADP ribosylation factor- dependent formation of Golgi coated vesicles. *The Journal of Cell Biology*. 134: 295-306.

Kumagai, M., E. Coustan-Smith, D. J. Murray, O. Silvennoinen, K. G. Murti, W. E. Evans, F. Malavasi, D. Campana. 1995. Ligation of CD38 suppresses human B lymphopoiesis. *Journal of Experimental Medicine*. 181: 1101-1110

Lambert, J. M., P. D. Senter, A. Yau-Young, W. A. Blattler, V. S. Goldmacher. 1985. Purified immunotoxins that are reactive with human lymphoid cells. Monoclonal antibodies conjugated to the ribosome-inactivating proteins gelonin and the pokeweed antiviral proteins. *The Journal of Biological Chemistry*. 260: 12035-12041

Lambert, J. M., V. S. Goldmacher, A. R. Collinson, L. M. Nadler, W. A. Blattler. 1991. An immunotoxin prepared with blocked ricin: a natural plant toxin adapted for therapeutic use. *Cancer Research*. 51: 6236-6242.

Lazarovits, A. I., N. Osman, C. E. L. Feuvre, S. C. Ley, M. J. Crumpton. 1994. CD7 Is Associated With CD3 And CD45 On Human T Cells. *The Journal of Immunology*. 153: 3956-3966

Ledbetter, J. A., C. H. June, L. S. Grosmaire, P. S. Rabinovitch. 1987. Cross-Linking Of Surface-Antigens Causes Mobilization Of Intracellular Ionized Calcium In T-Lymphocytes. *Proceedings Of The National Academy Of Sciences USA*. 84: 1384-1388

Lee, H. C., T. F. Walseth, G. T. Bratt, R. N. Hayes, D. I. Clapper. 1989. Structural Determination Of A Cyclic Metabolite Of NAD^+ With Intracellular $Ca\text{-}2^+$-Mobilizing Activity. *The Journal of Biological Chemistry*. 264: 1608-1615

Lee, H. C., E. Zocchi, L. Guida, L. Franco, U. Benatti, A. Deflora. 1993. Production And Hydrolysis Of Cyclic ADP-Ribose At The Outer Surface Of Human Erythrocytes. *Biochemical And Biophysical Research Communications*. 191: 639-645

Leikin, S., D. Miller, H. Sather, V. Albo, E. Esber, A. Johnson, N. Rogentine, D. Hammond. 1981. Immunologic evaluation in the prognosis of acute lymphoblastic leukemia. A report from Childrens Cancer Study Group. *Blood.* 58: 501-508

Lemichez, E., M. Bomsel, G. Devilliers, J. vanderSpek, J. R. Murphy, E. V. Lukianov, S. Olsnes, P. Boquet. 1997. Membrane translocation of diphtheria toxin fragment A exploits early to late endosome trafficking machinery. *Molecular Microbiology.* 23: 445-457

Leta, E., A. K. Roy, Z. Hou, L. K. Jung. 1995. Production and characterization of the extracellular domain of human CD7 antigen: further evidence that CD7 has a role in T cell signalling. *Cellular Immunology*. 165: 101-9.

Lewis, M. J., H. R. Pelham. 1990. A human homologue of the yeast HDEL receptor. *Nature*. 348: 162-3.

Lewis, M. J., H. R. Pelham. 1992. Ligand-induced redistribution of a human KDEL receptor from the Golgi complex to the endoplasmic reticulum. *Cell*. 68: 353-64.

Li, W. W., J. T. Lin, B. I. Schweitzer, W. P. Tong, D. Niedzwiecki, J. R. Bertino. 1992. Intrinsic resistance to methotrexate in human soft tissue sarcoma cell lines. *Cancer Research*. 52: 3908-3913.

Liou, W., H. J. Geuze, J. W. Slot. 1996. Improving structural integrity of cryosections for immunogold labelling. *Histochemistry and Cell Biology*. 106: 41-58.

Lippincott-Schwartz, J., L. C. Yuan, J. S. Bonifacino, R. D. Klausner. 1989. Rapid redistribution of Golgi proteins into the ER in cells treated with brefeldin A: evidence for membrane cycling from Golgi to ER. *Cell*. 56: 801-813.

Lippincott-Schwartz, J., J. G. Donaldson, A. Schweizer, E. G. Berger, H. P. Hauri, L. C. Yuan, R. D. Klausner. 1990. Microtubule-dependent retrograde transport of proteins into the ER in the presence of brefeldin A suggests an ER recycling pathway. *Cell*. 60: 821-836.

Lippincott-Schwartz, J., L. Yuan, C. Tipper, M. Amherdt, Lelio Orci , R. D. Klausner. 1991. Brefeldin A's Effects on Endosomes, Lysosomes, and the TGN Suggest a General Mechanism for Regulating Organelle Structure and Membrane Traffic. *Cell*. 67: 601-616

Lippincott-Schwartz, J., J. Glickman, J. G. Donaldson, J. Robbins, T. E. Kreis, K. B. Seamon, M. P. Sheetz, R. D. Klausner. 1991. Forskolin inhiits and reverses the effects of brefeldin A on golgi morphology by a cAMP-independent mechanism. *The Journal of Cell Biology*. 112: 567-577

Lippincott-Schwartz, J. 1993. Membrane cycling between the ER and Golgi apparatus and its role in biosynthetic transport. *Subcellular Biochemistry*. 21: 95-119

Lobach, D. F., L. I. Hensley, W. Ho, B. F. Haynes. 1985. Human T-Cell Antigen Expression During The Early Stages Of Fetal Thymic Maturation. *The Journal of Immunology*. 135: 1752-1759

Lopez-Otin, C., D. Barber, J. L. Fernandez-Luna, F. Soriano, E. Mendez. 1984. The primary structure of the cytotoxin restrictocin. *European Journal of Biochemistry*. 143: 621-634.

Lord, J. M., L. M. Roberts. 1998. Retrograde transport: Going against the flow. *Current Biology*. 8: R56-R58

Lyman, S. D., S. Escobar, A. M. Rousseau, A. Armstrong, W. C. Fanslow. 2000. Identification of CD7 as a cognate of the human K12 (SECTM1) protein. *The Journal of Biological Chemistry*. 275: 3431-7.

Malavasi, F., F. Caligariscappio, C. Milanese, P. Dellabona, P. Richiardi, A. O. Carbonara. 1984. Characterization Of A Murine Monoclonal-Antibody Specific For Human Early Lymphohemopoietic Cells. *Human Immunology*. 9: 9-20

Malavasi, F., A. Funaro, M. Alessio, L. B. Demonte, C. M. Ausiello, U. Dianzani, F. Lanza, E. Magrini, M. Momo, S. Roggero. 1992. CD38 - A Multilineage Cell Activation Molecule With A Split Personality. *International Journal Of Clinical & Laboratory Research*. 22: 73-80

Manetti, C., J. M. Le Doussal, E. Rouvier, A. Gruaz-Guyon, J. Barbet. 1995. Intracellular uptake and catabolism of anti-IgM antibodies and bi- specific antibody-targeted hapten by B-lymphoma cells. *International Journal of Cancer*. 63: 250-256.

Manske, J. M., D. J. Buchsbaum, S. M. Azemove, D. E. Hanna, D. A. Vallera. 1986. Antigenic modulation by anti-CD5 immunotoxins. *The Journal of Immunology*. 136: 4721-4728.

Marano, N., D. Holowka, B. Baird. 1989. Bivalent binding of an anti-CD3 antibody to Jurkat cells induces association of the T cell receptor complex with the cytoskeleton. *The Journal of Immunology*. 143: 931-938

Martinez-Climent, J. A. 1997. Molecular cytogenetics of childhood hematological malignancies. *Leukemia*. 11: 1999-2021.

Matthay, K.K., A.M.Abai, S. Cobb, K. Hong, D. Papahadjopoulos, R.M. Straubinger. 1989. Role of ligand in antibody-directed endocytosis of liposomes by human T-leukaemia cells. *Cancer Research*. 49: 4879-4886

Maxfield, F. R., J. Schlessinger, Y. Shechter, I. Pastan, M. C. Willingham. 1978. Collection of insulin, EGF and alpha2-macroglobulin in the same patches on the surface of cultured fibroblasts and common internalization. *Cell.* 14: 805-10.

May, R. D., F. D. Finkelman, H. T. Wheeler, J. W. Uhr, E. S. Vitetta. 1990. Evaluation of ricin A chain-containing immunotoxins directed against different epitopes on the delta-chain of cell surface-associated IgD on murine B cells. *The Journal of Immunology.* 144: 3637-3642.

May, R. D., T. H. Wheeler, F. D. Finkelman, J. W. Uhr, E. S. Vitetta. 1991. Intracellular routing rather than cross-linking or rate of internalisation determines the potency of immunotoxins directed against different epitopes of sIgD on murine B cells. *Cellular Immunology.* 135: 490-500

Mckeehan, W. 1972. The Ribosomal Subunit Requirements For GTP Hydrolysis By Reticulocyte Polypeptide Elongation Factors EF-1 And EF-2. *Biochemical and Biophysical Research Communications.* 48: 1117-1122

Mehta, K., U. Shahid, F. Malavasi. 1996. Human CD38, a cell-surface protein with multiple functions. *FASEB Journal.* 10: 1408-1417

Mellman, I. S., H. Plutner, R. M. Steinman, J. C. Unkeless, Z. A. Cohn. 1983. Internalization and degradation of macrophage Fc receptors during receptor-mediated phagocytosis. *The Journal of Cell Biology.* 96: 887-95.

Mellman, I., H. Plutner. 1984. Internalization and degradation of macrophage Fc receptors bound to polyvalent immune complexes. *The Journal of Cell Biology.* 98: 1170-1177

Mellman, I., H. Plutner, P. Ukkonen. 1984. Internalization and rapid recycling of macrophage Fc receptors tagged with monovalent antireceptor antibody: possible role of a prelysosomal compartment. *The Journal of Cell Biology.* 98: 1163-1169

Mellman, I., R. Fuchs, A. Helenius. 1986. Acidification of the endocytic and exocytic pathways. *Annual Review of Biochemistry.* 55: 663-700

Mellman, I. 1996. Endocytosis and molecular sorting. *Annual Review of Cell and Developmental Biology.* 12: 575-625

Michel, A., J. Dirkx. 1977. Occurrence Of Tryptophan In The Enzymically Active Site Of Diphtheria Toxin Fragment A. *Biochimica et Biophysica Acta.* 491: 286-295

Miller, D. R., S. Leikin, V. Albo, L. Vitale, H. Sather, P. Coccia, M. Nesbit, M. Karon, D. Hammond. 1980. Use of prognostic factors in improving the design and efficiency of clinical trials in childhood leukemia: Children's Cancer Study Group Report. *Cancer Treatment Reports.* 64: 381-392.

Miller, D. R., S. Leikin, V. Albo, H. Sather, D. Hammond. 1981. Prognostic importance of morphology (FAB classification) in childhood acute lymphoblastic leukaemia (ALL). *British Journal of Haematology.* 48: 199-206.

Miller, K., J. Beardmore, H. Kanety, J. Schlessinger, C. R. Hopkins. 1986. Localization of the epidermal growth factor (EGF) receptor within the endosome of EGF-stimulated epidermoid carcinoma (A431) cells. *The Journal of Cell Biology.* 102: 500-9.

Misumi, Y., K. Miki, A. Takatsuki, G. Tamura, Y. Ikehara. 1986. Novel blockade by brefeldin A of intracellular transport of secretory proteins in cultured rat hepatocytes. *Journal of Biological Chemistry.* 261: 11398-11403.

Mizumoto, K., K. Iwasaki, Y. Kaziro. 1974. Studies On Polypeptide Elongation Factor 2 From Pig Liver. III. Interaction With Guanine Nucleotides In The Presence And Absence Of Ribosomes. *Journal of Biochemistry (Tokyo).* 76: 1269-1280

Montanaro, L., S. Sperti, A. Mattioli. 1971. Interaction Of ADP-Ribosylated Aminoacyl-Transferase II With GTP And With Ribosomes. *Biochimica et Biophysica Acta.* 238: 493-497

Montanaro, L., S. Sperti, G. Testoni, A. Mattioli. 1976. Effect of elongation factor 2 and of adenosine diphosphate-ribosylated elongation factor 2 on translocation. *Biochemical Journal*. 156: 15-23

Montecucco, C., G. Schiavo, M. Tomasi. 1985. pH-dependence of the phospholipid interaction of diphtheria-toxin fragments. *Biochemical Journal*. 231: 123-128

Morin-Ganet, M. N., A. Rambourg, S. B. Deitz, A. Franzusoff, F. Kepes. 2000. Morphogenesis and dynamics of the yeast Golgi apparatus. *Traffic*. 1: 56-68.

Morland, B. J., J. Barley, D. Boehm, S. U. Flavell, N. Ghaleb, J. A. Kohler, K. Okayama, B. Wilkins, D. J. Flavell. 1994. Effectiveness of HB2 (anti-CD7) - saporin immunotoxin in an *in vivo* model of human T-cell leukaemia developed in severe combined immunodeficient mice. *British Journal of Cancer*. 69: 279-285

Morris, R. E., M. D. Manhart, C. B. Saelinger. 1983. Receptor-mediated entry of Pseudomonas toxin: methylamine blocks clustering step. *Infection and Immunity*. 40: 806-811

Morris, R. E., A. S. Gerstein, P. F. Bonventre, C. B. Saelinger. 1985. Receptor-mediated entry of diphtheria toxin into monkey kidney Vero cells: Electron microscopic evaluation. *Infection Immunity*. 50: 721-727

Moya, M., A. Dautry-Varsat, B. Goud, D. Louvard, P. Boquet. 1985. Inhibition Of Coated Pit Formation In Hep2 Cells Blocks The Cytotoxicity Of Diphtheria Toxin But Not That Of Ricin Toxin. *The Journal of Cell Biology*. 101: 548-559

Mullock, B. M., N. A. Bright, C. W. Fearon, S. R. Gray, J. P. Luzio. 1998. Fusion of lysosomes with late endosomes produces a hybrid organelle of intermediate density and is NSF dependent. *The Journal of Cell Biology*. 140: 591-601.

Myers, D. A., C. L. Villemez. 1988. Specific Chemical Cleavage Of Diphtheria Toxin With Hydroxylamine. Purification And Characterization Of The Modified Proteins. *The Journal of Biological Chemistry*. 263: 17122-17127

Nesbit, M. E. J., H. N. Sather, L. L. Robison, J. Ortega, P. S. Littman, G. J. D'Angio, G. D. Hammond. 1981. Presymptomatic central nervous system therapy in previously untreated childhood acute lymphoblastic leukaemia: comparison of 1800 rad and 2400 rad. A report for Children's Cancer Study Group. *Lancet.* 1: 461-466

Ness, B. G. v., J. B. Howard, J. W. Bodley. 1980. ADP-ribosylation of elongation factor 2 by diphtheria toxin NMR spectra and proposed structures of ribosyl-diphthamide and its hydrolysis products. *The Journal of Biological Chemistry.* 255: 10710-10716

Neville, D. M., Jr. 1987. Immunotoxins for in vivo therapy: Where are we? *Annals New York Academy of Sciences.* 507: 155-164

Novikoff, A. B., P. M. Novikoff. 1977. Cytochemical contributions to differentiating GERL from the Golgi apparatus. *Histochemical Journal.* 9: 525-51.

Nygard, O., L. Nilsson. 1984. Nucleotide-Mediated Interactions Of Eukaryotic Elongation Factor EF-2 With Ribosomes. *European Journal of Biochemistry.* 140: 93-96

Nygard, O., L. Nilsson. 1985. Reduced ribosomal binding of eukaryotic elongation factor 2 following ADP-ribosylation. Difference in binding selectivity between polyribosomes and reconstituted monoribosomes. *Biochimica et Biophysica Acta.* 824: 152-62.

Nygard, O., L. Nilsson. 1987. The Ribosomal Binding Site For Eukaryotic Elongation Factor EF-2 Contains 5 S Ribosomal RNA. *Biochimica et Biophysica Acta.* 908: 46-53

Nygard, O., L. Nilsson, P. Westermann. 1987. Characterisation Of The Ribosomal Binding Site For Eukaryotic Elongation Factor 2 By Chemical Cross-Linking. *Biochimica et Biophysica Acta.* 910: 245-253

O'Connor, O. A., M. Weiss. 1999. Recent advances in the biology and management of acute lymphoblastic leukemia in adults. *Cancer Treatment and Research*. 99: 307-733

Octave, J. N., Y. J. Schneider, R. R. Crichton, A. Trouet. 1983. Iron mobilization from cultured hepatocytes: effect of desferrioxamine B. *Biochemical Pharmacology*. 32: 3413-8.

Oda, K., S. Hirose, N. Takami, Y. Misumi, A. Takatsuki, Y. Ikehara. 1987. Brefeldin A arrests the intracellular transport of a precursor of complement C3 before its conversion site in rat hepatocytes. *FEBS Letters*. 214: 135-138.

Oeltmann, T. N., A. E. Frankel. 1991. Advances in immunotoxins. *FASEB Journal*. 5: 2334-2337

Ogata, M., V. K. Chaudhary, I. Pastan, D. J. FitzGerald. 1990. Processing of Pseudomonas exotoxin by a cellular protease results in the generation of a 37,000-Da toxin fragment that is translocated to the cytosol. *The Journal of Biological Chemistry*. 265: 20678-20685

Ogata, M., C. M. Fryling, I. Pastan, D. J. FitzGerald. 1992. Cell-mediated cleavage of Pseudomonas exotoxin between Arg279 and Gly280 generates the enzymatically active fragment which translocates to the cytosol. *The Journal of Biological Chemistry*. 267: 25396-25401.

Ohkuma, S., B. Poole. 1981. Cytoplasmic vacuolation of mouse peritoneal macrophages and the uptake into lysosomes of weakly basic substances. *The Journal of Cell Biology*. 90: 656-64.

Ohkuma, S., Y. Moriyama, T. Takano. 1982. Identification and characterization of a proton pump on lysosomes by fluorescein-isothiocyanate-dextran fluorescence. *Proceedings of the National Academy of Sciences USA*. 79: 2758-62.

Olsnes, S., C. Fernandez-Puentes, L. Carrasco, D. Vazquez. 1975. Ribosome inactivation by the toxic lectins abrin and ricin. Kinetics of the enzymic activity of the toxin A-chains. *European Journal of Biochemistry.* 60: 281-288.

Olsnes, S., J. V. Kozlov. 2001. Ricin. *Toxicon.* 39: 1723-8.

Omura, F., K. Kohno, T. Uchida. 1989. The histidine residue of codon 715 is essential function of elongation factor-II. *European Journal of Biochemistry.* 180: 1-8

Orci, L., B. S. Glick, J. E. Rothman. 1986. A new type of coated vesicular carrier that appears not to contain clathrin: its possible role in protein transport within the Golgi stack. *Cell.* 46: 171-84.

Orci, L., M. Tagaya, M. Amherdt, A. Perrelet, J. G. Donaldson, J. Lippincott-Schwartz, R. D. Klausner, J. E. Rothman. 1991. Brefeldin A, a drug that blocks secretion, prevents the assembly of non- clathrin-coated buds on Golgi cisternae. *Cell.* 64: 1183-1195.

Pagano, R. E. 1989. A fluorescent derivative of ceramide: physical properties and use in studying the Golgi apparatus of animal cells. *Methods in Cell Biology.* 29: 75-85

Palade, G. 1975. Intracellular aspects of the process of protein synthesis. *Science.* 189: 347-58.

Pappenheimer, A. M. J., R. Brown, J. T. Kurnick. 1969. Studies on the mode of action of diphtheria toxin. VII. Toxin-stimulated hydrolysis of nicotinamide adenine dinucleotide in mammalian cell extracts. *Journal of Experimental Medicine.* 129: 1-21

Pappenheimer, A. M. 1977. Diphtheria Toxin. *Annual Review of Biochemistry.* 46: 69-94

Pastan, I. H., M. C. Willingham. 1981. Receptor-mediated endocytosis of hormones in cultured cells. *Annual Review of Physiology.* 43: 239-50

Pastan, I., M. C. Willingham, D. J. P. FitzGerald. 1986. Immunotoxins. *Cell.* 47: 641-648

Pauletti, G., E. Lai, G. Attardi. 1990. Early appearance and long-term persistence of the submicroscopic extrachromosomal elements (amplisomes) containing the amplified DHFR genes in human cell lines. *Proceedings of the National Academy of Sciences USA.* 87: 2955-2959.

Pauza, M. E., S. O. Doumbia, C. A. Pennell. 1997. Construction and characterisation of human CD7-specific single-chain Fv immunotoxins. *The Journal of Immunology.* 158: 3259-3269

Pelham, H. R. 1988. Evidence that luminal ER proteins are sorted from secreted proteins in a post-ER compartment. *EMBO Journal.* 7: 913-8.

Pelham, H. R. 1989. Control of protein exit from the endoplasmic reticulum. *Annual Review of Cell Biology.* 5: 1-23

Pelham, H. R. B. 1991. Multiple Targets for Brefeldin A. *Cell.* 67: 449-451

Pelham, H. R. 1995. Sorting and retrieval between the endoplasmic reticulum and Golgi apparatus. *Current Opinion in Cell Biology.* 7: 530-5.

Piatak, M., J. A. Lane, W. Laird, M. J. Bjorn, A. Wang, M. Williams. 1988. Expression Of Soluble And Fully Functional Ricin-A Chain In Escherichia-Coli Is Temperature-Sensitive. *The Journal of Biological Chemistry.* 263: 4837-4843

Pirker, R., D. J. FitzGerald, T. C. Hamilton, R. F. Ozols, W. Laird, A. E. Frankel, M. C. Willingham, I. Pastan. 1985. Characterization of immunotoxins active against ovarian cancer cell lines. *Journal of Clinical Investigations.* 76: 1261-1267

Poole, B., S. Ohkuma. 1981. Effect of weak bases on the intralysosomal pH in mouse peritoneal macrophages. *The Journal of Cell Biology.* 90: 665-9.

Poplack, D. G., G. Reaman. 1988. Acute Lymphoblastic Leukaemia in Childhood. *Pediatric Clinics of North America*. 35: 903-931

Poplack, D. G. 1988. Acute Lymphoblastic Leukaemia. In *Principles and Practice of Pediatric Oncology*, eds. P. A. Pizzo, D. G. Poplack. Philadelphia:

Preijers, F. W. M. B. 1988. Relationship Between Internalisation and Cytotoxicity of Ricin A Chain Immunotoxins. *British Journal of Haematology*. 70: 289-294

Press, O. W., E. S. Vitetta, A. G. Farr, J. A. Hansen, P. J. Martin. 1986. Evaluation of ricin A-chain immunotoxins directed against human T cells. *Cellular Immunology*. 102: 10-20

Press, O. W., P. J. Martin, P. E. Thorpe, E. S. Vitetta. 1988. Ricin A-chain containing immunotoxins directed against different epitopes on the CD2 molecule differ in their ability to kill normal and malignant T cells. *The Journal of Immunology*. 141: 4410-4417

Press, O. W., A. G. Farr, K. I. Borroz, S. K. Anderson, P. J. Martin. 1989. Endocytosis and degradation of monoclonal antibodies targeting human B- cell malignancies. *Cancer Research*. 49: 4906-4912.

Press, O. W., J. Howell-Clark, S. Anderson, I. Bernstein. 1994. Retention of B-cell specific monoclonal antibodies by human lymphoma cells. *Blood*. 83: 1390-1397

Pui, C.-H. 1998. Recent advances in the biology and treatment of childhood acute lymphoblastic leukaemia. *Current Opinion in Hematology*. 5: 292-301

Rabinowich, H., L. Pricop, R. B. Herberman, T. I. Whiteside. 1994. Expression And Function Of CD7 Molecule On Human Natural-Killer-Cells. *Journal Of Immunology*. 152: 517-526

Rabinowich, H., W. C. Lin, R. B. Herberman, T. L. Whiteside. 1994. Signaling Via CD7 Molecules On Human NK Cells. Induction Of Tyrosine Phosphorylation And Beta 1 Integrin-Mediated Adhesion To Fibronectin. *The Journal of Immunology.* 153: 3504-3513

Rabinowitz, S., H. Horstmann, S. Gordon, G. Griffiths. 1992. Immunocytochemical characterization of the endocytic and phagolysosomal compartments in peritoneal macrophages. *The Journal of Cell Biology.* 116: 95-112.

Ramakrishnan, S., L. L. Houston. 1984. Comparison of the selective cytotoxic effects of immunotoxins containing ricin A chain or pokeweed antiviral protein and anti-Thy 1.1 monoclonal antibodies. *Cancer Research.* 44: 201-208

Ramakrishnan, S., F. M. Uckun, L. I. Houston. 1985. Anti-T Cell Immunotoxins Containing Pokeweed Anti-Viral Protein - Potential Purging Agents For Human Autologous Bone-Marrow Transplantation. *The Journal of Immunology.* 135: 3616-3622

Randy, M. P., B. J. Katzin. 1988. Ribosome-inhibiting proteins, retroviral reverse transcriptases, and RNase H share common structural elements. *Proteins: Structure, Function, and Genetics.* 3: 53-59

Randy, M. P., Y. Kim, J. D. Robertus. 1991. Site-directed mutagenesis of ricin A-chain and implications for the mechanism of action. *Proteins: Structure, Function, and Genetics.* 10: 270-278

Rapak, A., P. O. Falnes, S. Olsnes. 1997. Retrograde transport of mutant ricin to the endoplasmic reticulum with subsequent translocation to cytosol. *Proceedings of the National Academy of Sciences USA.* 94: 3783-3788

Raso, V., J. Lawrence. 1984. Carboxylic ionophores enhance the cytotoxic potency of ligand- and antibody-delivered ricin A chain. *Journal of Experimental Medicine.* 160: 1234-1240.

Raso, V., S. C. Watkins, H. Slayter, C. Fehrmann. 1987. Intracellular pathways of ricin A chain cytotoxins. *Annals New York Academy of Science*. 507: 172-186

Reaman, G., P. Zeltzer, W. A. Bleyer, B. Amendola, C. Level, H. Sather, D. Hammond. 1985. Acute lymphoblastic leukemia in infants less than one year of age: a cumulative experience of the Children's Cancer Study Group. *Journal of Clinical Oncology*. 3: 1513-1521

Reijngoud, D. J., J. M. Tager. 1977. The permeability properties of the lysosomal membrane. *Biochimica et Biophysica Acta*. 472: 419-49.

Renston, R. H., A. L. Jones, W. D. Christiansen, G. T. Hradek, B. J. Underdown. 1980. Evidence for a vesicular transport mechanism in hepatocytes for biliary secretion of immunoglobulin A. *Science*. 208: 1276-8.

Richter, D., F. Lipmann. 1970. Separation of mitochondrial and cytoplasmic peptide chain elongation factors from yeast. *Biochemistry*. 9: 5065-5070

Rihova, B. Receptor-mediated targeted drug or toxin therapy. *Advanced Drug Delivery Reviews*. 29: 273-289

Ritz, J., J. M. Pesando, S. E. Sallan, L. A. Clavell, J. Notismcconarty, P. Rosenthal, S. F. Schlossman. 1981. Serotherapy Of Acute Lymphoblastic-Leukemia With Monoclonal-Antibody. *Blood*. 58: 141-152

Rivera, G. K., A. M. Mauer. 1987. Controversies in the management of childhood acute lymphoblastic leukaemia: Treatment intensification, CNS leukaemia, and prognostic factors. *Seminars in Hematology*. 24: 12-26

Rogentine, G. N., R. J. Trapani, R. A. Yankee, E. S. Henderson. 1973. HL-A antigens and acute lymphocytic leukemia: the nature of the HL-A2 association. *Tissue Antigens*. 3: 470-476

Roth, J., E. G. Berger. 1982. Immunocytochemical localization of galactosyltransferase in HeLa cells: codistribution with thiamine pyrophosphatase in trans-Golgi cisternae. *The Journal of Cell Biology*. 93: 223-9.

Rothman, J. E. 1989. Polypeptide chain binding proteins: catalysts of protein folding and related processes in cells. *Cell*. 59: 591-601.

Rutenber, E., J. D. Robertus. 1991. Structure Of Ricin B-Chain At 2.5-A Resolution. *Proteins: Structure, Function, and Genetics*. 10: 260-269

Sandler, D. P., J. A. Ross. 1997. Epidemiology of acute leukemia in children and adults. *Seminars in Oncology*. 24: 3-16.

Sandvig, K., S. Olsnes, A. Pihl. 1976. Kinetics of binding of the toxic lectins abrin and ricin to surface receptors of human cells. *The Journal of Biological Chemistry*. 251: 3977-3984.

Sandvig, K., S. Olsnes. 1981. Rapid entry of nicked diphtheria toxin into cells at low pH. Characterization of the entry process and effects of low pH on the toxin molecule. *The Journal of Biological Chemistry*. 256: 9068-9076

Sandvig, K., S. Olsnes, O. W. Petersen, B. Van-Deurs. 1987. Acidification Of The Cytosol Inhibits Endocytosis From Coated Pits. *The Journal of Cell Biology*. 105: 679-689

Sandvig, K., B. V. Deurs. 1991. Endocytosis Without Clathrin (A Minireview). *Cell Biology International Reports*. 15: 3-8

Sandvig, K., B. V. Deurs. 1996. Endocytosis, Intracellular Transport, and Cytotoxic Action of Shiga Toxin and Ricin. *Physiological Reviews*. 76: 949-966

Sandvig, K., B. v. Deurs. 1999. Endocytosis and intracellular transport of ricin: recent discoveries. *FEBS Letters*. 452: 67-70

Santos-Argumedo, L., C. Teixeira, G. Preece, P. A. Kirkham, R. M. Parkhouse. 1993. A B lymphocyte surface molecule mediating activation and protection from apoptosis via calcium channels. *The Journal of Immunology*. 151: 3119-30.

Sather, H. N. 1986a. Age at diagnosis in childhood acute lymphoblastic leukemia. *Medical and Pediatric Oncology*. 14: 166-172.

Sather, H. N. 1986b. Statistical evaluation of prognostic factors in ALL and treatment results. *Medical and Pediatric Oncology*. 14: 158-165.

Sausville, E. A., D. Headlee, M. Stetler-Stevenson, E. S. Vitetta. 1995. Continuous infusion of the anti-CD22 immunotoxin IgG-RFB4-SMPT-dgA in patients with B-cell lymphoma: a Phase I study. *Blood*. 85: 3457-3465

Scales, S. J., R. Pepperkok, T. E. Kreis. 1997. Visualization of ER-to-Golgi transport in living cells reveals a sequential mode of action for COPII and COPI. *Cell*. 90: 1137-48.

Scatchard, G. 1949. The attractions of proteins for small molecules and ions. *Annals New York Academy of Science*. 51: 660-672

Schekman, R., I. Mellman. 1997. Does COPI go both ways? *Cell*. 90: 197-200.

Schmid, S. L., R. Fuchs, P. Male, I. Mellman. 1988. Two distinct subpopulations of endosomes involved in membrane recycling and transport to lysosomes. *Cell*. 52: 73-83.

Schweizer, A., J. A. Fransen, K. Matter, T. E. Kreis, L. Ginsel, H. P. Hauri. 1990. Identification of an intermediate compartment involved in protein transport from endoplasmic reticulum to Golgi apparatus. *European Journal of Cell Biology*. 53: 185-96.

Seetharam, S., V. K. Chaudhary, D. Fitzgerald, I. Pastan. 1991. Increased cytotoxic activity of Pseudomonas Exotoxin and two chimeric toxins ending in KDEL. *The Journal of Biological Chemistry*. 266: 17376-17381

Seglen, P. O., B. Grinde, A. E. Solheim. 1979. Inhibition of the lysosomal pathway of protein degradation in isolated rat hepatocytes by ammonia, methylamine, chloroquine and leupeptin. *European Journal of Biochemistry*. 95: 215-225

Sempowski, G. D., D. M. Lee, R. E. Kaufman, B. F. Haynes. 1999. Structure and Function of the CD7 Molecule. *Critical Reviews in Immunology*. 19: 331-348

Serafini, T., G. Stenbeck, A. Brecht, F. Lottspeich, L. Orci, J. E. Rothman, F. T. Wieland. 1991. A coat subunit of Golgi-derived non-clathrin-coated vesicles with homology to the clathrin-coated vesicle coat protein beta-adaptin. *Nature*. 349: 215-20.

Shan, D., O. W. Press. 1995. Constitutive endocytosis and degradation of CD22 by human B cells. *The Journal of Immunology*. 154: 4466-4475

Shao, R.-G., T. Shimizu, Y. Pommier. 1996. Brefeldin A is a potent inducer of apoptosis in human cancer cells independently of p53. *Experimental Cell Research*. 227: 190-196

Shen, G. L., J. L. Li, E. S. Vitetta. 1994. Bispecific anti-CD22/anti-CD3-ricin A chain immunotoxin is cytotoxic to Daudi lymphoma cells but not T cells in vitro and shows both A-chain- mediated and LAK-T-mediated killing. *The Journal of Immunology*. 152: 2368-76.

Shimizu, Y., G. A. Vanseventer, E. Ennis, W. Newman, K. J. Horgan, S. Shaw. 1992. Cross-Linking Of The T-Cell-Specific Accessory Molecules CD7 And CD28 Modulates-Cell Adhesion. *Journal Of Experimental Medicine*. 175: 577-582

Siegall, C. B., V. K. Chaudhary, D. J. FitzGerald, I. Pastan. 1989. Functional analysis of domains II, Ib, and III of Pseudomonas exotoxin. *The Journal of Biological Chemistry*. 264: 14256-14261

Siegall, C. B., M. Ogata, I. Pastan, D. J. Fitzgerald. 1991. Analysis Of Sequences In Domain-Ii Of Pseudomonas Exotoxin-A Which Mediate Translocation. *Biochemistry*. 30: 7154-7159

Siena, S., D. A. Lappi, M. Bregni, A. Formosa, S. Villa, M. Soria, G. Bonadonna, A. M. Gianni. 1988. Synthesis and characterization of an antihuman T-lymphocyte saporin immunotoxin (OKT1-SAP) with in vivo stability into nonhuman primates. *Blood*. 72: 756-765

Silverstein, S. C., R. M. Steinman, Z. A. Cohn. 1977. Endocytosis. *Annual Review of Biochemistry*. 46: 669-722.

Simpson, J. C., C. Dascher, L. M. Roberts, J. M. Lord, W. E. Balch. 1995. Ricin Cytotoxicity Is Sensitive to Recycling between the Endoplasmic Reticulum and the Golgi Complex. *The Journal of Biological Chemistry*. 270: 20078-20083

Simpson, J. C., L. M. Roberts, K. Romisch, J. Davey, D. H. Wolf, J. M. Lord. 1999. Ricin A chain utilises the endoplasmic reticulum-associated protein degradation pathway to enter the cytosol of yeast. *FEBS Letters*. 459: 80-84

Sitikov, A. S., E. K. Davydova, T. A. Bezlepkina, L. P. Ovchinnikov, A. S. Spirin. 1984. Eukaryotic elongation factor 2 loses its non-specific affinity for RNA and leaves polyribosomes as a result of ADP-ribosylation. *FEBS*. 176: 406-410

Skogerson, L., K. Moldave. 1967. The Binding Of Aminoacyl Transferase II To Ribosomes. *Biochemical and Biophysical Research Communications*. 27: 568-572

Sleight, R. G., R. E.Pagano. 1984. Transport of a fluorescent phosphatidylcholine analog from the plasma membrane to the Golgi apparatus. *The Journal of Cell Biology*. 99: 742-751

Smith, C. E. 1980. Ultrastructural localization of nicotinamide adenine dinucleotide phosphatase (NADPase) activity to the intermediate saccules of the Golgi apparatus in rat incisor ameloblasts. *Journal of Histochemistry and Cytochemistry*. 28: 16-26.

Spitler, L. E., M. del Rio, A. Khentigan, N. I. Wedel, N. A. Brophy, L. L. Miller, W. S. Harkonen, L. L. Rosendorf, H. M. Lee, R. P. Mischak, et al. 1987. Therapy of patients with malignant melanoma using a monoclonal antimelanoma antibody-ricin A chain immunotoxin. *Cancer Research*. 47: 1717-1723.

States, D. J., T. F. Walseth, H. C. Lee. 1992. Similarities In Amino Acid Sequences Of Aplysia ADP-Ribosyl Cyclase And Human Lymphocyte Antigen CD38. *Trends in Biochemical Sciences*. 17: 495

Steinman, R. M., S. E. Brodie, Z. A. Cohn. 1976. Membrane flow during pinocytosis. A stereologic analysis. *The Journal of Cell Biology*. 68: 665-87.

Steinman, R. M., I. S. Mellman, W. A. Muller, Z. A. Cohn. 1983. Endocytosis and the recycling of plasma membrane. *The Journal of Cell Biology*. 96: 1-27.

Stenmark, H., S. Olsnes, K. Sandvig. 1988. Requirement of specific receptors for efficient translocation of diphtheria toxin A fragment across the plasma membrane. *The Journal of Biological Chemistry*. 263: 13449-13455

Stevenson, F. K., A. J. Bell, R. Cusack, T. J. Hamblin, C. J. Slade, M. B. Spellerberg, G. T. Stevenson. 1991. Preliminary studies for an immunotherapeutic approach to the treatment of human myeloma using chimeric anti-CD38 antibody. *Blood*. 77: 1071-1079.

Stevenson, G. T. 1993. *Immunotherapy of tumours*. 5 ed. Clinical Aspects of Immunology, eds. P. J. Lachmann, K. D. Peters, F. S. Rosen, M. J. Walport. Oxford: Blackwell Scientific Publications

Stirpe, F., A. Gasperi-Campani, L. Barbieri, A. Falasca, A. Abbondanza, W. A. Stevens. 1983. Ribosome-inactivating proteins from the seeds of Saponaria officinalis L. (soapwort), of Agrostemma githago L.(corn cockle) and of Asparagus officinalis L.(asparagus), and from the latex of Hura crepitans L.(sandbox tree). *Biochemical Journal*. 216: 617-625

Stirpe, F., S. Bailey, S. P. Miller, J. W. Bodley. 1988. Modification of ribosomal RNA by ribosome-inactivating proteins from plants. *Nucleic Acids Research*. 16: 1349-1357

Strong, R. C., F. Uckun, R. J. Youle, J. H. Kersey, D. A. Vallera. 1985. Use of Multiple T-Cell-Directed Intact Ricin Immunotoxins for Autologous Bone Marrow Transplantation. *Blood*. 66: 627-635

Sullivan, M. P., T. Chen, P. G. Dyment, E. Hvizdala, C. P. Steuber. 1982. Equivalence of intrathecal chemotherapy and radiotherapy as central nervous system prophylaxis in children with acute lymphatic leukemia: a pediatric oncology group study. *Blood*. 60: 948-958

Suzuki, H., O. Zelphati, G. Hildebrand, L. Leserman. 1991. CD4 and CD7 molecules as targets for drug delivery from antibody bearing liposomes. *Experimental Cell Research*. 193: 112-119

Tanaka, M., K. Iwasaki, Y. Kaziro. 1977. Translocation Reaction Promoted By Polypeptide Chain Elongation Factor-2 From Pig Liver. *Journal of Biochemistry (Tokyo)*. 82: 1035-1043

Tanigawa, G., L. Orci, M. Amherdt, M. Ravazzola, J. B. Helms, J. E. Rothman. 1993. Hydrolysis of bound GTP by ARF protein triggers uncoating of Golgi- derived COP-coated vesicles. *The Journal of Cell Biology*. 123: 1365-71.

Taupiac, M. P., M. Alami, B. Beaumelle. 1996. Translocation of full-length Pseudomonas exotoxin from endosomes is driven by ATP hydrolysis but requires prior exposure to acidic pH. *The Journal of Biological Chemistry*. 271: 26170-26173.

Terhorst, C., A. Vanagthoven, K. Leclair, P. Snow, E. Reinherz, S. Schlossman. 1981. Biochemical-Studies Of The Human Thymocyte Cell-Surface Antigens T6, T9 And T10. *Cell.* 23: 771-780

Thandla, S., P. D. Aplan. 1997. Molecular biology of Acute Lymphoblastic Leukaemia. *Seminars in Oncology.* 24: 45-56

Theuer, C. P., J. Buchner, D. FitzGerald, I. Pastan. 1993. The N-terminal region of the 37-kDa translocated fragment of Pseudomonas exotoxin A aborts translocation by promoting its own export after microsomal membrane insertion. *Proceedings of the National Academy of Sciences USA.* 90: 7774-7778

Theuer, C., S. Kasturi, I. Pastan. 1994. Domain II of Pseudomonas exotoxin A arrests the transfer of translocating nascent chains into mammalian microsomes. *Biochemistry.* 33: 5894-5900

Thorpe, P. E., A. N. F. Brown, J. A. G. B. Jr., B. M. J. Foxwell, F. Stirpe. 1985. An Immunotoxin Composed of Monoclonal Anti-Thy 1.1 Antibody and a Ribosome-Inactivating Protein from *Saponaria Officinalis:* Potent Antitumor Effects In Vitro and In Vivo. *Journal of National Cancer Institute.* 75: 151-159

Thorpe, P. E., P. M. Wallace, P. P. Knowles, M. G. Relf, A. N. F. Brown, G. J. Watson, R. E. Knyba, E. J. Wawrzynczak, D. C. Blakey. 1987. New Coupling Agents for the Synthesis of Immunotoxins Containing a Hindered Disulfide Bond with Improved Stability *in vivo. Cancer Research.* 47: 5924-5931

Thorpe, P. E., P. M. Wallace, P. P. Knowles, M. G. Relf, A. N. Brown, G. J. Watson, D. C. Blakey, D. R. Newell. 1988. Improved anti-tumor effects of immunotoxins prepared with deglycosylated ricin A chain and hindered disulphide linkages. *Cancer Research.* 48: 6396-6403

Tonevitsky, A. G., I. I. Agapov, E. B. Mechetner, G. V. Ershova, A. Y. Toptygin, T. Sarma, A. T. Shamshiev, U. Pfueller. 1993. Comparison of the cytotoxic activity of the immunotoxins with different internalisation rate. *Biochemistry and Molecular Biology International*. 31: 1059-1069

Townsley, F. M., D. W. Wilson, H. R. Pelham. 1993. Mutational analysis of the human KDEL receptor: distinct structural requirements for Golgi retention, ligand binding and retrograde transport. *EMBO Journal*. 12: 2821-9.

Trippett, T., S. Schlemmer, Y. Elisseyeff, E. Goker, M. Wachter, P. Steinherz, C. Tan, E. Berman, J. E. Wright, A. Rosowsky, et al. 1992. Defective transport as a mechanism of acquired resistance to methotrexate in patients with acute lymphocytic leukemia. *Blood*. 80: 1158-1162.

Trowbridge, I. S., D. L. Domingo. 1981. Anti-transferrin Receptor Monoclonal Antibody and Toxin-Antibody Conjugates Affect Growth of Human Tumour Cells. *Nature*. 294(5837):171-173.

Tutt, A. L., R. R. French, T. M. Illidge, J. Honeychurch, H. M. McBride, C. A. Penfold, D. T. Fearon, R. M. E. Parkhouse, G. G. B. Klaus, M. J. Glennie. 1998. Monoclonal antibody therapy of B cell lymphoma: signaling activity on tumor cells appears more important than recruitment of effectors. *The Journal of Immunology*. 161: 3176-3185

Tycko, B., F. R. Maxfield. 1982. Rapid acidification of endocytic vesicles containing alpha 2- macroglobulin. *Cell*. 28: 643-51.

Uckun, F. M. 1993. Immunotoxins for the treatment of leukaemia. *British Journal of Haematology*. 85: 435-438

Uckun, F. M., G. H. Reaman. 1995. Immunotoxins for the treatment of leukemia and lymphoma. *Leukemia and Lymphoma*. 18: 195-201

Uckun, F. M., P. G. Steinherz, H. Sather, M. Trigg, D. Arthur, D. Tubergen, P. Gaynon, G. Reaman. 1996. CD2 antigen expression on leukeamic cells as a predictor of event-free survival after chemotherapy for T-lineage acute lymphoblastic leukaemia: A children's cancer group study. *Blood.* 88: 4288-4295

Umar, S., F. Malavasi, K. Mehta. 1996. Post-translational modification of CD38 protein into a high molecular weight form alters its catalytic properties. *The Journal of Biological Chemistry.* 271: 15922-15927.

Unanue, E. R., M. J. Karnovsky. 1973. Redistribution and fate of Ig complexes on surface of B lymphocytes: functional implications and mechanisms. *Transplantation Reviews.* 14: 184-210

Vallera, D. A. 1994. Immunotoxins: Will their clinical promise be fulfilled? *Blood.* 83: 309-317

Vallera, D. A., L. J. Burns, A. E. Frankel, A. R. Sicheneder, R. Gunther, K. Gajl-Peczalska, C. A. Pennell, J. H. Kersey. 1996. Laboratory preparation of a deglycosylated ricin toxin A chain containing immunotoxin directed against a CD7 T lineage differentiation antigen for phase I human clinical studies involving T cell malignancies. *Journal of Immunological Methods.* 197: 69-83

van der Sluijs, P., M. Hull, P. Webster, P. Male, B. Goud, I. Mellman. 1992. The small GTP-binding protein rab4 controls an early sorting event on the endocytic pathway. *Cell.* 70: 729-40.

van-Deurs, B., P. K. Holm, L. Kayser, K. Sandvig, S. H. Hansen. 1993. Multivesicular bodies in HEp-2 cells are maturing endosomes. *European Journal of Cell Biology.* 61: 208-24.

van Oosterhout, Y. V., I. E. van den Herik-Oudijk, H. M. Wessels, T. de Witte, J. G. van de Winkel, F. W. Preijers. 1994. Effect of isotype on internalization and cytotoxicity of CD19-ricin A immunotoxins. *Cancer Research.* 54: 3527-3532.

van-Deurs, B., L. R. Pedersen, A.Sundan, S.Olsnes, K.Sandvig. 1985. Receptor-mediated Endocytosis of a Ricin-Colloidal Gold Conjugate in Vero Cells. *Experimental Cell Research.* 159: 287-304

van-Deurs, B., T. I. Tonnessen, O. W. Petersen, K. Sandvig, S. Olsnes. 1986. Routing of internalised ricin and ricin conjugates to the Golgi complex. *The Journal of Cell Biology.* 102: 37-47

van-Deurs, B., O. W. Petersen, S. Olsnes, K. Sandvig. 1989. The Ways Of Endocytosis. *International Review of Cytology.* 117: 131-177

van-Horssen, P. J., Y. V. J. M. V. Oosterhout, T. D. Witte, F. W. M. B. Preijers. 1995. Cytotoxic Potency of CD22-Ricin A Depends on Intracellular Routing Rather than the Number of Internalised Molecules. *Scandinavian Journal of Immunology.* 41: 563-569

vanderSpek, J., D. Cassidy, F. Genbauffe, P. D. Huynh, J. R. Murphy. 1994. An intact transmembrane helix 9 is essential for the efficient delivery of the diphtheria toxin catalytic domain to the cytosol of target cells. *The Journal of Biological Chemistry.* 269: 21455-21459

Vervoordeldonk, S. F., P. A. Merle, E. F. v. Leeuwen, C. E. v. d. Schoot, A. E. G. K. v. d. Borne, I. C. M. Slaper-Cortenbach. 1994. Fcγ Receptor II (CD32) on malignant B cells influences modulation induced by anti-CD19 monoclonal antibody. *Blood.* 83: 1632-1639

Via, D. P., M. C. Willingham, I. Pastan, A. M. Gotto, Jr., L. C. Smith. 1982. Co-clustering and internalization of low-density lipoproteins and alpha 2-macroglobulin in human skin fibroblasts. *Experimental Cell Research.* 141: 15-22.

Vitetta, E. S., M. Stone, P. Amlot, J. Fay, R. May, M. Till, J. Newman, P. Clark, R. Collins, D. Cunningham. 1991. Phase I immunotoxin trial in patients with B-cell lymphoma. *Cancer Research.* 51: 4052-4058.

Vitetta, E. S., P. E. Thorpe, J. W. Uhr. 1993. Immunotoxins: Magic Bullets or Misguided Missiles? *Immunology today*. 14: 252-259

Vooijis, W. C., H. J. Schuurman, E. J. E. G. Bast, G. C. deGast. 1995. Evaluation of CD38 as target for immunotherapy in multiple myeloma. *Blood*. 85: 2282-2284

Vooijs, W. C., H. G. Otten, A. H. v. Hattum, M. v. Vlief, R. A. d. Weger, M. d. Boer, F. Stirpe, G. C. d. Gast. 1996. Enhanced Cytotoxicity Against Reed-Sternberg Cell Lines by the Combination of Anti-B7-1 (αCD80) and Anti-B7-2 (αCD86) Immunotoxins. *Blood*. 88: 87a

Waldmann, T. A. 1991. Monoclonal antibodies in diagnosis and therapy. *Science*. 252: 1657-1663

Wales, R., J. A. Chaddock, L. M. Roberts, J. M. Lord. 1992. Addition of an ER Retention Signal to the Ricin A Chain Increases the Cytotoxicity of the Holotoxin. *Experimental Cell Research*. 203: 1-4

Wales, R., L. M. Roberts, J. M. Lord. 1993. Addition of an endoplasmic reticulum retrieval sequence to ricin A chain significantly increases its cytotoxicity to mammalian cells. *The Journal of Biological Chemistry*. 268: 23986-23990.

Ware, R. E., R. M. Scearce, M. A. Dietz, C. F. Starmer, T. J. Palker, B. F. Haynes. 1989. Characterization Of The Surface-Topography And Putative Tertiary Structure Of The Human CD7 Molecule. *The Journal of Immunology*. 143: 3632-3640

Wargalla, U. C., R. A. Reisfeld. 1989. Rate of Internalization of an Immunotoxin Correlates with Cytotoxic Activity Against Human Tumor Cells. *Proceedings of the National Acadamy of Sciences USA*. 86: 5146-5150

Warren, G., V. Malhotra. 1998. The organisation of the Golgi apparatus. *Current Opinion in Cell Biology*. 10: 493-8.

Weil-Hillman, G., W. Runge, F. K. Jansen, D. A. Vallera. 1985. Cytotoxic Effect Of Anti-Mr 67,000 Protein Immunotoxins On Human Tumors In A Nude Mouse Model. *Cancer Research.* 45: 1328-1336

Wesche, J., A. Rapak, S. Olsnes. 1999. Dependence of Ricin Toxicity on Translocation of the toxin A-chain from the Endoplasmic reticulum to the Cytosol. *The Journal of Biological Chemistry.* 274: 34443-34449

Willingham, M. C., F. R. Maxfield, I. H. Pastan. 1979. alpha 2 Macroglobulin binding to the plasma membrane of cultured fibroblasts. Diffuse binding followed by clustering in coated regions. *The Journal of Cell Biology.* 82: 614-25.

Wood, S. A., J. E. Park, W. J. Brown. 1991. Brefeldin A causes a microtubule-mediated fusion of the trans-Golgi network and early endosomes. *Cell.* 67: 591-600

Wright, S. D., S. C. Silverstein. 1983. Receptors for C3b and C3bi promote phagocytosis but not the release of toxic oxygen from human phagocytes. *Journal of Experimental Medicine.* 158: 2016-23.

Yamaizumi, M., E. Mekada, T. Uchida, Y. Okada. 1978. One molecule of diphtheria toxin fragment A introduced into a cell can kill the cell. *Cell.* 15: 245-250

Yamashiro, D. J., B. Tycko, S. R. Fluss, F. R. Maxfield. 1984. Segregation of transferrin to a mildly acidic (pH 6.5) para-Golgi compartment in the recycling pathway. *Cell.* 37: 789-800.

Yoshida, T., C. Chen, M. Zhang, H. C. Wu. 1991. Disruption of the Golgi Apparatus by Brefeldin A Inhibits the Cytotoxicity of Ricin, Modeccin, and Pseudomonas Toxin. *Experimental Cell Research.* 192: 389-395

Youle, R. J., D. M. N. Jr. 1982. Kinetics of protein synthesis inactivation by ricin-anti-Thy 1.1 monoclonal antibody hybrids. Role of the ricin B subunit demonstrated by reconstitution. *The Journal of Biological Chemistry.* 257: 1598-1601

Youle, R. J., F. M. Uckun, D. A. Vallera, M. Colombatti. 1986. Immunotoxins show rapid entry of diphtheria toxin but not ricin via the T3 antigen. *The Journal of Immunology.* 136: 93-98

Zamboni, M., M. Brigotti, F. Rambelli, L. Montanaro, S. Sperti. 1989. High-pressure-liquid-chromatographic and fluorimetric methods for the determination of adenine released from ribosomes by ricin and gelonin. *Biochemical Journal.* 259: 639-643

Zocchi, E., L. Franco, L. Guida, U. Benatti, A. Bargellesi, F. Malavasi, H. C. Lee, A. Deflora. 1993. A Single Protein Immunologically Identified As CD38 Displays NAD^+ Glycohydrolase, ADP-Ribosyl Cyclase And Cyclic ADP-Ribose Hydrolase Activities At The Outer Surface Of Human Erythrocytes. *Biochemical And Biophysical Research Communications.* 196: 1459-1465

Zupo, S., E. Rugari, M. Dono, G. Taborelli, F. Malavasi, M. Ferrarini. 1994. CD38 Signaling By Agonistic Monoclonal-Antibody Prevents Apoptosis Of Human Germinal Center B-Cells. *European Journal Of Immunology.* 24: 1218-1222